

W.F. Chen
School of Civil Engineering
Purdue University
West Lafayette, Indiana 47907, USA

D.J. Han
Department of Civil Engineering
South China University of Technology
Guangzhou
People's Republic of China

Library of Congress Cataloging in Publication Data
Chen, Wai-Fah, 1936-

Plasticity for structural engineers/W.F. Chen and D.J. Han.
p. cm.
Bibliography: p.
Includes index.
1. Plasticity. 2. Structural design. I. Han, D.J. II. Title.
TA418.14.C49 1988
620.1'1233—dc19

88-2330

© 1988 by Springer-Verlag New York Inc.

All rights reserved. This work may not be translated or copied in whole or in part without the written permission of the publisher (Springer-Verlag, 175 Fifth Avenue, New York, NY 10010, USA), except for brief excerpts in connection with reviews or scholarly analysis. Use in connection with any form of information storage and retrieval, electronic adaptation, computer software, or by similar or dissimilar methodology now known or hereafter developed is forbidden.

The use of general descriptive names, trade names, trademarks, etc. in this publication, even if the former are not especially identified, is not to be taken as a sign that such names, as understood by the Trade Marks and Merchandise Marks Acts, may accordingly be used freely by anyone.

Typeset by J.W. Arrowsmith Ltd., Bristol, England.
Printed and bound by R.R. Donnelley & Sons, Harrisonburg, Virginia.
Printed in the United States of America.

9 8 7 6 5 4 3 2 1

ISBN 0-387-96711-7 Springer-Verlag New York Berlin Heidelberg
ISBN 3-540-96711-7 Springer-Verlag Berlin Heidelberg New York

Preface

This book is intended primarily for structural engineers familiar with the processes of elastic and plastic analysis and design of framed structures in steel and reinforced concrete, but less familiar with the elastic and plastic behavior of structural elements under combined stresses. The more complex structural elements are necessary for the solution of more general structural problems under the general heading of "nonlinear analysis" by either the finite-element or finite-difference method. In this book, we have attempted to present the topic of structural plasticity in a manner that is simple, concise, and reasonably comprehensive, encompassing the classical theory of metal plasticity as well as the modern development of concrete plasticity.

The scope of the book is indicated by the contents. It is divided into five parts. Part I examines, on the basis of simple test conditions, the elastic and plastic behaviors of metal and their possible generalizations under combined stresses. An understanding of stress and strain in three dimensions is essential for structural engineers to follow subsequent developments. To this end, index notation and the principles of stress and strain are developed briefly in the relevant parts of Chapters 1 to 3 of Part I.

Part II is concerned with the general developments of plastic stress-strain relations for perfectly plastic solids (Chapter 4) and for work-hardening plastic solids (Chapter 5). Part II ends with the detailed development of a constitutive equation that relates stress increments to total strain increments rather than to plastic strain increments, and that can be readily implemented for a finite-element or finite-difference code.

Part III deals with the application of the general theory of plasticity to metal. Constitutive formulations based on J_2 -theory together with procedures for their solution in a general nonlinear finite-element problem are discussed in some detail. The bounding surface theory recently developed for modeling the behavior of metal under cyclic loading is also presented. Part III closes with a brief discussion of the stress-strain relation for orthotropic materials.

Part IV deals with the application of the general theory of plasticity to reinforced concrete materials. It contains failure criteria of concrete

materials and their constitutive modeling in the pre- and post-fracture ranges. Computer implementation of these models together with model subroutines are included in a companion book entitled *Theory, Problems, and CAE Softwares of Structural Plasticity* by Chen and Zhang (1988).

Part V on limit analysis is devoted to the general limit theorems and their application to metal and concrete structures and the interaction of these structures with ice and soil media. It covers various aspects of modern techniques of limit analysis, and the discussion is illustrated by many examples dealing with practical problems in structural engineering.

The book can be used for courses of various lengths. The first six chapters can be reasonably covered in a three-hour one-semester course for the first-year graduate student who is learning about inelastic behavior of materials for the first time. In a course for graduate students who have already completed a course on plastic analysis of steel structures, the last two chapters on limit analysis can also be covered. The chapter on concrete plasticity may be skipped on a first reading. This part of the material is necessarily written at a slightly more advanced level, because it is directed toward the practicing engineer who is working on concrete structures in the general area of nonlinear analysis. The mathematics used here does not extend beyond the usual calculus so that the reader who has thoroughly studied the first six chapters has given himself most of the needed preparation. We have endeavored to give reasonably complete literature references to the topics covered in Part IV on concrete plasticity. The inclusion of a computer subroutine for a concrete model in the companion book cited previously is intended to encourage the reader to try out the proposed models.

Over the past years, Professor Chen has taught courses in plasticity and limit analysis at Lehigh University and Purdue University and has also given a series of lectures at the Swiss Federal Institute of Technology, National Taiwan University, and University of Kassel. Early drafts of this book have been tested as classroom notes in these courses. The material on concrete plasticity was prepared more recently and was presented as guest lectures at the 1985 Workshop on Recent Developments in Solid Mechanics at Peking University, Beijing, China.

Professor Chen wishes to thank Mr. Zhang Hung for preparing the Answers to Selected Problems as well as the Solution Manual during his course work on Structural Plasticity and later as a teaching and research assistant on this subject area in the School of Civil Engineering at Purdue University.

Contents

Preface	v
Notation	xi

Part I Fundamentals

Chapter 1 Introduction	3
1.1 Introduction	3
1.2 Historical Remarks	5
1.3 Plastic Behavior in Simple Tension and Compression	7
1.4 Modeling of Uniaxial Behavior in Plasticity	11
1.5 Index Notation	26
1.6 Summary	40
References	40
Problems	40
Answers to Selected Problems	44
Chapter 2 Yield and Failure Criteria	46
2.1 Stress	46
2.2 Yield Criteria Independent of Hydrostatic Pressure	72
2.3 Failure Criterion for Pressure-Dependent Materials	84
2.4 Anisotropic Failure/Yield Criteria	99
2.5 Summary	103
References	104
Problems	104
Answers to Selected Problems	111
Chapter 3 Elastic Stress-Strain Relations	117
3.1 Strain	117
3.2 Linear Elastic Isotropic Stress-Strain Relation—Hooke's Law	138
3.3 Nonlinear Elastic Isotropic Stress-Strain Relation	148
3.4 Principle of Virtual Work	161
3.5 Drucker's Stability Postulate	163
3.6 Normality, Convexity, and Uniqueness for an Elastic Solid	165

November, 1987

W.F. CHEN
D.J. HAN

3.7 Incremental Stress-Strain Relations	171
3.8 Summary	172
References	173
Problems	174
Answers to Selected Problems	176

Part II Plastic Stress-Strain Relations

Chapter 4 Stress-Strain Relations for Perfectly Plastic Materials	179
4.1 Introduction	179
4.2 Plastic Potential and Flow Rule	181
4.3 Flow Rule Associated with von Mises Yield Function	183
4.4 Flow Rule Associated with Tresca Yield Function	185
4.5 Flow Rule Associated with Mohr-Coulomb Yield Function	189
4.6 Convexity, Normality, and Uniqueness for Elastic-Perfectly Plastic Materials	192
4.7 A Simple Elastic-Plastic Problem: The Expansion of a Thick-Walled Cylinder	197
4.8 Incremental Stress-Strain Relationships	207
4.9 Prandtl-Reuss Material Model (J_2 Theory)	210
4.10 Drucker-Prager Material Model	216
4.11 General Isotropic Material	221
References	225
Problems	226
Answers to Selected Problems	230
Chapter 5 Stress-Strain Relations for Work-Hardening Materials	232
5.1 Introduction	232
5.2 Deformation Theory of Plasticity	233
5.3 Loading Surface and Hardening Rules	239
5.4 Flow Rule and Drucker's Stability Postulate	250
5.5 Effective Stress and Effective Strain	256
5.6 Illustrative Examples	261
5.7 Incremental Stress-Strain Relationships	267
References	281
Problems	282
Answers to Selected Problems	286

Part III Metal Plasticity

Chapter 6 Implementation in Metals	293
6.1 Introduction	293
6.2 Formulation of the Elastic-Plastic Matrix	294
6.3 Finite-Element Formulation	296
6.4 Numerical Algorithms for Solving Nonlinear Equations	299
6.5 Numerical Implementation of the Elastic-Plastic Incremental Constitutive Relations	308

6.6 Bounding Surface Theory	317
6.7 Extension to Anisotropic Case	326
References	340

Part IV Concrete Plasticity

Chapter 7 Implementation in Concretes	345
7.1 Introduction	345
7.2 Failure Criteria	353
7.3 Plasticity Modeling: Hardening Behavior	368
7.4 Plasticity Modeling: Softening Behavior	383
References	399
Appendix	401

Part V Limit Analysis

Chapter 8 General Theorems of Limit Analysis and Their Applications	409
8.1 Introduction	409
8.2 Theorems of Limit Analysis	411
8.3 Applications of the General Theorems	421
8.4 Discontinuous Stress Fields	427
8.5 Basic Techniques in Applications of the Upper-Bound Method	447
8.6 Example Problems in Plane Stress, Plane Strain, and 3-D	468
References	486
Problems	486
Answers to Selected Problems	489

Chapter 9 Limit Analysis of Engineering Structures	492
9.1 Introduction	492
9.2 Bending of Beams and Frames	497
9.3 Combined Axial and Bending Forces in Frames and Arches	506
9.4 Effect of Shear Force	518
9.5 Limit Analysis of Plates	526
9.6 Limit Analysis of Plates on Elastic Foundations	533
9.7 Limit Analysis of Shells	568
References	589
Problems	590
Answers to Selected Problems	596

Index	601
-----------------	-----

Notation

Stresses and Strains

$\sigma_1, \sigma_2, \sigma_3$	principal stresses, tensile stress positive
σ_{ii}	stress tensor
s_{ij}	stress deviator tensor
σ	normal stress
τ	shear stress
$p = \frac{1}{3}I_1$	hydrostatic pressure or spherical stress
$\sigma_{oct} = \frac{1}{3}I_1$	octahedral normal stress
$\tau_{oct} = \sqrt{\frac{2}{3}}J_2$	octahedral shear stress
$\sigma_m = \sigma_{oct}$	mean normal stress
$\tau_m = \sqrt{\frac{2}{3}}J_2$	mean shear stress
s_1, s_2, s_3	principal stress deviators
$\epsilon_1, \epsilon_2, \epsilon_3$	principal strains, tensile strain positive
ϵ_{ij}	strain tensor
e_{ij}	strain deviator tensor
ϵ	normal strain
γ	engineering shear strain
$\epsilon_v = I'_1$	volumetric strain
$\epsilon_{oct} = \frac{1}{3}I'_1$	octahedral normal strain
$\gamma_{oct} = 2\sqrt{\frac{2}{3}}J'_2$	octahedral engineering shear strain
e_1, e_2, e_3	principal strain deviators

Invariants

$$I_1 = \sigma_1 + \sigma_2 + \sigma_3 = \sigma_{ii} = \text{first invariant of stress tensor}$$

$$\begin{aligned} J_2 &= \frac{1}{2}s_{ij}s_{ij} \\ &= \frac{1}{6}[(\sigma_x - \sigma_y)^2 + (\sigma_y - \sigma_z)^2 + (\sigma_z - \sigma_x)^2] + \tau_{xy}^2 + \tau_{yz}^2 + \tau_{zx}^2 \\ &= \text{second invariant of stress deviator tensor} \end{aligned}$$

$J_3 = \frac{1}{3} s_{ij} s_{jk} s_{ki} = s_{ij} $	= third invariant of stress deviator
$\cos 3\theta = \frac{3\sqrt{3}}{2} \frac{J_3}{J_2^{3/2}}$, where θ is the angle of similarity defined in Fig. 2.9	
$I'_1 = \epsilon_1 + \epsilon_2 + \epsilon_3$	= first invariant of strain tensor
$\rho = \sqrt{2J_2}$	= deviatoric length defined in Fig. 2.8
$\xi = \frac{1}{\sqrt{3}} I_1$	= hydrostatic length defined in Fig. 2.8
$J'_2 = \frac{1}{2} e_{ij} e_{ij}$	
$= \frac{1}{6} [(\epsilon_x - \epsilon_y)^2 + (\epsilon_y - \epsilon_z)^2 + (\epsilon_z - \epsilon_x)^2] + \epsilon_{xy}^2 + \epsilon_{yz}^2 + \epsilon_{zx}^2$	
	= second invariant of strain deviator tensor

Material Parameters

f'_c	uniaxial compressive cylinder strength ($f'_c > 0$)
f'_t	uniaxial tensile strength ($f'_t = m f'_c$)
f'_{bc}	equal biaxial compressive strength ($f'_{bc} > 0$)
E	Young's modulus
ν	Poisson's ratio
K	$\frac{E}{3(1-2\nu)}$ = bulk modulus
G	$\frac{E}{2(1+\nu)}$ = shear modulus
c, ϕ	cohesion and friction angle in Mohr-Coulomb criterion
α, k	constants in Drucker-Prager criterion
k	yield (failure) stress in pure shear

Miscellaneous

{ }	vector
[]	matrix
	determinant
C_{ijkl}	material stiffness tensor
D_{ijkl}	material compliance tensor
$f()$	failure criterion or yield function
x, y, z or x_1, x_2, x_3	Cartesian coordinates

δ_{ij}	Kronecker delta
$W(\epsilon_{ij})$	strain energy density
$\Omega(\sigma_{ij})$	complementary energy density
l_{ij}	$\cos(x'_i, x_j)$ = the cosine of the angle between the x'_i and x_j axes (see Section 1.5.3)

Part I: Fundamentals

1

Introduction

1.1. Introduction

1.1.1. Role of Plasticity in Structural Engineering

The engineering design of large structures often involves a two-stage process: first, the internal force field acting on the structural material must be defined, and second, the response of the material to that force field must be determined. The first stage involves an analysis of the stresses acting within the structural elements; the second involves a knowledge of the properties of the structural material. The linear relationship between stress and strain in an idealized material forms the basis of the *mathematical theory of elasticity*, which has in turn been applied widely in practice to actual materials to estimate stress or strain in the structural elements under a specified working load condition. These stresses are restricted to be less than the specified *working* or *allowable* stress that is chosen as some fraction of the yield strength of the material. A safe design thus is evolved, not due to the adequacy of the structural analysis and the understanding of the properties of the material, but by reliance upon the experience of decades or centuries.

An actual structure is a very complex body with an extremely complicated state of stress. Many secondary stresses arise owing to fabrication, erection, and localization. The combination of unknown initial stress, secondary stresses, and stress concentration and redistribution due to discontinuities of the structure defy an idealized calculation based on the theory of elasticity. The *theory of plasticity* represents a necessary extension of the theory of elasticity and is concerned with the analysis of stresses and strains in the structure in the plastic as well as the elastic ranges. It furnishes more realistic estimates of load-carrying capacities of structures and provides a better understanding of the reaction of the structural elements to the forces induced in the material. An understanding of the role of the relevant mechanical variables that define the characteristic reaction of the material to the applied force is therefore essential to the engineer designing structures. These

stress-strain relationships and their applications to structural engineering problems are developed and discussed in the following chapters. The more comprehensive this knowledge, the more exact will be the design and the more perfect will be the structure. This book attempts to achieve this goal for the case of structural analysis and design of metal and concrete structures.

1.1.2. Scope

Both the theory of elasticity and the theory of plasticity are phenomenological in nature. They are the formalization of experimental observations of the macroscopic behavior of a deformable solid and do not inquire deeply into the physical and chemical basis of this behavior.

A complete account of the theory and application of plasticity must deal with two equally important aspects: (1) the general technique used in the development of stress-strain relationships for inviscid elastic-plastic materials with work hardening as well as strain softening; and (2) the general numerical solution procedure for solving an elastic-plastic structural problem under the action of loads or displacements, each of which varies in a specified manner. Such an account will be given in the following chapters.

The first task of plasticity theory is to set up relationships between stress and strain under a complex stress state that can describe adequately the observed plastic deformation. This is a difficult task. However, deformational rules for metals that, in general, agree well with experimental evidence have been firmly established and successfully used in engineering applications. Moreover, in recent years, the methods of plasticity have also been extended and applied to study the deformational behavior of geological materials, such as rocks, soils, and concretes. The extension of plasticity theory to nonmetallic materials is probably the most active research subject in the field of mechanics of materials at present, and various material models have been developed.

The second task of the theory is to develop numerical techniques for implementing these stress-strain relationships in the analysis of structures. Because of the nonlinear nature of the plastic deformation rules, solutions of the basic equations of solid mechanics inevitably present considerable difficulties. However, in recent years, the rapid development of high-speed computers and modern techniques of finite-element analysis has provided the engineer with a powerful tool for the solution of virtually any nonlinear structural problem. It also has provoked newer developments and wider applications of the classical plasticity theory. Research activity in this field has increased tremendously during the last decade or so.

This book attempts to give a concise description of the basic concepts of the theory and its modern developments, as well as its computer implementations.

1.2. Historical Remarks

1.2.1. Pioneering Work

It is generally regarded that the origin of plasticity, as a branch of mechanics of continua, dates back to a series of papers from 1864 to 1872 by Tresca on the extrusion of metals, in which he proposed the first *yield condition*, which states that a metal yields plastically when the maximum shear stress attains a critical value. The actual formulation of the theory was done in 1870 by St. Venant, who introduced the basic *constitutive relations* for what today we would call rigid, perfectly plastic materials in plane stress. The salient feature of this formulation was the suggestion of a *flow rule* stating that the principal axes of the strain increment (or strain rate) coincide with the principal axes of stress. It remained for Levy later in 1870 to obtain the general equations in three dimensions. A generalization similar to the results of Levy was arrived at independently by von Mises in a landmark paper in 1913, accompanied by his well-known, pressure-insensitive yield criterion (J_2 -theory, or octahedral shear stress yield condition).

In 1924, Prandtl extended the St. Venant-Levy-von Mises equations for the plane continuum problem to include the elastic component of strain, and Reuss in 1930 carried out their extension to three dimensions. In 1928, von Mises generalized his previous work for a rigid, perfectly plastic solid to include a general yield function and discussed the relation between the direction of plastic strain rate (increment) and the *regular or smooth* yield surface, thus introducing formally the concept of using the yield function as a *plastic potential* in the incremental stress-strain relations of flow theory. As is well known now, the von Mises yield function may be regarded as a plastic potential for the St. Venant-Levy-von Mises-Prandtl-Reuss stress-strain relations. The appropriate flow rule associated with the Tresca yield condition, which contains singular regimes (i.e., corners or discontinuities in derivatives with respect to stress), was discussed by Reuss in 1932 and 1933.

Since greater emphasis was placed on problems involving flow or perfect plasticity in the years before 1940, the development of incremental constitutive relationships for hardening materials proceeded more slowly. For example, in 1928, Prandtl attempted to formulate general relations for hardening behavior, and Melan, in 1938, generalized the foregoing concepts of perfect plasticity and gave incremental relations for hardening solids with smooth (regular) yield surface. Also, *uniqueness theorems* for elastic-

plastic incremental problems were discussed by Melan in 1938 for both perfectly plastic and hardening materials based on some limiting assumptions.

1.2.2. Classical Theory

The nearly twenty years after 1940 saw the most intensive period of development of basic concepts and fundamental ingredients in what is now referred to as the *classical theory of metal plasticity*.

Independently of the work of Melan in 1938, Prager, in a significant paper published in 1949, arrived at a general framework (similar to that discussed by Melan in 1938) for the plastic constitutive relations for *hardening materials* with smooth (regular) yield surfaces. The yield function (also termed the *loading function*) and the *loading-unloading* conditions were precisely formulated. Such conditions as the *continuity* condition (near neutral loading), the *consistency* condition (for loading from plastic states), the *uniqueness* condition, and the condition of *irreversibility* of plastic deformation were formulated and discussed. Also, the interrelationship between the *convexity* of the (smooth) yield surface, the *normality* to the yield surface, and the uniqueness of the associated boundary-value problem was clearly recognized. In 1958, Prager further extended this general framework to include thermal effects (nonisothermal plastic deformation), by allowing the yield surface to change its shape with temperature.

A very significant concept of work hardening, termed the *material stability postulate*, was proposed by Drucker in 1951 and amplified in his further papers. With this concept, the plastic stress-strain relations together with many related fundamental aspects of the subject may be treated in a unified manner. We may note here that Drucker in 1959 also extended his postulate to include time-dependent phenomena such as creep and linear viscoelasticity. Based on this postulate, *uniqueness* of perfectly plastic and work-hardening solids has been proved, and various *variational theorems* have been formulated.

Postulates providing assumptions which play an equivalent role in the development of the framework of plasticity relations have been given by Hill in 1948, and extended by Bishop and Hill in 1951 in a study of polycrystalline aggregates, and by Ilyushin in 1961 through consideration of non-negative work in a cycle of straining (known as *Ilyushin's postulate* for material stability). However, it may be noted that the approach for developing the plasticity relations based entirely on Drucker's postulate seems so far to be the most plausible.

Precise formulations of the two fundamental *theorems of limit analysis* (the so-called upper-bound and lower-bound theorems) were given in two papers by Drucker, Greenberg, and Prager in 1951 and in 1952 for an elastic-perfectly (or ideally) plastic material, and by Hill (1951, 1952) from the point of view of rigid-ideally plastic materials. It appears, however,

that the earliest reference to the theorems of limit analysis was probably due to Gvozdev in 1936; (a translation of his paper from Russian was provided by Haythornthwaite in 1960). The theorems are remarkably simple and in accord with intuition. Since then, the application of these theorems to the analysis of various classes of problems (e.g., beams and frames, plates and shells, metal-forming processes) has increased very rapidly (not only for metallic structures, but also for concrete and soil materials).

Further generalization of the plastic stress-strain relations for *singular yield surfaces* (i.e., in the presence of corners or discontinuities in the direction of the normal vector to the yield surface), as well as the uniqueness and variational theorems for such cases, is due to Koiter published in 1953. He introduced the device of using more than one yield (or loading) function in the stress-strain relationships, the plastic strain increment receiving a contribution from each active yield (loading) surface and falling within the fan of normals to the contributing surfaces. In this 1953 illuminating paper, Koiter has shown that the so-called slip theory of plasticity, introduced originally by Batdorf and Budiansky in 1949 and conceived as an alternative formulation to the classical flow theory, is a particular type of incremental (flow) theory with a singular yield condition composed of infinitely many *independently acting* regular (smooth or continuously differentiable), plane yield functions. The concept was further extended by Sanders in 1955, who also proposed a mechanism for the formulation of subsequent yield surfaces.

The introduction of the "corner" concept has ended a period of considerable controversy in which supposedly alternative frameworks for constitutive relations which admitted singular regimes in the yield surface were advanced. Further discussions on this subject may be found in the 1960 paper by Koiter and in the 1953 paper by Prager, among many others.

1.3. Plastic Behavior in Simple Tension and Compression

The simplest type of loading is represented by the uniaxial stress condition, e.g., the simple tension test, for which $\sigma_1 > 0$, $\sigma_2 = \sigma_3 = 0$, or the simple compression test, for which $\sigma_1 = \sigma_2 = 0$, $\sigma_3 < 0$. The well-known uniaxial stress-strain diagram, in which the axial principal stress σ_1 (or σ_3) is plotted against the axial strain ϵ_1 (or ϵ_3), affords a useful representation of the plastic as well as the elastic behavior.

1.3.1. Monotonic Loading

Figure 1.1a shows the typical curve for a simple tension specimen of mild steel. The initial elastic region generally appears as a straight line OA where A defines the *limit of proportionality*. On further straining, the relation between stress and strain is no longer linear but the material is still elastic,

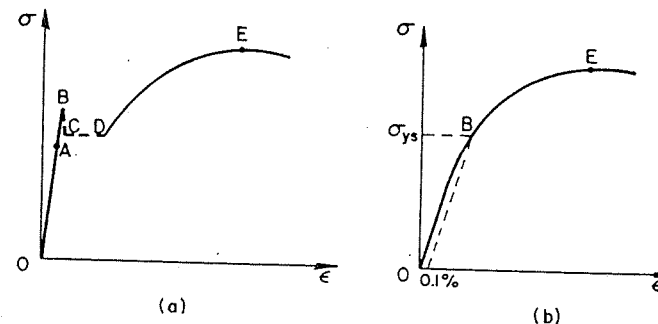


FIGURE 1.1. Stress-strain diagram for mild steel (a) and for some other metals (b).

and upon release of the load, the specimen reverts to its original length. The maximum stress point *B* at which the load can be applied without causing any permanent deformation defines the *elastic limit*. Point *B* is also called the *yield point*, for it marks the initiation of plastic or irreversible deformation. Usually, there is little difference between the proportional limit, *A*, and the elastic limit, *B*. Mild steel exhibits an upper yield point *B* and a lower yield point *C*. Beyond point *C*, there is an extension at approximately constant load. The behavior in the flat region *CD* is generally referred to as *plastic flow*. For most metals, however, neither a sharp yield point nor plastic flow is discernible, and a yield strength is generally defined by an *offset yield stress*, σ_{ys} , corresponding usually to a 0.1% definition of strain as shown in Fig. 1.1b. This offset yield stress is defined as the *initial yield stress*.

Above the yield point, the response of the material is both elastic and plastic. The slope of the curve decreases steadily, monotonically, and eventually failure of the specimen occurs at point *E*. A *ductile material* like mild steel is able to incur comparatively large strains without failure. On the other hand, cast iron is a *brittle material* since it fails after very little straining. It is generally considered when discussing the failure of metals that there are two types of failure modes: *cleavage type* such as exhibited by cast iron and *shear type* such as exhibited by mild steel. Failure characteristics of geological materials are much more complicated. They also depend on loading type: for example, concrete exhibits brittle behavior under tensile loadings, but under compressive loadings with confining pressure, it may exhibit a certain degree of ductility before failure.

1.3.2. Unloading and Reloading

Now, consider the test in which the specimen is first loaded monotonically to some value beyond the initial yield point and then completely unloaded.

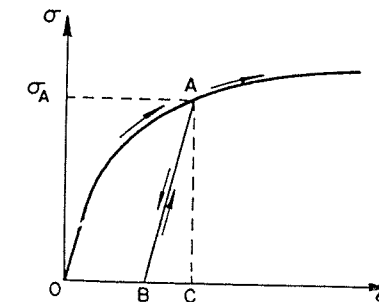


FIGURE 1.2. Loading, unloading, and reloading paths.

The behavior is as indicated in Fig. 1.2. When the stress is reduced, the strain decreases along an almost elastic unloading line *AB* which is parallel to the initially linear region of the curve. When the load is again zero at the end of unloading, the strain is not zero; there remains a *residual strain* *OB*. The irrecoverable strain *OB* is referred to as *plastic strain* while the recoverable strain *BC* is the *elastic strain*. Now, if this specimen is reloaded, the stress-strain curve follows the reloading path *BA*, which is identical to the unloading path *AB*. The material is therefore elastic until the previous maximum stress at point *A* is reached again. The stress σ_A is regarded as the *subsequent yield stress*, beyond which further plastic deformation is induced and the stress-strain curve again follows the original one for monotonic loading.

For most materials, after the initial yield point has been reached, the stress-strain curve continues to rise although the slope becomes progressively less, until the slope falls to zero as failure occurs. Thus, the subsequent yield stress increases with further straining. This effect of the material being able to withstand a greater stress after plastic deformation is known as *strain hardening* or *work hardening*, in the sense that the material gets stronger the more it is strained or worked.

For some materials, such as concrete or rock in a simple compression test, there is a region beyond the failure or peak point in which the slope of the curve is negative. Such a behavior is called *strain softening*. This type of material gets weaker with a continuous straining beyond a certain limit or peak stress.

1.3.3. Reversed Loading

If we perform a simple compression test on a metal, we will obtain an almost identical stress-strain curve as in a simple tension test. However,

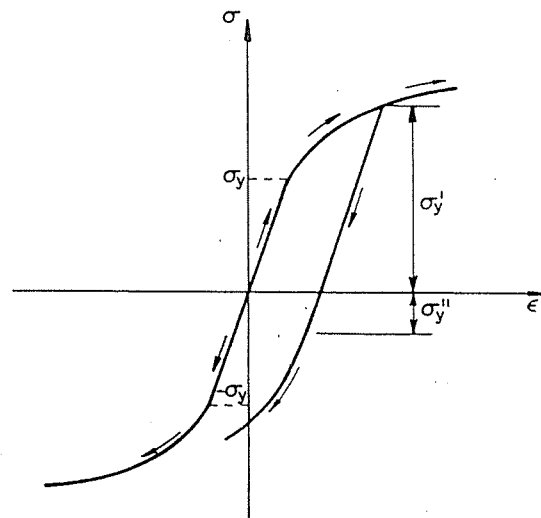


FIGURE 1.3. Bauschinger effect.

after a plastic prestraining in tension of a specimen, the stress-strain curve of this specimen in compression differs considerably from the curve which would be obtained on reloading of this specimen in tension, or on loading an undisturbed specimen in compression. As illustrated in Fig. 1.3, for the specimen with a preloading σ'_y in tension, its corresponding compressive yielding occurs at a stress level σ''_y which is less than the initial yield stress σ_y , and much less than the subsequent yield point σ'_y . This phenomenon is known as the *Bauschinger effect* and is usually present whenever there is a stress reversal.

It is evident from the previous discussion that there is no one-to-one correspondence between stress and strain in a plastically deformed solid. In other words, the strain is not a function of stress alone, but depends on the previous *loading history*. Thus, the material is *load path dependent*. This can be illustrated by the simple case of zero stress, when residual strains of different magnitudes can be established by varying the loading history with the stress starting and finishing at zero.

In this discussion so far, we have assumed that there is a single stress-strain curve for tension or compression, independent of the rate of straining. This assumption is referred to as *time independence*. It is reasonably true for structural metals at room temperature under a static loading condition. Rate effects are very important for materials under dynamic loading conditions. The case is not considered in this book.

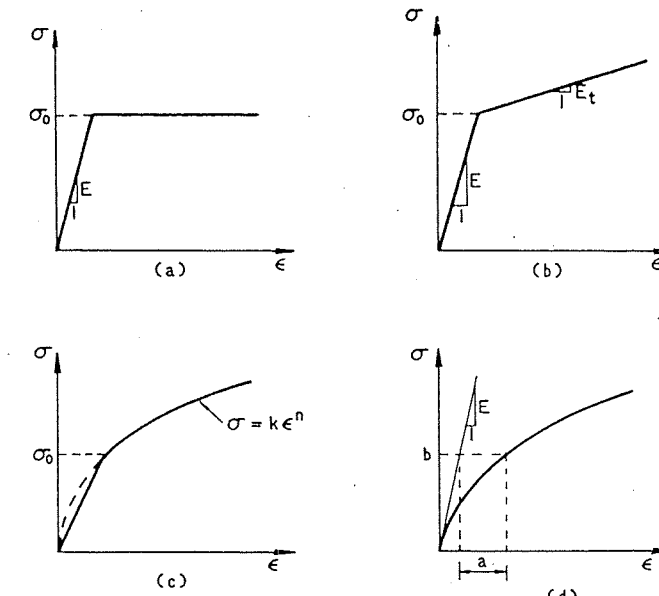


FIGURE 1.4. Idealized stress-strain curves.

1.4. Modeling of Uniaxial Behavior in Plasticity

1.4.1. Simplified Uniaxial Tensile Stress-Strain Curves

In order to obtain a solution to a deformation problem, it is necessary to idealize the stress-strain behavior of the material. The following idealized models deserve note.

1.4.1.1. ELASTIC-PERFECTLY PLASTIC MODEL (FIG. 1.4a)

In some instances, it is permissible and convenient to neglect the effect of work hardening, assume that the plastic flow occurs as the stress has reached the yield stress σ_0 . Thus, the uniaxial tension stress-strain relation may be expressed as

$$\epsilon = \frac{\sigma}{E} \quad \text{for } \sigma < \sigma_0 \quad (1.1)$$

$$\epsilon = \frac{\sigma}{E} + \lambda \quad \text{for } \sigma = \sigma_0$$

where E is Young's modulus, and λ is a scalar to be determined and is greater than 0.

1.4.1.2. ELASTIC-LINEAR WORK-HARDENING MODEL (FIG. 1.4b)

In the elastic-linear work-hardening model, the continuous curve is approximated by two straight lines, thus replacing the smooth transition curve by a sharp breaking point, the ordinate of which is taken to be the elastic limit stress or the yield strength σ_0 . The first straight-line branch of the diagram has a slope of Young's modulus, E . The second straight-line branch, representing in an idealized fashion the strain-hardening range, has a slope of $E_t < E$. The stress-strain relation for a monotonic loading in tension has the form

$$\begin{aligned}\epsilon &= \frac{\sigma}{E} && \text{for } \sigma \leq \sigma_0 \\ \epsilon &= \frac{\sigma_0}{E} + \frac{1}{E_t} (\sigma - \sigma_0) && \text{for } \sigma > \sigma_0\end{aligned}\quad (1.2)$$

1.4.1.3. ELASTIC-EXPONENTIAL HARDENING MODEL (FIG. 1.4c)

Consider a power expression of the type

$$\begin{aligned}\sigma &= E\epsilon && \text{for } \sigma \leq \sigma_0 \\ \sigma &= k\epsilon^n && \text{for } \sigma > \sigma_0\end{aligned}\quad (1.3)$$

where k and n are two characteristic constants of the material to be determined to best fit the experimentally obtained curve. If ϵ represents the total strain, the curve should pass through the point representing the yield stress and the corresponding elastic strain. The power expression (1.3) should be used only in the strain-hardening range (see Fig. 1.4c).

1.4.1.4. RAMBERG-OSGOOD MODEL (FIG. 1.4d)

The nonlinear stress-strain curve as shown in Fig. 1.4d has the following expression:

$$\epsilon = \frac{\sigma}{E} + a \left(\frac{\sigma}{b} \right)^n \quad (1.4)$$

in which a , b , and n are material constants. The initial slope of the curve takes the value of Young's modulus E at $\sigma = 0$, and decreases monotonically with increasing loading. Since the model has three parameters, it allows for a better fit of real stress-strain curves.

1.4.2. Tangent Modulus E_t and Plastic Modulus E_p

Because the elastic-plastic stress-strain response of a material is nonlinear in nature, an incremental procedure is generally adopted in solution of a deformation problem. We assume therefore that a *strain increment*, $d\epsilon$, consists of two parts: the *elastic strain increment*, $d\epsilon^e$, and the *plastic strain increment*, $d\epsilon^p$ (see Fig. 1.5a), such that

$$d\epsilon = d\epsilon^e + d\epsilon^p \quad (1.5)$$

The *stress increment* $d\sigma$ is related to the *strain increment* $d\epsilon$ by

$$d\sigma = E_t d\epsilon \quad (1.6)$$

where E_t is the *tangent modulus* which is changing during plastic deformation. In the case of uniaxial loading, E_t is the current slope of the σ - ϵ curve (Fig. 1.5a). If we separate the plastic strain ϵ^p from the total strain ϵ , then the plastic strain increment $d\epsilon^p$ and the stress increment $d\sigma$ are related by

$$d\sigma = E_p d\epsilon^p \quad (1.7)$$

where E_p is referred to as the *plastic modulus*, which in the case of uniaxial loading is the slope of the σ - ϵ^p curve as shown in Fig. 1.5b. For the elastic strain increment $d\epsilon^e$, we have the usual relationship

$$d\sigma = E d\epsilon^e \quad (1.8)$$

where E is the *elastic modulus*.

Substitution of $d\epsilon$ in Eq. (1.6), $d\epsilon^p$ in Eq. (1.7), and $d\epsilon^e$ in Eq. (1.8) into Eq. (1.5) leads to the relationship between the three moduli E_t , E , and E_p ,

$$\frac{1}{E_t} = \frac{1}{E} + \frac{1}{E_p} \quad (1.9)$$

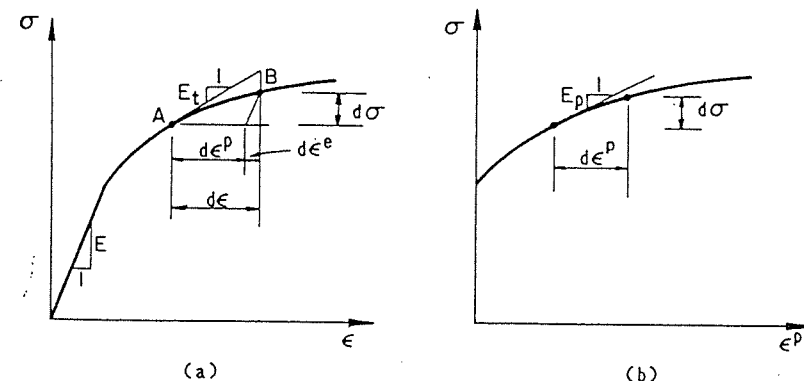


FIGURE 1.5. Tangent modulus E_t and plastic modulus E_p .

1.4.3. Hardening Rules

As described previously, the phenomenon whereby yield stress increases with further plastic straining is known as work hardening or strain hardening. To describe this behavior, we introduce a *hardening parameter* κ to characterize various stages of hardening, and assume that the plastic modulus E_p is a function of this hardening parameter κ as

$$E_p = E_p(\kappa) \quad (1.10)$$

where κ may be taken as the *plastic work* W_p

$$W_p = \int \sigma d\epsilon^p \quad (1.11)$$

or the *plastic strain* ϵ^p or, more realistically, the accumulative plastic strain

$$\epsilon_p = \int (d\epsilon^p d\epsilon^p)^{1/2}$$

which is the sum of the *effective plastic strain increments* defined by

$$|d\epsilon_p| = \sqrt{d\epsilon^p d\epsilon^p} \quad (1.12)$$

Since the uniaxial tensile $\sigma-\epsilon$ curve for a material is generally known from a simple test, the functional form of the plastic modulus E_p in Eq. (1.10) can be determined from this test in terms of a given definition of the hardening parameter κ .

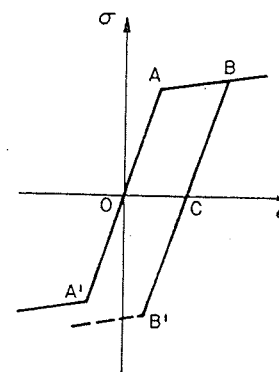
For a material element under a reversed loading condition, the subsequent yield stress is usually determined by one of the following three simple rules:

1. *Isotropic hardening rule*: The reversed compressive yield stress is assumed equal to the tensile yield stress. As illustrated in Fig. 1.6a, where $|\overline{B'C}| = |\overline{BC}|$, the reversed compressive yield stress $\sigma_{B'}$ is equal to the tensile yielding stress σ_B before load reversal. Thus, the isotropic hardening rule neglects completely the Bauschinger effect, as it assumes that a raised yield point in tension carries over equally in compression. This hardening rule may be expressed mathematically in the form

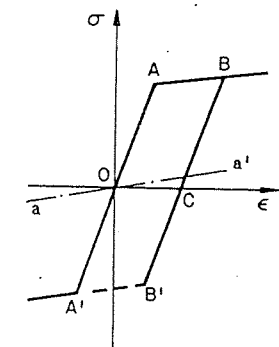
$$|\sigma| = |\sigma(\kappa)| \quad (1.13)$$

where $\sigma(\kappa)$ is a function of the hardening parameter κ and the parameter κ must be defined such that it is always a non-negative scalar, such as the plastic work or accumulative plastic strain mentioned before.

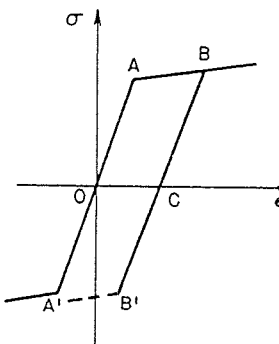
2. *Kinematic hardening rule*: The elastic range is assumed to be unchanged during hardening. Thus, the kinematic hardening rule considers the Bauschinger effect to its full extent. Kinematic hardening for a linear hardening material is shown in Fig. 1.6b, where $|\overline{BB'}| = |\overline{AA'}|$. The center of the elastic region is moved along the straight line aa' . This hardening



(a) ISOTROPIC HARDENING



(b) KINEMATIC HARDENING



(c) INDEPENDENT HARDENING

FIGURE 1.6. Hardening rules.

rule may be expressed mathematically in the form

$$|\sigma - c(\kappa)| = \sigma_0 \quad (1.14)$$

where c is a function of the hardening parameter κ .

3. *Independent hardening rule:* The material is assumed to be hardened independently in tension and in compression. This hardening rule is exemplified in Fig. 1.6c, where $\overline{BC} > \overline{OA}$, but $|\overline{CB'}| = |\overline{OA}'|$; the material has hardened only in tension, but it behaves like a virgin material under a reversed compressive loading condition. It may be expressed mathematically in the form

$$\begin{aligned}\sigma &= \sigma_t(\kappa_t) && \text{if } \sigma > 0 \\ \sigma &= \sigma_c(\kappa_c) && \text{if } \sigma < 0\end{aligned}$$

where κ_t and κ_c are hardening parameters accumulated during the tension and compression loading, respectively.

1.4.4. Examples

EXAMPLE 1.1. The behavior of a polycrystal metallic material composed of many monocrystals is analogous to a truss structure composed of many individual bars. Therefore, it is possible to use a simple truss model to simulate the elastic-plastic behavior of metallic materials. In this example, an overlay truss structure shown in Fig. 1.7 is considered. The Bauschinger effect will be simulated by the model.

In Fig. 1.7, two pairs of bar elements in parallel carry the load P . The vertical bars are made of elastic-perfectly plastic materials with different yield strength. Discuss the loading, unloading, and reloading characteristics of this structural model.

LOADING BEHAVIOR. With the load P increasing from zero, the first two significant stages occur when bars 1 yield followed by the yielding of bars

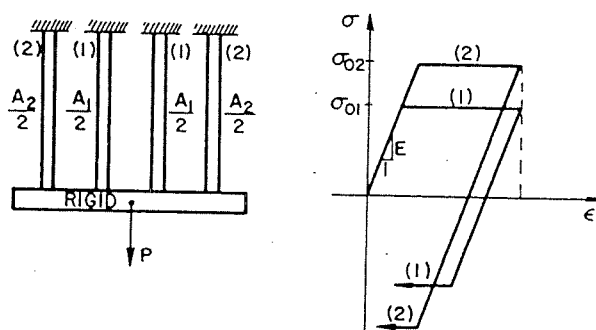


FIGURE 1.7. Overlay model.

1.4. Modeling of Uniaxial Behavior in Plasticity 17

2. Noting that both materials have the same elastic modulus, the load at first yield is found as

$$P_a = \sigma_{01}A_1 + \sigma_{01}A_2 \quad (1.15)$$

The equivalent stress can be expressed as

$$\sigma_a = \frac{\sigma_{01}A_1 + \sigma_{01}A_2}{A_1 + A_2} = \sigma_{01} \quad (1.16)$$

The corresponding strain is

$$\epsilon_a = \frac{\sigma_{01}}{E} \quad (1.17)$$

At the yielding of bars 2, the load, the stress, and the strain may be expressed as

$$P_b = \sigma_{01}A_1 + \sigma_{02}A_2 \quad (1.18)$$

$$\sigma_b = \frac{\sigma_{01}A_1 + \sigma_{02}A_2}{A_1 + A_2} \quad (1.19)$$

$$\epsilon_b = \frac{\sigma_{02}}{E} \quad (1.20)$$

UNLOADING BEHAVIOR. After this, further elongation of the bars does not result in any increase in load. Therefore, the next significant occurrence will be an unloading phase. During unloading, the modulus is the same as the initial modulus E . Therefore, load P reaches zero when the strain has been reduced by an amount

$$\epsilon = \frac{\sigma_{01}A_1 + \sigma_{02}A_2}{E(A_1 + A_2)} \quad (1.21)$$

At this point, the stress in bars 1, σ_1 , and that in bars 2, σ_2 , are represented by

$$\sigma_1 = \sigma_{01} - E\epsilon = \frac{(\sigma_{01} - \sigma_{02})A_2}{A_1 + A_2} \quad (1.22)$$

$$\sigma_2 = \sigma_{02} - E\epsilon = \frac{(\sigma_{02} - \sigma_{01})A_1}{A_1 + A_2} \quad (1.23)$$

Because $\sigma_{02} > \sigma_{01}$, we have $\sigma_1 < 0$, $\sigma_2 > 0$, indicating that there exists a residual compression in the lower-yield-strength bars 1 and a residual tension in the higher-yield-strength bars 2 with the applied load being reduced to zero.

Since we assume that the bar itself is elastic-perfectly plastic, compressive yield will occur in bars 1 when the strain has been reduced by an amount

$$\epsilon = 2 \frac{\sigma_{01}}{E} \quad (1.24)$$

At this instance, the load in bars 1 is

$$P_1 = -\sigma_{01}A_1 \quad (1.25)$$

The load in bars 2 is

$$P_2 = (\sigma_{02} - 2\sigma_{01})A_2 \quad (1.26)$$

The equivalent stress is

$$\sigma_d = \frac{(\sigma_{02} - 2\sigma_{01})A_2 - \sigma_{01}A_1}{A_1 + A_2} \quad (1.27)$$

Noting that the reversed yield load in Eq. (1.27) is less in magnitude than the initial yield load in Eq. (1.16), it follows therefore that bars 1 yield much earlier than they would have on initial loading, because they are already in compression when $P=0$ as indicated in Eq. (1.22).

Compressive yielding occurs in bars 2 when the strain has been reduced by the amount

$$\epsilon = 2 \frac{\sigma_{02}}{E} \quad (1.28)$$

At this point, the load and the equivalent stress can be expressed as

$$P_c = -\sigma_{01}A_1 - \sigma_{02}A_2 \quad (1.29)$$

$$\sigma_e = \frac{-\sigma_{01}A_1 - \sigma_{02}A_2}{A_1 + A_2} \quad (1.30)$$

The σ - ϵ curve for this loading path is shown in Fig. 1.8 by 0-a-b-c-d-e. If more bar elements with different yield strengths are included in the structural model, a more smooth σ - ϵ curve will be obtained.

RELOADING BEHAVIOR. Consider now the case in which compressive loading is terminated at point h before compressive plastic flow in bars 2 begins. Reloading of the structural system in tension will follow the linear response with the initial modulus E but bars 1 will eventually yield again in tension at point i and plastic flow begins at point f. The σ - ϵ curve for this loading cycle is shown in Fig. 1.8 by f-g-h-i.

This structural model with an assemblage of bars of different yield strengths may be considered, qualitatively, to represent a real specimen with slip planes of different strengths, and therefore explains why a real specimen generally exhibits the Bauschinger effect.

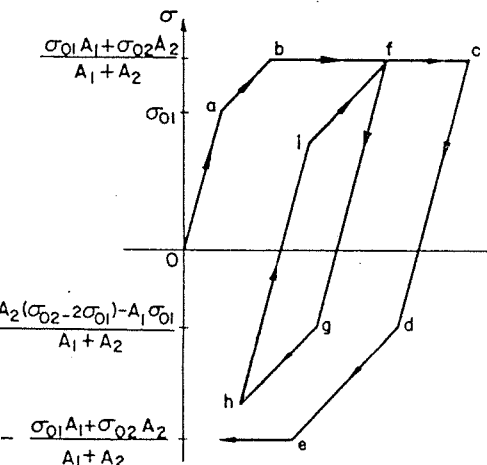


FIGURE 1.8. Loading and unloading characteristics of the overlay model.

EXAMPLE 1.2. The σ - ϵ response in simple tension for an elastic-linear hardening plastic material is approximated by the following expressions.

$$\sigma = \sigma_0 + m\epsilon^p \quad \text{for } \sigma \geq \sigma_0$$

$$\epsilon^p = \frac{\sigma}{E}$$

where $\sigma_0 = 207$ MPa, $E = 207$ GPa, and $m = 25.9$ GPa. A material sample is first stretched to a total strain $\epsilon = 0.007$, is subsequently returned to its initial strain-free state ($\epsilon = 0$) by continued compressive stressing, and then is unloaded and reloaded in tension again to reach the same strain $\epsilon = 0.007$ (see Fig. 1.9). Sketch the stress-strain curve for the following hardening rules: (i) isotropic hardening, (ii) kinematic hardening, (iii) independent acting tensile and compressive hardening.

SOLUTION. According to the definition of the plastic modulus in Eq. (1.7), we have

$$E_p = \frac{d\sigma}{d\epsilon^p} = m = 25,900 \text{ MPa}$$

and the tangent modulus E_t is found from Eq. (1.9) as

$$E_t = \frac{1}{\frac{1}{E} + \frac{1}{E_p}} = \frac{1}{\frac{1}{207,000} + \frac{1}{25,900}} = 23,020 \text{ MPa}$$

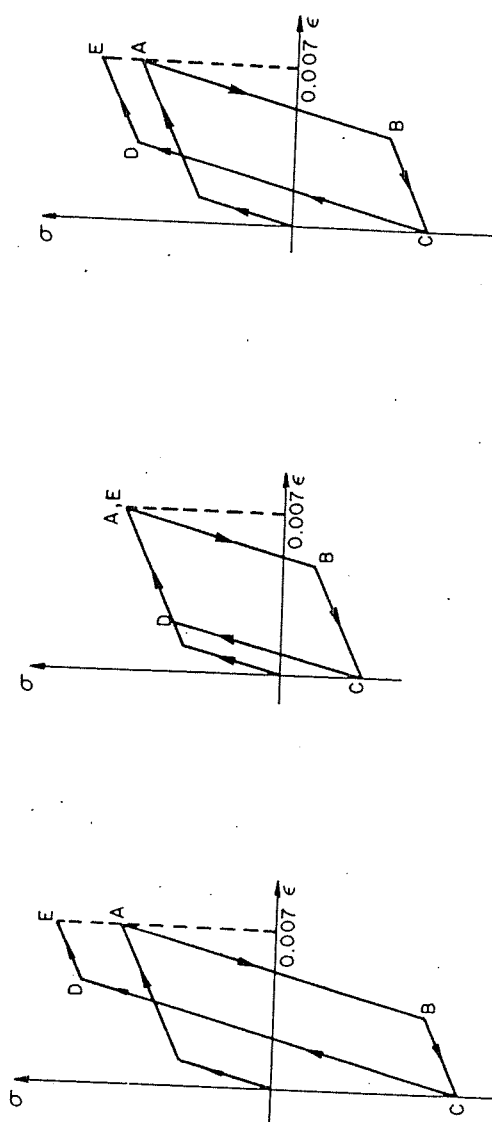


FIGURE 1.9. Stress-strain curve for a strain cycle $\epsilon = 0 \rightarrow 0.007 \rightarrow 0 \rightarrow 0.007$.

which assumes the constant value 23,020 MPa for the linear hardening material.

With the material sample stretching, yielding occurs at the point with strain

$$\epsilon = \frac{\sigma_0}{E} = 0.001$$

Then, the sample is further stretched to point *A* with strain $\epsilon = 0.007$, at which the stress σ_A is found as

$$\begin{aligned}\sigma_A &= \sigma_0 + \Delta\sigma \\ &= \sigma_0 + E_i \Delta\epsilon \\ &= 207 + 23,020(0.007 - 0.001) = 345 \text{ MPa}\end{aligned}$$

The subsequent stresses are determined for the three hardening rules as follows:

(i) *Isotropic hardening case* [Fig. 1.9(i)]: During unloading and reversed loading in compression, the sample behaves elastically until it yields again in compression at point *B*. According to the isotropic hardening rule, we have

$$\begin{aligned}\sigma_B &= -\sigma_A = -345 \text{ MPa} \\ \epsilon_B &= \epsilon_A - 2 \frac{\sigma_A}{E} = 0.007 - 2 \left(\frac{345}{207,000} \right) = 0.00367\end{aligned}$$

Now, the material sample is yielding until load reversal occurs at point *C* as $\epsilon = 0$.

$$\begin{aligned}\sigma_C &= \sigma_B + E_i \Delta\epsilon \\ &= -345 + 23,020(0 - 0.00367) = -429 \text{ MPa}\end{aligned}$$

Upon reversal of the straining, the material is elastic up to point *D* at which

$$\begin{aligned}\sigma_D &= 429 \text{ MPa} \\ \epsilon_D &= \epsilon_C + \frac{2\sigma_D}{E} = 0 + 2 \left(\frac{429}{207,000} \right) = 0.004145\end{aligned}$$

As the strain ϵ reaches 0.007 at point *E*, the stress is

$$\begin{aligned}\sigma_E &= \sigma_D + E_i \Delta\epsilon \\ &= 429 + 23,020(0.007 - 0.004145) \\ &= 495 \text{ MPa}\end{aligned}$$

(ii) *Kinematic hardening case* [Fig. 1.9(ii)]: The yield stress at point *B* is

$$\sigma_B = \sigma_A - 2\sigma_0 = 345 - 2(207) = -69 \text{ MPa}$$

$$\epsilon_B = \epsilon_A - 2 \frac{\sigma_0}{E} = 0.007 - 2 \left(\frac{207}{207,000} \right) = 0.005$$

At point *C*,

$$\begin{aligned} \sigma_C &= \sigma_B + E_t \Delta \epsilon \\ &= -69 + 23,020(0 - 0.005) = -184 \text{ MPa} \end{aligned}$$

At point *D*, the sample yields again in tension at a stress

$$\begin{aligned} \sigma_D &= \sigma_C + 2\sigma_0 \\ &= -184 + 2(207) = 230 \text{ MPa} \\ \epsilon_D &= \epsilon_C + \frac{2\sigma_0}{E} = 0 + 2 \left(\frac{207}{207,000} \right) = 0.002 \end{aligned}$$

At point *E*, the stress is

$$\begin{aligned} \sigma_E &= \sigma_D + E_t \Delta \epsilon \\ &= 230 + 23,020(0.007 - 0.002) = 345 \text{ MPa} \end{aligned}$$

(iii) *Independent hardening case* [Fig. 1.9(iii)]: Because the material has not yielded in compression before, the yield stress at point *B* is

$$\begin{aligned} \sigma_B &= -\sigma_0 = -207 \text{ MPa} \\ \epsilon_B &= \epsilon_A - \frac{\sigma_A}{E} - \frac{\sigma_0}{E} \\ &= 0.007 - \frac{345}{207,000} - \frac{207}{207,000} = 0.00433 \end{aligned}$$

At point *C*,

$$\begin{aligned} \sigma_C &= \sigma_B + E_t \Delta \epsilon \\ &= -207 + 23,020(0 - 0.00433) = -307 \text{ MPa} \end{aligned}$$

At point *D*, the material yields again in tension at a stress equal to σ_A , i.e.,

$$\begin{aligned} \sigma_D &= \sigma_A = 345 \text{ MPa} \\ \epsilon_D &= \epsilon_C - \frac{\sigma_C}{E} + \frac{\sigma_D}{E} = 0 - \frac{(-307)}{207,000} + \frac{345}{207,000} \\ &= 0.00315 \end{aligned}$$

At point *E*, the stress is

$$\begin{aligned} \sigma_E &= \sigma_D + E_t \Delta \epsilon \\ &= 345 + 23,020(0.007 - 0.00315) = 434 \text{ MPa} \end{aligned}$$

The stress-strain curves for each of the three cases are shown in Fig. 1.9.

EXAMPLE 1.3. Consider a nonlinear kinematic hardening material with a simple tension σ - ϵ curve obtained from a simple test in the form

$$\begin{aligned} \sigma &= \sigma_0 + m(\epsilon^p)^n & \text{for } \sigma \geq \sigma_0 \\ \sigma &= E\epsilon^e & \text{for } \sigma < \sigma_0 \end{aligned} \quad (1.31)$$

where $m = 500 \text{ MPa}$, $n = 0.3$, $E = 70,000 \text{ MPa}$, and $\sigma_0 = 200 \text{ MPa}$. Equation (1.31) represents the elastoplastic behavior of the material under the simple tension stress path. This relationship cannot be used directly for a general loading path other than the simple tension stress path. To generalize it, we shall follow the discussion in Section 1.4.3 and introduce a non-negative hardening parameter κ to represent the plastic deformation of the material under a general loading condition. The relationship between the hardening parameter κ and the plastic modulus E_p , Eq. (1.10), is assumed to be of the same form as Eq. (1.31). This strategy extends and generalizes the elastoplastic behavior of a material observed in a simple loading test to the general loading case. This is a basic strategy used frequently in the theory of plasticity.

A material element is first loaded to point *A* in tension at which $\sigma_A = 350 \text{ MPa}$, and is then unloaded and continuously loaded in compression. State *B* is the yield point in compression during reversed loading (Fig. 1.10).

- Find the expressions describing the σ - ϵ^p curve during plastically compressive loading starting from state *B* for hardening parameter κ defined as: case (i), $\kappa = \int (d\epsilon^p d\epsilon^p)^{1/2}$; case (ii), $\kappa = \epsilon^p$. Sketch the σ - ϵ^p curve.
- For κ defined as case (iii), $\kappa = W_p = \int \sigma d\epsilon^p$, sketch the σ - ϵ^p curve using a simple incremental procedure.

SOLUTION. (a) In the initial plastic tension range, $d\epsilon^p > 0$, so we have

$$\kappa = \int_0^{\epsilon^p} (d\epsilon^p d\epsilon^p)^{1/2} = \int_0^{\epsilon^p} d\epsilon^p = \epsilon^p$$

which takes the same form as case (ii). From the given σ - ϵ relation (1.31) for simple tension, the plastic modulus E_p can be expressed in terms of κ as

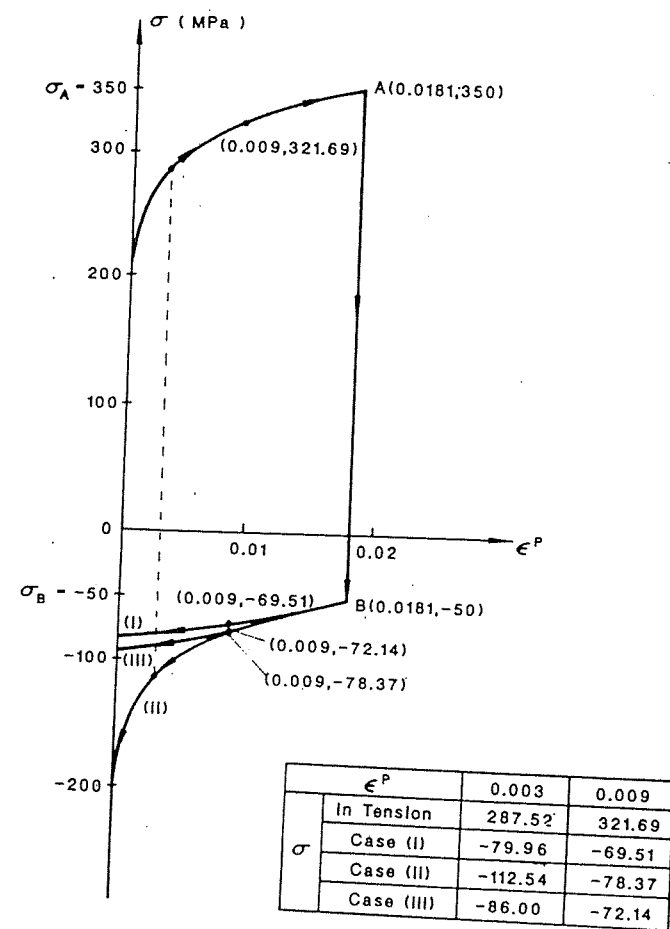
$$E_p = \frac{d\sigma}{d\epsilon^p} = mn(\epsilon^p)^{n-1} = mn\kappa^{n-1} \quad (1.32)$$

In the compressive loading range starting from point *B*, the hardening parameter κ for case (i) is the total accumulated plastic strain up to the current state ϵ^p :

$$\kappa = \epsilon_A^p + (\epsilon_A^p - \epsilon^p) = 2\epsilon_A^p - \epsilon^p \quad (1.33a)$$

and for case (ii), it is ϵ^p itself:

$$\kappa = \epsilon^p \quad (1.33b)$$

FIGURE 1.10. $\sigma-\epsilon^p$ relations for various definitions of κ .

The plastic modulus E_p is given by

$$E_p = mn\kappa^{n-1} = mn(2\epsilon_A^p - \epsilon^p)^{n-1} \quad \text{for case (i)} \quad (1.34a)$$

$$E_p = mn(\epsilon^p)^{n-1} \quad \text{for case (ii)} \quad (1.34b)$$

Hence, the $\sigma-\epsilon^p$ curve in this range can be found by

$$\sigma = \sigma_B + \int_{\epsilon_B^p}^{\epsilon^p} E_p d\epsilon^p \quad (1.35)$$

Substituting Eq. (1.34) for E_p and noting that $\sigma_B = \sigma_A - 2\sigma_0$ and $\epsilon_B^p = \epsilon_A^p$, carrying out the integration leads to

$$\sigma = -m(2\epsilon_A^p - \epsilon^p)^n + m(\epsilon_A^p)^n + \sigma_A - 2\sigma_0 \quad \text{for case (i)} \quad (1.36a)$$

and

$$\sigma = m[(\epsilon^p)^n - (\epsilon_A^p)^n] + \sigma_A - 2\sigma_0 \quad \text{for case (ii)} \quad (1.36b)$$

At point A, the stress σ_A is already given as $\sigma_A = 350$ MPa, so the strain can easily be determined by Eq. (1.31) as

$$\epsilon_A^p = 0.0181$$

Substituting the values of m , n , σ_0 , σ_A , and ϵ_A^p into Eqs. (1.36a) and (1.36b) leads to

$$\sigma = -500(0.0362 - \epsilon^p)^{0.3} + 100.06 \quad \text{for case (i)} \quad (1.37a)$$

$$\sigma = 500(\epsilon^p)^{0.3} - 200.06 \quad \text{for case (ii)} \quad (1.37b)$$

The $\sigma-\epsilon^p$ curves for cases (i) and (ii) are sketched in Fig. 1.10.

(b) For case (iii), the hardening parameter κ is defined by W_p , and according to assumption (1.10), the plastic modulus is now a function of W_p , i.e.,

$$E_p = E_p(W_p) \quad (1.38)$$

From the given $\sigma-\epsilon$ relation (1.31), W_p is given by

$$\begin{aligned} W_p &= \int \sigma d\epsilon^p \\ &= \int_0^{\epsilon^p} [\sigma_0 + m(\epsilon^p)^n] d\epsilon^p \\ &= \sigma_0 \epsilon^p + \frac{m}{n+1} (\epsilon^p)^{n+1} \end{aligned} \quad (1.39a)$$

From Eq. (1.31) also we have

$$E_p = mn(\epsilon^p)^{n-1} \quad (1.39b)$$

The relationship (1.38) is now established from Eqs. (1.39a) and (1.39b) by canceling out the variable ϵ_p .

In the compressive loading range starting from point B, there is no explicit expression for $E_p = E(W_p)$. Thus, the $\sigma-\epsilon^p$ curve cannot be found by direct integration; we can only use the incremental procedure to find the $\sigma-\epsilon^p$ relation numerically. The steps in the calculation are the following:

1. Calculate σ , ϵ^p , W_p , and E_p at the starting point B.
2. Take the plastic strain increment $d\epsilon^p = -0.0015$ (first increment, -0.0016).

TABLE 1.1. Calculation of $\sigma-\epsilon^p$ relation by simple incremental procedure for case (iii) in Example 1.3.

σ	ϵ^p	W_p	E_p	\dot{W}_p	$\dot{\sigma}$
-50.00	0.0181	5.709	2487.23	0.0800	-3.980
-53.98	0.0165	5.789	2465.35	0.0810	-3.698
-57.68	0.0150	5.870	2443.93	0.0865	-3.666
-61.34	0.0135	5.957	2421.14	0.0920	-3.632
-64.98	0.0120	6.049	2397.99	0.0975	-3.597
-68.57	0.0105	6.146	2374.50	0.1029	-3.562
-72.13	0.0090	6.249	2349.89	0.1082	-3.525
-75.66	0.0075	6.357	2324.26	0.1135	-3.486
-79.15	0.0060	6.471	2298.50	0.1187	-3.448
-82.59	0.0045	6.590	2272.65	0.1239	-3.409
-86.00	0.0030	6.713	2245.99	0.1290	-3.369
-89.37	0.0015	6.842	2219.35	0.1341	-3.329
-92.70	0.0000	6.977	2192.04	0.1391	-3.288

3. Calculate the stress increment $d\sigma = E_p d\epsilon^p$ and the plastic work increment $dW_p = \sigma d\epsilon^p$.
4. Update stress, plastic strain, and plastic work by adding up the corresponding increments: $\sigma + d\sigma$, $\epsilon^p + d\epsilon^p$, $W_p + dW_p$.
5. Update plastic modulus E_p by solving Eq. (1.39a) for ϵ^p , then substituting ϵ^p so obtained into Eq. (1.39b) to find E_p . Note here that ϵ^p is not the current plastic strain.
6. Go to step 2.

The results of this calculation are given in Table 1.1 and the corresponding $\sigma-\epsilon^p$ curve is shown in Fig. 1.10.

1.5. Index Notation

Because index notation allows a drastic reduction in the number of terms in an expression or equation and the simplification of the general formulation to a great extent, it is commonly used in the current literature when stress, strain, and constitutive equations are discussed. A basic knowledge of these notations is therefore essential in studying plasticity theory and constitutive modeling of materials. With such notations, the various stress-strain relationships can be expressed in a compact form, thereby allowing greater attention to be paid to physical principles rather than to the equations themselves.

1.5.1. Indicial Notation and Summation Convention

For the present, we restrict ourselves to right-handed Cartesian coordinate systems. In a three-dimensional space, a right-handed Cartesian coordinate system is pictured as a set of three mutually orthogonal axes denoted as the x -, y -, and z -axes. For future convenience, the axes are more conveniently designated as x_1 -, x_2 -, and x_3 -axes, rather than the more familiar notation x , y , and z . The sketch shown in Fig. 1.11 is based on the right-handed notation, where the x_2 - and x_3 -axes lie in the plane of the paper and the x_1 -axis is directed towards the reader.

1.5.1.1. INDICIAL NOTATION

In this coordinate system, a vector \mathbf{V} is denoted as

$$\mathbf{V} = (v_1, v_2, v_3) = v_1 \mathbf{e}_1 + v_2 \mathbf{e}_2 + v_3 \mathbf{e}_3 \quad (1.40)$$

where \mathbf{e}_1 , \mathbf{e}_2 , and \mathbf{e}_3 are unit vectors as shown in Fig. 1.11, and v_1 , v_2 , and v_3 are three components of the vector. It is useful to abbreviate the latter by a single component with a generalized index. Thus, in the *indicial notation*, v_i represents the components of vector \mathbf{V} . It is implicitly understood that the index i ranges in value from 1 to 3 when v_i is written for \mathbf{V} .

As an example, the statement $x_i = 0$ implies that each of the components x_1 , x_2 , x_3 of the vector \mathbf{X} is zero, or \mathbf{X} is a null vector. Similarly,

$$f(\mathbf{X}) = f(x_i) = f(x_j) = f(x_1, x_2, x_3) \quad (1.41)$$

The index may be freely chosen. Hence, x_i and x_j represent one and the same vector.

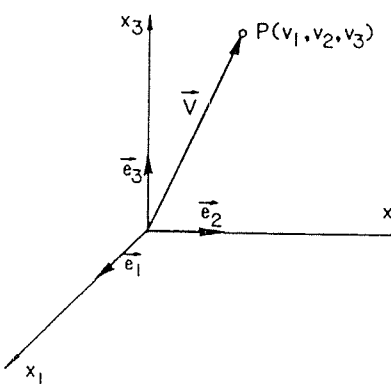


FIGURE 1.11. Right-handed Cartesian coordinate system.

1.5.1.2. SUMMATION CONVENTION

The *summation convention* is complementary to the indicial notation and allows for further brevity when dealing with summations. We adopt the following convention: whenever a subscript occurs twice in the same term, it is understood that the subscript is to be summed from 1 to 3. Consider, for example, the dot product of two vectors, \mathbf{U} and \mathbf{V} . It has the form

$$\mathbf{U} \cdot \mathbf{V} = u_1 v_1 + u_2 v_2 + u_3 v_3 = \sum_{i=1}^3 u_i v_i \quad (1.42)$$

The expression on the far right may be abbreviated as $u_i v_i$ since the summation always involves three components. The summation convention requires that the index i be repeated, but eliminates the use of the summation symbol Σ . Again, however, the index itself may be freely chosen. Thus, $u_i v_i$ and $u_k v_k$ represent the same sum, $u_1 v_1 + u_2 v_2 + u_3 v_3$. Such repeated subscripts are often called *dummy* subscripts because of the fact that the particular letter used in the subscript is not important; thus, $u_i v_i = u_k v_k$.

In this context, it is necessary to point out that $u_i + v_i$ represents a vector sum, say, w_i , but not a scalar sum of any kind. Explicitly, the following equation is true:

$$(w_1, w_2, w_3) = (u_1 + v_1, u_2 + v_2, u_3 + v_3) \quad (1.43)$$

but the following form is incorrect:

$$u_i + v_i = u_1 + v_1 + u_2 + v_2 + u_3 + v_3 \quad (1.44)$$

Further, the index in a term of an equation or expression should occur only twice in this same term for the summation convention to be valid. An expression such as $u_i v_{ii}$ conveys no special sense.

The effectiveness of the convention is more apparent when it is applied to a set of three simultaneous equations. Consider the set

$$\begin{aligned} a_{11}x_1 + a_{12}x_2 + a_{13}x_3 &= b_1 \\ a_{21}x_1 + a_{22}x_2 + a_{23}x_3 &= b_2 \\ a_{31}x_1 + a_{32}x_2 + a_{33}x_3 &= b_3 \end{aligned} \quad (1.45)$$

As a first stage in abbreviation, these may be written as

$$\begin{aligned} a_{1j}x_j &= b_1 \\ a_{2j}x_j &= b_2 \\ a_{3j}x_j &= b_3 \end{aligned} \quad (1.46)$$

and, in the final stage, as

$$a_{ij}x_j = b_i \quad (1.47)$$

In the first stage, the index j assumes the values 1 to 3 and summation is understood on the left-hand side of the equations since the index is repeated. As mentioned before, the repeated index is referred to as a *dummy* index quite often because the choice of the letter for the index is immaterial. The three equations of the first stage may be represented as in the final stage by the use of the *free* index i . To be consistent, it is necessary to use the same index i on both sides of the equation. The existence of one free index indicates that vectors are involved. Later, it will be seen that when two free indices appear, tensors are involved.

Based on the previous discussion, the simultaneous equations (1.45) may also be written as

$$a_{rs}x_s = b_r \quad (1.48)$$

As a review, equivalent vector and indicial (or component) forms are presented in Table 1.2 for study.

The divergence of vector \mathbf{V} is $\nabla \cdot \mathbf{V}$ or the scalar sum

$$\nabla \cdot \mathbf{V} = \frac{\partial v_1}{\partial x_1} + \frac{\partial v_2}{\partial x_2} + \frac{\partial v_3}{\partial x_3} \quad (1.49)$$

In the summation convention,

$$\nabla \cdot \mathbf{V} = \frac{\partial v_i}{\partial x_i} \quad (1.50)$$

where i is a dummy index.

The conventions regarding subscripts described above can now be summarized as a set of three rules:

Rule 1: If a subscript occurs precisely *once* in one term of an expression or equation, it is called a "*free index*." This must occur precisely once in each term of the expression or equation.

Rule 2: If a subscript occurs precisely *twice* in one term of an expression or equation, it is called a "*dummy index*." It is to be summed from 1 to 3. The dummy index may or may not occur precisely twice in any other term.

Rule 3: If a subscript occurs more than twice in one term of an expression or equation, it is a *mistake*.

TABLE 1.2. Equivalent vector and indicial notation.

Vector	Components	Indicial notation
\mathbf{V}	(v_1, v_2, v_3)	v_i
$\mathbf{U} + \mathbf{V}$	$(u_1 + v_1, u_2 + v_2, u_3 + v_3)$	$u_i + v_i$
$\nabla \phi$	$\left(\frac{\partial \phi}{\partial x_1}, \frac{\partial \phi}{\partial x_2}, \frac{\partial \phi}{\partial x_3} \right)$	$\frac{\partial \phi}{\partial x_i}$

1.5.1.3. DIFFERENTIATION NOTATION

In subscript notation, we use a *comma* to indicate differentiation; thus, for example, the partial derivative form of Eq. (1.50) can be further simplified to the form $v_{i,i}$. The first subscript refers to the component of \mathbf{V} , and the *comma* indicates the partial derivative with respect to the second subscript corresponding to the relevant coordinate axis. Thus

$$v_{i,i} = v_{1,1} + v_{2,2} + v_{3,3} \quad (1.51)$$

and the gradient of ϕ is conveniently written in the form $\phi_{,i}$, which indicates clearly the vector character of the gradient of ϕ . The divergence of $\nabla\phi$ would be written as $\phi_{,ii} = \phi_{,11} + \phi_{,22} + \phi_{,33}$. It is a scalar, known as the Laplacian of ϕ , and is often denoted by $\nabla^2\phi = \nabla \cdot \nabla\phi$.

1.5.2. The Symbol δ_{ij} (Kronecker Delta)

The *Kronecker delta* is a special matrix, denoted as δ_{ij} :

$$\delta_{ij} = \begin{bmatrix} 1 & 0 & 0 \\ 0 & 1 & 0 \\ 0 & 0 & 1 \end{bmatrix} \quad (1.52)$$

Thus, the components of δ_{ij} are 1 if $i=j$, and 0 if $i \neq j$:

$$\delta_{11} = \delta_{22} = \delta_{33} = 1 \quad (1.53)$$

$$\delta_{12} = \delta_{21} = \delta_{13} = \delta_{31} = \delta_{23} = \delta_{32} = 0 \quad (1.54)$$

Further, the δ_{ij} matrix is symmetric since $\delta_{ij} = \delta_{ji}$. Note that, because of the summation convention,

$$\delta_{jj} = \delta_{11} + \delta_{22} + \delta_{33} = 3 \quad (1.55)$$

The Kronecker delta may be regarded as an operator and serves a useful function when so used. Consider, for example, the projection $\delta_{ij}v_j$. According to the summation convention, this yields an expansion of the vector

$$\delta_{i1}v_1 + \delta_{i2}v_2 + \delta_{i3}v_3 \text{ or } v_i \quad (1.56)$$

This can be easily verified since on assigning values 1, 2, and 3 to i , the components obtained are v_1 , v_2 , and v_3 . Hence,

$$\delta_{ij}v_j = v_i \quad (1.57)$$

This final answer may be visualized as the result of substituting i for j (or j for i , if need be) in the quantity operated on (by the operator δ_{ij}). It appears, therefore, that the application of δ_{ij} to v_j has merely substituted i for j in v_j ; the δ_{ij} symbol is therefore often called a *substitution operator*.

As another example, $\delta_{ij}\delta_{ji}$ represents a scalar sum in the summation convention. Using the concept of substitution operator,

$$\delta_{ij}\delta_{ji} = \delta_{ii} = \delta_{11} + \delta_{22} + \delta_{33} = 3 \quad (1.58)$$

Similarly,

$$\delta_{ij}a_{ji} = a_{ii} = a_{11} + a_{22} + a_{33} \quad (1.59)$$

Finally, noting that the dot product $\mathbf{e}_i \cdot \mathbf{e}_j$ is 1 if $i=j$ and 0 if $i \neq j$, then matching the components of δ_{ij} , we can write

$$\mathbf{e}_i \cdot \mathbf{e}_j = \delta_{ij} \quad (1.60)$$

1.5.3. Transformation of Coordinates

1.5.3.1. DIRECTION COSINES

The values of the components of a vector \mathbf{V} , designated by v_1 , v_2 , v_3 or simply v_i , are associated with the chosen set of coordinate axes. Often it is necessary to reorient the reference axes and evaluate the new values for the components of \mathbf{V} in the new coordinate system.

Let x_i and x'_i be two sets of right-handed Cartesian coordinate systems having the same origin. Vector \mathbf{V} , then, has components v_i and v'_i in the two systems. Since the vector is the same, the components must be related through the cosines of the angles between the positive x'_i - and x_i -axes.

If l_{ij} represents $\cos(x'_i, x_j)$, that is, the cosines of the angles between x'_i and x_j axes for i and j ranging from 1 to 3, it can be shown as follows that $v'_i = l_{ij}v_j$. These cosines may be conveniently tabulated as in Table 1.3. It should be noted that the elements of l_{ij} (a matrix) are not symmetrical, $l_{ij} \neq l_{ji}$. For example, l_{12} is the cosine of the angle between x'_1 and x_2 and l_{21} is that between x'_2 and x_1 (see Fig. 1.12). The angle is assumed to be measured from the primed system to the unprimed system.

1.5.3.2. RELATION BETWEEN THE l_{ij}

From the definition of l_{ij} , we know

$$l_{ij} = \mathbf{e}'_i \cdot \mathbf{e}_j \quad (1.61)$$

TABLE 1.3. Direction cosines (l_{ij}).

Axis	Axis		
	x_1	x_2	x_3
x'_1	l_{11}	l_{12}	l_{13}
x'_2	l_{21}	l_{22}	l_{23}
x'_3	l_{31}	l_{32}	l_{33}

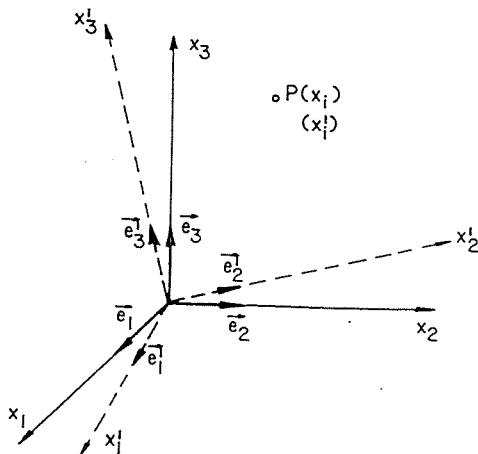


FIGURE 1.12. Transformation of coordinates.

The base (or unit) vector e'_i may be expressed, in reference to the x_i -axes, as

$$\begin{aligned} e'_i &= (e'_i \cdot e_1)e_1 + (e'_i \cdot e_2)e_2 + (e'_i \cdot e_3)e_3 \\ &= l_{i1}e_1 + l_{i2}e_2 + l_{i3}e_3 = l_{ij}e_j \end{aligned} \quad (1.62)$$

Conversely,

$$e_i = l_{ji}e'_j \quad (1.63)$$

Hence,

$$e'_i \cdot e'_j = \delta_{ij} = l_{ir}e_r \cdot l_{jr}e_k = l_{ir}l_{jk}\delta_{rk} = l_{ir}l_{jr} \quad (1.64)$$

or

$$l_{ir}l_{jr} = \delta_{ij} \quad (1.65)$$

which implies the following six equations:

$$\begin{aligned} l_{11}^2 + l_{12}^2 + l_{13}^2 &= 1 \\ l_{21}^2 + l_{22}^2 + l_{23}^2 &= 1 \\ l_{31}^2 + l_{32}^2 + l_{33}^2 &= 1 \\ l_{11}l_{21} + l_{12}l_{22} + l_{13}l_{23} &= 0 \\ l_{11}l_{31} + l_{12}l_{32} + l_{13}l_{33} &= 0 \\ l_{21}l_{31} + l_{22}l_{32} + l_{23}l_{33} &= 0 \end{aligned} \quad (1.66)$$

Similarly,

$$e_i \cdot e_j = \delta_{ij} = l_{ri}e'_r \cdot l_{kj}e'_k = l_{ri}l_{kj}\delta_{rk} = l_{ri}l_{rj} \quad (1.67)$$

or

$$l_{ri}l_{rj} = \delta_{ij} \quad (1.68)$$

The arbitrary vector V can be expressed either in the form $v_i e_i$ or $v'_i e'_i$:

$$v'_i = V \cdot e'_i = v_j e_j \cdot e'_i = v_j e_j \cdot l_{ik}e_k = l_{ik}v_j \delta_{jk} = l_{ij}v_i \quad (1.69)$$

or

$$v'_i = l_{ij}v_j \quad (1.70)$$

Conversely,

$$v_i = V \cdot e_i = v'_j e'_j \cdot l_{ri}e'_r = l_{ri}v'_j \delta_{jr} = l_{ji}v'_j \quad (1.71)$$

or

$$v_i = l_{ji}v'_j \quad (1.72)$$

In a similar manner, if the point P (Fig. 1.12) has coordinates x_i in the unprimed system and x'_i in the primed system, then

$$x'_i = l_{ij}x_j \quad \text{and} \quad x_i = l_{ji}x'_j \quad (1.73)$$

It follows that

$$l_{ij} = \frac{\partial x'_i}{\partial x_j} = \frac{\partial x_j}{\partial x'_i} \quad (1.74)$$

EXAMPLE 1.4. Table 1.4 gives the direction cosines (l_{ij}) for the x_i and x'_i coordinate systems. Show that the point $(0, 1, -1)$ in the x_i system coincides with the point $(-\frac{29}{25}, \frac{4}{5}, -\frac{3}{25})$ in the x'_i system.

TABLE 1.4. Direction cosines (l_{ij}) for Example 1.4.

Axis	Axis		
	x_1	x_2	x_3
x'_1	$\frac{12}{25}$	$-\frac{9}{25}$	$\frac{4}{5}$
x'_2	$\frac{3}{5}$	$\frac{4}{5}$	0
x'_3	$-\frac{16}{25}$	$\frac{12}{25}$	$\frac{3}{5}$

SOLUTION. The relations between the coordinates of the point in the two coordinate systems x_i and x'_i are given by [Eq. (1.73)]

$$x'_i = l_{ij}x_j$$

where $x_j = (0, 1, -1)$. Hence, the x'_i coordinates of the point can be calculated. For $i = 1$,

$$x'_1 = l_{1j}x_j$$

Substituting from Table 1.4, we obtain

$$\begin{aligned} x'_1 &= l_{11}x_1 + l_{12}x_2 + l_{13}x_3 \\ &= \left(\frac{12}{25}\right)(0) + \left(-\frac{9}{25}\right)(1) + \left(\frac{4}{5}\right)(-1) \\ &= -\frac{29}{25} \end{aligned}$$

Similarly,

$$x'_2 = l_{2j}x_j = l_{21}x_1 + l_{22}x_2 + l_{23}x_3$$

and

$$x'_3 = l_{3j}x_j = l_{31}x_1 + l_{32}x_2 + l_{33}x_3$$

which upon substituting from Table 1.4 give

$$x'_2 = \frac{4}{5} \quad \text{and} \quad x'_3 = -\frac{3}{25}$$

Therefore, the point $(0, 1, -1)$ in the x_i system coincides with the point $(-\frac{29}{25}, \frac{4}{5}, -\frac{3}{25})$ in the x'_i system.

1.5.4. Definition of Cartesian Tensors

In the preceding section, we proved that a vector at any point in a space is completely determined by a knowledge of its three components. If we know the components of a vector v_i in the x_i coordinate system, then the components of the same vector in the x'_i coordinate system can be obtained by the transformation $v'_i = l_{ij}v_j$. This transformation equation holds for any vector, whether it is a physical quantity such as velocity or force, a geometric quantity such as a radius vector from the origin, or a less easily visualized quantity such as the gradient of a scalar. For example, if

$$G_i = \frac{\partial \phi}{\partial x_i} \quad (1.75)$$

then

$$G'_i = \frac{\partial \phi}{\partial x'_i} = \frac{\partial \phi}{\partial x_k} \frac{\partial x_k}{\partial x'_i} = l_{ik}G_k \quad (1.76)$$

The foregoing transformation rule, in which each new vector component in a new coordinate system is a linear combination of the old components, is very convenient and of considerable use. In the following, we adopt it as the definition of a vector, thus replacing the previous definition of a vector as a quantity possessing direction and magnitude. The basic reason for adopting this new definition of a vector is that it can be easily generalized to apply to more complicated physical quantities called *tensors* whereas the "magnitude and direction" definition cannot.

In the following, we first define a *tensor* of the first order to be a set of three quantities (called its components) possessing the property that if their values at a fixed point in any coordinate system x_i are v_i , then their values at this point in any other coordinate system x'_i are given by the relationship $v'_i = l_{ij}v_j$. An equivalent statement is, of course, $v_i = l_{ji}v'_j$. Since all vectors transform according to this law, vectors are tensors of the first order. A scalar, such as temperature, has the same value irrespective of the coordinate system used to specify it at a point, and hence a scalar is unaffected by transformations and is defined as a tensor of order zero. A *first-order tensor* (or a vector) is a set of $3^1 = 3$ components, and a *zero-order tensor* (or a scalar) is a set of $3^0 = 1$ component.

The definition is now extended to higher-order tensors similarly. A *second-order tensor* is defined as a set of $3^2 = 9$ components, such that if their values at a given point are a_{ij} in a coordinate system x_i , their values a'_{ij} at the same point in any other coordinate system x'_i are given by

$$a'_{ij} = l_{im}l_{jn}a_{mn} \quad (1.77)$$

A second-order tensor may be interpreted to be defined completely by three vectors just as a vector is completely defined by three scalars. It will subsequently appear that the quantities expressing the state of stress at a point in a body form a second-order tensor. In other words, the state of stress at a point is completely defined by three *stress vectors*.

A *third-order tensor* is a set of $3^3 = 27$ components, such that if their values at a given point are a_{ijk} in a coordinate system x_i , their values a'_{ijk} in any other coordinate system x'_i are given by

$$a'_{ijk} = l_{im}l_{jn}l_{kp}a_{mnp} \quad (1.78)$$

Tensors may be of any order; the general transformation equation is evident from the previous definitions. All such tensors are called *Cartesian tensors* because of the restriction to Cartesian coordinate systems.

As an example, suppose that the nine "components" of a second-order tensor are known:

$$a_{11} = 1, \quad a_{12} = -1, \quad a_{32} = 2, \quad \text{all other } a_{ij} = 0$$

in the coordinate system x_i . Consider a new coordinate system x'_i , related to the x_i system by the direction cosines (l_{ij}) table given below:

New axis	Old axis		
	x_1	x_2	x_3
x'_1	$\frac{1}{\sqrt{2}}$	$\frac{1}{\sqrt{2}}$	0
x'_2	$\frac{-1}{\sqrt{2}}$	$\frac{1}{\sqrt{2}}$	0
x'_3	0	0	1

The new components a'_{ij} in the x'_i system are then given by

$$\begin{aligned} a'_{11} &= l_{1k} l_{1r} a_{kr} \\ &= l_{11} l_{11} a_{11} + l_{11} l_{12} a_{12} + l_{13} l_{12} a_{32} + 0 \\ &= \frac{1}{2}(1) + \frac{1}{2}(-1) + 0 = 0 \end{aligned} \quad (1.79)$$

Similarly, $a'_{12} = -1$, $a'_{32} = \sqrt{2}$, and so on.

1.5.5. Properties of Tensors

Operations on tensors parallel those on vectors.

1.5.5.1. EQUALITY

Two tensors A and B are defined to be equal when their respective components are equal. For example, the condition for equality of tensors a_{ij} and b_{ij} is that

$$a_{ij} = b_{ij} \quad (1.80)$$

1.5.5.2. ADDITION

The sum or difference of two tensors of the same order is a tensor, also of the same order, which is defined by adding or subtracting the corresponding components of the two tensors. For example, if two second-order tensors a_{ij} and b_{ij} are added, the resulting nine quantities c_{ij} also comprise a second-order tensor defined by

$$c_{ij} = a_{ij} + b_{ij} \quad (1.81)$$

It is obvious that the sum or difference of two tensors of different order cannot be defined.

1.5.5.3. TENSOR EQUATIONS

As previously mentioned, a tensor equation that is true in one coordinate system is true in all systems, for if two tensors satisfy $a_{ij} = b_{ij}$ in the x_i

system, we can define $c_{ij} = a_{ij} - b_{ij}$ in all systems. Then, by the preceding reasoning that the difference of two tensors of the same order is a tensor, also of the same order, it follows that c_{ij} is a tensor of second order. Now, c_{ij} vanishes in the x_i system, and hence in all systems. This can also be seen easily from the fact that c'_{ij} in any system is a linear combination of the c_{ij} .

1.5.5.4. MULTIPLICATION

Multiplication of a tensor a_{ij} by a scalar quantity α yields a tensor b_{ij} of the same order:

$$b_{ij} = \alpha a_{ij} \quad (1.82)$$

Consider the two tensors a_i of order one and b_{ij} of order two. We may define a new set of quantities c_{ijk} by a process called tensor multiplication:

$$c_{ijk} = a_i b_{jk} \quad (1.83)$$

It is, of course, understood that a similar rule of definition is to be used in other coordinate systems.

$$\begin{aligned} c'_{ijk} &= a'_i b'_{jk} \\ &= (l_{im} a_m)(l_{jn} l_{ko} b_{no}) \\ &= l_{im} l_{jn} l_{ko} a_m b_{no} \\ &= l_{im} l_{jn} l_{ko} c_{mno} \end{aligned} \quad (1.84)$$

It follows from Eq. (1.84) that c_{ijk} is a third-order tensor. In general, tensor multiplication yields a new tensor whose order is the sum of the orders of the original tensors.

1.5.5.5. CONTRACTION

Consider the tensor a_{ijk} —a set of 27 quantities. If we give two indices the same letter, say, replacing the j by a k , resulting in a_{ikk} , then only three quantities remain, each being the sum of three of the original components. It is easy to show that this set of three quantities is a first-order tensor. For the third-order tensor a_{ijk} , we have

$$a'_{ijk} = l_{ip} l_{jq} l_{kr} a_{pqr}$$

and therefore

$$\begin{aligned} a'_{ikk} &= l_{ip} (l_{kq} l_{kr}) a_{pqr} \\ &= l_{ip} \delta_{qr} a_{pqr} \\ &= l_{ip} a_{prr} \end{aligned} \quad (1.85)$$

which is the transformation rule for the first-order tensor; that is, a_{ikk} is a first-order tensor.

TABLE 1.5. Examples of tensor properties.

Tensor	Order	Remarks
$u_i + v_i$	1	Addition
cd	0	Multiplication
cu_i	1	Multiplication
$u_i v_j$	2	Multiplication
$u_i a_{jk}$	3	Multiplication
$u_i v_i$	0	Scalar (or dot) product (Length) ²
$u_i u_i$	0	
$a_{ii} = a_{11} + a_{22} + a_{33}$	0	First invariant of a_{ij}
$u_i a_{rk}$	1	Contraction
$u_{,j}$	2	Differentiation
$u_{,i} = u_{1,1} + u_{2,2} + u_{3,3}$	0	Divergence, $\nabla \cdot U$

1.5.5.6. EXAMPLES

Suppose that c and d are scalars, u_i or v_i are the three components of a vector, and a_{ij} are the nine components of a second-order tensor. Then we have the results given in Table 1.5.

1.5.6. Isotropic Tensors

A tensor is isotropic if its components have the same value in all coordinate systems. A scalar (tensor of order zero) is a simple example. The tensor δ_{ij} is isotropic. For δ_{ij} , the transformation rule yields

$$\delta'_{ij} = l_{ir} l_{js} \delta_{rs} = l_{ir} l_{jr} = \delta_{ij} \quad (1.86)$$

which is the definition for the second-order isotropic tensor.

It can be shown that any second-order isotropic tensor must be of the form of a constant times δ_{ij} , and the most general fourth-order isotropic tensor has the form:

$$a_{ijkl} = \alpha \delta_{ij} \delta_{kl} + \beta \delta_{ik} \delta_{jl} + \gamma \delta_{il} \delta_{jk} \quad (1.87)$$

EXAMPLE 1.5. If ϕ is a scalar, show the following:

- (a) $\phi_{,i}$ is a first-order tensor.
- (b) $\phi_{,ij}$ is a second-order tensor.
- (c) $\phi_{,kk}$ is a scalar (zero-order tensor).

SOLUTION. Since ϕ is a scalar,

$$\phi(\text{in } x_i \text{ system}) = \phi'(\text{in } x'_i \text{ system}) \quad (1.88)$$

(a) Define

$$G_i = \frac{\partial \phi}{\partial x_i} = \phi_{,i} \quad (1.89)$$

Thus,

$$G'_i = \frac{\partial \phi'}{\partial x'_i} = \frac{\partial \phi}{\partial x'_i} = \frac{\partial \phi}{\partial x_j} \frac{\partial x_j}{\partial x'_i} \quad (1.90)$$

From Eqs. (1.74) and (1.90),

$$G'_i = l_{ij} G_j$$

or

$$\phi'_{,i} = l_{ij} \phi_{,j} \quad (i \text{ is a free index}) \quad (1.91)$$

Hence $\phi_{,i}$ is a first-order tensor.

(b) Define

$$c_{ij} = \frac{\partial^2 \phi}{\partial x_i \partial x_j} = \phi_{,ij} \quad (1.92)$$

Thus,

$$c'_{ij} = \frac{\partial^2 \phi'}{\partial x'_i \partial x'_j} = \frac{\partial}{\partial x'_i} \left(\frac{\partial \phi}{\partial x_k} \frac{\partial x_k}{\partial x'_j} \right)$$

or

$$\begin{aligned} c'_{ij} &= \frac{\partial}{\partial x'_i} \left(\frac{\partial \phi}{\partial x_k} l_{jk} \right) \\ &= \frac{\partial}{\partial x_m} \left(\frac{\partial \phi}{\partial x_k} l_{jk} \right) \frac{\partial x_m}{\partial x'_i} \end{aligned}$$

Hence,

$$c'_{ij} = \frac{\partial^2 \phi}{\partial x_m \partial x_k} l_{jk} l_{im} \quad (1.93)$$

or, using Eqs. (1.92) and (1.93), we get

$$\phi'_{,ij} = l_{im} l_{jk} \phi_{,mk} \quad (1.94)$$

That is, $\phi_{,ij}$ is a second-order tensor.

(c) Replacing subscript j by i in Eq. (1.94), we have

$$\phi'_{,ii} = l_{im} l_{ik} \phi_{,mk} \quad (1.95)$$

But from Eq. (1.65)

$$l_{im} l_{ik} = \delta_{mk} \quad (1.96)$$

Substituting Eq. (1.95) into Eq. (1.96), we get

$$\phi'_{,ii} = \delta_{mk} \phi_{,mk}$$

or

$$\phi'_{,ii} = \phi_{,mm}$$

Hence, $\phi_{,ii}$ is a scalar (zero-order tensor).

1.6. Summary

The theory of plasticity is concerned with the analysis of stresses and strains in the plastic range of ductile materials, especially metals. This chapter introduced the fundamental concepts of plasticity theory by discussing the uniaxial stress-strain behavior of metals. Important concepts, such as elastic deformation, plastic deformation, yielding, plastic flow, hardening, softening, and the Bauschinger effect for reversed loading have all been illustrated. The most significant feature of plastic deformation is its *irreversibility* and *load path dependence*. For a hardening material, a hardening parameter relating to plastic work or plastic strain was introduced to record the history of loading. The plastic modulus is then related to this hardening parameter. The general characteristics of materials discussed in this chapter in terms of the uniaxial stress-strain behavior of metals can be used in the later chapters to extract rather far-reaching information regarding the two-dimensional and three-dimensional stress-strain relations of materials in general and metals and concretes in particular.

The relationship between stress and strain in general loading cases characterizing the properties of a material is generally referred to in the open literature as the *constitutive relation*. The following chapters are concerned with the general techniques used in the necessary extension of stress-strain behavior in uniaxial conditions to the three-dimensional situation. Generally, six stress components and six strain components are involved in constitutive equations. To simplify the mathematical expressions, we shall use index notations. A concise introduction to tensor notations in preparation for the subsequent discussion has also been given in this chapter.

References

- Chen, W.F., and G.Y. Baladi, 1985. *Soil Plasticity: Theory and Implementation*, Elsevier, Amsterdam, The Netherlands.
- Chen, W.F., 1982. *Plasticity in Reinforced Concrete*, McGraw-Hill, New York.
- Chen, W.F., and A.F. Saleeb, 1982. *Constitutive Equations for Engineering Materials, Volume 1: Elasticity and Modeling*, Wiley-Interscience, New York.

PROBLEMS

- 1.1. The σ - ϵ response in simple tension for a material is approximated by the following form of the Ramberg-Osgood formula

$$\epsilon = \epsilon^r + \epsilon^p = \frac{\sigma}{E} + \left(\frac{\sigma}{b}\right)^n$$

- (a) Find the tangent modulus E_t and the plastic modulus E_p as functions of stress σ and of plastic strain ϵ^p .
- (b) Find the plastic work W_p as a function of stress σ and of plastic strain ϵ^p .
- (c) Express the stress σ and the plastic modulus E_p in terms of the plastic work W_p .
- (d) What is the initial yield stress?

- (e) Assuming $n = 1$, sketch the σ - ϵ curve for loading followed by a complete unloading.
- (f) Assuming $n = 5$, find the offset tensile stresses for the permanent offsets $\epsilon^p = 0.1\%$ and $\epsilon^p = 0.2\%$, respectively.
- 1.2. For the material of Problem 1.1, assume $n = 4$, $E = 73,000$ MPa, and $b = 800$ MPa. A material element is pretrained in tension up to a state with $\epsilon^p = 0.015$ and is subsequently unloaded and then reversely loaded until plastic flow in compression commences; further compressive yielding continues until $\epsilon^p = -0.015$. The material is assumed to follow: (i) the isotropic hardening rule; (ii) the independent hardening rule, both with the plastic modulus E_p taken to depend on a single hardening modulus κ defined as $\kappa = \int (d\epsilon^p d\sigma^p)^{1/2}$.
 - (a) Find the stress at the initiation of compressive yielding.
 - (b) Sketch the σ - ϵ^p curve.
- 1.3. For the material of Problem 1.1, assume $n = 3$, $E = 69,000$ MPa, and $b = 690$ MPa. A material element is firstly strained in tension up to a State 1 with $W_p = 113.85$ kN · m/m³ and is subsequently unloaded and reversely loaded until plastic flow in compression commences at State 2. Further, it is loaded with a stress increment $d\sigma = -2.07$ MPa up to State 3, and then with another stress increment $d\sigma = -2.07$ MPa up to State 4. After that, the element is unloaded and loaded in tension again until plastic flow occurs at State 5. The material is assumed to follow the isotropic hardening rule with the plastic modulus E_p taken to depend on a hardening parameter κ defined as $\kappa = W_p$.
 - (a) Find the tensile stress σ_1 and the plastic strain ϵ_1^p at State 1.
 - (b) Find the stress σ , strain ϵ , plastic strain ϵ^p , plastic work W_p , and plastic modulus E_p at States 2, 3, and 4, respectively.
 - (c) Find the stress σ_5 and plastic modulus E_p at State 5.
- 1.4. For the overlay material model of Example 1.1 (see Fig. 1.7), assume that the material parameters are selected as $A_1 = \frac{2}{3}$, $A_2 = \frac{1}{3}$, $\sigma_{01} = 138$ MPa, $\sigma_{02} = 345$ MPa, and $E = 69,000$ MPa. The strains at points *c* and *f* in Fig. 1.8 are taken to be $\epsilon_c = 0.013$ and $\epsilon_f = 0.011$, and State *h* is assumed to correspond to a compressive stress in bars 2 of value $\sigma_{02}/2$.
 - (a) Find the residual stresses in bars 1 and 2 when $\sigma = 0$ along the unloading path *f-g* and during reloading along path *h-i*.
 - (b) Determine the stress in bars 2, corresponding to States *g* and *i*.
 - (c) What are the values of the stress in bars 2, σ_2 , and the strain ϵ when stress in bars 1 is completely relieved (i.e., $\sigma_1 = 0$) during unloading along path *f-g* and during reloading along path *h-i*.
 - (d) For the σ - ϵ paths in Fig. 1.8, plot bar stresses σ_1 vs. σ_2 , showing the line of equivalent stress $\sigma = 0$.
- 1.5. An initially unstressed and unstrained element of the same linear strain-hardening material as in Example 1.2 is subjected to different loading histories which produce the stress paths given below. For each of the three hardening rules considered in Example 1.2, find the final strain state, ϵ , and the corresponding ϵ^p attained at the end of each loading path. In the following, stress σ is in MPa.
 - (i) $\sigma = 0 \rightarrow 414 \rightarrow -414 \rightarrow 0 \rightarrow 414$
 - (ii) $\sigma = 0 \rightarrow 621 \rightarrow 0$

For each case, show schematic representations of the stress-strain paths followed in the σ - ϵ and σ - ϵ^p spaces.

- 1.6. The σ - ϵ response in simple tension for an elastic-plastic material is approximated by the piecewise linear curve expressed as

Elastic	$\sigma = E\epsilon$	$(\epsilon < \epsilon_0)$
Elastic-plastic	$\sigma = \sigma_0 + E_{pl}(\epsilon - \epsilon_0)$	$(\epsilon_0 \leq \epsilon \leq \epsilon_1)$
	$\sigma = \sigma_1 + E_{pl}(\epsilon - \epsilon_1)$	$(\epsilon_1 \leq \epsilon \leq \epsilon_2)$
Perfectly plastic	$\sigma = \sigma_2$	$(\epsilon > \epsilon_2)$

where the material constants are given as $\sigma_0 = 207$ MPa, $\epsilon_0 = 0.001$; $\sigma_1 = 414$ MPa, $\epsilon_1 = 0.005$; $\sigma_2 = 587$ MPa, $\epsilon_2 = 0.013$. An element of the material is prestrained in tension up to a State A with $\epsilon_A = 0.015$ and is subsequently unloaded until plastic flow in compression commences at State C. Further compressive yielding continues until $\epsilon^p = 0$. The material is assumed to harden kinematically, with the plastic modulus taken to depend on a single hardening parameter κ as defined below.

- (a) Sketch the loading-unloading-reverse loading σ - ϵ^p curves for each of the following assumptions: (i) $\kappa = \int (d\epsilon^p d\epsilon^p)^{1/2}$; (ii) $\kappa = \epsilon^p$ (for $\epsilon^p \geq 0$); (iii) $\kappa = \int \sigma d\epsilon^p$; (iv) $\kappa = \int (\sigma - \alpha) d\epsilon^p$ where α (in stress units) is the center of the current elastic region.
- (b) What are the values σ and ϵ when $\epsilon^p = 0$ during reversed (compression) flow, for each of the four assumptions in (a).

- 1.7. A bar with two fixed ends is subjected to an axial force P at the point with the left-end distance equal to a and the right-end distance equal to b and $a < b$, as shown in Fig. P1.7. The bar is made of an elastic-perfectly plastic material with yield stress σ_y . The axial force P is first increased from zero until plastic flow occurs in the entire bar, and then is unloaded to zero, followed by a reloading in the reverse direction.

- (a) Determine the elastic and plastic limit loads P_e and P_p during the loading.
- (b) Determine the residual stress and plastic strain in the bar when the axial load P is unloaded to zero.
- (c) Determine the plastic limit load P_p during the reversed loading.

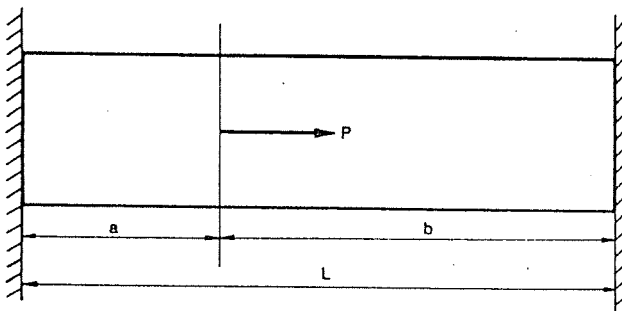


FIGURE P1.7.

- (d) Sketch the P vs. u curve for the complete load-reversed load cycle for the case $b = 2a$, where u is the axial displacement of the bar at the load point.

- 1.8. Using the table of direction cosines (l_{ij}) as given in Example 1.4 (Table 1.4), show that the following two planes coincide:

$$2x_1 - \frac{1}{3}x_2 + x_3 = 1 \quad \text{in } (x_i) \text{ system}$$

$$\frac{47}{25}x'_1 + \frac{14}{15}x'_2 - \frac{21}{25}x'_3 = 1 \quad \text{in } (x'_i) \text{ system}$$

- 1.9. If $B_i = A_i/\sqrt{(A_j A_j)}$, show that B_i is a unit vector.

- 1.10. Given the relations

$$\sigma_{ij} = s_{ij} + \frac{1}{3}\sigma_{kk}\delta_{ij}$$

$$J_2 = \frac{1}{2}s_{ij}s_{ji}$$

where σ_{ij} and s_{ij} are symmetric second-order tensors, show that (a) $s_{ii} = 0$ and (b) $\partial J_2 / \partial \sigma_{ij} = s_{ij}$.

- 1.11. Prove that there is no pair of vectors A_i and B_i such that $\delta_{ij} = A_i B_j$.

- 1.12. Show that an arbitrary second-order tensor σ_{ij} may be written in the form

$$\sigma_{ij} = s_{ij} + \alpha\delta_{ij}$$

where $s_{ii} = 0$.

- 1.13. Consider a truss consisting of three bars with cross-sectional area A and subjected to a vertical load P at joint D as shown in Fig. P1.13. The bars are made of an elastic-perfectly plastic material with elastic modulus E and yield stress σ_y . As P is continuously increased, bar 2 is first yielded at State a (P_a , Δ_a), and subsequently bars 1 and 3 are yielded at State b (P_b , Δ_b). Plastic flow occurs at a constant load P_b until joint D has an additional amount of displacement $\sigma_0 L/E$ (State c); then P is completely unloaded (State d). Afterward, P is increased in a reversed direction until all three bars are reversely yielded again (State f).

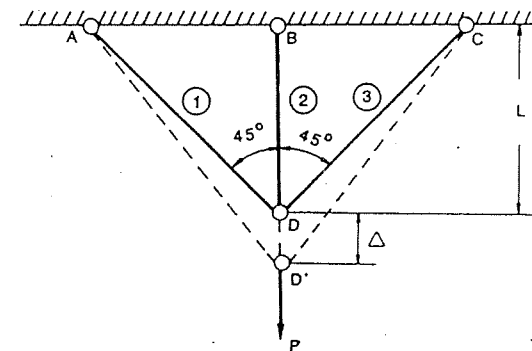


FIGURE P1.13.

- Find the residual stresses and residual strains at state *d* for three truss bars.
- Find the reversed yield load.
- Plot the load vs. displacement (*P* vs. Δ) curve for the whole loading-unloading-reversed loading program.
- Referring to the parallel bar model of Example 1.1, what conclusion can be drawn from this truss model?

ANSWERS TO SELECTED PROBLEMS

- 1.1. (d) 0; (f) $\sigma_{0.1\%} = 0.25b$, $\sigma_{0.2\%} = 0.289b$.
- 1.2. (a) (i) $\sigma_c = -280$ MPa; (ii) $\sigma_c = 0$.
 (b) Equation of $\sigma-\epsilon^p$ curve on reversed loading is (i) $\sigma = -800(0.03 - \epsilon^p)^{1/4}$; (ii) $\sigma = -800(0.03 - \epsilon^p)^{1/4} + 280$.
- 1.3. (a) $\sigma_1 = 84.07$ MPa, $\epsilon_1^p = 0.001806$.
 (b) $\sigma_2 = -84.07$ MPa, $\epsilon_2 = 0.000588$, $\epsilon_2^p = \epsilon_1^p$, $(W_p)_2 = 113.85$ kN · m/m³, $(E_p)_2 = 15,504$ MPa; $\sigma_3 = -86.15$ MPa, $\epsilon_3 = 0.000424$, $\epsilon_3^p = 0.001672$, $(W_p)_3 = 125.3$ kN · m/m³, $(E_p)_3 = 14,793$ MPa; $\sigma_4 = -88.22$ MPa, $\epsilon_4 = 0.000254$, $\epsilon_4^p = 0.001532$, $(W_p)_4 = 137.5$ kN · m/m³, $(E_p)_4 = 14,117$ MPa.
 (c) $\sigma_5 = 88.22$ MPa, $(E_p)_5 = 14,117$ MPa.

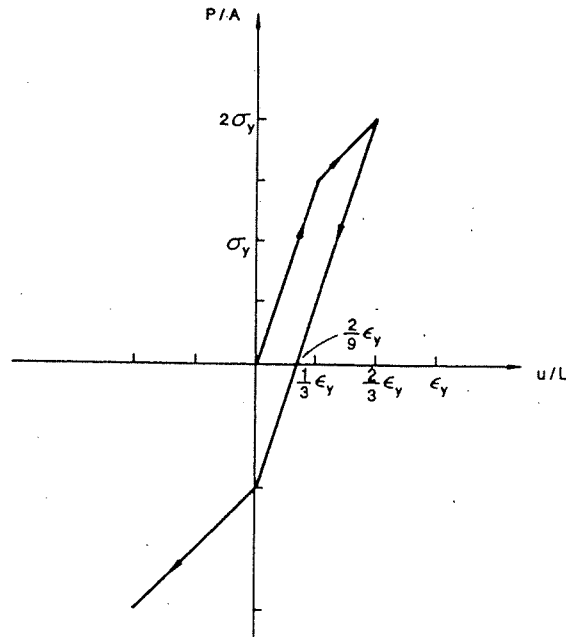


FIGURE S1.7.

- 1.4. (a) Path *c-d* and Path *f-g*: $\sigma_1 = -69$ MPa, $\sigma_2 = 138$ MPa; Path *h-i*: $\sigma_1 = 11.5$ MPa, $\sigma_2 = -23$ MPa.
 (b) At Point *g*: $\sigma_2 = 69$ MPa; at Point *i*: $\sigma_2 = 103.5$ MPa.
 (c) For Path *f-g*: $\sigma_2 = 207$ MPa; for Path *h-i*: $\sigma_2 = -34.5$ MPa.
- 1.5. Isotropic hardening: (i) $\epsilon = 0 \rightarrow 0.01 \rightarrow 0.006 \rightarrow 0.008 \rightarrow 0.01$, $\epsilon^p = 0 \rightarrow 0.008 \rightarrow 0.008 \rightarrow 0.008$; (ii) $\epsilon = 0 \rightarrow 0.019 \rightarrow 0.016$, $\epsilon^p = 0 \rightarrow 0.016 \rightarrow 0.016$.
 Kinematic hardening: (i) $\epsilon = 0 \rightarrow 0.01 \rightarrow -0.01 \rightarrow -0.008 \rightarrow 0.01$, $\epsilon^p = 0 \rightarrow 0.008 \rightarrow -0.008 \rightarrow -0.008$; (ii) $\epsilon = 0 \rightarrow 0.019 \rightarrow 0.008$, $\epsilon^p = 0 \rightarrow 0.016 \rightarrow 0.008$.
 Independent hardening: (i) $\epsilon = 0 \rightarrow 0.01 \rightarrow -0.002 \rightarrow 0 \rightarrow 0.002$, $\epsilon^p = 0 \rightarrow 0.008 \rightarrow 0 \rightarrow 0 \rightarrow 0$; (ii) $\epsilon = 0 \rightarrow 0.019 \rightarrow 0.016$, $\epsilon^p = 0 \rightarrow 0.016 \rightarrow 0.016$.
- 1.6. (b) (i) $\sigma = 172.6$ MPa, $\epsilon = 0.0008$; (ii) $\sigma = -207.1$ MPa, $\epsilon = -0.001$; (iii) $\sigma = 43.3$ MPa, $\epsilon = 0.0002$; (iv) same as (i).

1.7. Figure S1.7.

1.13. Figure S1.13.

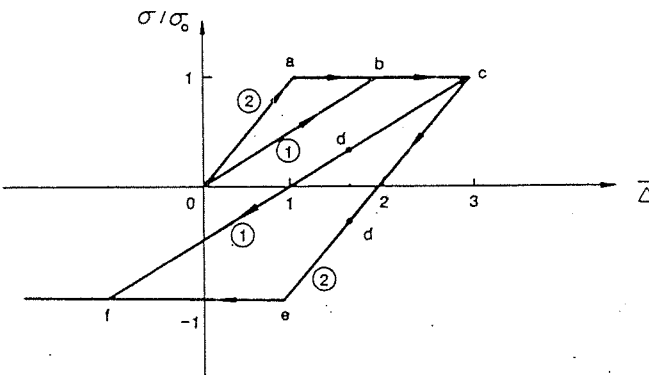
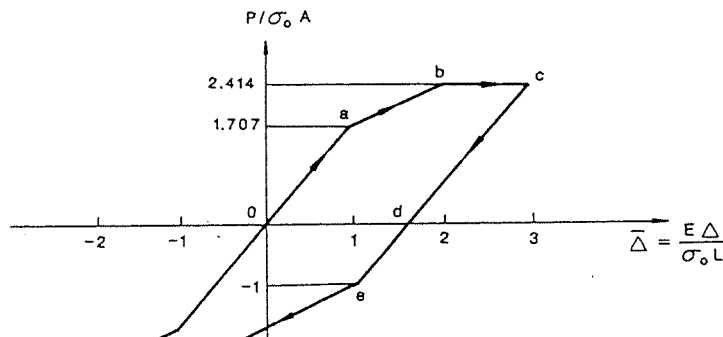


FIGURE S1.13.

2 Yield and Failure Criteria

In Chapter 1, we have discussed the characteristics of the uniaxial behavior of a material, introducing some important concepts in plasticity theory for the uniaxial case. The main task of the subsequent chapters is to generalize these concepts to a combined state of stress. This chapter deals with the limits of elasticity and the limits of strength under all possible combinations of stresses. Before we proceed to this subject, an analysis of the state of combined stresses is first introduced to provide the necessary background for the subsequent study.

2.1. Stress

2.1.1. Stress at a Point and the Stress Tensor

As we know, stress is defined as the intensity of internal forces acting between particles of a body across imaginary internal surfaces. Consider a surface area ΔA passing through a point P_0 with a unit vector \mathbf{n} normal to the area ΔA as shown in Fig. 2.1. Let \mathbf{F}_n be the resultant force due to the action across the area ΔA of the material from one side onto the other side of the cut plane \mathbf{n} . Then the stress vector at point P_0 associated with the cut plane \mathbf{n} is defined by

$$\lim_{\Delta A \rightarrow 0} \frac{\mathbf{F}_n}{\Delta A} = \mathbf{T} = \vec{\mathbf{T}} \quad (2.1)$$

The state of stress at a point is defined as the totality of *all* stress vectors $\vec{\mathbf{T}}$ at that point.

Since we can make an infinite number of cuts through a point, we have an infinite number of values of $\vec{\mathbf{T}}$ which, in general, are different from each other. This infinite number of values of $\vec{\mathbf{T}}$ characterizes the state of stress (or the stress state) at the point. Fortunately, as shown later, there is no need to know all the values of the stress vectors on the infinite numbers of planes containing the point. If the stress vectors $\vec{\mathbf{T}}^1$, $\vec{\mathbf{T}}^2$, and $\vec{\mathbf{T}}^3$ on three

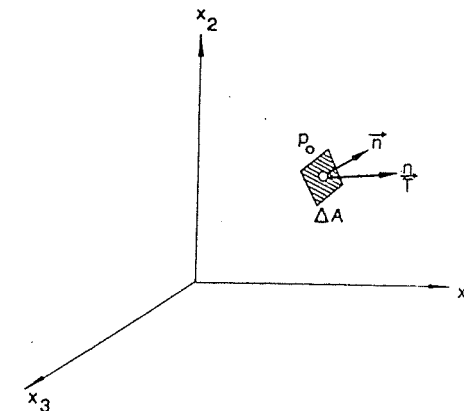


FIGURE 2.1. Stress vector $\vec{\mathbf{T}}$ at point P_0 associated with cut \mathbf{n} .

mutually perpendicular planes are known, as shown in Fig. 2.2, the stress vector on any plane containing this point can be found from equilibrium conditions at that point.

Figure 2.3 shows an element $OABC$ with the stress vectors $\vec{\mathbf{T}}^1$, $\vec{\mathbf{T}}^2$, and $\vec{\mathbf{T}}^3$ acting on its faces OBC , OAC , OAB , and ABC , respectively. Stress vector $\vec{\mathbf{T}}(\vec{\mathbf{T}}^1, \vec{\mathbf{T}}^2, \vec{\mathbf{T}}^3)$ represents the stress acting across the cut plane normal to unit vector $\mathbf{e}_1(\mathbf{e}_2, \mathbf{e}_3)$ from the negative side onto the positive side.

The unit vector \mathbf{n} can be written in the component form

$$\mathbf{n} = (n_1, n_2, n_3) \quad (2.2)$$

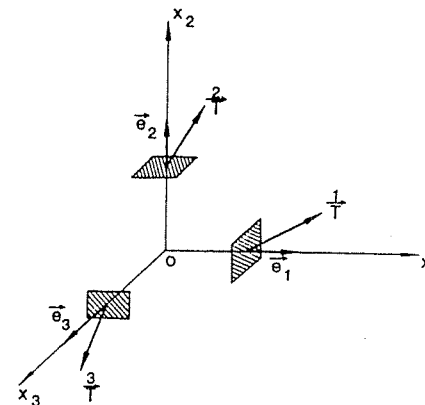
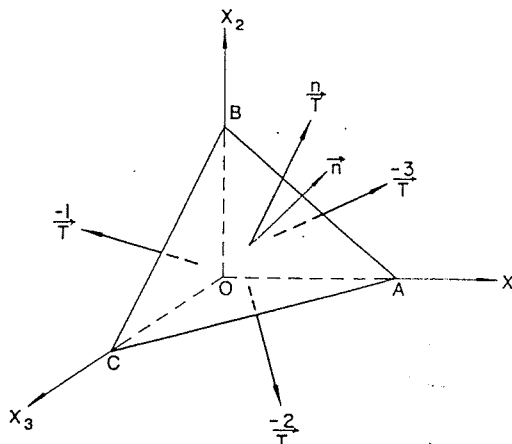


FIGURE 2.2. Stress vectors on three mutually perpendicular planes at a point.

FIGURE 2.3. Stress vectors acting on arbitrary plane n and on the coordinate planes.

where the direction cosines n_1 , n_2 , and n_3 are given by

$$\begin{aligned}n_1 &= \cos(\mathbf{e}_1, \mathbf{n}) \\n_2 &= \cos(\mathbf{e}_2, \mathbf{n}) \\n_3 &= \cos(\mathbf{e}_3, \mathbf{n})\end{aligned}\quad (2.3)$$

Let A be the area of ΔABC . Then the area of the face perpendicular to the x_i -axis, denoted by A_i , is given by

$$A_i = A \cos(\mathbf{e}_i, \mathbf{n}) = An_i \quad (2.4)$$

From equilibrium of the body $OABC$ (Fig. 2.3) and using Eq. (2.4), we get

$$\bar{T}(A) + \bar{T}^1(An_1) + \bar{T}^2(An_2) + \bar{T}^3(An_3) = 0 \quad (2.5)$$

Dividing Eq. (2.5) by A , we have

$$\bar{T} = -\bar{T}^1 n_1 - \bar{T}^2 n_2 - \bar{T}^3 n_3 \quad (2.6)$$

But

$$\bar{T}^i = -\bar{T} \quad \text{for } i = 1, 2, \text{ and } 3$$

Therefore,

$$\bar{T} = \bar{T}^1 n_1 + \bar{T}^2 n_2 + \bar{T}^3 n_3 \quad (2.7)$$

or in the xyz coordinate system,

$$\bar{T} = \bar{T}_x n_x + \bar{T}_y n_y + \bar{T}_z n_z \quad (2.8)$$

Equation (2.7) or (2.8) expresses the stress vector \bar{T} at any point associated with the cut plane n in terms of the stress vectors on the planes perpendicular to the three coordinate axes, x_1 , x_2 , and x_3 , at the same point. Therefore, it is clear that the three stress vectors \bar{T} , \bar{T}^1 , and \bar{T}^2 define the state of stress at a point completely.

The stress vector, \bar{T} , of course, need not be perpendicular to the plane on which it acts. In practice, therefore, the stress vector \bar{T} is decomposed into two components, one normal to the plane n , called the *normal stress*, and the other parallel to this plane, called the *shearing stress*.

The stress vectors associated with each of the three coordinate planes x_1 , x_2 , and x_3 are also decomposed into components in the direction of the three coordinate axes. For example, the stress vector \bar{T}^1 associated with the coordinate plane x_1 , has three stress components: normal stress σ_{11} , and shearing stresses σ_{12} and σ_{13} in the direction of the three coordinate axes x_1 , x_2 , and x_3 , respectively, as shown in Fig. 2.4. Thus, we have

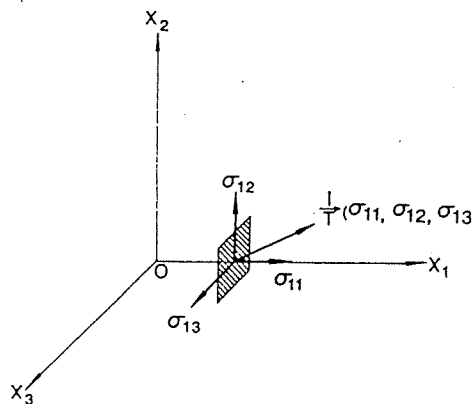
$$\bar{T}^1 = \sigma_{11} \mathbf{e}_1 + \sigma_{12} \mathbf{e}_2 + \sigma_{13} \mathbf{e}_3 \quad (2.9)$$

$$\bar{T}^2 = \sigma_{21} \mathbf{e}_1 \quad (2.10)$$

Similarly, for the coordinate planes x_2 and x_3 ,

$$\bar{T}^2 = \sigma_{22} \mathbf{e}_2 \quad (2.11)$$

$$\bar{T}^3 = \sigma_{32} \mathbf{e}_2 \quad (2.12)$$

FIGURE 2.4. Components of a stress vector associated with the coordinate plane normal to x_1 .

In general,

$$\vec{T} = \sigma_{ij} \mathbf{e}_j \quad (2.13)$$

where σ_{ij} denotes the j -th component of the stress vector \vec{T} acting on an area element (at P) whose normal is in the direction of the positive x_i -axis (Fig. 2.4).

The nine quantities σ_{ij} required to define the three stress vectors \vec{T}_1 , \vec{T}_2 , and \vec{T}_3 are called the components of the *stress tensor*, which is given by

$$\sigma_{ij} = \begin{bmatrix} \frac{1}{3} \vec{T} \\ \frac{2}{3} \vec{T} \\ \frac{3}{3} \vec{T} \end{bmatrix} = \begin{bmatrix} \sigma_{11} & \sigma_{12} & \sigma_{13} \\ \sigma_{21} & \sigma_{22} & \sigma_{23} \\ \sigma_{31} & \sigma_{32} & \sigma_{33} \end{bmatrix} \quad (2.14)$$

where σ_{11} , σ_{22} , and σ_{33} are normal components of stress and σ_{12} , σ_{21} , ... are shearing components of stress.

The components of the stress tensor can be written using von Karman's notation in the form

$$\sigma_{ij} = \begin{bmatrix} \sigma_x & \tau_{xy} & \tau_{xz} \\ \tau_{yx} & \sigma_y & \tau_{yz} \\ \tau_{zx} & \tau_{zy} & \sigma_z \end{bmatrix} \quad (2.15)$$

where σ represents a normal component of stress, and τ represents a shearing component of stress. Also, the symbols σ_{xx} , σ_{xy} , ... may be used instead of σ_{ij} to designate the components of the stress tensor in Eqs. (2.14) and (2.15). Thus, the following forms are dual notations for the stress tensor σ_{ij} :

$$\sigma_{ij} = \begin{bmatrix} \sigma_{11} & \sigma_{12} & \sigma_{13} \\ \sigma_{21} & \sigma_{22} & \sigma_{23} \\ \sigma_{31} & \sigma_{32} & \sigma_{33} \end{bmatrix} \equiv \begin{bmatrix} \sigma_{xx} & \sigma_{xy} & \sigma_{xz} \\ \sigma_{yx} & \sigma_{yy} & \sigma_{yz} \\ \sigma_{zx} & \sigma_{zy} & \sigma_{zz} \end{bmatrix} \equiv \begin{bmatrix} \sigma_x & \tau_{xy} & \tau_{xz} \\ \tau_{yx} & \sigma_y & \tau_{yz} \\ \tau_{zx} & \tau_{zy} & \sigma_z \end{bmatrix} \quad (2.16)$$

Upon substitution of Eq. (2.13) into Eq. (2.7), the components of the stress vector \vec{T} can be written as

$$\vec{T}_i = \sigma_{ij} n_j \quad (2.17)$$

From the consideration of the equilibrium of moments of a material element, it can be shown that the stress tensor, σ_{ij} , is symmetric, that is, $\sigma_{ij} = \sigma_{ji}$. Thus, Eq. (2.17) may be conveniently rewritten as

$$\vec{T}_i = \sigma_{ij} n_j \quad i = 1, 2, 3 \quad (2.18)$$

where σ_{ij} is given by Eq. (2.16).

Equation (2.18) expresses the components of the stress vector acting on an arbitrary plane n at a given point in terms of the components of the

stress tensor, σ_{ij} , at that point. It therefore follows that T_i for any n_i may be calculated from a knowledge of the nine basic quantities σ_{ij} .

In Eq. (2.18), \vec{T}_i and n_i are vectors. From this equation, we can show that σ_{ij} is a tensor of second order; that is, the stress components σ_{ij} in the x_i system and the components σ'_{ij} in the x'_i system are related by following equations:

$$\sigma'_{ij} = l_{im} l_{jn} \sigma_{mn} \quad (2.19)$$

and

$$\sigma_{ij} = l_{mi} l_{nj} \sigma'_{mn} \quad (2.20)$$

where the l_{ij} are the direction cosines shown in Table 1.3.

2.1.2. Cauchy's Formulas for Stresses

Equations (2.7) and (2.18) derived in the preceding section are different forms of Cauchy's formulas for stresses. In practice, however, it is desirable to express directly the normal and shear stress components, σ_n and S_n , respectively, of any stress vector \vec{T} acting on an arbitrary plane n at a given point in terms of the components of the stress tensor σ_{ij} at that point. The magnitude of the normal stress component is given by

$$\sigma_n = \vec{T} \cdot \mathbf{n} = \vec{T}_i n_i \quad (2.21)$$

Substituting from Eq. (2.18) for \vec{T}_i , Eq. (2.21) then becomes

$$\sigma_n = \sigma_{ij} n_i n_j \quad (2.22)$$

The magnitude of the shear stress component is given by

$$S_n^2 = (\vec{T})^2 - \sigma_n^2 \quad (2.23)$$

where, from Eq. (2.18), $(\vec{T})^2$ is obtained as

$$(\vec{T})^2 = \vec{T} \cdot \vec{T} = \vec{T}_i \vec{T}_i = (\sigma_{ij} n_j)(\sigma_{ik} n_k) \quad (2.24)$$

or

$$(\vec{T})^2 = \sigma_{ij} \sigma_{ik} n_j n_k \quad (2.25)$$

Equations (2.22) and (2.23), for the determination of the normal and shearing components of stress acting on an arbitrary plane n , are the most useful forms of Cauchy's formulas for stresses.

The vector σ_n is in the direction of the normal vector n , and the vector S_n lies in the plane formed by the two vectors \vec{T} and n .

EXAMPLE 2.1. The state of stress at a point is represented by the given stress tensor σ_{ij} :

$$\sigma_{ij} = \begin{bmatrix} -80 & 16 & 26 \\ 16 & 26 & -28 \\ 26 & -28 & -36 \end{bmatrix} \text{ (units of stress)}$$

For a plane with unit normal $n = (\frac{1}{4}, \frac{1}{2}, \sqrt{11}/4)$, calculate:

- (a) The magnitude of the stress vector, \vec{T} , for plane n .
- (b) The normal and shear stress components, σ_n and S_n , for plane n .

SOLUTION. (a) The components \vec{T}_i of the stress vector \vec{T} are calculated using Eq. (2.18), which gives

$$\vec{T}_1 = \sigma_{ij}n_j = \sigma_{11}n_1 + \sigma_{12}n_2 + \sigma_{13}n_3 = 9.56$$

Similarly,

$$\vec{T}_2 = \sigma_{2j}n_j = -6.22$$

$$\vec{T}_3 = \sigma_{3j}n_j = -37.35$$

Thus, the magnitude of the stress vector \vec{T} is given by

$$|\vec{T}| = [(\vec{T}_1)^2 + (\vec{T}_2)^2 + (\vec{T}_3)^2]^{1/2} = 39.10$$

- (b) Substituting into Eq. (2.22), we get

$$\sigma_n = \sigma_{ij}n_i n_j = \sigma_{11}n_1^2 + \sigma_{22}n_2^2 + \sigma_{33}n_3^2 + 2(\sigma_{12}n_1 n_2 + \sigma_{23}n_2 n_3 + \sigma_{31}n_3 n_1)$$

or

$$\sigma_n = -31.69$$

Thus, the magnitude of the shear stress component, S_n , is calculated using Eq. (2.23),

$$|S_n| = [(\vec{T})^2 - \sigma_n^2]^{1/2} = [(39.10)^2 - (-31.69)^2]^{1/2} = 22.90$$

2.1.3. Principal Stresses and Invariants of the Stress Tensor

Suppose that the direction n at a point in a body is so oriented that the resultant stress, stress vector \vec{T} , associated with direction n is in the same direction as the unit normal n ; that is, $\vec{T} = \sigma_n n$ and $S_n = 0$ (no shear stress). The plane n is then called a *principal plane* at the point, its normal direction n is called a *principal direction*, and the normal stress σ_n is called a *principal stress*. At every point in a body, there exist at least three principal directions. From the definition, we have

$$\vec{T} = \sigma n \quad (2.26)$$

or in component form

$$\vec{T}_i = \sigma n_i \quad (2.27)$$

Substituting for \vec{T}_i from Eq. (2.18) leads to

$$\sigma_{ij}n_j = \sigma n_i \quad (2.28)$$

which implies the following three equations:

$$\sigma_{11}n_1 + \sigma_{12}n_2 + \sigma_{13}n_3 = \sigma n_1 \quad (2.29)$$

$$\sigma_{21}n_1 + \sigma_{22}n_2 + \sigma_{23}n_3 = \sigma n_2 \quad (2.29)$$

$$\sigma_{31}n_1 + \sigma_{32}n_2 + \sigma_{33}n_3 = \sigma n_3 \quad (2.29)$$

or in von Karman's notation

$$(\sigma_x - \sigma)n_x + \tau_{xy}n_y + \tau_{xz}n_z = 0 \quad (2.30)$$

$$\tau_{yx}n_x + (\sigma_y - \sigma)n_y + \tau_{yz}n_z = 0 \quad (2.30)$$

$$\tau_{zx}n_x + \tau_{zy}n_y + (\sigma_z - \sigma)n_z = 0 \quad (2.30)$$

These three linear simultaneous equations are homogeneous for n_x , n_y , and n_z . In order to have a nontrivial solution, the determinant of the coefficients must vanish:

$$\begin{vmatrix} \sigma_x - \sigma & \tau_{xy} & \tau_{xz} \\ \tau_{yx} & \sigma_y - \sigma & \tau_{yz} \\ \tau_{zx} & \tau_{zy} & \sigma_z - \sigma \end{vmatrix} = 0 \quad (2.31)$$

so that this requirement determines the value of σ . There are, in general, three roots, σ_1 , σ_2 , and σ_3 . Since the basic equation was $\vec{T}_i = \sigma n_i$, these three possible values of σ are the three possible magnitudes of the normal stress corresponding to zero shear stress. In the abbreviated notation, Eqs. (2.30) and (2.31) have the forms

$$(\sigma_{ij} - \sigma\delta_{ij})n_j = 0 \quad (2.32)$$

and

$$|\sigma_{ij} - \sigma\delta_{ij}| = 0 \quad (2.33)$$

Expanding Eq. (2.31) leads to the *characteristic equation*

$$\sigma^3 - I_1\sigma^2 + I_2\sigma - I_3 = 0 \quad (2.34)$$

where

I_1 = sum of the diagonal terms of σ_{ij}

or

$$I_1 = \sigma_{11} + \sigma_{22} + \sigma_{33} = \sigma_x + \sigma_y + \sigma_z \quad (2.35)$$

I_2 = sum of the cofactors of diagonal terms of σ_{ij}

or

$$\begin{aligned} I_2 &= \left| \begin{array}{cc} \sigma_{22} & \sigma_{23} \\ \sigma_{32} & \sigma_{33} \end{array} \right| + \left| \begin{array}{cc} \sigma_{11} & \sigma_{13} \\ \sigma_{31} & \sigma_{33} \end{array} \right| + \left| \begin{array}{cc} \sigma_{11} & \sigma_{12} \\ \sigma_{21} & \sigma_{22} \end{array} \right| \\ &= \left| \begin{array}{cc} \sigma_y & \tau_{yz} \\ \tau_{zy} & \sigma_z \end{array} \right| + \left| \begin{array}{cc} \sigma_x & \tau_{xz} \\ \tau_{zx} & \sigma_z \end{array} \right| + \left| \begin{array}{cc} \sigma_x & \tau_{xy} \\ \tau_{yx} & \sigma_y \end{array} \right| \end{aligned} \quad (2.36)$$

I_3 = determinant of σ_{ij}

or

$$I_3 = \left| \begin{array}{ccc} \sigma_{11} & \sigma_{12} & \sigma_{13} \\ \sigma_{21} & \sigma_{22} & \sigma_{23} \\ \sigma_{31} & \sigma_{32} & \sigma_{33} \end{array} \right| = \left| \begin{array}{ccc} \sigma_x & \tau_{xy} & \tau_{xz} \\ \tau_{yx} & \sigma_y & \tau_{yz} \\ \tau_{zx} & \tau_{zy} & \sigma_z \end{array} \right| \quad (2.37)$$

From the property of the roots of a cubic equation, it can be shown that [refer to Eq. (2.34)],

$$\begin{aligned} I_1 &= \sigma_1 + \sigma_2 + \sigma_3 \\ I_2 &= \sigma_1\sigma_2 + \sigma_2\sigma_3 + \sigma_3\sigma_1 \\ I_3 &= \sigma_1\sigma_2\sigma_3 \end{aligned} \quad (2.38)$$

where σ_1 , σ_2 , and σ_3 are the roots of Eq. (2.34).

The cubic Eq. (2.34) must therefore be the same whether we derive it from x , y , z coordinates or from the principal directions 1, 2, 3. Hence quantities I_1 , I_2 , and I_3 are the *invariants of the stress tensor*; that is, their values would be the same regardless of rotation of the coordinate axes.

Substituting σ_1 , σ_2 , and σ_3 in turn into Eq. (2.32), and also employing the identity

$$n_1^2 + n_2^2 + n_3^2 = 1 \quad (2.39)$$

we can determine the components (n_1, n_2, n_3) of the unit normal n_i corresponding to each value of σ (principal stress),

$$\begin{aligned} n^{(1)} &= (n_1^{(1)}, n_2^{(1)}, n_3^{(1)}) & \text{for } \sigma = \sigma_1 \\ n^{(2)} &= (n_1^{(2)}, n_2^{(2)}, n_3^{(2)}) & \text{for } \sigma = \sigma_2 \\ n^{(3)} &= (n_1^{(3)}, n_2^{(3)}, n_3^{(3)}) & \text{for } \sigma = \sigma_3 \end{aligned} \quad (2.40)$$

These three directions are called *principal directions* at the point.

The need for Eq. (2.39) arises from the fact that when σ in Eq. (2.32) is set equal to, say, σ_1 , Eq. (2.33) implies from linear-algebra theory that at most two of the three equations (2.32) can be independent. It can be shown that if the three σ -roots are all different, *exactly* two of the three equations are independent. The special case in which two or more σ -roots coincide may subsequently be treated as a limiting case. In the meantime, we need only the resulting fact that whether two or only one of Eqs. (2.32) is independent, at least one solution $n_i^{(1)}$ satisfying Eqs. (2.32) and also Eq. (2.39) exists. Similarly, an $n_i^{(2)}$ corresponding to σ_2 and an $n_i^{(3)}$ corresponding to σ_3 may be found.

2.1.4. Principal Shear Stresses and Maximum Shear Stress

In describing the stress state at a point, let us take the principal axes 1, 2, and 3 as the reference axes instead of the general x_1 , x_2 , x_3 coordinate system. Note that on these coordinate planes 1, 2, and 3, all shear stresses are zero (Fig. 2.5). So, the magnitude of the stress acting on an arbitrary plane n at this point as given by Eq. (2.25) turns out to be

$$(\frac{\sigma}{T})^2 = \sigma_1^2 n_1^2 + \sigma_2^2 n_2^2 + \sigma_3^2 n_3^2 \quad (2.41)$$

Equation (2.22) gives the normal stress component as

$$\sigma_n = \sigma_1 n_1^2 + \sigma_2 n_2^2 + \sigma_3 n_3^2 \quad (2.42)$$

From Eq. (2.23), the magnitude of the shear stress component is expressed as

$$S_n^2 = (\frac{\sigma}{T})^2 - \sigma_n^2 = (\sigma_1^2 n_1^2 + \sigma_2^2 n_2^2 + \sigma_3^2 n_3^2) - (\sigma_1 n_1^2 + \sigma_2 n_2^2 + \sigma_3 n_3^2)^2 \quad (2.43)$$

The condition for n is given by

$$n_1^2 + n_2^2 + n_3^2 = 1 \quad (2.44)$$

From Eqs. (2.42) and (2.44), and eliminating n_3 , we obtain σ_n as a function of n_1 and n_2 . For stationary values of σ_n , letting $\partial\sigma_n/\partial n_1 = 0$ and $\partial\sigma_n/\partial n_2 = 0$, we can show that $\sigma_n = \sigma_3$ is a stationary value. Similarly, we can also prove σ_1 and σ_2 are stationary values of the normal stress σ_n .

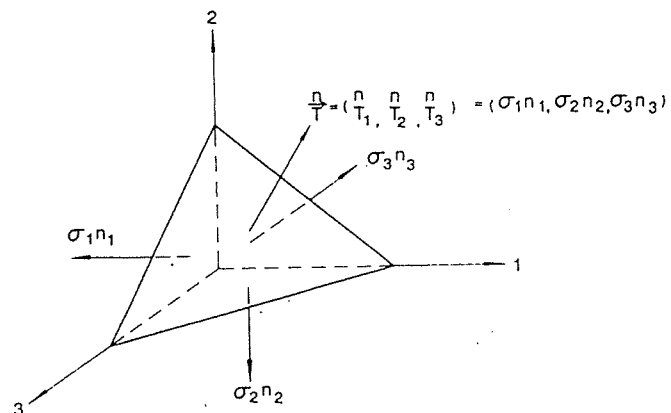


FIGURE 2.5. Components of stress on any plane referred to principal stress axes 1, 2, and 3.

Now, let us examine the stationary values of shear stress S_n . From Eqs. (2.43) and (2.44), and eliminating n_3 , we obtain

$$S_n^2 = (\sigma_1^2 - \sigma_3^2)n_1^2 + (\sigma_2^2 - \sigma_3^2)n_2^2 + \sigma_3^2 - [(\sigma_1 - \sigma_3)n_1^2 + (\sigma_2 - \sigma_3)n_2^2 + \sigma_3]^2 \quad (2.45)$$

Hence, for stationary values of S_n , we have

$$\frac{1}{2} \frac{\partial S_n^2}{\partial n_1} = (\sigma_1 - \sigma_3)n_1\{(\sigma_1 - \sigma_3) - 2[(\sigma_1 - \sigma_3)n_1^2 + (\sigma_2 - \sigma_3)n_2^2]\} = 0 \quad (2.45a)$$

and

$$\frac{1}{2} \frac{\partial S_n^2}{\partial n_2} = (\sigma_2 - \sigma_3)n_2\{(\sigma_2 - \sigma_3) - 2[(\sigma_1 - \sigma_3)n_1^2 + (\sigma_2 - \sigma_3)n_2^2]\} = 0 \quad (2.45b)$$

Assuming that σ_1 , σ_2 , and σ_3 are distinct and $\sigma_1 > \sigma_2 > \sigma_3$, we obtain the conditions that can satisfy Eqs. (2.45a,b), and Eq. (2.44) in the following:

(i) $n_1 = n_2 = 0, n_3 = \pm 1 \quad (2.46)$

Equation (2.43) gives $S_n = 0$, a minimum value, and this shear stress component S_n acts on the principal plane with the normal in the direction of axis 3.

(ii) $n_1 = 0, n_2 = \pm \frac{1}{\sqrt{2}}$, and $n_3 = \pm \frac{1}{\sqrt{2}} \quad (2.47)$

These values define two planes passing through the principal axis of σ_1 at an angle of 45° to the principal axes of σ_2 and σ_3 . The stationary value of S_n in this case is given by

$$S_n^2 = \frac{1}{4}(\sigma_2 - \sigma_3)^2 \quad (2.48)$$

or

$$|S_n| = \frac{1}{2}|\sigma_2 - \sigma_3| \quad (2.49)$$

(iii) $n_2 = 0, n_1 = \pm \frac{1}{\sqrt{2}}$, and $n_3 = \pm \frac{1}{\sqrt{2}} \quad (2.50)$

The stationary value of S_n in this case is

$$|S_n| = \frac{1}{2}|\sigma_1 - \sigma_3| \quad (2.51)$$

These values of n_1 , n_2 , and n_3 define two planes passing through the principal axis of σ_2 at an angle of 45° to the principal axes of σ_1 and σ_3 . Similarly, we can determine another stationary value of shear stress S_n given by

$$|S_n| = \frac{1}{2}|\sigma_1 - \sigma_2| \quad (2.52)$$

This shear stress acts on planes passing through the principal axis of σ_3 at an angle of 45° to the principal axes of σ_1 and σ_2 ($n_1 = \pm 1/\sqrt{2}$, $n_2 = \pm 1/\sqrt{2}$, $n_3 = 0$).

Stationary values $\frac{1}{2}|\sigma_1 - \sigma_2|$, $\frac{1}{2}|\sigma_2 - \sigma_3|$, $\frac{1}{2}|\sigma_1 - \sigma_3|$ are called *principal shear stresses* since they occur on planes which bisect the angle between principal planes. It should be noted that these principal shear planes are not pure shear planes; the normal stresses on the principal shear planes can be calculated using Eq. (2.41) and the corresponding values of n_1 , n_2 , and n_3 . The largest value of the principal shear stresses, called the *maximum shearing stress*, τ_{\max} , is equal to $\frac{1}{2}|\sigma_1 - \sigma_3|$ for $\sigma_1 > \sigma_2 > \sigma_3$.

2.1.5. Stress Deviation Tensor and Its Invariants

It is convenient in material modeling to decompose the stress tensor into two parts, one called the *spherical* or the *hydrostatic stress tensor* and the other called the *stress deviator tensor*. The hydrostatic stress tensor is the tensor whose elements are $p\delta_{ij}$, where p is the mean stress and is given by

$$p = \frac{1}{3}\sigma_{kk} = \frac{1}{3}(\sigma_x + \sigma_y + \sigma_z) = \frac{1}{3}I_1 \quad (2.53)$$

From Eq. (2.53), it is apparent that p is the same for all possible orientations of the axes; hence, it is called the *spherical* or the *hydrostatic stress*. The *stress deviator tensor* s_{ij} is defined by subtracting the spherical state of stress from the actual state of stress. Therefore, we have

$$\sigma_{ij} = s_{ij} + p\delta_{ij} \quad (2.54)$$

$$s_{ij} = \sigma_{ij} - p\delta_{ij} \quad (2.55)$$

Equation (2.55) gives the required definition of the stress deviator tensor s_{ij} . The components of this tensor are given by

$$s_{ij} = \begin{bmatrix} s_{11} & s_{12} & s_{13} \\ s_{21} & s_{22} & s_{23} \\ s_{31} & s_{32} & s_{33} \end{bmatrix} = \begin{bmatrix} (\sigma_{11} - p) & \sigma_{12} & \sigma_{13} \\ \sigma_{21} & (\sigma_{22} - p) & \sigma_{23} \\ \sigma_{31} & \sigma_{32} & (\sigma_{33} - p) \end{bmatrix} \quad (2.56)$$

or, using von Karman's notation,

$$s_{ij} = \begin{bmatrix} s_x & s_{xy} & s_{xz} \\ s_{yx} & s_y & s_{yz} \\ s_{zx} & s_{zy} & s_z \end{bmatrix} = \begin{bmatrix} (\sigma_x - p) & \tau_{xy} & \tau_{xz} \\ \tau_{yx} & (\sigma_y - p) & \tau_{yz} \\ \tau_{zx} & \tau_{zy} & (\sigma_z - p) \end{bmatrix} \quad (2.57)$$

Note that $\delta_{ij} = 0$ and $s_{ij} = \sigma_{ij}$ for $i \neq j$ in Eq. (2.55).

It is apparent that subtracting a constant normal stress in all directions does not change the principal directions. The principal directions are therefore the same for the stress deviator tensor as for the original stress tensor. In terms of the principal stresses, the stress deviator tensor s_{ij} is

$$s_{ij} = \begin{bmatrix} \sigma_1 - p & 0 & 0 \\ 0 & \sigma_2 - p & 0 \\ 0 & 0 & \sigma_3 - p \end{bmatrix} \quad (2.58)$$

or

$$s_{ij} = \begin{bmatrix} \frac{2\sigma_1 - \sigma_2 - \sigma_3}{3} & 0 & 0 \\ 0 & \frac{2\sigma_2 - \sigma_3 - \sigma_1}{3} & 0 \\ 0 & 0 & \frac{2\sigma_3 - \sigma_1 - \sigma_2}{3} \end{bmatrix} \quad (2.59)$$

To obtain the invariants of the stress deviator tensor s_{ij} , a similar derivation is followed as was used to derive Eq. (2.34). Thus, we can write

$$|s_{ij} - s\delta_{ij}| = 0 \quad (2.60)$$

or

$$s^3 - J_1 s^2 - J_2 s - J_3 = 0 \quad (2.61)$$

where J_1 , J_2 , and J_3 are the invariants of the stress deviator tensor. Using Eq. (2.54) and definitions similar to those given in Eqs. (2.35) to (2.37), the invariants J_1 , J_2 , and J_3 may be expressed in different forms in terms of the components of s_{ij} or its principal values, s_1 , s_2 , and s_3 , or alternatively, in terms of the components of the stress tensor σ_{ij} or its principal values, σ_1 , σ_2 , and σ_3 . Thus, we have

$$J_1 = s_{ii} = s_{11} + s_{22} + s_{33} = s_1 + s_2 + s_3 = 0 \quad (2.62)$$

$$\begin{aligned} J_2 &= \frac{1}{2}s_{ij}s_{ji} = \frac{1}{2}(s_{11}^2 + s_{22}^2 + s_{33}^2 + s_{12}s_{21} + s_{21}s_{12} + \dots) = \frac{1}{2}(s_1^2 + s_2^2 + s_3^2) \\ &= \frac{1}{2}(s_{11}^2 + s_{22}^2 + s_{33}^2 + 2\sigma_{12}^2 + 2\sigma_{23}^2 + 2\sigma_{31}^2) \\ &= -s_{11}s_{22} - s_{22}s_{33} - s_{33}s_{11} + \sigma_{12}^2 + \sigma_{23}^2 + \sigma_{31}^2 = -(s_1s_2 + s_2s_3 + s_3s_1) \\ &= \frac{1}{6}[(s_{11} - s_{22})^2 + (s_{22} - s_{33})^2 + (s_{33} - s_{11})^2] + \sigma_{12}^2 + \sigma_{23}^2 + \sigma_{31}^2 \\ &= \frac{1}{6}[(\sigma_x - \sigma_y)^2 + (\sigma_y - \sigma_z)^2 + (\sigma_z - \sigma_x)^2] + \tau_{xy}^2 + \tau_{yz}^2 + \tau_{zx}^2 \\ &= \frac{1}{6}[(\sigma_1 - \sigma_2)^2 + (\sigma_2 - \sigma_3)^2 + (\sigma_3 - \sigma_1)^2] \end{aligned} \quad (2.63)$$

$$J_3 = \frac{1}{3}s_{ij}s_{jk}s_{ki} = \begin{vmatrix} s_x & \tau_{xy} & \tau_{xz} \\ \tau_{yx} & s_y & \tau_{yz} \\ \tau_{zx} & \tau_{zy} & s_z \end{vmatrix} = \frac{1}{3}(s_1^3 + s_2^3 + s_3^3) = s_1s_2s_3 \quad (2.64)$$

It can be shown that the invariants J_1 , J_2 , and J_3 are related to the invariants I_1 , I_2 , and I_3 of the stress tensor σ_{ij} through the following relations:

$$\begin{aligned} J_1 &= 0 \\ J_2 &= \frac{1}{3}(I_1^2 - 3I_2) \\ J_3 &= \frac{1}{27}(2I_1^3 - 9I_1I_2 + 27I_3) \end{aligned} \quad (2.65)$$

One advantage of using the stress deviator tensor is now apparent. The first invariant of this tensor, J_1 , is always zero. This can also be seen by taking the sum of the diagonal elements in Eq. (2.56) or (2.58).

It can be shown that the necessary and sufficient condition for a state of stress σ_{ij} to be a pure shear state is that $\sigma_{ii} = 0$, or its first invariant $I_1 = 0$ (see Problem 2.11). Therefore, the stress deviator tensor s_{ij} is a state of pure shear.

2.1.6. Octahedral Stresses

An *octahedral (stress) plane* is a plane whose normal makes equal angles with each of the principal axes of stress. Thus, the planes with normal $\mathbf{n} = (n_1, n_2, n_3) = [1/\sqrt{3}(1, 1, 1)]$ in the principal coordinate system are called *octahedral planes*. Note that we can have eight octahedral planes, as shown in Fig. 2.6, with $OA = OB = OC = OA' = OB' = OC'$. Referring to the principal stress axes, 1, 2, and 3, the stress tensor σ_{ij} is written as

$$\sigma_{ij} = \begin{bmatrix} \sigma_1 & 0 & 0 \\ 0 & \sigma_2 & 0 \\ 0 & 0 & \sigma_3 \end{bmatrix} \quad (2.66)$$

The normal component of a stress vector at point O associated with any direction, \mathbf{n} , can be obtained by Cauchy's formula in Eq. (2.22),

$$\sigma_n = \sigma_{ij}n_i n_j$$

or

$$\sigma_n = \sigma_1 n_1 n_1 + \sigma_2 n_2 n_2 + \sigma_3 n_3 n_3 \quad (2.67)$$

Therefore, the normal stress on a face of the octahedron will be

$$\sigma_{oct} = \sigma_1 n_1^2 + \sigma_2 n_2^2 + \sigma_3 n_3^2 = \frac{1}{3}(\sigma_1 + \sigma_2 + \sigma_3) = \frac{1}{3}I_1 \quad (2.68)$$

Note that the magnitude of σ_{oct} on all the eight faces is the same and that the quantity σ_{oct} is the mean normal stress (or hydrostatic stress).

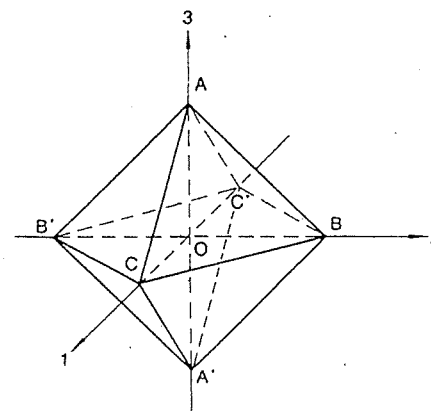


FIGURE 2.6. Octahedral planes in principal coordinate system.

The shear stress on a face of the octahedron, τ_{oct} , can be obtained from the formula in Eq. (2.23):

$$\tau_{\text{oct}}^2 = (\bar{T}_{\text{oct}})^2 - \sigma_{\text{oct}}^2 \quad (2.69)$$

Using Eq. (2.24) to calculate $(\bar{T}_{\text{oct}})^2$, we get

$$(\bar{T}_{\text{oct}})^2 = \sigma_1^2 n_1^2 + \sigma_2^2 n_2^2 + \sigma_3^2 n_3^2 = \frac{1}{3}(\sigma_1^2 + \sigma_2^2 + \sigma_3^2) \quad (2.70)$$

Therefore,

$$\begin{aligned} \tau_{\text{oct}}^2 &= \frac{1}{3}(\sigma_1^2 + \sigma_2^2 + \sigma_3^2) - \frac{1}{3^2}(\sigma_1 + \sigma_2 + \sigma_3)^2 \\ &= \frac{1}{9}[(\sigma_1 - \sigma_2)^2 + (\sigma_2 - \sigma_3)^2 + (\sigma_3 - \sigma_1)^2] \end{aligned} \quad (2.71)$$

Recalling the results we have obtained for the principal shear stresses, τ_{oct} can be expressed as

$$\tau_{\text{oct}}^2 = \frac{1}{3}(\tau_{12}^2 + \tau_{23}^2 + \tau_{31}^2) \quad (2.72)$$

where τ_{12} , τ_{23} , and τ_{31} are the principal shear stresses. Therefore,

$$\tau_{\text{oct}} = \sqrt{\frac{2}{3}(\tau_{12}^2 + \tau_{23}^2 + \tau_{31}^2)} = \sqrt{\frac{2}{3}J_2} \quad (2.73)$$

where J_2 is an invariant of the stress deviator tensor. In terms of the invariants of the stress tensor, the octahedral shear stress can be written as [see Eq. (2.65)]

$$\tau_{\text{oct}} = \frac{\sqrt{2}}{3}(I_1^2 - 3J_2)^{1/2} \quad (2.74)$$

and in terms of general nonprincipal stresses, it becomes [see Eq. (2.63)]

$$\tau_{\text{oct}} = \sqrt{\frac{1}{3}[(\sigma_x - \sigma_y)^2 + (\sigma_y - \sigma_z)^2 + (\sigma_z - \sigma_x)^2 + 6(\tau_{xy}^2 + \tau_{yz}^2 + \tau_{zx}^2)]} \quad (2.75)$$

which gives the *octahedral shear stress* at a point in terms of the stress components referred to an arbitrary set of coordinate axes, x , y , and z .

Note that the magnitude of τ_{oct} on all the eight faces is the same and that the quantity τ_{oct} is somewhat an average principal shear stress as given by Eq. (2.73).

EXAMPLE 2.2. Given the state of stress σ_{ij} in Eq. (2.76) below, calculate the following:

- (a) The octahedral normal and shear stresses.
- (b) The hydrostatic stress.
- (c) The stress deviator tensor, s_{ij} .

$$\sigma_{ij} = \begin{bmatrix} 1 & 2 & 4 \\ 2 & 2 & 1 \\ 4 & 1 & 3 \end{bmatrix} \text{ (units of stress)} \quad (2.76)$$

SOLUTION. (a) The first invariant I_1 is calculated from Eq. (2.35):

$$I_1 = \sigma_{ii} = 1 + 2 + 3 = 6$$

Therefore, from Eq. (2.68), we have

$$\sigma_{\text{oct}} = \frac{1}{3}I_1 = 2$$

Using Eq. (2.75) for τ_{oct} , we get

$$\tau_{\text{oct}} = \sqrt{\frac{2}{3}[(1-2)^2 + (2-3)^2 + (3-1)^2 + 6(4+1+16)]} = 3.83$$

(b) The hydrostatic (mean) stress is given by Eq. (2.53):

$$p = \frac{1}{3}(6) = 2$$

(c) The stress deviator tensor s_{ij} is obtained from Eq. (2.55):

$$\begin{aligned} s_{ij} &= \sigma_{ij} - p\delta_{ij} \\ s_{ij} &= \begin{bmatrix} 1 & 2 & 4 \\ 2 & 2 & 1 \\ 4 & 1 & 3 \end{bmatrix} - 2 \begin{bmatrix} 1 & 0 & 0 \\ 0 & 1 & 0 \\ 0 & 0 & 1 \end{bmatrix} \\ &= \begin{bmatrix} -1 & 2 & 4 \\ 2 & 0 & 1 \\ 4 & 1 & 1 \end{bmatrix} \end{aligned}$$

Since s_{ij} is a pure shear state, as a check, the condition $s_{ii} = 0$ is found to be satisfied.

EXAMPLE 2.3. The states of stress $\sigma_{ij}^{(1)}$ and $\sigma_{ij}^{(2)}$ at two different points in a body are given by Eqs. (2.77) and (2.78) below. Determine which state is more critical to yielding if the following criteria of yielding are used:

- (a) Octahedral normal stress, σ_{oct} .
- (b) Octahedral shear stress, τ_{oct} .
- (c) Maximum shear stress, τ_{max} .

$$\sigma_{ij}^{(1)} = \begin{bmatrix} 10 & 0 & 3 \\ 0 & 3 & 0 \\ 3 & 0 & 2 \end{bmatrix} \text{ (units of stress)} \quad (2.77)$$

$$\sigma_{ij}^{(2)} = \begin{bmatrix} 3 & 0 & 0 \\ 0 & -7 & 0 \\ 0 & 0 & -5 \end{bmatrix} \text{ (units of stress)} \quad (2.78)$$

SOLUTION. (a) From Eq. (2.68), σ_{oct} can be calculated in both cases. Thus we have

$$\sigma_{\text{oct}}^{(1)} = \frac{1}{3}(10+3+2) = 5$$

$$\sigma_{\text{oct}}^{(2)} = \frac{1}{3}(3-7-5) = -3$$

Therefore, based on σ_{oct} , yielding occurs first at the first point.

(b) Using Eq. (2.75), we have

$$\tau_{\text{oct}}^{(1)} = \frac{1}{3}[49+1+64+6(9)]^{1/2} = 4.32$$

$$\tau_{\text{oct}}^{(2)} = \frac{1}{3}[100+4+64]^{1/2} = 4.32$$

Thus, based on τ_{oct} , yielding will occur at both points at the same time.

(c) Following the procedure given in Section 2.1.3, we can find the principal stresses of the first state of stress. The results are

$$\sigma_1^{(1)} = 11, \quad \sigma_2^{(1)} = 3, \quad \sigma_3^{(1)} = 1$$

Equation (2.78) represents a principal state of stress in which

$$\sigma_1^{(2)} = 3, \quad \sigma_2^{(2)} = -5, \quad \sigma_3^{(2)} = -7$$

Thus, the maximum shear stresses are given by Eq. (2.51):

$$\tau_{\text{max}}^{(1)} = \left| \frac{(11)-(1)}{2} \right| = 5$$

$$\tau_{\text{max}}^{(2)} = \left| \frac{(3)-(-7)}{2} \right| = 5$$

Again, based on τ_{max} , yielding will occur at both points at the same time.

2.1.7. Physical Interpretations of Stress Invariants I_1 and J_2

There are several interpretations of stress invariants I_1 and J_2 , one of which has been shown by Eqs. (2.68) and (2.73). Namely, $I_1/3$ is the octahedral normal stress σ_{oct} , while $\sqrt{2/3}J_2$ is the octahedral shear stress. Other interpretations are presented in the following sections.

2.1.7.1. ELASTIC STRAIN ENERGY

The total elastic strain energy W per unit volume of a linear elastic material can be divided into two parts, associated respectively with the change in volume, W_1 , and with the change in shape, W_2 :

$$W = W_1 + W_2 \quad (2.79)$$

where

$$W_1 = \text{dilatational energy} = \frac{1-2\nu}{6E} I_1^2 \quad (2.80)$$

$$W_2 = \text{distortional energy} = \frac{1+\nu}{E} J_2 \quad (2.81)$$

and where E and ν are the modulus of elasticity and Poisson's ratio, respectively. The invariants I_1 and J_2 are seen to be directly proportional to the energy of dilatation and the energy of distortion, respectively.

2.1.7.2. MEAN STRESSES

Consider an infinitesimal spherical element of volume. At any point on the surface of this sphere, the stress vector on the tangent plane has a shear stress component τ_s and a normal stress component σ_s . The mean value of the normal stress σ_s over the spherical surface can be defined by

$$\sigma_m = \lim_{s \rightarrow 0} \left(\frac{1}{S} \int_S \sigma_s dS \right) \quad (2.82)$$

where S denotes the surface of the sphere. Evaluation of this expression gives

$$\sigma_m = \frac{1}{3}(\sigma_1 + \sigma_2 + \sigma_3) = \frac{1}{3}I_1 \quad (2.83)$$

For the shear stress τ_s on the surface of the sphere, the mean value of τ_s can be based upon stresses existing on all possible planes of orientation through the point by carrying out the averaging process over the spherical surface. Since the sign of shear stress has no significance with respect to the physical mechanism of failure, it is expedient to take the average in the sense of the root mean. Thus,

$$\tau_m = \lim_{s \rightarrow 0} \left(\frac{1}{S} \int_S \tau_s^2 dS \right)^{1/2} \quad (2.84)$$

Carrying out the indicated operations leads to

$$\tau_m = \frac{1}{\sqrt{15}} [(\sigma_1 - \sigma_2)^2 + (\sigma_2 - \sigma_3)^2 + (\sigma_3 - \sigma_1)^2]^{1/2} \quad (2.85)$$

or, in terms of the invariant J_2 ,

$$\tau_m = \sqrt{\frac{2}{3}} J_2 \quad (2.86)$$

2.1.7.3. ROOT MEAN OF THE PRINCIPAL SHEAR STRESS

Equations (2.49), (2.51), and (2.52) give the principal shear stresses, whose root mean is

$$\sqrt{\frac{1}{3} \left[\left(\frac{\sigma_1 - \sigma_2}{2} \right)^2 + \left(\frac{\sigma_2 - \sigma_3}{2} \right)^2 + \left(\frac{\sigma_3 - \sigma_1}{2} \right)^2 \right]} = \frac{\sqrt{2}J_2}{2} \quad (2.87)$$

2.1.8. Mohr's Circles for Three-Dimensional Stress Systems

Mohr's diagram is a useful graphical representation of the stress state at a point. In this graphical representation, the state of stress at a point is represented by the Mohr circle diagram, in which the abscissa, σ_n , and ordinate, S_n , of each point give the normal and shear stress components, respectively, acting on a particular cut plane with a fixed normal direction.

In the general three-dimensional case, for a given state of stress at a point, the values of the principal stresses σ_1 , σ_2 , and σ_3 must first be calculated from Eq. (2.34), and the corresponding principal axes are calculated from Eqs. (2.40). Once the values of σ_1 , σ_2 , and σ_3 are known, a Mohr circle diagram can be constructed as shown in Fig. 2.7, for the case $\sigma_1 > \sigma_2 > \sigma_3$. In this figure, the centers of the three Mohr circles C_1 , C_2 , and C_3 have the coordinates $[\frac{1}{2}(\sigma_2 + \sigma_3), 0]$, $[\frac{1}{2}(\sigma_1 + \sigma_3), 0]$, and $[\frac{1}{2}(\sigma_1 + \sigma_2), 0]$, respectively. The three radii R_1 , R_2 , and R_3 are equal to $\frac{1}{2}(\sigma_2 - \sigma_3)$, $\frac{1}{2}(\sigma_1 - \sigma_3)$, and $\frac{1}{2}(\sigma_1 - \sigma_2)$, respectively. Associated with the cut plane n at the considered point with respect to the principal coordinate system, the corresponding normal and shear stresses can be plotted as a point in the σ_n - S_n stress space. Let us consider the positive values of S_n , that is, in the upper half of the σ_n - S_n stress space.

Assuming that the components of the unit normal n are n_1 , n_2 , and n_3 in the direction of the principal axes 1, 2, and 3, respectively, and that $\sigma_1 > \sigma_2 > \sigma_3$, Eqs. (2.42) and (2.43) give

$$\sigma_n^2 + S_n^2 = (\vec{n})^2 = \sigma_1^2 n_1^2 + \sigma_2^2 n_2^2 + \sigma_3^2 n_3^2 \quad (2.88)$$

$$\sigma_n = \sigma_1 n_1^2 + \sigma_2 n_2^2 + \sigma_3 n_3^2 \quad (2.89)$$

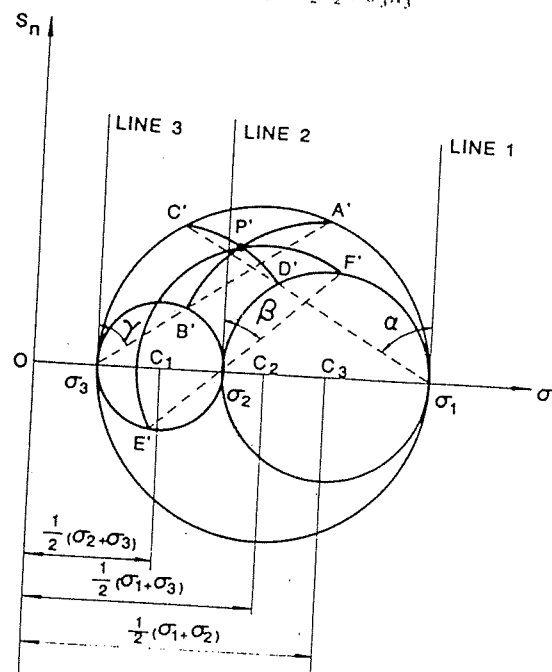


FIGURE 2.7. Mohr's circles in three-dimensional case ($\sigma_1 > \sigma_2 > \sigma_3$).

For the unit vector n , we have

$$n_1^2 + n_2^2 + n_3^2 = 1 \quad (2.90)$$

Solving Eqs. (2.88) to (2.90) for n_1^2 , n_2^2 , and n_3^2 leads to

$$n_1^2 = \frac{S_n^2 + (\sigma_n - \sigma_2)(\sigma_n - \sigma_3)}{(\sigma_1 - \sigma_2)(\sigma_1 - \sigma_3)} \quad (2.91)$$

$$n_2^2 = \frac{S_n^2 + (\sigma_n - \sigma_3)(\sigma_n - \sigma_1)}{(\sigma_2 - \sigma_3)(\sigma_2 - \sigma_1)} \quad (2.92)$$

$$n_3^2 = \frac{S_n^2 + (\sigma_n - \sigma_1)(\sigma_n - \sigma_2)}{(\sigma_3 - \sigma_1)(\sigma_3 - \sigma_2)} \quad (2.93)$$

Since $\sigma_1 > \sigma_2 > \sigma_3$, and the left-hand sides of Eqs. (2.91) to (2.93) are non-negative, it follows that

$$S_n^2 + (\sigma_n - \sigma_2)(\sigma_n - \sigma_3) \geq 0 \quad (2.94)$$

$$S_n^2 + (\sigma_n - \sigma_3)(\sigma_n - \sigma_1) \leq 0 \quad (2.95)$$

$$S_n^2 + (\sigma_n - \sigma_1)(\sigma_n - \sigma_2) \geq 0 \quad (2.96)$$

which may be rewritten as

$$S_n^2 + [\sigma_n - \frac{1}{2}(\sigma_2 + \sigma_3)]^2 \geq \frac{1}{4}(\sigma_2 - \sigma_3)^2 \quad (2.97)$$

$$S_n^2 + [\sigma_n - \frac{1}{2}(\sigma_1 + \sigma_3)]^2 \leq \frac{1}{4}(\sigma_1 - \sigma_3)^2 \quad (2.98)$$

$$S_n^2 + [\sigma_n - \frac{1}{2}(\sigma_1 + \sigma_2)]^2 \geq \frac{1}{4}(\sigma_1 - \sigma_2)^2 \quad (2.99)$$

Relations (2.97) to (2.99) show that the admissible values of σ_n and S_n lie inside, or on the boundaries of, the region bounded by the circles C_1 , C_2 , and C_3 , as shown in Fig. 2.7.

For any fixed value of n_1 , eliminating n_2 and n_3 from Eqs. (2.88) to (2.90) gives

$$[\sigma_n - \frac{1}{2}(\sigma_2 + \sigma_3)]^2 + S_n^2 = \frac{1}{4}(\sigma_2 - \sigma_3)^2 + n_1^2(\sigma_1 - \sigma_2)(\sigma_1 - \sigma_3) \quad (2.100)$$

Therefore, for a given value of n_1 , the point (σ_n, S_n) corresponding to this particular value of n_1 lies on the arc $C'D'$ as shown in Fig. 2.7. To construct this arc, we draw line 1 parallel to the S_n -axis passing through the point $(\sigma_1, 0)$ and measure an angle $\alpha = \cos^{-1} n_1$ from that line. This line making an angle α with line 1 intersects circles C_2 and C_3 in points C' and D' , respectively. Using $[\frac{1}{2}(\sigma_2 + \sigma_3), 0]$ as the center, we draw the arc $C'D'$.

Similarly, for a fixed value of n_2 , eliminating n_1 and n_3 from Eqs. (2.88) to (2.90) gives

$$[\sigma_n - \frac{1}{2}(\sigma_1 + \sigma_3)]^2 + S_n^2 = \frac{1}{4}(\sigma_1 - \sigma_3)^2 + n_2^2(\sigma_2 - \sigma_1)(\sigma_2 - \sigma_3) \quad (2.101)$$

Thus, (σ_n, S_n) corresponding to this particular value of n_2 lies on the arc $E'F'$ in Fig. 2.7. This arc $E'F'$ is drawn from the center $[\frac{1}{2}(\sigma_1 + \sigma_3), 0]$ between the points of intersection, E' and F' , of circles C_1 and C_3 , respectively, with the line making an angle $\beta = \cos^{-1} n_2$ with line 2.

Finally, for a fixed value of n_3 , the relation between the values of (σ_n, S_n) for this particular value of n_3 is given by

$$[\sigma_n - \frac{1}{2}(\sigma_1 + \sigma_2)]^2 + S_n^2 = \frac{1}{4}(\sigma_1 - \sigma_2)^2 + n_3^2(\sigma_3 - \sigma_1)(\sigma_3 - \sigma_2) \quad (2.102)$$

and in this case, the point (σ_n, S_n) lies on arc $A'B'$ in Fig. 2.7.

For a given point P with known values of n_1 , n_2 , and n_3 , one can find (σ_n, S_n) corresponding to these values graphically. Since only two values of n_1 , n_2 , and n_3 are independent, we can use any two values, for example, n_1 and n_3 , to determine the values (σ_n, S_n) corresponding to these values. For a fixed value of n_1 , we construct the arc $C'D'$. Similarly, for a fixed value of n_3 , we construct the arc $A'B'$, as shown in Fig. 2.7. The point of intersection, P' , of the two arcs gives the required values σ_n and S_n corresponding to the given values n_1 , n_2 , and n_3 . The third value, n_2 , is used to check the procedure since the third arc $E'F'$ must pass through the same point P' .

2.1.9. Haigh-Westergaard Stress Space

This geometric representation of the stress state at a point is very useful in the study of plasticity theory and failure criteria. Since the stress tensor σ_{ij} has six independent components, it is, of course, possible to consider these components as positional coordinates in a six-dimensional space. However, this is too difficult to deal with. The simplest alternative is to take the three principal stresses σ_1 , σ_2 , σ_3 as coordinates and represent the stress state at a point as a point in this three-dimensional stress space. This space is called the *Haigh-Westergaard stress space*. In this principal stress space, every point having coordinates σ_1 , σ_2 , and σ_3 represents a possible stress state. Any two stress states at a point P which differ in the orientation of their principal axes, but not in the principal stress values, would then be represented by the same point in the three-dimensional stress space. This implies that this type of stress space representation is focused primarily on the geometry of stress and not on the orientation of the stress state with respect to the material body.

Consider the straight line ON passing through the origin and making the same angle with each of the coordinate axes, as shown in Fig. 2.8. Then, for every point on this line, the state of stress is one for which $\sigma_1 = \sigma_2 = \sigma_3$. Thus, every point on this line corresponds to a hydrostatic or spherical state of stress, while the deviatoric stresses, $s_1 = (2\sigma_1 - \sigma_2 - \sigma_3)/3$, etc., are equal to zero. This line is therefore termed the *hydrostatic axis*. Furthermore, any plane perpendicular to ON is called the *deviatoric plane*. Such a plane has the form

$$\sigma_1 + \sigma_2 + \sigma_3 = \sqrt{3}\xi \quad (2.103)$$

where ξ is the distance from the origin to the plane measured along the

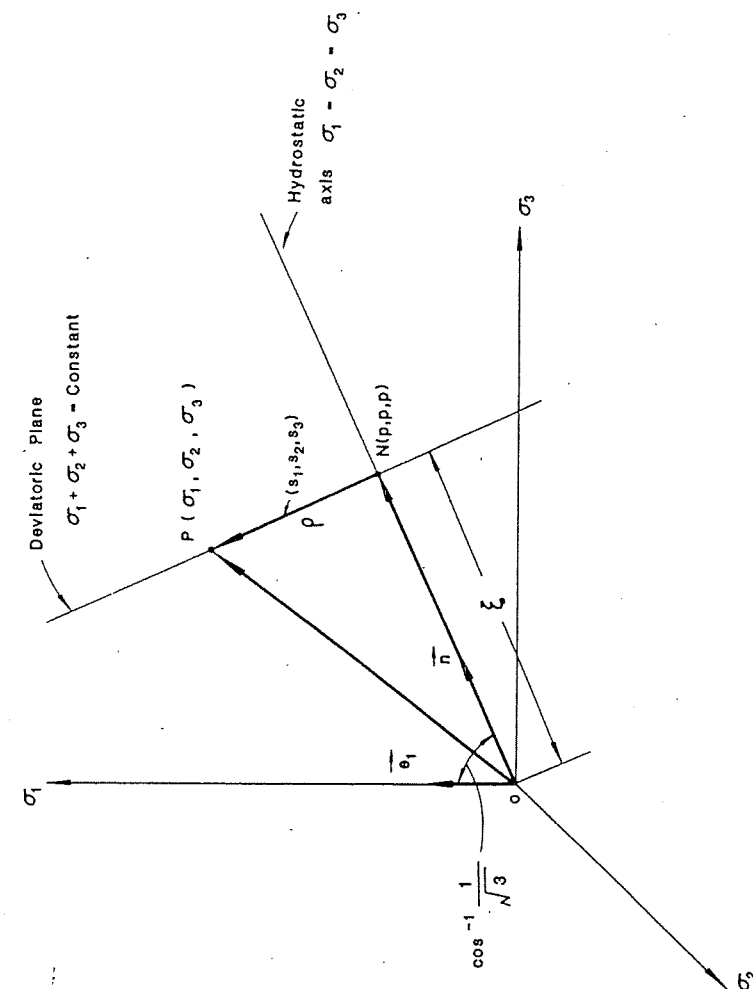


FIGURE 2.8. Haigh-Westergaard stress space.

normal ON . The particular deviatoric plane passing through the origin O ,

$$\sigma_1 + \sigma_2 + \sigma_3 = 0 \quad (2.104)$$

is called the π -plane.

Consider an arbitrary state of stress at a given point with stress components σ_1 , σ_2 , and σ_3 . This state of stress is represented by point $P(\sigma_1, \sigma_2, \sigma_3)$ in the principal stress space in Fig. 2.8. The stress vector OP can be decomposed into two components, the component ON in the direction of the unit vector $n = (1/\sqrt{3}, 1/\sqrt{3}, 1/\sqrt{3})$ and the component NP perpendicular to ON (parallel to the π -plane). Thus,

$$|ON| = OP \cdot n = (\sigma_1, \sigma_2, \sigma_3) \cdot \left(\frac{1}{\sqrt{3}}, \frac{1}{\sqrt{3}}, \frac{1}{\sqrt{3}} \right) \quad (2.105)$$

or

$$|ON| = \frac{1}{\sqrt{3}} (\sigma_1 + \sigma_2 + \sigma_3) = \frac{I_1}{\sqrt{3}} = \sqrt{3} p \quad (2.106)$$

The components of vector NP are given by

$$NP = OP - ON \quad (2.107)$$

But

$$ON = |ON|n = (p, p, p) \quad (2.108)$$

Therefore, substituting from Eq. (2.108) into Eq. (2.107),

$$NP = (\sigma_1, \sigma_2, \sigma_3) - (p, p, p) = [(\sigma_1 - p), (\sigma_2 - p), (\sigma_3 - p)] \quad (2.109)$$

which, using Eq. (2.55), reduces to

$$NP = (s_1, s_2, s_3) \quad (2.110)$$

Hence, the length ρ of vector NP is given by

$$\rho = |NP| = (s_1^2 + s_2^2 + s_3^2)^{1/2} = \sqrt{2J_2} \quad (2.111)$$

or, by Eq. (2.73),

$$\rho = |NP| = \sqrt{3}\tau_{oct} \quad (2.112)$$

Thus, the vectors ON and NP represent the hydrostatic components ($p\delta_{ij}$) and the deviatoric stress components (s_{ij}), respectively, of the state of stress (σ_{ij}) represented by point P in Fig. 2.8.

Now consider the projections of vector NP and the coordinate axes σ_i on a deviatoric plane as shown in Fig. 2.9. In this figure, the axes σ'_1 , σ'_2 , and σ'_3 are the projections of the axes σ_1 , σ_2 , and σ_3 on the deviatoric plane, and NP is the projection of vector NP on the same plane. Since the

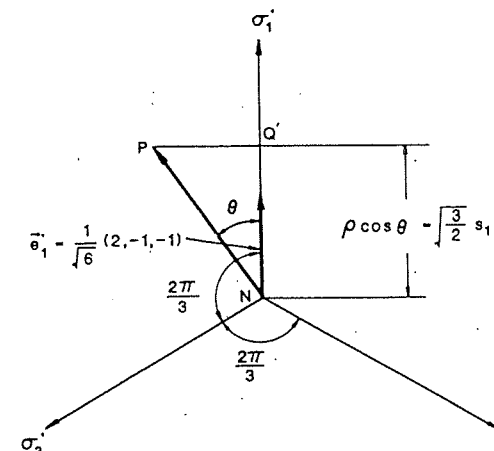


FIGURE 2.9. State of stress at a point projected on a deviatoric plane.

unit vector e'_1 in the direction of the σ'_1 -axis has components $(1/\sqrt{6}) \times (2, -1, -1)$ with respect to the axes σ_1 , σ_2 , and σ_3 , then the projection of vector NP in the direction of the unit vector e'_1 , denoted by NQ' , is given by

$$NQ' = \rho \cos \theta = NP \cdot e'_1 = (s_1, s_2, s_3) \cdot \frac{1}{\sqrt{6}} (2, -1, -1)$$

or

$$\rho \cos \theta = \frac{1}{\sqrt{6}} (2s_1 - s_2 - s_3) \quad (2.113)$$

Substituting for $s_2 + s_3 = -s_1$, we have

$$\rho \cos \theta = \sqrt{\frac{3}{2}} s_1 \quad (2.114)$$

Substituting for ρ from Eq. (2.111) into Eq. (2.114) results in

$$\cos \theta = \frac{\sqrt{3}}{2} \frac{s_1}{\sqrt{2J_2}} \quad (2.115)$$

Using the trigonometric identity $\cos 3\theta = 4\cos^3 \theta - 3\cos \theta$ and substituting for $\cos \theta$ from Eq. (2.115) leads to

$$\cos 3\theta = 4 \left(\frac{\sqrt{3}}{2} \frac{s_1}{\sqrt{2J_2}} \right)^3 - 3 \left(\frac{\sqrt{3}}{2} \frac{s_1}{\sqrt{2J_2}} \right)$$

or

$$\cos 3\theta = \frac{3\sqrt{3}}{2J_2^{3/2}} (s_1^3 - s_1 J_2) \quad (2.116)$$

Substituting for $J_2 = -(s_1 s_2 + s_2 s_3 + s_3 s_1)$ gives

$$\cos 3\theta = \frac{3\sqrt{3}}{2J_2^{3/2}} [s_1^3 + s_1^2(s_2 + s_3) + s_1 s_2 s_3] \quad (2.117)$$

Finally, substituting for $s_2 + s_3 = -s_1$ and $J_3 = s_1 s_2 s_3$, we get

$$\cos 3\theta = \frac{3\sqrt{3}}{2} \frac{J_3}{J_2^{3/2}} \quad (2.118)$$

Equation (2.118) shows that the value of $\cos 3\theta$ is an invariant related to the deviatoric stress invariants J_2 and J_3 . Now, we see that a state of stress $(\sigma_1, \sigma_2, \sigma_3)$ can be expressed by (ξ, ρ, θ) , which are referred to as the Haigh-Westergaard coordinates. Later, in the discussion of the yield and failure conditions, ξ , ρ , and θ are used as parameters required to represent the yield and failure functions in stress space. The relations between $(\sigma_1, \sigma_2, \sigma_3)$ and (ξ, ρ, θ) can be established in the following manner.

From Eq. (2.115), we know

$$s_1 = \frac{2}{\sqrt{3}} \sqrt{J_2} \cos \theta \quad (2.119)$$

In a similar manner, the deviatoric stress components s_2 and s_3 can also be obtained in terms of the angle θ . From Fig. 2.9, these components are given by

$$s_2 = \frac{2}{\sqrt{3}} \sqrt{J_2} \cos \left(\frac{2\pi}{3} - \theta \right) \quad (2.120)$$

$$s_3 = \frac{2}{\sqrt{3}} \sqrt{J_2} \cos \left(\frac{2\pi}{3} + \theta \right) \quad (2.121)$$

These relations are satisfied only if the angle lies in the range (for $\sigma_1 \geq \sigma_2 \geq \sigma_3$)

$$0 \leq \theta \leq \frac{\pi}{3} \quad (2.122)$$

In view of Eqs. (2.58), (2.103), (2.111), and (2.119)–(2.121), the three principal stresses of σ_{ij} are therefore given by

$$\begin{aligned} \begin{Bmatrix} \sigma_1 \\ \sigma_2 \\ \sigma_3 \end{Bmatrix} &= \begin{Bmatrix} p \\ p \\ p \end{Bmatrix} + \frac{2}{\sqrt{3}} \sqrt{J_2} \begin{Bmatrix} \cos \theta \\ \cos(\theta - 2\pi/3) \\ \cos(\theta + 2\pi/3) \end{Bmatrix} \\ &= \frac{1}{\sqrt{3}} \begin{Bmatrix} \xi \\ \xi \\ \xi \end{Bmatrix} + \sqrt{\frac{2}{3}} p \begin{Bmatrix} \cos \theta \\ \cos(\theta - 2\pi/3) \\ \cos(\theta + 2\pi/3) \end{Bmatrix} \end{aligned} \quad (2.123)$$

2.1.10. Equation of Equilibrium

For any volume V of a material body and having S as the surface area of V , as shown in Fig. 2.10, we have the following condition of equilibrium:

$$\int_S \vec{T}_i dS + \int_V F_i dV = 0 \quad (2.124)$$

Substituting \vec{T}_i from Eq. (2.18), Eq. (2.124) may be written as

$$\int_S \sigma_{ij} n_j dS + \int_V F_i dV = 0 \quad (2.125)$$

Using the divergence theorem

$$\int_S u_i n_i dS = \int_V u_{ii} dV \quad (2.126)$$

Eq. (2.125) can be expressed as

$$\int_V (\sigma_{ij,j} + F_i) dV = 0 \quad (2.127)$$

For an arbitrary volume,

$$\sigma_{ij,j} + F_i = 0 \quad (2.128)$$

Equation (2.128) may be written in the (x, y, z) notation as

$$\begin{aligned} \frac{\partial \sigma_x}{\partial x} + \frac{\partial \tau_{xy}}{\partial y} + \frac{\partial \tau_{xz}}{\partial z} + F_x &= 0 \\ \frac{\partial \tau_{yx}}{\partial x} + \frac{\partial \sigma_y}{\partial y} + \frac{\partial \tau_{yz}}{\partial z} + F_y &= 0 \\ \frac{\partial \tau_{zx}}{\partial x} + \frac{\partial \tau_{zy}}{\partial y} + \frac{\partial \sigma_z}{\partial z} + F_z &= 0 \end{aligned} \quad (2.129)$$

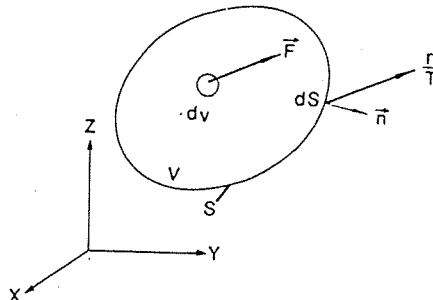


FIGURE 2.10. Equilibrium of a material body.

2.2. Yield Criteria Independent of Hydrostatic Pressure

2.2.1. General Considerations

The yield criterion defines the elastic limits of a material under combined states of stress. As we know, the elastic limit in a simple tension test is the yield stress σ_0 , while in a simple shear test, it is the yield stress τ_0 . In general, the elastic limit or yield stress is a function of the state of stress, σ_{ij} . Hence, the yield condition can generally be expressed as

$$f(\sigma_{ij}, k_1, k_2, \dots) = 0 \quad (2.130)$$

where k_1, k_2, \dots are material constants, which, like σ_0 and τ_0 , are to be determined experimentally.

For isotropic materials, the orientation of the principal stresses is immaterial, and the values of the three principal stresses suffice to describe the state of stress uniquely. A yield criterion therefore consists in a relation of the form

$$f(\sigma_1, \sigma_2, \sigma_3, k_1, k_2, \dots) = 0 \quad (2.131)$$

We have shown that the three principal stresses σ_1, σ_2 , and σ_3 can be expressed in terms of the combinations of the three stress invariants I_1, J_2 , and J_3 , where I_1 is the first invariant of the stress tensor σ_{ij} and J_2 and J_3 are the second and third invariants of the deviatoric tensor s_{ij} . Thus, one can replace Eq. (2.131) by

$$f(I_1, J_2, J_3, k_1, k_2, \dots) = 0 \quad (2.132)$$

Furthermore, these three particular principal invariants are directly related to Haigh-Westergaard coordinates ξ, ρ, θ in stress space [see Eq. (2.123)]. Therefore, Eq. (2.132) can also be rewritten as

$$f(\xi, \rho, \theta, k_1, k_2, \dots) = 0 \quad (2.133)$$

Yield criteria of materials should be determined experimentally. An important experimental fact for metals, shown by Bridgman and others [see Hill (1950)], is that the influence of hydrostatic pressure on yielding is not appreciable. The absence of a hydrostatic pressure effect means that the yield function can be reduced to the form

$$f(J_2, J_3, k_1, k_2, \dots) = 0 \quad (2.134)$$

A stress-strain curve in simple tension does not, in itself, provide any information on the behavior under combined stress. The combined stress tests, analogous to simple tension, are termed proportional or radial loading tests. In these tests, all stresses are increased proportionately. In a biaxial state of stress, for example, σ_1 and σ_2 are increased so as to keep the ratio σ_1/σ_2 constant. It seems that we would need to perform a number of tests

in order to construct a yield locus. However, we will show that one point on the yield locus may give rise to twelve points (Fig. 2.11) if the material (1) is isotropic, (2) is hydrostatic pressure independent, and (3) has equal yield stresses in tension and compression.

Now suppose that a material yields in a state of stress, $(3\sigma, \sigma, 0)$. Point $A_1(3\sigma, \sigma, 0)$ in Fig. 2.11 then lies on the yield locus on the $\sigma_1-\sigma_2$ plane. If the material is isotropic, there is no reason why we should not relabel the axes in an alternative way. We thus conclude that point $A_2(\sigma, 3\sigma, 0)$ also lies on the yield locus. Further, if the material has the same response to tension and compression, points $A_3(-3\sigma, -\sigma, 0)$ and $A_4(-\sigma, -3\sigma, 0)$ will also lie on the yield locus. Now considering A_1 and A_2 or A_3 and A_4 , we see that they are mirror images about a line aa' bisecting the σ_1 and σ_2 axes. Similarly, A_1 and A_4 or A_2 and A_3 , are symmetric about another line bb' perpendicular to line aa' . Hence, there are two symmetric axes for the yield locus.

Moreover, if hydrostatic pressure has no effect on yielding, we can add a hydrostatic state of stress, (h, h, h) say, to a yield stress state to generate another yield point. For example, if a hydrostatic pressure $(-3\sigma, -3\sigma, -3\sigma)$ is added to the yield stress point $(3\sigma, \sigma, 0)$, then the stress state $(0, -2\sigma, -3\sigma)$ is another yield point. Now, we alter its coordinates such that a yield point $B_1(-2\sigma, -3\sigma, 0)$ is obtained on the $\sigma_1-\sigma_2$ plane. Similarly, one can get another new yield point $C_1(2\sigma, -\sigma, 0)$ on the $\sigma_1-\sigma_2$ plane by adding $(-\sigma, -\sigma, -\sigma)$ to $(3\sigma, \sigma, 0)$ and altering the coordinates correspondingly. Finally, because of symmetry, points B_1 and C_1 , like point A_1 , can generate four points B_1, B_2, B_3, B_4 and C_1, C_2, C_3, C_4 , respectively, lying on the

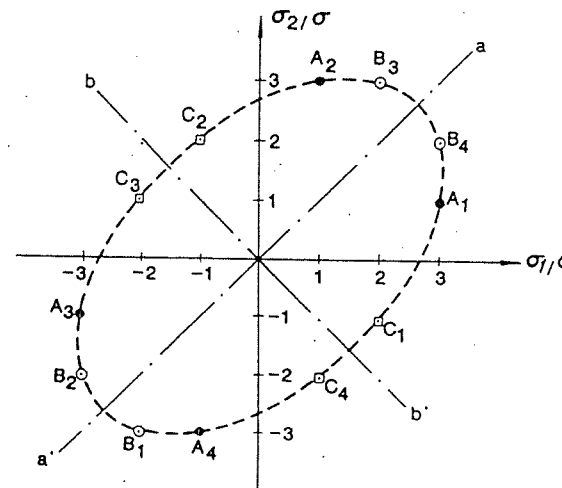


FIGURE 2.11. Yield locus on $\sigma_1-\sigma_2$ plane ($\sigma_3=0$) generated from one test point, A_1 .

yield locus. Now, we have generated a total of twelve yield points on the $\sigma_1-\sigma_2$ plane from one test point. Connecting these points with a smooth curve, we construct a yield locus as shown in Fig. 2.11. Noting that this locus is generated from only one radial test point, it can be considered an approximation of the yield function of a biaxial state of stress for a material with isotropy, with the same response to tension and compression, and with no hydrostatic pressure effect on yielding.

We have discussed so far the general form and some characteristics of a yield function. The very useful yield criteria of Tresca and von Mises for metals will be studied in the following sections.

2.2.2. The Tresca Yield Criterion

Historically, the first yield criterion for a combined state of stress for metals was that proposed in 1864 by Tresca, who suggested that yielding would occur when the maximum shearing stress at a point reaches a critical value k . Stating this in terms of principal stresses (see Section 2.1.4), one-half of the greatest absolute value of the differences between the principal stresses taken in pairs must be equal to k at yield, namely,

$$\text{Max}(\frac{1}{2}|\sigma_1 - \sigma_2|, \frac{1}{2}|\sigma_2 - \sigma_3|, \frac{1}{2}|\sigma_3 - \sigma_1|) = k \quad (2.135)$$

where the material constant k may be determined from the simple tension test. Then

$$k = \frac{\sigma_0}{2} \quad (2.136)$$

in which σ_0 is the yield stress in simple tension.

There are six different expressions in various regions of the $\sigma_1-\sigma_2$ plane, depending upon the relative magnitudes and the signs of σ_1 and σ_2 (see Fig. 2.12). In the first quadrant, between the σ_1 -axis and the bisector of the two axes, the order of the stresses requires that

$$\tau_{\max} = \frac{\sigma_1}{2}$$

Hence, the yield criterion becomes $\sigma_1 = \sigma_0$ and gives the line AB . In the same quadrant, between the bisector and the σ_2 -axis, we have

$$\tau_{\max} = \frac{\sigma_2}{2}$$

and the yield criterion $\sigma_2 = \sigma_0$ is represented by the line BC . In the second quadrant, we have

$$\tau_{\max} = \frac{\sigma_2 - \sigma_1}{2}$$

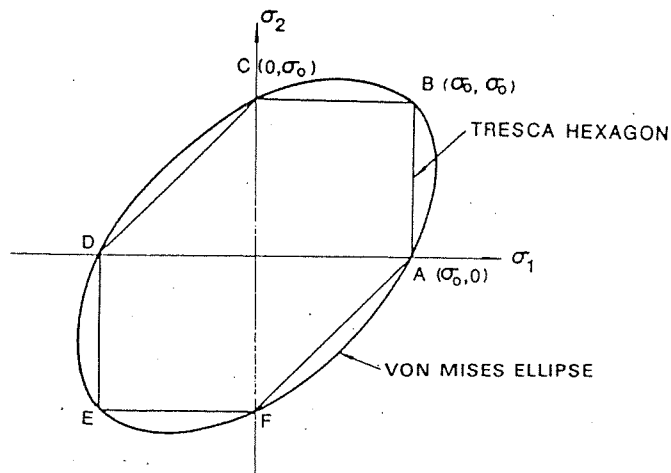


FIGURE 2.12. Yield criteria matched in tension in the coordinate plane $\sigma_3 = 0$.

Thus, the yield criterion becomes $\sigma_2 - \sigma_1 = \sigma_0$, and line CD is obtained. By proceeding similarly for the third and fourth quadrants, it can be found that the yield locus for plane stress is a hexagon $ABCDEF$ as shown in Fig. 2.12.

To represent the yield surface in the principal stress space, Eq. (2.123) is used here for the principal stresses. Assuming the ordering of stresses to be $\sigma_1 > \sigma_2 > \sigma_3$, we can rewrite Eq. (2.135) in the form

$$\frac{1}{2}(\sigma_1 - \sigma_3) = \frac{1}{\sqrt{3}}\sqrt{J_2} \left[\cos \theta - \cos \left(\theta + \frac{2}{3}\pi \right) \right] = k \quad (0 \leq \theta \leq 60^\circ) \quad (2.137)$$

Expanding this equation and noting Eq. (2.136), we obtain the Tresca criterion in terms of stress invariants,

$$f(J_2, \theta) = 2\sqrt{J_2} \sin(\theta + \frac{1}{3}\pi) - \sigma_0 = 0 \quad (0 \leq \theta \leq 60^\circ) \quad (2.138)$$

or identically in terms of the variables ξ, ρ, θ ,

$$f(\rho, \theta) = \sqrt{2}\rho \sin(\theta + \frac{1}{3}\pi) - \sigma_0 = 0 \quad (2.139)$$

Since the hydrostatic pressure has no effect on the yield surface, Eq. (2.138) or Eq. (2.139) must be independent of hydrostatic pressure I_1 or ξ , representing a cylindrical surface whose generator is parallel to the hydrostatic axis. On the deviatoric plane, Eq. (2.138) or Eq. (2.139) is a straight line passing through point A (with $\theta = 0$, and $\rho = \sqrt{2/3}\sigma_0$) and point B (with $\theta = 60^\circ$ and the same ρ as point A), as shown in Fig. 2.13. This is one sector of the yield locus on the deviatoric plane. Each of the five other possible orderings of the magnitudes of the principal stresses gives similar lines in the appropriate sectors of the yield locus on the deviatoric plane, and a regular hexagon

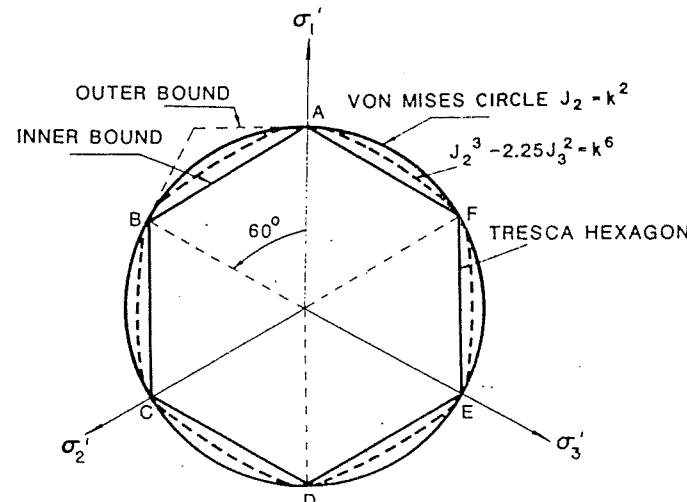


FIGURE 2.13. Yield criteria matched in tension in a deviatoric plane.

$ABCDEF$ is thus obtained. Now we can see that the yield surface is a regular hexagonal prism in principal stress space, as shown in Fig. 2.14. The yield locus for a biaxial state of stress shown in Fig. 2.12 is the intersection of the cylinder with the coordinate plane $\sigma_3 = 0$.

Isotropy means that there is no need to draw the yield surface in a general stress space (σ_{ij}). Nevertheless, some intersections of particular planes with

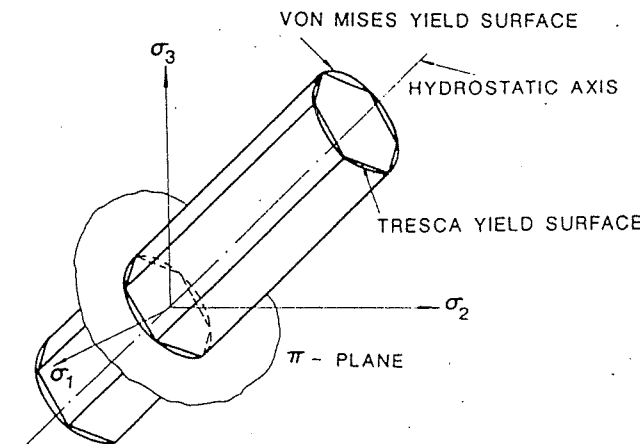
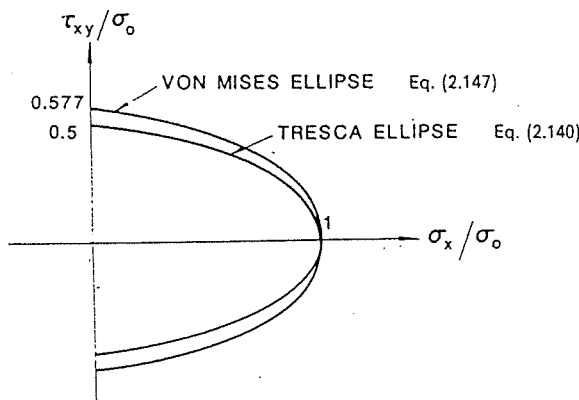


FIGURE 2.14. Yield surfaces in principal stress space.

FIGURE 2.15. Intersection of the $\sigma_x - \tau_{xy}$ plane with the yield surface.

the surface in general stress space are of interest, e.g., the intersection with the $\sigma_x - \tau_{xy}$ plane. In simpler language, the latter intersection is the yield locus for combined normal stress and shear (Fig. 2.15), which is an ellipse

$$\sigma_x^2 + 4\tau_{xy}^2 = \sigma_0^2 \quad (2.140)$$

It is of interest to note that the invariant form of Eq. (2.137) can also be expressed explicitly in terms of the invariants J_2 and J_3 as

$$f(J_2, J_3) = 4J_2^3 - 27J_3^2 - 36k^2J_2^2 + 96k^4J_2 - 64k^6 = 0 \quad (2.141)$$

2.2.3: The von Mises Yield Criterion

Although the maximum shearing stress criterion is simple, it does not reflect any influence of the intermediate principal stress. The octahedral shearing stress or the strain energy of distortion is a convenient alternative choice to the maximum shearing stress as the key variable for causing yielding of materials which are pressure independent. The von Mises yield criterion, dating from 1913, is based on this alternative. It states that yielding begins when the octahedral shearing stress reaches a critical value k . From Eq. (2.73), it must have the form

$$\tau_{oct} = \sqrt{\frac{2}{3}}J_2 = \sqrt{\frac{2}{3}}k \quad (2.142)$$

which reduces to the simple form

$$f(J_2) = J_2 - k^2 = 0 \quad (2.143)$$

or, written in terms of principal stresses,

$$(\sigma_1 - \sigma_2)^2 + (\sigma_2 - \sigma_3)^2 + (\sigma_3 - \sigma_1)^2 = 6k^2 \quad (2.144)$$

where k is the yield stress in pure shear. Yielding will occur in a uniaxial tension test when $\sigma_1 = \sigma_0$, $\sigma_2 = \sigma_3 = 0$. On substitution of these values into Eq. (2.144), one finds

$$k = \frac{\sigma_0}{\sqrt{3}} \quad (2.145)$$

We know from our earlier discussions that for pressure-independent materials, the yield criterion for an isotropic material must have the general form of Eq. (2.134). It follows that the simplest mathematical form compatible with this requirement is Eq. (2.143). This equation represents a circular cylinder whose intersection with the deviatoric plane is a circle with radius $\rho = \sqrt{2}k$.

Note that the constant k , both in Eq. (2.143) for the von Mises criterion and in Eq. (2.135) for the Tresca criterion, is the yield stress in pure shear. However, relations between the yield stress in simple tension, σ_0 , and the parameter k defined by Eq. (2.136) of the Tresca criterion and by Eq. (2.145) of the von Mises criterion are different. If the two criteria are made to agree for a simple tension yield stress σ_0 , the ratio of the yield stress in shear, k , between the von Mises and Tresca criteria is $2/\sqrt{3} = 1.15$, and graphically, the von Mises circle circumscribes the Tresca hexagon as shown in Fig. 2.13. However, if the two criteria are made to agree for the case of pure shear (same k value), the circle will inscribe the hexagon.

The von Mises criterion for a biaxial state of stress is represented by the intersection of the circular cylinder with the coordinate plane $\sigma_3 = 0$, i.e.,

$$\sigma_1^2 + \sigma_2^2 - \sigma_1 \sigma_2 = \sigma_0^2 \quad (2.146)$$

which is an ellipse shown in Fig. 2.12. The intersection of the von Mises surface in general stress space with the $\sigma_x - \tau_{xy}$ plane is also an ellipse, given by

$$\sigma_x^2 + 3\tau_{xy}^2 = \sigma_0^2 \quad (2.147)$$

as shown in Fig. 2.15.

EXAMPLE 2.4. A thin-walled steel cylindrical vessel with diameter $D = 50.8$ cm and wall thickness $t = 6.35$ mm is subjected to an interior pressure p as shown in Fig. 2.16a. The ends of the tube are closed. The yield stress of the steel is $\sigma_0 = 225$ MPa. According to (a) the Tresca criterion and (b) the von Mises criterion, find the pressure p_y under which the vessel begins to yield.

SOLUTION. The state of stress for an element at the wall of the thin-walled pressure vessel is considered biaxial as shown in Fig. 2.16b, in which the circumferential stress σ_c and the axial stress σ_a are given by

$$\sigma_c = \frac{pD}{2t}, \quad \sigma_a = \frac{pD}{4t} \quad (2.148)$$

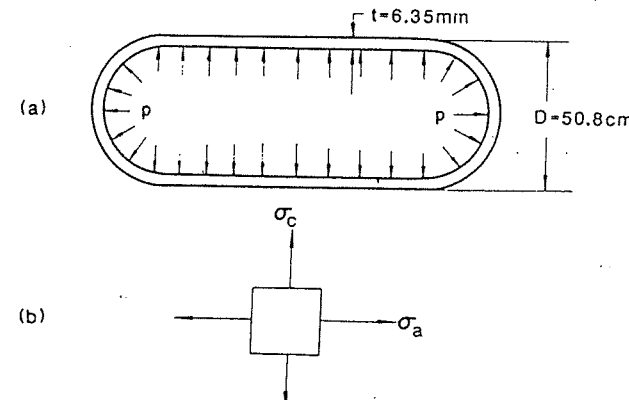


FIGURE 2.16. (a) A thin-walled cylindrical pressure vessel. (b) An element at the wall considered to be in a state of biaxial stress.

although the interior pressure acting on the wall causes a local compressive stress equal to this pressure p . Actually, a triaxial state of stress exists on the inside of the vessel. However, for a thin-walled cylindrical vessel, $D/t \gg 1$, this latter stress, $\sigma_r = p$, is much smaller than σ_a and σ_c and thus is ignored.

(a) Tresca criterion: Clearly, the ordering of the principal stresses is

$$\sigma_1 = \sigma_c, \sigma_2 = \sigma_a, \sigma_3 = \sigma_r = 0 \quad (2.149)$$

Hence, the Tresca yield condition is represented as

$$\tau_{\max} = \frac{\sigma_1 - \sigma_3}{2} = \frac{\sigma_c}{2} = \frac{\sigma_0}{2} \quad (2.150)$$

Substituting Eq. (2.148) into Eq. (2.150), solve for the yield pressure p_y as

$$p_y = \frac{2t\sigma_0}{D} = \frac{(2)(0.00635)(225)}{0.508} = 5.625 \text{ MPa}$$

(b) von Mises criterion: For a state of biaxial stress, the von Mises criterion of Eq. (2.146) is applied, i.e.,

$$\sigma_a^2 + \sigma_c^2 - \sigma_a \sigma_c = \sigma_0^2 \quad (2.151)$$

Substitution of Eq. (2.148) into Eq. (2.151) yields

$$\frac{p^2 D^2}{16t^2} + \frac{p^2 D^2}{4t^2} - \frac{p^2 D^2}{8t^2} = \sigma_0^2$$

The pressure satisfying the above condition is obtained as

$$p_y = \frac{4}{\sqrt{3}} \frac{t}{D} \sigma_0 = \frac{4}{\sqrt{3}} \frac{(0.00635)(225)}{0.508} = 6.495 \text{ MPa}$$

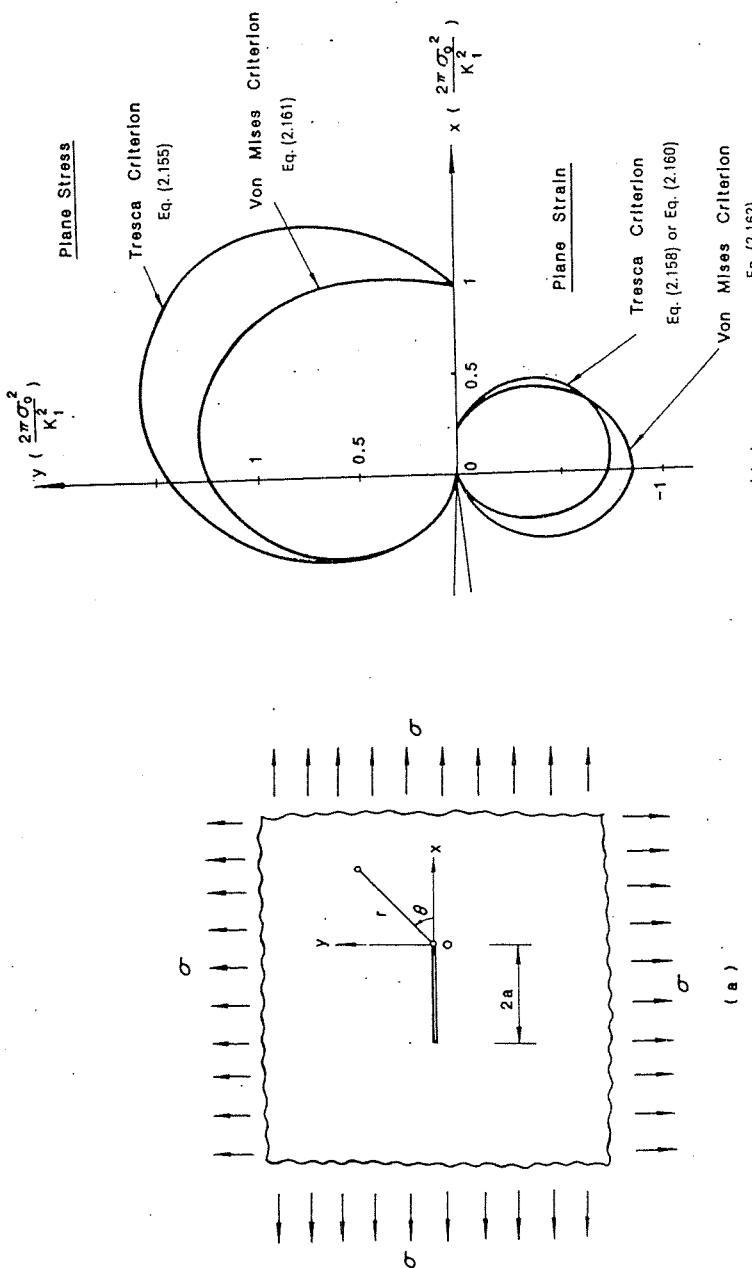


FIGURE 2.17. (a) A plane with a line crack of length $2a$ subjected to biaxial stress at infinity. (b) Elastic-plastic boundary near the crack tip (considered symmetrical about the x -axis).

EXAMPLE 2.5. A plane with a line crack of length $2a$ is subjected to a biaxial stress at infinity as shown in Fig. 2.17a. If the origin of the coordinate system is located at the crack tip, the stress field near the crack tip can be expressed by

$$\begin{aligned}\sigma_x &= \frac{K_1}{\sqrt{2\pi r}} \cos \frac{\theta}{2} \left[1 - \sin \frac{\theta}{2} \sin \frac{3\theta}{2} \right] \\ \sigma_y &= \frac{K_1}{\sqrt{2\pi r}} \cos \frac{\theta}{2} \left[1 + \sin \frac{\theta}{2} \sin \frac{3\theta}{2} \right] \\ \tau_{xy} &= \frac{K_1}{\sqrt{2\pi r}} \sin \frac{\theta}{2} \cos \frac{3\theta}{2} \cos \frac{\theta}{2}\end{aligned}\quad (2.152)$$

where K_1 is the *stress intensity factor*. Determine the plastic zone boundary based on (a) the Tresca criterion and (b) the von Mises criterion.

SOLUTION. (a) Tresca criterion: First we must find the principal stresses from Mohr's circle as below:

$$\sigma_{1,2} = \frac{1}{2} (\sigma_x + \sigma_y) \pm \sqrt{\left(\frac{\sigma_x - \sigma_y}{2}\right)^2 + \tau_{xy}^2}$$

From substitution, we obtain

$$\begin{aligned}\sigma_1 &= \frac{K_1}{\sqrt{2\pi r}} \cos \frac{\theta}{2} \left(1 + \sin \frac{\theta}{2} \right) \\ \sigma_2 &= \frac{K_1}{\sqrt{2\pi r}} \cos \frac{\theta}{2} \left(1 - \sin \frac{\theta}{2} \right)\end{aligned}\quad (2.153)$$

(i) Plane stress case: From $\sigma_3 = 0$, we have

$$\sigma_1 > \sigma_2 > \sigma_3 = 0 \quad \text{for } 0 \leq \theta \leq \pi$$

and the governing yield criterion is

$$\sigma_1 = \frac{K_1}{\sqrt{2\pi r}} \cos \frac{\theta}{2} \left(1 + \sin \frac{\theta}{2} \right) = \sigma_0 \quad (2.154)$$

The plastic zone boundary is obtained as

$$r = \frac{K_1^2}{2\pi\sigma_0^2} \cos^2 \frac{\theta}{2} \left(1 + \sin \frac{\theta}{2} \right)^2 \quad (2.155)$$

(ii) Plane strain case:

$$\sigma_3 = \nu(\sigma_x + \sigma_y) = \nu(\sigma_1 + \sigma_2) \quad (2.156)$$

For $\nu < 0.5$, σ_1 is always the largest of the principal stresses. However, for σ_2 and σ_3 , there are two possibilities, i.e.,

$$\sigma_1 > \sigma_2 > \sigma_3$$

or

$$\sigma_1 > \sigma_3 > \sigma_2$$

depending on the value of Poisson's ratio ν .

If $\sigma_1 > \sigma_2 > \sigma_3$, the condition

$$\sigma_1(1 - \nu) - \nu\sigma_2 = \sigma_0 \quad (2.157)$$

governs yielding. Substituting Eq. (2.153) into Eq. (2.157) and rearranging leads to the following expression for the boundary of the plastic zone:

$$r_1 = \frac{K_1^2}{2\pi\sigma_0^2} \cos^2 \frac{\theta}{2} \left[(1 - 2\nu) + \sin \frac{\theta}{2} \right]^2 \quad (2.158)$$

On the other hand, if $\sigma_1 > \sigma_3 > \sigma_2$, the yield condition becomes

$$\sigma_1 - \sigma_2 = \sigma_0 \quad (2.159)$$

and the plastic zone boundary is obtained as

$$r_2 = \frac{K_1^2}{2\pi\sigma_0^2} \sin^2 \frac{\theta}{2} \quad (2.160)$$

In summary, the real plastic zone boundary r is determined by taking the larger value of r_1 and r_2 given by Eq. (2.158) or Eq. (2.160) respectively, depending on the value of Poisson's ratio ν .

(b) von Mises criterion: We have already determined the three principal stresses σ_1 , σ_2 , and σ_3 . The procedure to obtain the plastic zone boundary is quite straightforward.

(i) Plane stress case: Substituting Eq. (2.153) and $\sigma_3 = 0$ into the von Mises yield condition given by Eqs. (2.144) and (2.145) and rearranging leads to

$$r = \frac{K_1^2}{2\pi\sigma_0^2} \cos^2 \frac{\theta}{2} \left(1 + 3 \sin^2 \frac{\theta}{2} \right) \quad (2.161)$$

(ii) Plane strain case: Using Eq. (2.156) for σ_3 and following the same procedure, we get

$$r = \frac{K_1^2}{2\pi\sigma_0^2} \cos^2 \frac{\theta}{2} \left[(1 - 2\nu)^2 + 3 \sin^2 \frac{\theta}{2} \right] \quad (2.162)$$

The plastic zone boundaries given by Eqs. (2.155), (2.158), (2.160), (2.161) and (2.162) are sketched for $\nu = 0.25$ in terms of the dimensionless ratio $r(2\pi\sigma_0^2/K_1^2)$ in Fig. 2.17b.

2.2.4. Comments on the Tresca and von Mises Criteria

For an isotropic material whose yielding is independent of hydrostatic pressure, the yield criterion must be a cylinder with generator parallel to

the hydrostatic axis. Hence, the complete shape of the yield surface is determined by the cross section with the deviatoric plane. Further, if the yield stresses in tension and in compression are equal, such a cross section must have the sixfold symmetry shown in Fig. 2.13. It follows that a typical section can be determined experimentally by exploring only one of the typical 30° sectors. On the basis of energy considerations, it can be shown that for a wide class of materials, the yield surface must be convex (see Chapters 3 and 4). If we accept the fact that the yield surface is convex, it must lie between the two hexagons shown in Fig. 2.13. The inner Tresca hexagon is obviously a lower bound on the yield curve, and the von Mises cylinder gives a somewhat average value between the outer and inner bounds.

In short, on the basis of the four assumptions of (1) isotropy, (2) hydrostatic pressure independence, (3) equal yield stresses in tension and compression, and (4) convexity, the general shape of the yield surface can be well defined, and the von Mises cylinder cannot deviate much from the actual yield surface $f(J_2, J_3) = 0$.

As a matter of fact, there have been many experimental results showing that the yield points fall between the Tresca hexagon and the von Mises circle and closer to the latter. Osgood in 1947, among many others, performed radial loading tests on thin-wall aluminum tubes, and the results were correlated to an equivalent shearing stress defined by

$$\tau_{eq} = \sqrt[3]{J_2^3 - 2.25J_3^2} = \tau_{oct}\sqrt[3]{1 - 2.25J_3^2/J_2^3} \quad (2.163)$$

A plot of τ_{eq} against the octahedral shear strain γ_{oct} , as shown in Fig. 2.18, shows that the equivalent shearing stress τ_{eq} is a good parameter for

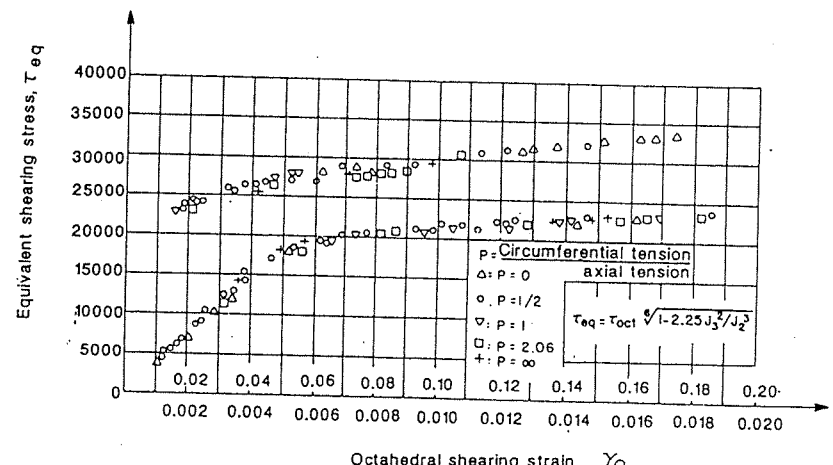


FIGURE 2.18. Osgood's test on thin-walled tubes under tension and interior pressure.

characterizing yielding as well as hardening of the material. The yield criterion is therefore expressed as

$$J_2^3 - 2.25 J_3^2 = k^6 \quad (2.164)$$

where k is the yield stress in pure shear, which is related to the yield stress σ_0 in simple tension by

$$k = \sqrt{\frac{2}{\pi}} \sigma_0 = 0.54 \sigma_0 \quad (2.165)$$

Comparing to $k = 0.5\sigma_0$ of Tresca and $k = 0.577\sigma_0$ of von Mises, the yield stress in pure shear falls between the values predicted by Tresca and von Mises. The yield curve of Eq. (2.165) as plotted in Fig. 2.13 does lie between the Tresca hexagon and the von Mises circle and passes through most of the experimental points.

2.3. Failure Criterion for Pressure-Dependent Materials

2.3.1. Characteristics of the Failure Surface of an Isotropic Material

Failure of a material is usually defined in terms of its load-carrying capacity. However, for perfectly plastic materials, yielding itself implies failure, so the yield stress is also the limit of strength.

As in the case of the yield criteria, a general form of the failure criteria can be given by Eq. (2.130) for anisotropic materials and by Eqs. (2.131) through (2.133) for isotropic ones. As we already know, yielding of most ductile metals is hydrostatic pressure independent. However, the behavior of many nonmetallic materials, such as soils, rocks, and concrete, is characterized by its hydrostatic pressure dependence. Therefore, the stress invariant I_1 or ξ should not be omitted from Eq. (2.132) and Eq. (2.133), respectively.

The general shape of a failure surface, $f(I_1, J_2, J_3) = 0$ or $f(\xi, \rho, \theta) = 0$, in a three-dimensional stress space can be described by its cross-sectional shapes in the deviatoric planes and its meridians in the meridian planes. The cross sections of the failure surface are the intersection curves between this surface and a deviatoric plane which is perpendicular to the hydrostatic axis with $\xi = \text{const}$. The meridians of the failure surface are the intersection curves between this surface and a plane (the meridian plane) containing the hydrostatic axis with $\theta = \text{const}$.

For an isotropic material, the labels 1, 2, 3 attached to the coordinate axes are arbitrary; it follows that the cross-sectional shape of the failure surface must have a threefold symmetry of the type shown in Fig. 2.19b. Therefore, when performing experiments, it is necessary to explore only the sector $\theta = 0^\circ$ to 60° , the other sectors being known by symmetry.

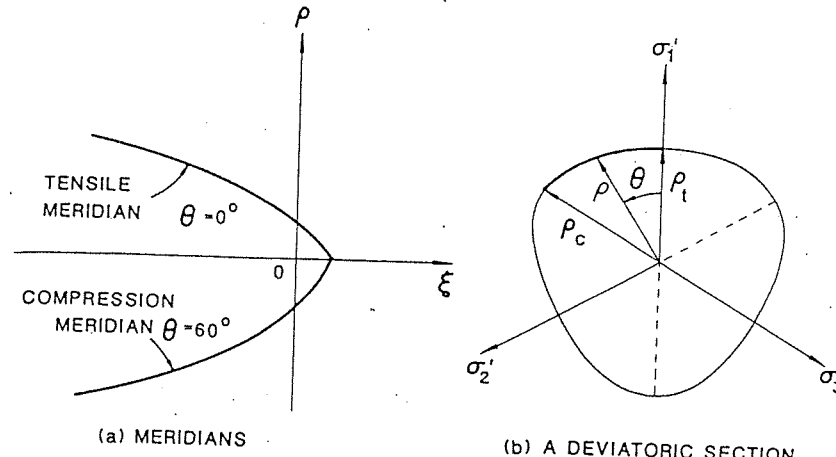


FIGURE 2.19. General shape of the failure surface for an isotropic material.

The typical sector shown in Fig. 2.19b by a heavy line corresponds to the regular ordering of the principal stresses, $\sigma_1 \geq \sigma_2 \geq \sigma_3$. Within this ordering, there are two extreme cases:

$$\sigma_1 = \sigma_2 > \sigma_3 \quad (2.166)$$

and

$$\sigma_1 > \sigma_2 = \sigma_3 \quad (2.167)$$

corresponding to $\theta_1 = 60^\circ$ and $\theta_2 = 0^\circ$, respectively. To show this, we substitute Eqs. (2.166) and (2.167) into Eq. (2.115) and get

$$\cos \theta_1 = \frac{\sqrt{3}}{2} \frac{s_1}{\sqrt{J_2}} = \frac{2\sigma_1 - \sigma_1 - \sigma_3}{2\sqrt{3}\sqrt{\frac{2}{6}(\sigma_1 - \sigma_3)^2}} = \frac{1}{2}$$

and

$$\cos \theta_2 = \frac{2\sigma_1 - \sigma_3 - \sigma_3}{2\sqrt{3}\sqrt{\frac{2}{6}(\sigma_1 - \sigma_3)^2}} = 1$$

respectively. The meridian corresponding to $\theta_1 = 60^\circ$ is called the *compression meridian* in that Eq. (2.166) represents a stress state corresponding to a hydrostatic stress state with a compressive stress superimposed in one direction. The meridian determined by $\theta = 0^\circ$, corresponding to Eq. (2.167), represents a hydrostatic stress state with a tensile stress superimposed in one direction and is therefore called the *tensile meridian*.

Furthermore, the meridian determined by $\theta = 30^\circ$ is sometimes called the *shear meridian*. It also follows from the definition of $\cos \theta$ in Eq. (2.115) that this equation is fulfilled for $\theta = 30^\circ$, when the stresses are $\sigma_1, (\sigma_1 + \sigma_3)/2$,

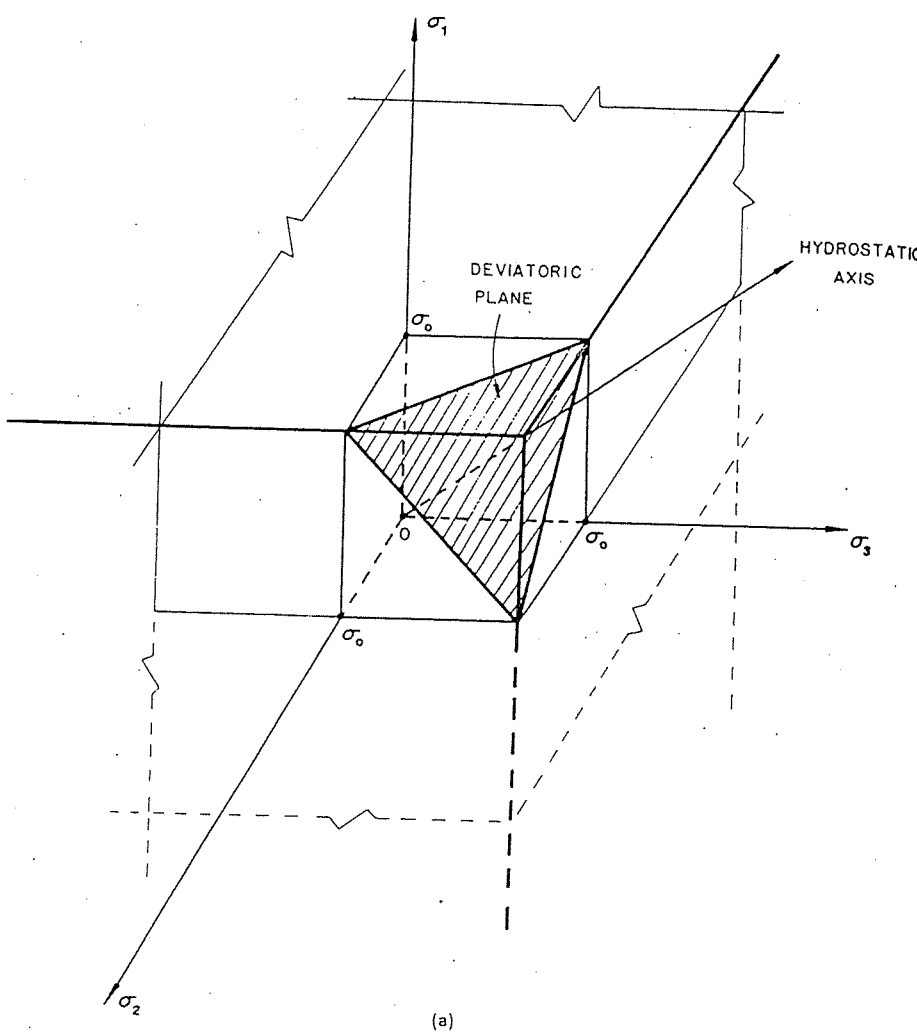


FIGURE 2.20. (a) Rankine maximum-principal-stress criterion; cross sections of Rankine criterion: (b) meridian plane ($\theta = 0^\circ$); (c) π -plane. Figure continues on next page.

and σ_3 , which is a pure shear state $\frac{1}{2}(\sigma_1 - \sigma_3, 0, \sigma_3 - \sigma_1)$ with a hydrostatic stress state $\frac{1}{2}(\sigma_1 + \sigma_3)$ superimposed.

Based on the above considerations, a general shape of the failure surface for an isotropic material may be illustrated in Haigh-Westergaard stress space as shown in Fig. 2.19a. We shall consider this in more detail in the following discussion of some simple failure criteria.

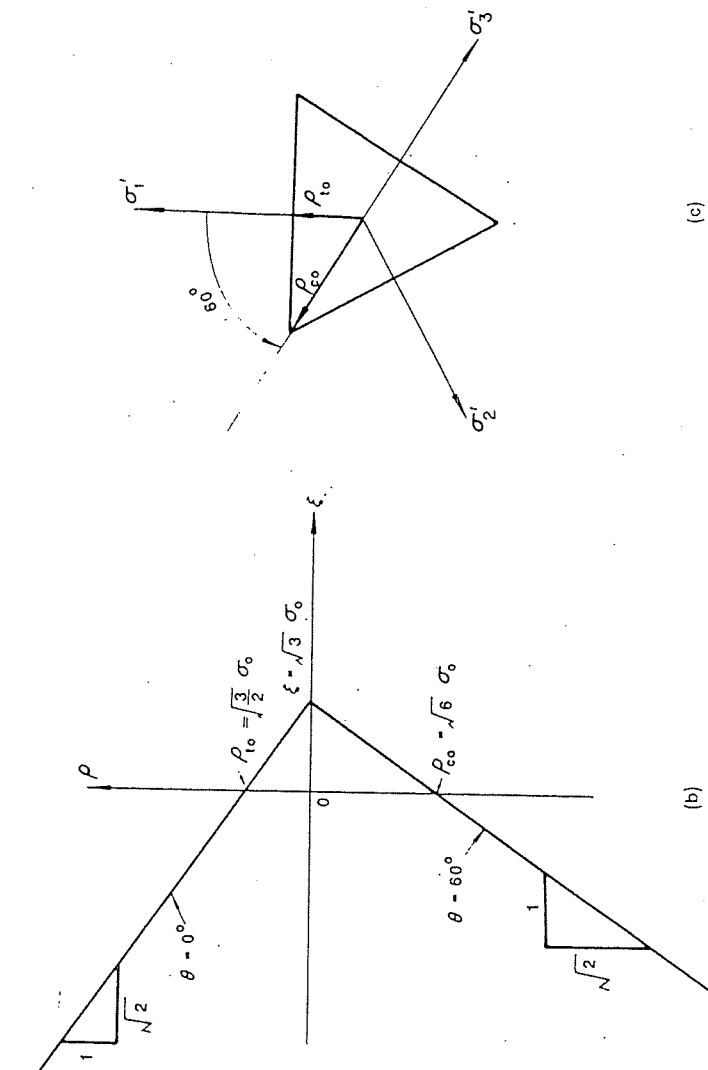


FIGURE 2.20. (b) and (c).

2.3.2. The Maximum-Tensile-Stress Criterion (Rankine)

The maximum-tensile-stress criterion of Rankine, dating from 1876, is generally accepted today to determine whether a tensile failure has occurred for a brittle material. According to this criterion, brittle failure takes place when the maximum principal stress at a point inside the material reaches a value equal to the tensile strength σ_0 as found in a simple tension test, regardless of the normal or shearing stresses that occur on other planes through this point. The equations for the failure surface defined by this criterion are

$$\sigma_1 = \sigma_0, \quad \sigma_2 = \sigma_0, \quad \sigma_3 = \sigma_0 \quad (2.168)$$

which result in three planes perpendicular to the σ_1 , σ_2 , and σ_3 axes, respectively as shown in Fig. 2.20a. This surface will be referred to as the tension-failure surface or the simple tension cutoff. When the variables ξ , ρ , θ or I_1 , J_2 , θ are used, the failure surface can be fully described by the following equations within the range $0 \leq \theta \leq 60^\circ$ using Eq. (2.123).

$$f(I_1, J_2, \theta) = 2\sqrt{3}J_2 \cos \theta + I_1 - 3\sigma_0 = 0 \quad (2.169)$$

or identically

$$f(\xi, \rho, \theta) = \sqrt{2}\rho \cos \theta + \xi - \sqrt{3}\sigma_0 = 0 \quad (2.170)$$

Figures (2.20b and c) show the cross-sectional shape on the π -plane ($\xi = 0$) and the tensile ($\theta = 0^\circ$) and compressive ($\theta = 60^\circ$) meridians of the failure surface.

As we know, some of the nonmetallic materials, such as concrete, rocks, and soils, have a good compressive strength. Under compression loading with confining pressure, this kind of material may even exhibit some ductile and shear failure behavior. Under tension loads, however, a brittle failure behavior with a very low tensile strength is generally observed. Hence, the Rankine criterion is sometimes combined with the Tresca or the von Mises criterion to approximate the failure behavior of such materials. The combined criteria are referred to as the Tresca or the von Mises criterion with a tension cutoff, and their graphical representations consist of two surfaces, corresponding to a combined behavior of shear failure in compression and tensile failure in tension. An example of such failure surfaces is shown in Fig. 2.21, in which the compressive strength is assumed three times as large as the tensile strength.

2.3.3. The Mohr-Coulomb Criterion

Mohr's criterion, dating from 1900, may be considered as a generalized version of the Tresca criterion. Both criteria are based on the assumption that the maximum shear stress is the only decisive measure of impending failure. However, while the Tresca criterion assumes that the critical value

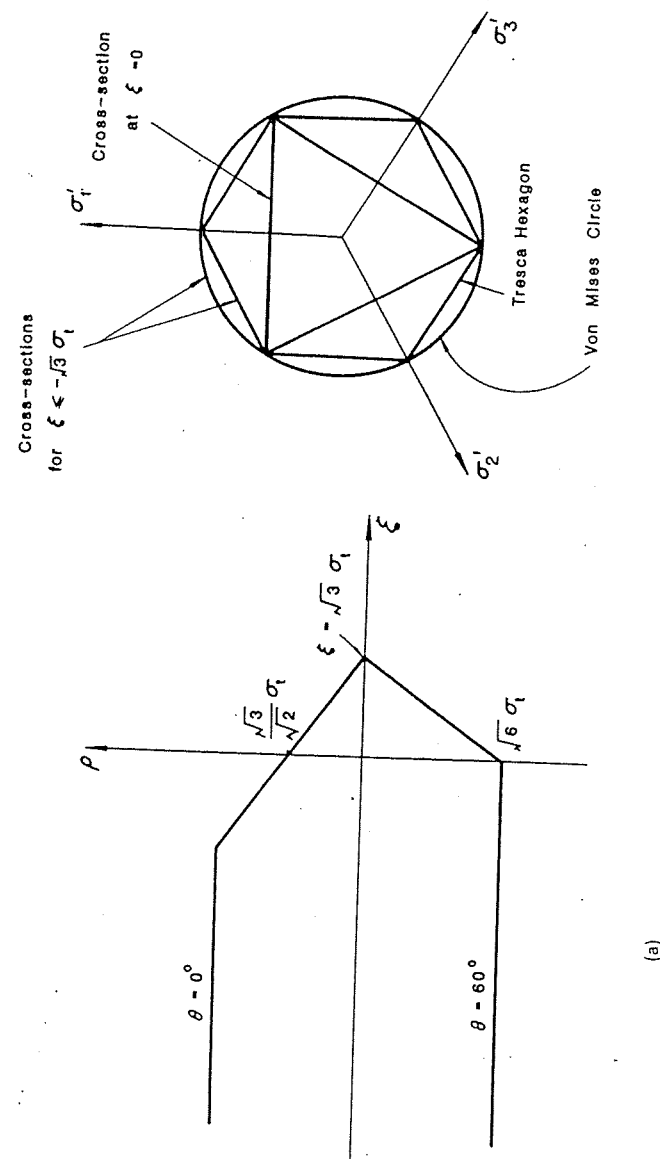


FIGURE 2.21. Tresca and von Mises criteria with tension cutoff: (a) meridian section ($\theta = 0^\circ$); (b) cross sections.

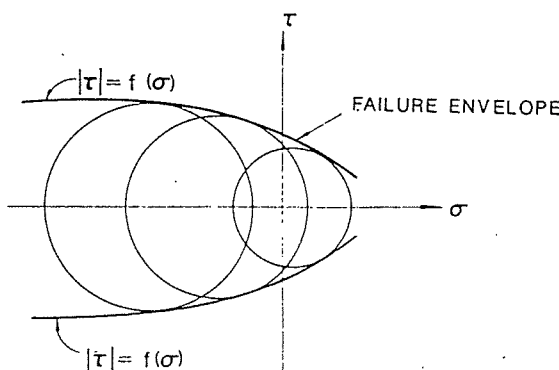


FIGURE 2.22. Graphical representation of Mohr's criterion.

of the shear stress is a constant, Mohr's failure criterion considers the limiting shear stress τ in a plane to be a function of the normal stress σ in the same plane at a point, i.e.,

$$|\tau| = f(\sigma) \quad (2.171)$$

where $f(\sigma)$ is an experimentally determined function.

In terms of Mohr's graphical representation of the state of stress, Eq. (2.171) means that failure of material will occur if the radius of the largest principal circle is tangent to the envelope curve $f(\sigma)$ as shown in Fig. 2.22. In contrast to the Tresca criterion, it is seen that Mohr's criterion allows for the effect of the mean stress or the hydrostatic stress.

The simplest form of the Mohr envelope $f(\sigma)$ is a straight line, illustrated in Fig. 2.23. The equation for the straight-line envelope is known as Coulomb's equation, dating from 1773,

$$|\tau| = c - \sigma \tan \phi \quad (2.172)$$

in which c is the cohesion and ϕ is the angle of internal friction; both are material constants determined by experiment. The failure criterion associated with Eq. (2.172) will be referred to as the Mohr-Coulomb criterion. In the special case of frictionless materials, for which $\phi = 0$, Eq. (2.172) reduces to the maximum-shear-stress criterion of Tresca, $\tau = c$, and the cohesion becomes equal to the yield stress in pure shear $c = k$.

From Eq. (2.172) and for $\sigma_1 \geq \sigma_2 \geq \sigma_3$, the Mohr-Coulomb criterion can be written as

$$\frac{1}{2}(\sigma_1 - \sigma_3) \cos \phi = c - \left[\frac{1}{2}(\sigma_1 + \sigma_3) + \frac{\sigma_1 - \sigma_3}{2} \sin \phi \right] \tan \phi \quad (2.173)$$

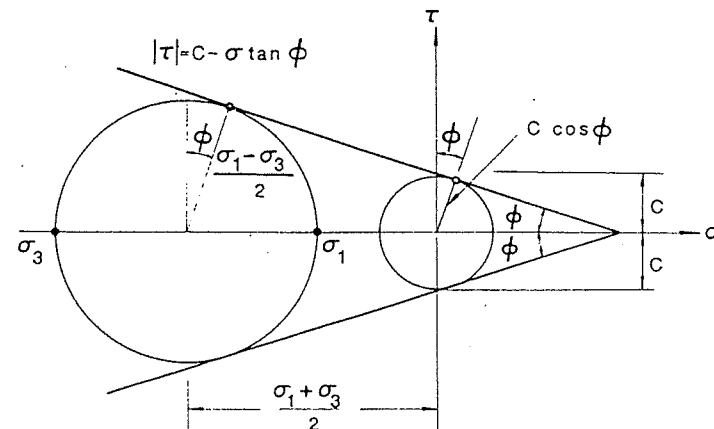


FIGURE 2.23. Mohr-Coulomb criterion: with straight line as failure envelope.

or rearranging

$$\sigma_1 \frac{1 + \sin \phi}{2c \cos \phi} - \sigma_3 \frac{1 - \sin \phi}{2c \cos \phi} = 1 \quad (2.174)$$

If we define

$$f'_c = \frac{2c \cos \phi}{1 - \sin \phi} \quad (2.175)$$

and

$$f'_t = \frac{2c \cos \phi}{1 + \sin \phi} \quad (2.176)$$

Eq. (2.174) is further reduced to

$$\frac{\sigma_1 - \sigma_3}{f'_t - f'_c} = 1 \quad \text{for } \sigma_1 \geq \sigma_2 \geq \sigma_3 \quad (2.177)$$

It is clear from Eq. (2.177) that f'_t is the strength in simple tension while f'_c is the strength in simple compression.

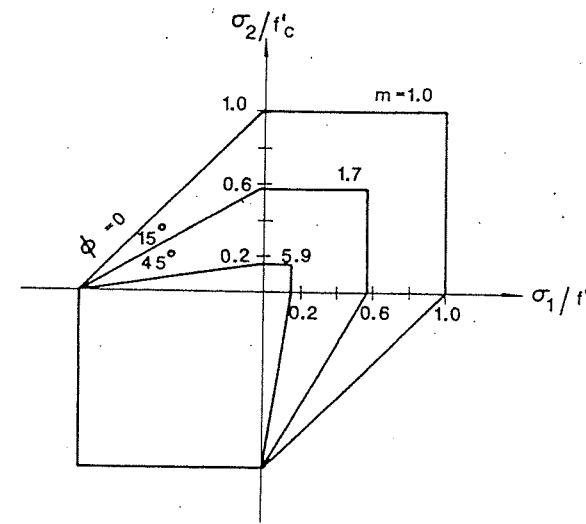
It is sometimes convenient to introduce a parameter m , where

$$m = \frac{f'_c}{f'_t} = \frac{1 + \sin \phi}{1 - \sin \phi} \quad (2.178)$$

Then Eq. (2.177) can be written in the slope-intercept form

$$m\sigma_1 - \sigma_3 = f'_c \quad \text{for } \sigma_1 \geq \sigma_2 \geq \sigma_3 \quad (2.179)$$

Similarly to what we have done for the Tresca criterion, $\sigma_1 - \sigma_3 = \sigma_0$, the failure locus for the Mohr-Coulomb criterion in the $\sigma_1 - \sigma_2$ plane can be sketched based on Eq. (2.179) for several values of m . The failure loci are irregular hexagons as shown in Fig. 2.24.

FIGURE 2.24. Mohr-Coulomb criterion in the coordinate plane $\sigma_3 = 0$.

To demonstrate the shape of the three-dimensional failure surface of the Mohr-Coulomb criterion, we again use Eq. (2.123) and rewrite Eq. (2.174) in the following form:

$$\begin{aligned} f(I_1, J_2, \theta) &= \frac{1}{3} I_1 \sin \phi + \sqrt{J_2} \sin \left(\theta + \frac{\pi}{3} \right) \\ &+ \frac{\sqrt{J_2}}{\sqrt{3}} \cos \left(\theta + \frac{\pi}{3} \right) \sin \phi - c \cos \phi = 0 \end{aligned} \quad (2.180)$$

or identically in terms of variables ξ, ρ, θ :

$$\begin{aligned} f(\xi, \rho, \theta) &= \sqrt{2} \xi \sin \phi + \sqrt{3} \rho \sin \left(\theta + \frac{\pi}{3} \right) \\ &+ \rho \cos \left(\theta + \frac{\pi}{3} \right) \sin \phi - \sqrt{6} c \cos \phi = 0 \end{aligned} \quad (2.181)$$

with $0 \leq \theta \leq \pi/3$.

In principal stress space, this gives an irregular hexagonal pyramid. Its meridians are straight lines (Fig. 2.25a), and its cross section in the π -plane is an irregular hexagon (Fig. 2.25b). Only two characteristic lengths are required to draw this hexagon: the lengths ρ_{t0} and ρ_{c0} , which can be obtained directly from Eq. (2.181) with $\xi = 0, \theta = 0^\circ, \rho = \rho_{t0}$ and $\xi = 0, \theta = 60^\circ, \rho = \rho_{c0}$. Using Eqs. (2.175) and (2.176), we have the following alternative forms for

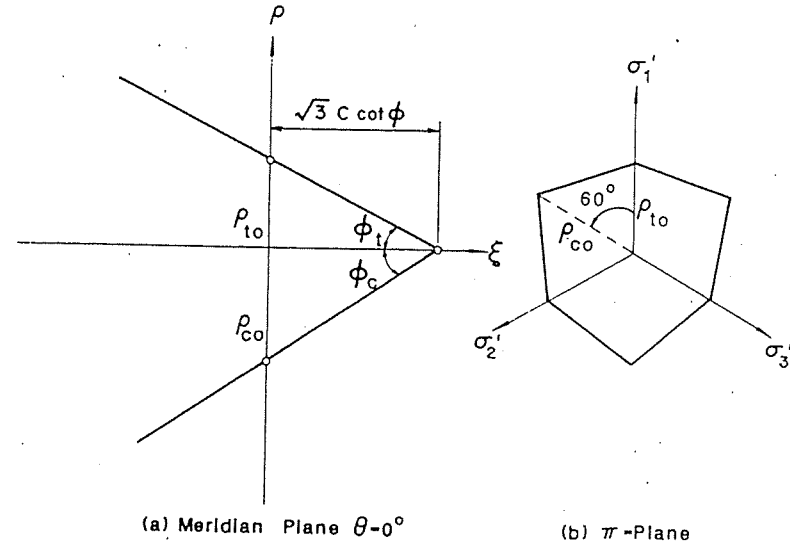


FIGURE 2.25. Graphical representation of Mohr-Coulomb criterion in principal stress space.

ρ_{t0} and ρ_{c0} on the π -plane:

$$\rho_{t0} = \frac{2\sqrt{6}c \cos \phi}{3 + \sin \phi} = \frac{\sqrt{6}f'_c(1 - \sin \phi)}{3 + \sin \phi} \quad (2.182)$$

$$\rho_{c0} = \frac{2\sqrt{6}c \cos \phi}{3 - \sin \phi} = \frac{\sqrt{6}f'_c(1 - \sin \phi)}{3 - \sin \phi} \quad (2.183)$$

and the ratio of these lengths is given by

$$\frac{\rho_{t0}}{\rho_{c0}} = \frac{3 - \sin \phi}{3 + \sin \phi} \quad (2.184)$$

A family of Mohr-Coulomb cross sections in the π -plane for several values of ϕ is shown in Fig. 2.26, where the stresses have been normalized with respect to the compressive strength f'_c . Obviously, the hexagons shown in Fig. 2.24 are the intersections of the pyramid with the coordinate plane $\sigma_3 = 0$. When $f'_c = f'_t$ (or equivalently, when $\phi = 0$ or $m = 1$), the hexagon becomes identical with Tresca's hexagon, as it should.

To obtain a better approximation when tensile stresses occur, it is sometimes necessary to combine the Mohr-Coulomb criterion with a maximum-tensile-strength cutoff. It should be noted that this combined criterion is a three-parameter criterion. We need two stress states to determine the values of c and ϕ and one stress state to determine the maximum tensile stress.

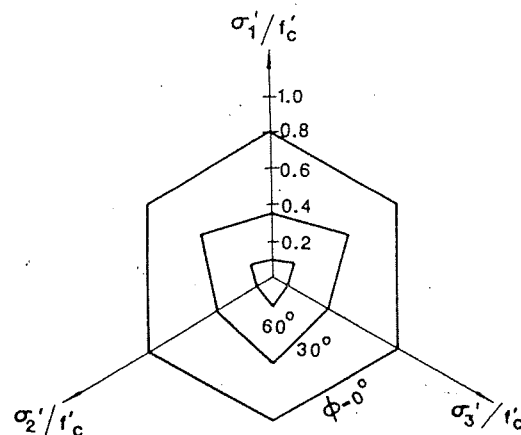


FIGURE 2.26. Failure curves for Mohr-Coulomb criterion in the deviatoric planes.

2.3.4. The Drucker-Prager Criterion

As we have seen, the Mohr-Coulomb failure criterion can be considered a generalized Tresca criterion accounting for the hydrostatic pressure effect. The Drucker-Prager criterion, formulated in 1952, is a simple modification of the von Mises criterion, where the influence of a hydrostatic stress component on failure is introduced by inclusion of an additional term in the von Mises expression to give

$$f(I_1, J_2) = \alpha I_1 + \sqrt{J_2} - k = 0 \quad (2.185)$$

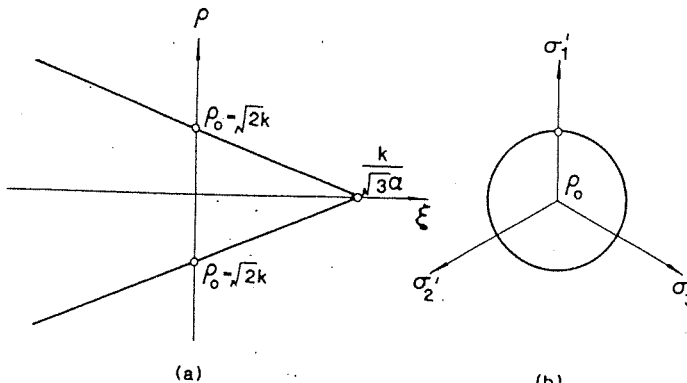
Using variables ξ and ρ leads to

$$f(\xi, \rho) = \sqrt{6}\alpha\xi + \rho - \sqrt{2}k = 0 \quad (2.186)$$

where α and k are material constants. When α is zero, Eq. (2.186) reduces to the von Mises criterion.

The failure surface of Eq. (2.186) in principal stress space is clearly a right-circular cone. Its meridian and cross section on the π -plane are shown in Fig. 2.27.

The Mohr-Coulomb hexagonal failure surface is mathematically convenient only in problems where it is obvious which one of the six sides is to be used. If this information is not known in advance, the corners of the hexagon can cause considerable difficulty and give rise to complications in obtaining a numerical solution. The Drucker-Prager criterion, as a smooth approximation to the Mohr-Coulomb criterion, can be made to match the latter by adjusting the size of the cone. For example, if the Drucker-Prager circle is made to agree with the outer apices of the Mohr-Coulomb hexagon, i.e., the two surfaces are made to coincide along the compression meridian

FIGURE 2.27. Drucker-Prager criterion: (a) meridian plane, $\theta = 0^\circ$; (b) π -plane.

ρ_c , where $\theta = 60^\circ$, then the constants α and k in Eq. (2.185) are related to the constants c and ϕ in Eq. (2.174) by

$$\alpha = \frac{2 \sin \phi}{\sqrt{3}(3 - \sin \phi)}, \quad k = \frac{6c \cos \phi}{\sqrt{3}(3 - \sin \phi)} \quad (2.187)$$

The cone corresponding to the constants in Eq. (2.187) circumscribes the hexagonal pyramid and represents an outer bound on the Mohr-Coulomb failure surface (Fig. 2.28). On the other hand, the inner cone passes through the tension meridian ρ_t , where $\theta = 0$, and will have the constants

$$\alpha = \frac{2 \sin \phi}{\sqrt{3}(3 + \sin \phi)}, \quad k = \frac{6c \cos \phi}{\sqrt{3}(3 + \sin \phi)} \quad (2.188)$$

However, the approximation given by either the inner or the outer cone to the Mohr-Coulomb failure surface can be poor for certain stress states. Other approximations made to match another meridian, say, the shear meridian, may be better.

The Drucker-Prager criterion for a biaxial stress state is represented by the intersection of the circular cone with the coordinate plane of $\sigma_3 = 0$. Substituting $\sigma_3 = 0$ into Eq. (2.185) leads to

$$\alpha(\sigma_1 + \sigma_2) + \sqrt{\frac{1}{3}(\sigma_1^2 - \sigma_1\sigma_2 + \sigma_2^2)} = k \quad (2.189)$$

or rearranging

$$(1 - 3\alpha^2)(\sigma_1^2 + \sigma_2^2) - (1 + 6\alpha^2)\sigma_1\sigma_2 + 6k\alpha(\sigma_1 + \sigma_2) - 3k^2 = 0 \quad (2.190)$$

which is an off-center ellipse as shown in Fig. 2.29.

EXAMPLE 2.6. A material has a tensile strength f'_t equal to one-tenth of its compressive strength f'_c . Consider a material element subjected to a combination of normal stress σ and shear stress τ . On the basis of (a) the

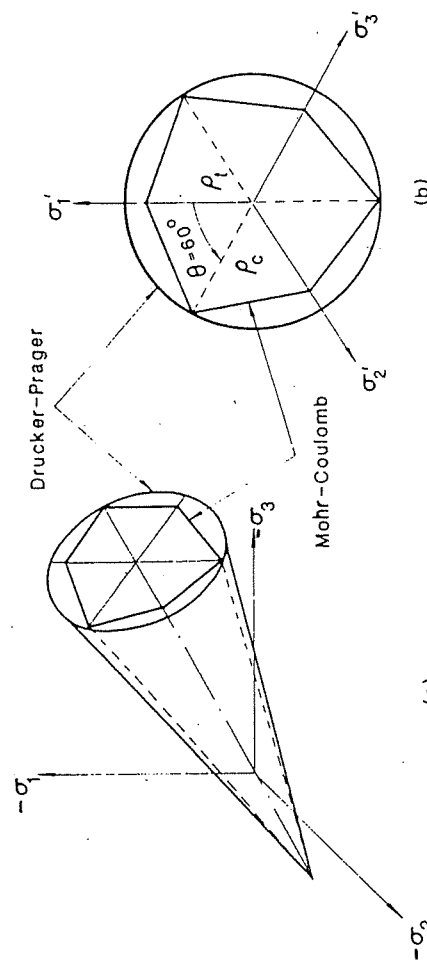


FIGURE 2.28. Drucker-Prager and Mohr-Coulomb criteria matched along the compressive meridian:
(a) in principal stress space; (b) in the deviatoric plane.

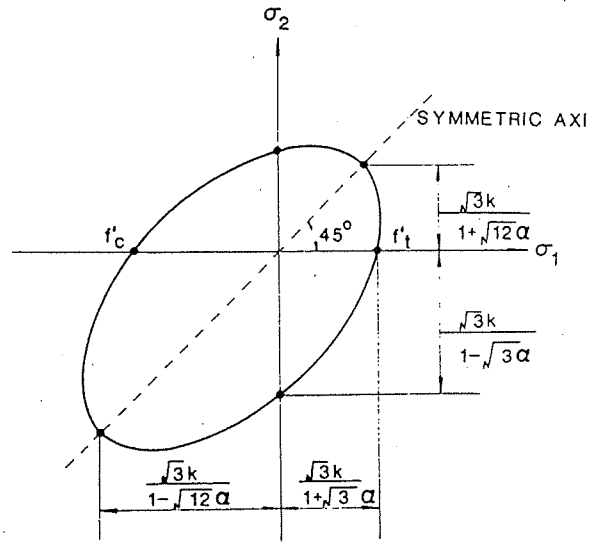


FIGURE 2.29. Drucker-Prager criterion in the coordinate plane $\sigma_3 = 0$.

Mohr-Coulomb criterion and (b) the Drucker-Prager criterion, sketch the interaction curves which govern the failure of the element.

SOLUTION. (a) Mohr-Coulomb criterion: To use the failure condition of Eq. (2.177), we must find the principal stresses from Mohr's circle as

$$\begin{aligned} \frac{\sigma}{2} + \sqrt{\left(\frac{\sigma}{2}\right)^2 + \tau^2} &= \sigma_1 > 0 \\ \frac{\sigma}{2} - \sqrt{\left(\frac{\sigma}{2}\right)^2 + \tau^2} &= \sigma_3 < 0 \end{aligned} \quad (2.191)$$

and the stress in the direction perpendicular to the $\sigma_1-\sigma_3$ plane is zero,

$$\sigma_2 = 0$$

Substituting Eq. (2.191) into Eq. (2.177) yields

$$\frac{\sigma + \sqrt{\sigma^2 + 4\tau^2}}{2f'_t} - \frac{\sigma - \sqrt{\sigma^2 + 4\tau^2}}{2f'_c} = 1 \quad (2.192)$$

Noting that $f'_t = \frac{1}{10}f'_c$ and rearranging, one gets

$$\left[\frac{\sigma + \frac{9}{20}f'_c}{\frac{11}{20}f'_c} \right]^2 + \left(\frac{\tau}{f'_c/\sqrt{40}} \right)^2 = 1 \quad (2.193)$$

which is an ellipse as shown in Fig. 2.30.

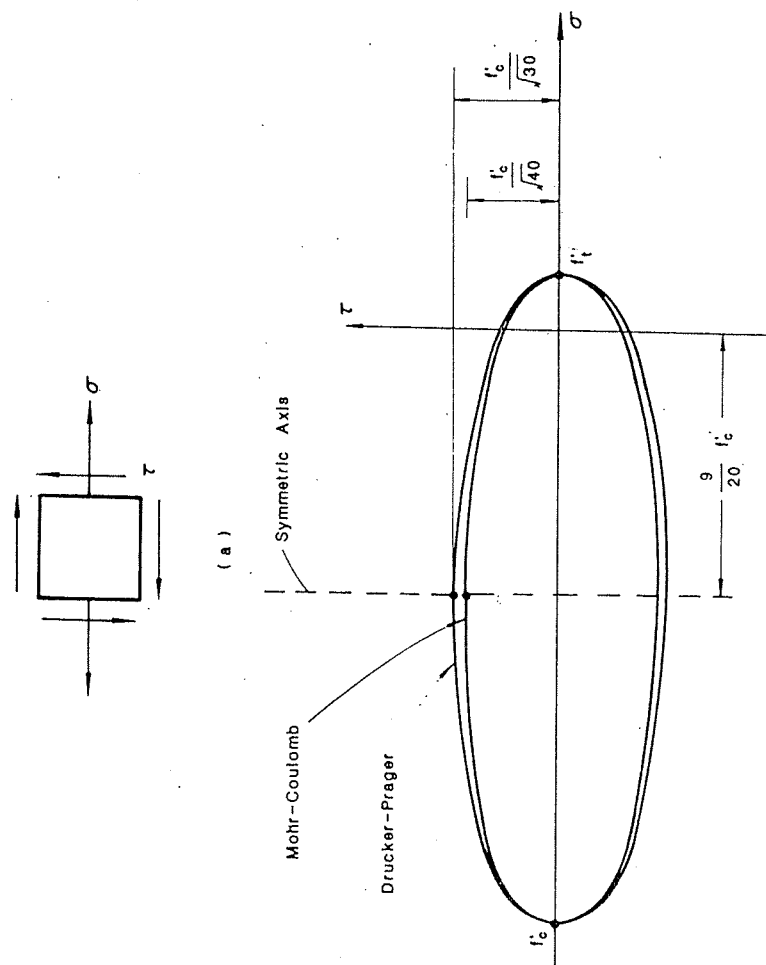


FIGURE 2.30. (a) An element subjected to normal stress σ and shear stress τ . (b) Failure curves based on Mohr-Coulomb and Drucker-Prager criteria.

(b) Drucker-Prager criterion: The material constants α and k can be determined from the given tensile failure stress f'_t and compression failure strength f'_c . Substituting stress states ($\sigma_1 = f'_t$, $\sigma_2 = \sigma_3 = 0$) and ($\sigma_1 = \sigma_2 = 0$, $\sigma_3 = -f'_c$) into the failure condition of Eq. (2.185), one gets

$$\begin{aligned}\alpha f'_t + \frac{1}{\sqrt{3}} f'_t - k &= 0 \\ -\alpha f'_c + \frac{1}{\sqrt{3}} f'_c - k &= 0\end{aligned}\quad (2.194)$$

Noting that $f'_c = 10f'_t$ and solving Eq. (2.194) for k and α leads to

$$k = \frac{2}{11\sqrt{3}} f'_c, \quad \alpha = \frac{9}{11\sqrt{3}} \quad (2.195)$$

For the stress state (σ, τ) , $I_1 = \sigma$, $J_2 = \frac{1}{3}\sigma^2 + \tau^2$, Eq. (2.185) becomes

$$\alpha\sigma + \sqrt{\frac{1}{3}\sigma^2 + \tau^2} - k = 0 \quad (2.196)$$

Substituting Eq. (2.195) into Eq. (2.196) and rearranging, we obtain the failure condition for the given stress state as

$$\left[\frac{\sigma + \frac{9}{20}f'_c}{\frac{11}{20}f'_c} \right]^2 + \left[\frac{\tau}{f'_c/\sqrt{30}} \right]^2 = 1 \quad (2.197)$$

which is also an ellipse as shown in Fig. 2.30.

2.4. Anisotropic Failure/Yield Criteria

Although most materials can be treated as isotropic approximately, strictly speaking, all materials are anisotropic to some extent; that is, the material properties are not the same in every direction. The general form of the failure/yield criteria for anisotropic materials has been expressed by Eq. (2.130). However, the definite form of the function $f(\sigma_{ij}, k_1, k_2, \dots)$ depends very much on the characteristics of the material.

2.4.1. A Yield Criterion for Orthotropic Materials

An orthotropic material has three mutually orthogonal planes of symmetry at every point. The intersection of these planes are known as the principal axes of anisotropy. The yield criterion proposed by Hill (1950), when referred to these axes, has the form

$$\begin{aligned}f(\sigma_{ij}) = a_1(\sigma_y - \sigma_z)^2 + a_2(\sigma_z - \sigma_x)^2 + a_3(\sigma_x - \sigma_y)^2 \\ + a_4\tau_{yz}^2 + a_5\tau_{zx}^2 + a_6\tau_{xy}^2 - 1 = 0\end{aligned}\quad (2.198)$$

where a_1, a_2, \dots, a_6 are material parameters. Equation (2.198) is a quadratic expression of the stresses, representing some kind of energy that governs

yielding of the orthotropic materials. The Hill criterion is therefore considered an extended form of the distortion-energy criterion of von Mises. The omission of the linear terms and the appearance of only differences between normal stress components in the yield criterion implies the assumptions that the material responses are equal in tension and compression and that a hydrostatic stress does not influence yielding.

The material parameters may be determined from three simple tension tests in the directions of the principal axes of anisotropy and three simple shear tests along the planes of symmetry. Denote the tensile strengths as X , Y , and Z , corresponding to the x -, y -, and z -axes, and the shear strengths as S_{23} , S_{31} , and S_{12} , corresponding to the three coordinate planes. Substituting these six states of stress into Eq. (2.198) and solving for the parameters, we obtain

$$\begin{aligned} 2a_1 &= \frac{1}{Y^2} + \frac{1}{Z^2} - \frac{1}{X^2} \\ 2a_2 &= \frac{1}{Z^2} + \frac{1}{X^2} - \frac{1}{Y^2} \\ 2a_3 &= \frac{1}{X^2} + \frac{1}{Y^2} - \frac{1}{Z^2} \\ a_4 &= \frac{1}{S_{23}^2} \\ a_5 &= \frac{1}{S_{31}^2} \\ a_6 &= \frac{1}{S_{12}^2} \end{aligned} \quad (2.199)$$

If the material is transversely isotropic (rotational symmetry about the z -axis), Eq. (2.198) must remain invariant for arbitrary x -, y -axes of reference. It follows that the parameters must satisfy the relations:

$$a_1 = a_2, \quad a_4 = a_5, \quad a_6 = 2(a_1 + 2a_3) \quad (2.200)$$

For a complete isotropy,

$$6a_1 = 6a_2 = 6a_3 = a_4 = a_5 = a_6 \quad (2.201)$$

and Eq. (2.198) reduces to the von Mises criterion.

2.4.2. A Criterion for Ice Crushing Failure

Ice is columnar-grained in structure. It may be treated as an orthotropic material. However, the strength of ice is sensitive to hydrostatic pressure. Its tensile strength is much lower than its compressive strength. The Hill criterion of Eq. (2.198) cannot model such behavior, and therefore, is not

applicable to ice. A yield function including linear terms of normal stresses and having the following form has been proposed:

$$\begin{aligned} f(\sigma_{ij}) = & a_1(\sigma_y - \sigma_z)^2 + a_2(\sigma_z - \sigma_x)^2 + a_3(\sigma_x - \sigma_y)^2 + a_4\tau_{yz}^2 \\ & + a_5\tau_{zx}^2 + a_6\tau_{xy}^2 + a_7\sigma_x + a_8\sigma_y + a_9\sigma_z - 1 = 0 \end{aligned} \quad (2.202)$$

This function, being a special case of the n -type yield functions presented by Pariseau (1968), can describe materials with differing tensile and compressive strengths and predicts a nonlinear (parabolic) increase in strength with confining pressure. If the material is completely anisotropic, nine independent strength measurements would be required to determine the coefficients of Eq. (2.202). Any isotropy, such as transverse isotropy, will reduce the number of required tests. Obviously, this is the case for an ice sheet. Its strength within the horizontal plane is isotropic (see Fig. 2.31). This implies that the coefficients in Eq. (2.202) are not independent, but are subjected to the restrictions

$$a_1 = a_2, \quad a_4 = a_5, \quad a_7 = a_8, \quad a_6 = 2(a_1 + 2a_3) \quad (2.203)$$

which is similar to Eq. (2.200). Thus, Eq. (2.202) reduces to

$$\begin{aligned} f(\sigma_{ij}) = & a_1[(\sigma_y - \sigma_z)^2 + (\sigma_z - \sigma_x)^2] + a_3(\sigma_x - \sigma_y)^2 + a_4(\tau_{yz}^2 + \tau_{zx}^2) \\ & + 2(a_1 + 2a_3)\tau_{xy}^2 + a_7(\sigma_x + \sigma_y) + a_9\sigma_z - 1 = 0 \end{aligned} \quad (2.204)$$

This criterion is employed by Ralston (1977) for ice crushing failure analysis. The values of the coefficients a_1 , a_3 , a_7 , and a_9 can be determined from

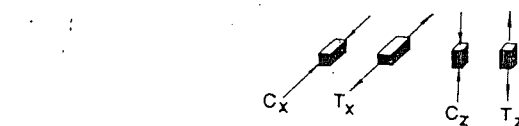
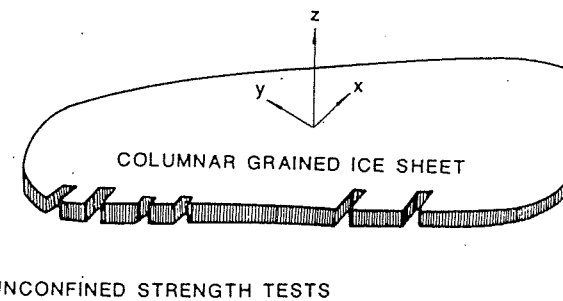


FIGURE 2.31. An example of transversely isotropic material with different tensile and compressive strengths.

compressive and tensile strength measurements as follows:

$$\begin{aligned} a_1 &= \frac{1}{2C_z T_z}, & a_3 &= \frac{1}{T_x C_x} - \frac{1}{2C_z T_z} \\ a_7 &= \frac{1}{T_x} - \frac{1}{C_x}, & a_9 &= \frac{1}{T_z} - \frac{1}{C_z} \end{aligned} \quad (2.205)$$

where T_x, C_x, T_z, C_z are the absolute values of the horizontal and vertical tensile and compressive strengths, respectively (see Fig. 2.31). The value of a_4 could be determined from either a shear test or a compression test on a sample inclined away from the vertical direction.

The ice strength data used in Ralston's work are

$$\begin{aligned} T_x &= 1.01 \text{ MPa}, & T_z &= 1.21 \text{ MPa} \\ C_x &= 7.11 \text{ MPa}, & C_z &= 13.5 \text{ MPa} \end{aligned} \quad (2.206)$$

As can be seen, the compressive strengths are 7 to 11 times as large as the tensile strengths. With the uniaxial strengths given, the coefficients are calculated from Eq. (2.205) as

$$\begin{aligned} a_1 &= 3.06 \times 10^{-2} \text{ MPa}^{-2}, & a_3 &= 10.9 \times 10^{-2} \text{ MPa}^{-2} \\ a_7 &= 84.9 \times 10^{-2} \text{ MPa}^{-1}, & a_9 &= 75.2 \times 10^{-2} \text{ MPa}^{-1} \end{aligned} \quad (2.207)$$

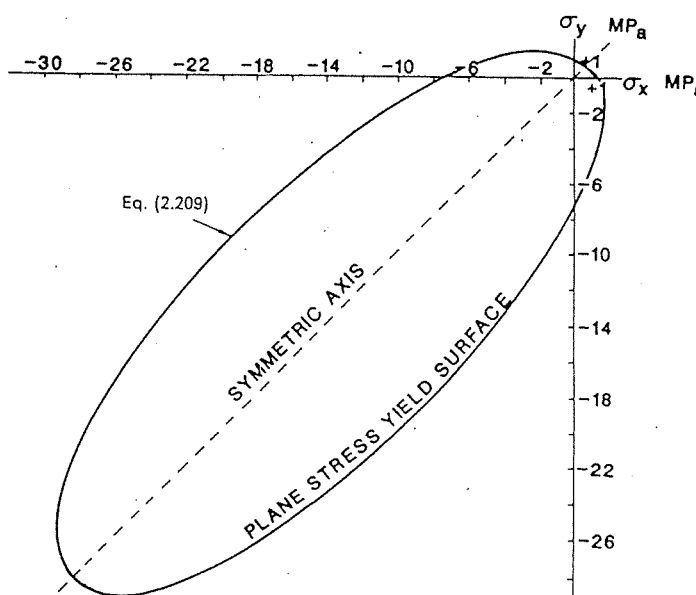


FIGURE 2.32. Yield curve under plane stress condition.

In contrast, if the strength in tension is equal to that in compression, i.e., $T_x = C_x$ and $T_z = C_z$, the coefficients a_7 and a_9 vanish, so the linear terms disappear. In this case, Eq. (2.202) reduces to Eq. (2.198) for an orthotropic material without hydrostatic stress effect. Now, we assume a plane stress condition, i.e.,

$$\sigma_z = \tau_{yz} = \tau_{xz} = 0$$

With this assumption, the yield function (2.204) further reduces to

$$a_1(\sigma_x^2 + \sigma_y^2) + a_3(\sigma_x - \sigma_y)^2 + 2(a_1 + 2a_3)\tau_{xy}^2 + a_7(\sigma_x + \sigma_y) = 1 \quad (2.208)$$

If x and y are the principal stress directions, then τ_{xy} vanishes and we arrive at

$$a_1(\sigma_x^2 + \sigma_y^2) + a_3(\sigma_x - \sigma_y)^2 + a_7(\sigma_x + \sigma_y) = 1 \quad (2.209)$$

The yield surface given by Eq. (2.209) with the coefficients given in Eq. (2.207) is plotted in Fig. 2.32. This yield surface is a long narrow ellipse symmetric about the line $\sigma_x = \sigma_y$.

2.5. Summary

This chapter deals with the yield/failure criteria of materials under combined stress conditions. The stress analysis of Section 2.1 at the beginning of this chapter gives the necessary background for the later discussion. As we have already seen, a better understanding of the yield/failure criteria can be obtained if their geometric shapes can be described intuitively in the principal stress space.

There are four types of criteria introduced in this chapter: isotropic and independent of hydrostatic pressure; isotropic and dependent on hydrostatic pressure; orthotropic and independent of hydrostatic pressure; and orthotropic and dependent on hydrostatic pressure. Characteristics of these criteria may be summarized as follows:

Isotropic without hydrostatic pressure effect. This type of yield function, $f(J_2, J_3, k_1, k_2, \dots) = 0$, independent of the variable J_1 or ξ , suggests that the shearing stress is the only decisive factor which governs yielding. Its geometric shape is a cylinder with meridians parallel to the hydrostatic axis. The cross sections with the deviatoric planes have sixfold symmetry. The Tresca and von Mises criteria are the most useful yield functions of this type.

Isotropic with hydrostatic pressure effect. The yield/failure functions of this type depend on both the hydrostatic stress and the shearing stresses, having the form $f(I_1, J_2, J_3, k_1, k_2, \dots) = 0$. The corresponding yield/failure surface may have either curved or straight meridians, which are no longer parallel to the hydrostatic axis. Its deviatoric sections

generally have threefold symmetry. The Mohr-Coulomb and Drucker-Prager criteria, including a linear term in I_1 and ξ in their expressions and having conical shapes in the principal stress space, are the simplest functions of this type.

Orthotropic with and without hydrostatic pressure effect. It should be noted that for anisotropic materials, the yield function, $f(\sigma_{ij}, k_1, k_2, \dots) = 0$, is established in a certain reference coordinate system which is fixed with respect to the orientation of the material body. We cannot change the reference coordinates without changing the form of the function. Thus, it is impossible to illustrate the yield surface in the three-dimensional principal stress space, as we have done for isotropic materials. The yield functions of Eq. (2.198) and Eq. (2.202), suitable only for materials with orthotropic anisotropy, are referenced from the three principal axes of anisotropy of the material. Equation (2.202) is different from Eq. (2.198) in that the linear terms of normal stresses are included in the yield function, reflecting the influence of hydrostatic pressure.

References

- Chen, W.F., 1982. *Plasticity in Reinforced Concrete*, McGraw-Hill, New York.
 Chen, W.F., and A.F. Sallab, 1982. *Constitutive Equations for Engineering Materials, Volume 1: Elasticity and Modeling*, Wiley-Interscience, New York.
 Drucker, D.C., "The Relation of Experiments to Mathematical Theories of Plasticity," *Journal of Applied Mechanics* 16: 349-357 (1949).
 Hill, R., 1950. *The Mathematical Theory of Plasticity*, Oxford University Press, New York.
 Pariseau, W.G., 1968. "Plasticity Theory for Anisotropic Rocks and Solids," *Proceedings of the Tenth Symposium of Rock Mechanics*, Chapter 10, University of Texas, Austin.
 Ralston, T.D., 1977. "Yield and Plastic Deformation in Ice Crushing Failure" (Preprint), ICSI/AIDJEX Symposium on Sea Ice-Processes and Models, Seattle, Washington.

PROBLEMS

- 2.1. The stress tensor σ_{ij} at a point is given by

$$\sigma_{ij} = \begin{bmatrix} 0 & 0 & 0 \\ 0 & 300 & 100\sqrt{3} \\ 0 & 100\sqrt{3} & 100 \end{bmatrix} \text{ (stress unit)}$$

Find:

- (a) The magnitude of the normal and shear stresses on an area element whose unit normal vector is given by $n = (\frac{1}{2}, \frac{1}{2}, 1/\sqrt{2})$.
- (b) The magnitude of the principal stresses.
- (c) The orientation of the principal axes of stresses.
- (d) The octahedral stresses.
- (e) The maximum shear stress.

- 2.2. For the given stress tensor σ_{ij} :

$$\sigma_{ij} = \begin{bmatrix} \frac{3}{2} & -\frac{1}{2\sqrt{2}} & -\frac{1}{2\sqrt{2}} \\ -\frac{1}{2\sqrt{2}} & \frac{11}{4} & -\frac{5}{4} \\ -\frac{1}{2\sqrt{2}} & -\frac{5}{4} & \frac{11}{4} \end{bmatrix} \text{ (stress unit)}$$

- (a) find the principal stresses and their associated principal directions;
- (b) find the deviatoric stress tensor, s_{ij} , and the principal deviatoric stresses s_1 , s_2 , and s_3 ;
- (c) determine the deviatoric stress invariants J_1 , J_2 , and J_3 .
- 2.3. (a) If $s_1 > s_2 > s_3$, can $s_3 = 0$? Explain.
 (b) Can J_2 be negative? Explain.
 (c) Can J_3 be positive? Explain.
- 2.4. Show that the ratio $\tau_{\text{oct}}/\tau_{\text{max}}$ is bounded by

$$\frac{\sqrt{6}}{3} \leq \frac{\tau_{\text{oct}}}{\tau_{\text{max}}} \leq \frac{2\sqrt{2}}{3}$$

- 2.5. Prove the following relations:

- (a) $J_2 = \frac{1}{3}I_1^2 - I_2$.
- (b) $J_3 = I_3 - \frac{1}{3}I_1I_2 + \frac{2}{27}I_1^3$.
- (c) $\tau_{\text{oct}} = \frac{\sqrt{2}}{3}(I_1^2 - 3I_2)^{1/2}$.
- (d) $J_2 = -(s_1s_2 + s_2s_3 + s_3s_1)$.

- 2.6. Given Cauchy's formula for stress at a point as

$$T_i = \sigma_{ij}n_j$$

where T_i is the stress vector acting on a plane-area element with normal vector n_i , show that the stress components σ_{ij} form a second-order tensor using the definition of tensors.

- 2.7. Show that subtracting a hydrostatic stress from a given state of stress does not change the principal directions.
- 2.8. Prove that the shear stress component S_n acting on any plane passing through a given point is unchanged by the addition of hydrostatic tension or compression to the original state of stress.
- 2.9. The stress state at a point is given by

$$\sigma_{ij} = \begin{bmatrix} 30 & 45 & 60 \\ 45 & 20 & 50 \\ 60 & 50 & 10 \end{bmatrix} \text{ MPa}$$

- (a) Determine the stress invariants I_1 , J_2 , J_3 , and θ .
- (b) Based on the expressions for principal stresses in terms of the stress invariants I_1 , J_2 , and θ , find the magnitudes of the principal stresses σ_1 , σ_2 , and σ_3 .

2.10. (a) Show that

$$\frac{\partial J_3}{\partial \sigma_{ij}} = s_{ik}s_{kj} - \frac{2}{3}J_2\delta_{ij}$$

(b) Find $\partial\theta/\partial\sigma_{ij}$.

- 2.11. Show that if $I_1 = \sigma_x + \sigma_y + \sigma_z = 0$, the stress state σ_{ij} is a pure shear state. Note that the state of stress is termed a pure shear state if there exists some coordinate system $0x'y'z'$ such that $\sigma_{x'}^* = \sigma_{y'}^* = \sigma_{z'}^* = 0$. $\sigma_{x'} = \sigma_{y'} = \sigma_{z'} = 0$

- 2.12. If a stress state is obtained by superposing two other stress states, show that:

- (a) The maximum principal stress is not greater than the sum of the individual maximum principal stresses.
- (b) The maximum shear stress is not greater than the sum of the individual maximum shear stresses.
- (c) The resultant hydrostatic pressure component is simply the algebraic summation of the hydrostatic components of the two individual states, but the resultant shear component is the vectorial summation of the shear components of the two individual states.

- 2.13. Considering Eq. (2.61) for the principal deviatoric stresses,

$$s^3 - J_2s - J_3 = 0$$

and making the substitution $s = r \sin \psi$ leads to

$$\sin^3 \psi - \frac{J_2}{r^2} \sin \psi - \frac{J_3}{r^3} = 0$$

- (a) Considering the similarity of the latter equation to the trigonometric identity,

$$\sin^3 \psi - \frac{1}{3} \sin \psi + \frac{1}{4} \sin 3\psi = 0$$

show that r and ψ are invariants related to J_2 and J_3 through

$$r = \frac{2}{\sqrt{3}} \sqrt{J_2} \quad \text{and} \quad \sin 3\psi = -\frac{3\sqrt{3}}{2} \frac{J_3}{J_2^{3/2}}$$

- (b) Using the results obtained in (a) with Eqs. (2.111) and (2.118), prove that:
(i) $r = \sqrt{2/3}\rho$; (ii) $\psi = [\theta - (\pi/6)]$ and ψ varies in the range $-\pi/6 \leq \psi \leq \pi/6$ for $0 \leq \theta \leq \pi/3$.
(c) For an arbitrary state of stress defined by the principal stresses $\sigma_1 \geq \sigma_2 \geq \sigma_3$ and considering the projection on the π -plane (as shown in Fig. 2.9), show the corresponding values of θ and ψ for the following cases: (i) $\sigma_2 = \sigma_3$; (ii) $\sigma_2 = \sigma_1$; (iii) $\sigma_2 = \frac{1}{2}(\sigma_1 + \sigma_3)$. (Note: In many cases, the invariants ψ or θ are conveniently used to replace J_3 in writing the general expressions for yield or failure functions.)

- 2.14. A metal yields when the maximum shear stress, τ_{max} , reaches the value of 125 MPa. A material element of this metal is subjected to a biaxial state of stress:

$$\sigma_1 = \sigma, \quad \sigma_2 = \alpha\sigma, \quad \sigma_3 = 0$$

where α is a constant. For what values of (σ, α) will yielding occur?

- 2.15. A metal yields at a state of plane stress with

$$\sigma_x = 80 \text{ MPa}, \quad \sigma_y = 40 \text{ MPa}, \quad \tau_{xy} = 80 \text{ MPa}$$

Assume isotropy, independence of hydrostatic pressure, and equality of properties in tension and compression.

- (a) Find all other biaxial states of stress at yield in (σ_1, σ_2) space.
- (b) Plot the results in part (a) in (σ_1, σ_2) space and estimate the yield stress (i) in axial tension and (ii) in simple shear, and give limits of possible error of your estimates, based on convexity.
- (c) Determine the yield stresses in (b), based on (i) the von Mises criterion; (ii) the Tresca criterion; (iii) $F(J_2, J_3) = J_2^3 - 2.25J_3^2 - k^6 = 0$.

- 2.16. A long steel circular tube of 25.4-cm diameter and 0.32-cm wall thickness is subjected to an interior pressure of 4.83 MPa. The ends of the tube are closed. The yield stress of the steel is 227 MPa. Find the additional axial tensile load P which is needed to cause yielding of the tube, based on (i) the von Mises criterion; (ii) the Tresca criterion; (iii) $f(J_2, J_3) = J_2^3 - 2.25J_3^2 - k^6 = 0$.

- 2.17. The stress tensor at a point under the working load condition is given by

$$\sigma_{ij} = \begin{bmatrix} 25 & 50 & 0 \\ 50 & 100 & 0 \\ 0 & 0 & -50 \end{bmatrix} \text{ MPa}$$

The yield stress of the material is 250 MPa. Based on (a) the Tresca criterion and (b) the von Mises criterion, calculate the factor of safety of the stress state against failure (i) if all stresses are increased proportionally to reach the yield surface and (ii) if only the normal stress σ_x is increased to a critical failure value at the yield surface.

- 2.18. A material fails under confined compression loading with stresses $\sigma_1 = \sigma_2 = -\frac{1}{3}f'_c$, $\sigma_3 = -2.0f'_c$, where f'_c is its uniaxial compressive strength.

- (a) Determine the constants c and ϕ in terms of f'_c for the Mohr-Coulomb criterion.
- (b) Determine the constants k and α for the Drucker-Prager criterion.
- (c) Illustrate the Mohr-Coulomb and Drucker-Prager failure surfaces by plotting their cross sections in the π -plane and the meridian section in the meridian plane of $\theta = 0^\circ$.
- (d) Find the largest discrepancy in a deviatoric plane between the Mohr-Coulomb and Drucker-Prager criteria.
- (e) Find the tensile strength f'_t predicted by these two criteria.

- 2.19. Assume that the material described in Problem 2.18 has a tensile strength $f'_t = 0.1f'_c$. (a) Plot the failure surfaces defined by (i) the Mohr-Coulomb criterion with tension cutoff; (ii) the Drucker-Prager criterion with tension cutoff, in the meridian plane of $\theta = 0^\circ$ and in the deviatoric planes, respectively.

- (b) Plot the intersections of the failure surfaces with the $\sigma_1-\sigma_2$ plane ($\sigma_3 = 0$) and with the $\sigma_x-\tau_{xy}$ plane.

- 2.20. Find the constants α and k of the Drucker-Prager criterion in terms of the cohesion, c , and the angle of internal friction, ϕ , of the Mohr-Coulomb criterion for the following cases:

- (a) to match the shear meridian;
- (b) to match the simple compression and the simple tension points;
- (c) to match the equal biaxial compression and simple tension points.

- 2.21. Prove Eq. (2.200) for transversely isotropic materials.

- 2.22. Because of the similarity of the elastic-plastic behavior of a truss structure to that of a polycrystal metal, we may simulate the elastic-plastic behavior of a metal by an analysis of a simple truss structure. A three-component truss structure is subjected to a pair of forces, F_H and F_V , at Joint D as shown in Fig. P2.22a. The three bars have the same cross-sectional area A , Young's modulus E , and yielding stress σ_y , and A is considered large enough such that no buckling will occur. Define a two-dimensional force space $F_H - F_V$. A point with coordinate $(F_H/N_y, F_V/N_y)$, where $N_y = A\sigma_y$, in the force space represents a pair of forces F_H and F_V acting on the structure. Define the elastic limit state in the force space corresponding to the force state at which one of the three bars starts to yield, and the plastic collapse state at which the structure reaches its plastic collapse state.

- (a) Write explicitly the three sets of general equations required for a solution of this problem.
- (b) Sketch the initial elastic limit locus in the force space (a simulation of the initial yield surface in the two-dimensional stress space).
- (c) Show that the closed curve of Fig. 2.22b is the locus of the plastic collapse limit envelope (a simulation of the failure surface in the two-dimensional stress space).
- (d) Calculate the stress history of the three bars for the load-unload cycle: $(F_H/N_y, F_V/N_y) = (0, 0) \rightarrow (0, 2) \rightarrow (0, 0)$.
- (e) Sketch the subsequent elastic limit locus of the structure after it completes the load-unload cycle (kinematic hardening).
- (f) What are the relationships and the differences between the elastic limit locus and the plastic collapse limit locus?

- 2.23. As discussed in Section 2.3.3, when the ratio of the two characteristic lengths, ρ_{10}/ρ_{c0} [Eq. (2.184)], of the Mohr-Coulomb failure surface on the π -plane becomes unity, the Mohr-Coulomb surface will be reduced to the Tresca surface. What surface will the Mohr-Coulomb surface be reduced to when $\rho_{10}/\rho_{c0} = \frac{1}{2}$? Discuss the characteristics of the failure surface and plot the locus of the surface on a deviatoric plane and also show its tensile and compressive meridians on a meridian plane.

- 2.24. A long thin-walled steel cylindrical vessel with diameter D and wall thickness t is subjected to an internal pressure p_1 and an external pressure p_2 , as shown in Fig. P2.24. Suppose that the external pressure p_2 does not contribute to the axial stress of the tube, and let $p_2 = rp_1$, $r \geq 0$. The tube begins to yield under $p_1 = p_0$, and $p_2 = 0$.

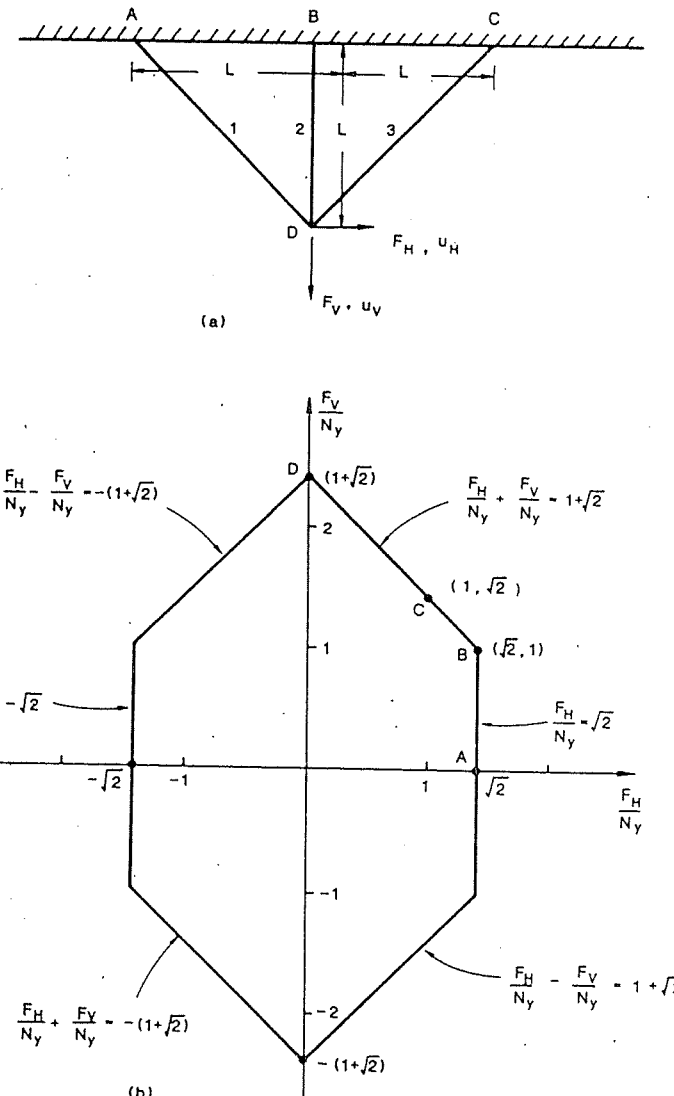


FIGURE P2.22. (a) Three-bar truss; (b) limit state locus of plastic collapse.

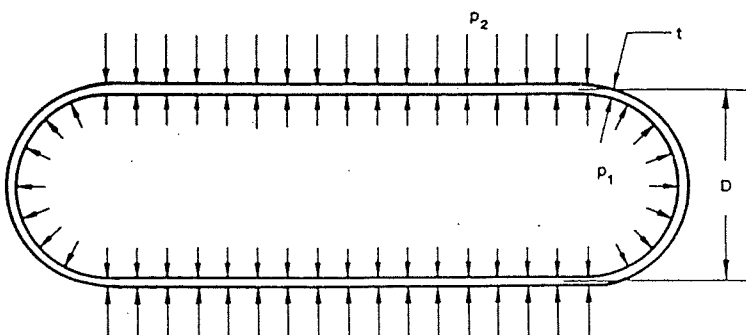


FIGURE P2.24. A thin-walled cylindrical vessel subjected to internal and external pressure.

- Find the limit pressure, $p_1 = p_1$, at which the tube begins to yield, in terms of p_0 and r for the case $r > 0$, according to (i) the von Mises criterion and (ii) the Tresca criterion.
- Sketch the p_y vs. r curve for the two criteria.
- Find the value of r at which the limit pressures predicted by the two criteria have the largest difference, and give the reason. Assume that the two criteria are matched at the pure shear yield point.

2.25. Show that

$$s_{ik}s_{kj}s_{il}s_{lj} = 2J_2^2$$

2.26. The Lode parameter of stress is defined by

$$\mu_\sigma = \frac{2\sigma_2 - \sigma_1 - \sigma_3}{\sigma_1 - \sigma_3} = \frac{\tau_{12} - \tau_{23}}{\tau_{13}}, \quad \sigma_1 \geq \sigma_2 \geq \sigma_3$$

- Show that the parameter μ_σ is related to the Lode angle θ or ψ as

$$\tan \psi = \tan \left(\theta - \frac{\pi}{6} \right) = \frac{\mu_\sigma}{\sqrt{3}}, \quad |\theta| \leq 60^\circ$$

- Show that the von Mises yield criterion can be expressed in terms of μ_σ as

$$\frac{2\tau_{\max}}{\sigma_0} = \frac{\sigma_1 - \sigma_3}{\sigma_0} = \frac{2}{\sqrt{3 + \mu_\sigma^2}}, \quad -1 \leq \mu_\sigma \leq 1$$

where σ_0 is the yield stress in uniaxial tension.

- Plot the $2\tau_{\max}/\sigma_0$ vs. μ_σ curve and discuss the discrepancy between the von Mises and Tresca criteria.

2.27. Assume that the uniaxial compressive strength is f'_c and the uniaxial tensile strength is $f'_t = f'_c/10$ for a concrete material. Predict the stress state at failure of a concrete cube specimen in the triaxial compression test shown in Fig. P2.27 for the following loading paths. Use the Mohr-Coulomb criterion.

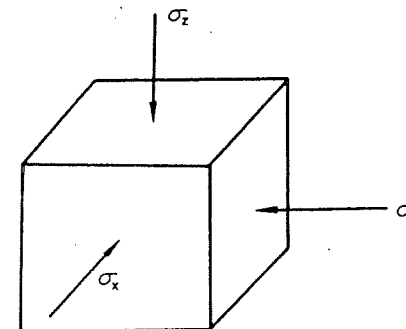


FIGURE P2.27. A concrete cube subjected to a triaxial compression stress state.

- Proportional loading, $\sigma_x = \sigma_y = -p$, $\sigma_z = -Ap$, where A is a constant greater than 1. Express the stress state at failure in terms of f'_c and A . What is the minimum value of A , A_{\min} , such that if $A \leq A_{\min}$, the specimen will never fail?
- Increase $\sigma_x = \sigma_y$ first until the stress state $\sigma_x = \sigma_y = -Rf'_c$, $\sigma_z = 0$, where R is a constant greater than zero, is reached; then, increase σ_z . Express the stress state at failure in terms of f'_c and R . What is the maximum value of R , R_{\max} , such that if $R \geq R_{\max}$, the specimen will fail before reaching the state $\sigma_x = \sigma_y = -Rf'_c$.

2.28. The σ - ϵ response in a simple tension test for an elastic-linear hardening plastic material is approximated by the following expression

$$\sigma = \begin{cases} \sigma_0 + m\epsilon^p, & \text{for } \sigma \geq \sigma_0 \\ E\epsilon, & \text{for } \sigma < \sigma_0 \end{cases}$$

where σ_0 is the initial tensile yield stress. A material sample is first stretched to a state at which the accumulated plastic strain $\epsilon^p = \epsilon_0^p$ and is subsequently unloaded and reversely loaded to a compression state at which the accumulated plastic strain $\epsilon^p = 0$. According to (i) the isotropic hardening rule, (ii) the kinematic hardening rule, and (iii) the independent hardening rule, determine the current tensile and compression yield strengths of the material at this stress state.

ANSWERS TO SELECTED PROBLEMS

- (a) $\sigma_n = 247.5$, $S = 194.3$.
 (b) $\sigma_1 = 400$, $\sigma_2 = \sigma_3 = 0$.
 (c) $n^{(1)} = (0, \pm 0.866, \pm 0.5)$, $n^{(2)} = (0, \mp 0.5, \pm 0.866)$, $n^{(3)} = (\pm 1, 0, 0)$. Note that the principal directions 2 and 3 are not unique, and any two mutually perpendicular axes normal to axis 1 can be chosen.
 (d) $\sigma_{oct} = 133.33$, $\tau_{oct} = 188.56$.
 (e) $\tau_{\max} = 200$.

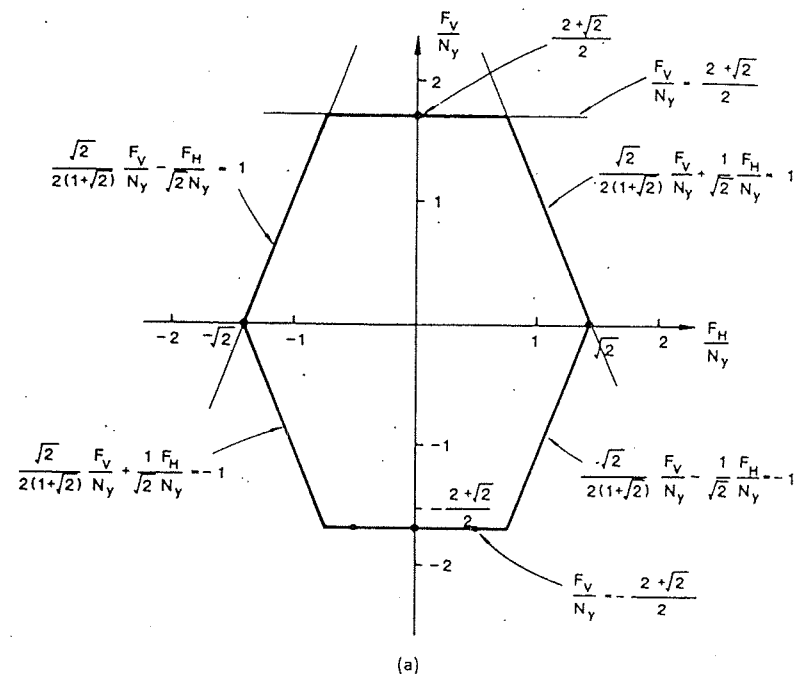


FIGURE S2.22. (a).

2.2. (a) $\sigma_1 = 4$, $\sigma_2 = 2$, $\sigma_3 = 1$, $n^{(1)} = (0, \pm 1/\sqrt{2}, \mp 1/\sqrt{2})$, $n^{(2)} = (\pm 1/\sqrt{2}, \mp \frac{1}{2}, \mp \frac{1}{2})$, $n^{(3)} = (\pm 1/\sqrt{2}, \pm \frac{1}{2}, \pm \frac{1}{2})$.

(b) $s_1 = \frac{5}{3}$, $s_2 = -\frac{1}{3}$, $s_3 = -\frac{4}{3}$.

(c) $J_1 = 0$, $J_2 = 2.333$, $J_3 = 0.741$.

2.4. Hint: $\tau_{oct} = \sqrt{\frac{2}{3}} J_2$; $\tau_{max} = (\sigma_1 - \sigma_3)/2 = \sqrt{J_2/3} [\cos \theta - \cos(\theta + \frac{2}{3}\pi)]$, for $0^\circ \leq \theta \leq 60^\circ$.

2.9. (a) $I_1 = 60$, $J_2 = 8225$, $J_3 = 265,250$, $\theta = 7^\circ 30'$.

$$(b) \begin{Bmatrix} \sigma_1 \\ \sigma_2 \\ \sigma_3 \end{Bmatrix} = \frac{1}{3} \begin{Bmatrix} I_1 \\ I_1 \\ I_1 \end{Bmatrix} + \frac{2}{\sqrt{3}} \sqrt{J_2} \begin{Bmatrix} \cos \theta \\ \cos(\theta - 2\pi/3) \\ \cos(\theta + 2\pi/3) \end{Bmatrix} = \begin{Bmatrix} 123.83 \\ -20.08 \\ -43.75 \end{Bmatrix} \text{ MPa}$$

$$\begin{aligned} 2.10. (a) \frac{\partial J_3}{\partial \sigma_{ij}} &= \frac{\partial}{\partial \sigma_{ij}} \left(\frac{1}{3} s_{mn} s_{nk} s_{km} \right) = \frac{\partial s_{mn}}{\partial \sigma_{ij}} s_{nk} s_{km} \\ &= \frac{\partial}{\partial \sigma_{ij}} (\sigma_{mn} - \frac{1}{3} \delta_{ll} \delta_{mn}) s_{nk} s_{km} \\ &= (\delta_{mi} \delta_{nj} - \frac{1}{3} \delta_{ij} \delta_{mn}) s_{nk} s_{km} = s_{jk} s_{ki} - \frac{1}{3} s_{mk} s_{km} \delta_{ij} \\ &= s_{ik} s_{kj} - \frac{2}{3} J_2 \delta_{ij} \end{aligned}$$

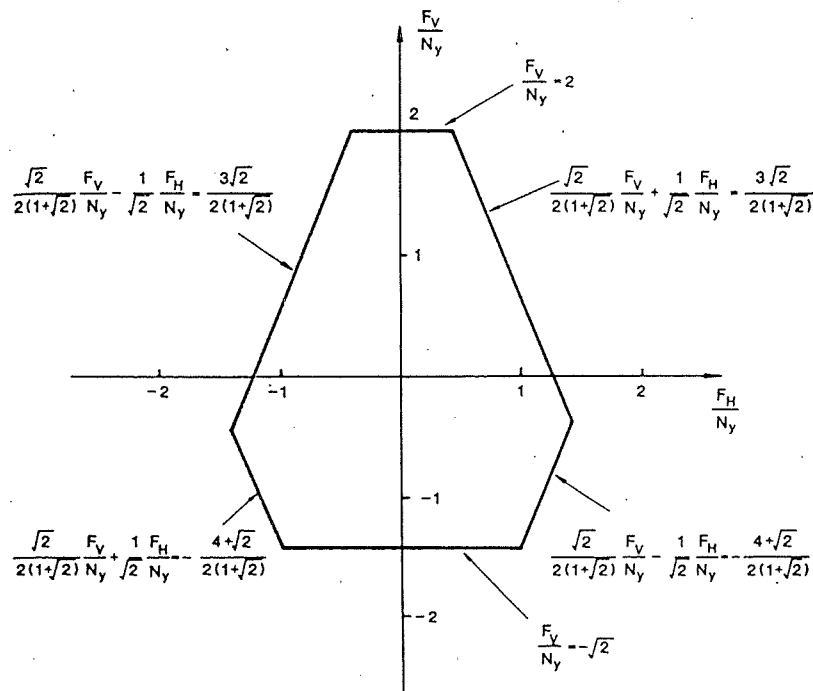


FIGURE S2.22. (b)

2.13. (c) Case (i): $\sigma_2 = \sigma_3$; $\theta = 0^\circ$, $\psi = -30^\circ$. Case (ii): $\sigma_2 = \sigma_1$; $\theta = 60^\circ$, $\psi = 30^\circ$. Case (iii): $\sigma_2 = \frac{1}{2}(\sigma_1 + \sigma_3)$; $\theta = 30^\circ$, $\psi = 0^\circ$.

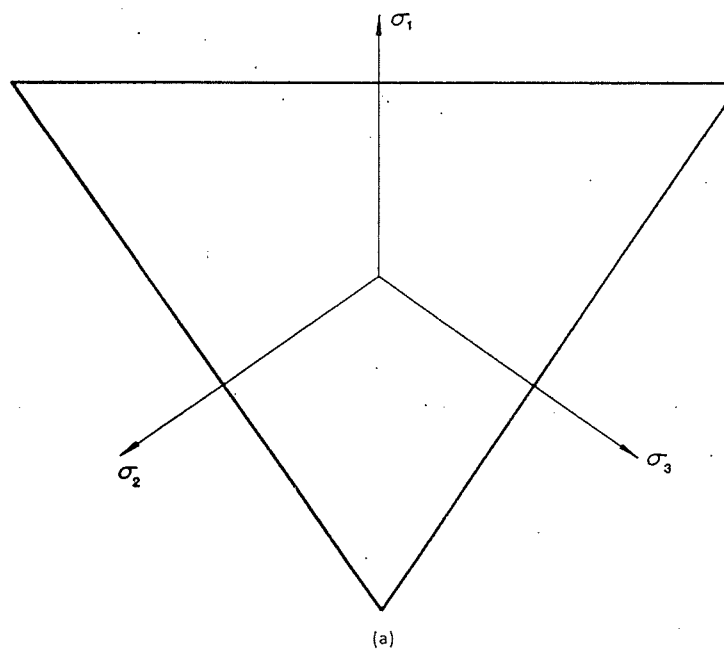
2.14.

$$|\sigma| = \begin{cases} 2\tau_{max} & \text{for } 0 \leq \alpha \leq 1 \\ \frac{2}{\alpha} \tau_{max} & \text{for } \alpha > 1 \\ \frac{2}{1-\alpha} \tau_{max} & \text{for } \alpha < 0 \end{cases}$$

2.15. (a) (142.5, -22.5), (-22.5, 142.5), (-142.5, 22.5), (22.5, -142.5), (-165, -142.5), (-142.5, -165), (165, 142.5), (142.5, 165), (165, 22.5), (22.5, 165), (-165, -22.5), (-22.5, -165).

(b) (i) $153.8 \text{ MPa} \leq \sigma_y \leq 165 \text{ MPa}$; (ii) $82.5 \text{ MPa} \leq \tau_y \leq 102.5 \text{ MPa}$.

(c) (i) $\sigma_y = 155 \text{ MPa}$, $\tau_y = 89.4 \text{ MPa}$; (ii) $\sigma_y = 165 \text{ MPa}$, $\tau_y = 82.5 \text{ MPa}$; (iii) $\sigma_y = 156.6 \text{ MPa}$, $\tau_y = 84.5 \text{ MPa}$.

FIGURE S2.23. (a) The failure surface on a deviatoric plane with $I_1 < 0$.2.16. (i) $P = 395$ kN; (ii) $P = 335$ kN; (iii) $P = 375$ kN.2.17. (a) (i) S.F. = 1.43; (ii) S.F. = 7.0.
(b) (i) S.F. = 1.60; (ii) S.F. = 8.81.2.18. (a) $c = 0.2887f'_c$, $\phi = 30^\circ$.
(b) $k = 0.3465f'_c$, $\alpha = 0.2309$.
(c) On π -plane, for Mohr-Coulomb: $\rho_{t0} = 0.3499f'_c$, $\rho_{c0} = 0.4899f'_c$; for Drucker-Prager: $\rho = 0.49f'_c$.
On the $\theta = 0^\circ$ meridian plane, the coordinate of the apex: for Mohr-Coulomb, $\xi_0 = \sqrt{3}c \cot \phi = 0.8661f'_c$; for Drucker-Prager, $\xi_0 = k/(\sqrt{3}\alpha) = 0.8664f'_c$.
(e) For Mohr-Coulomb, $f'_t = \frac{1}{3}f'_c$; for Drucker-Prager, $f'_t = 0.4287f'_c$.2.20. (a) $\alpha = \frac{1}{3} \sin \phi$, $k = c \cos \phi$.
(b) $\alpha = (1/\sqrt{3}) \sin \phi$, $k = (2/\sqrt{3})c \cos \phi$.
(c) $\alpha = 2 \sin \phi / [\sqrt{3}(3 + \sin \phi)]$, $k = 6c \cos \phi / [\sqrt{3}(3 + \sin \phi)]$.

2.22. (b) Figure S2.22a; (e) Figure S2.22b.

2.23. Figures S2.23a and b.

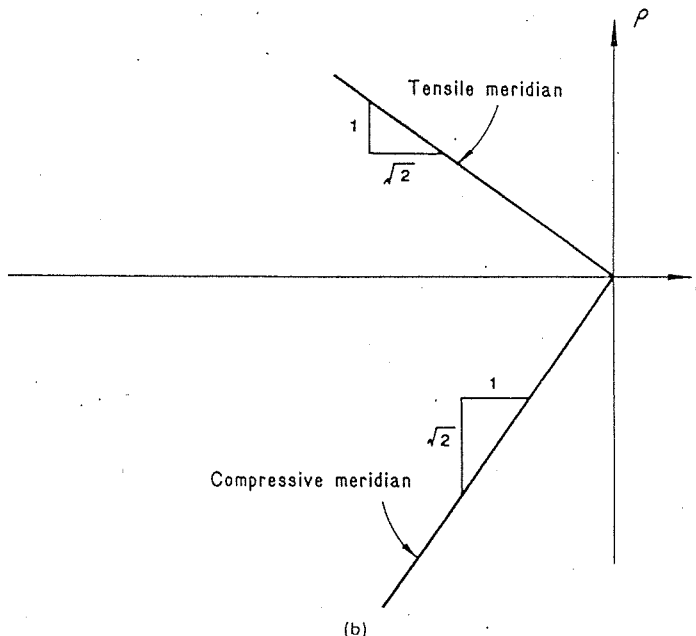
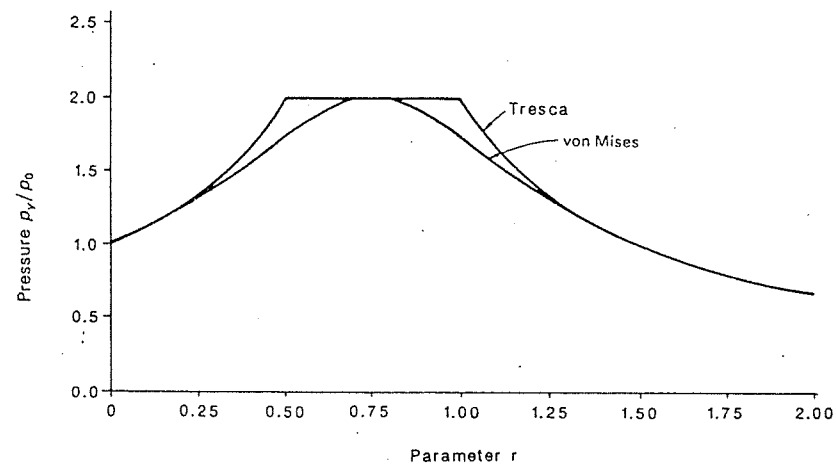


FIGURE S2.23. (b) The tensile and compressive meridians of the failure surface on a meridian plane.

FIGURE S2.24. p_y vs. r curves.

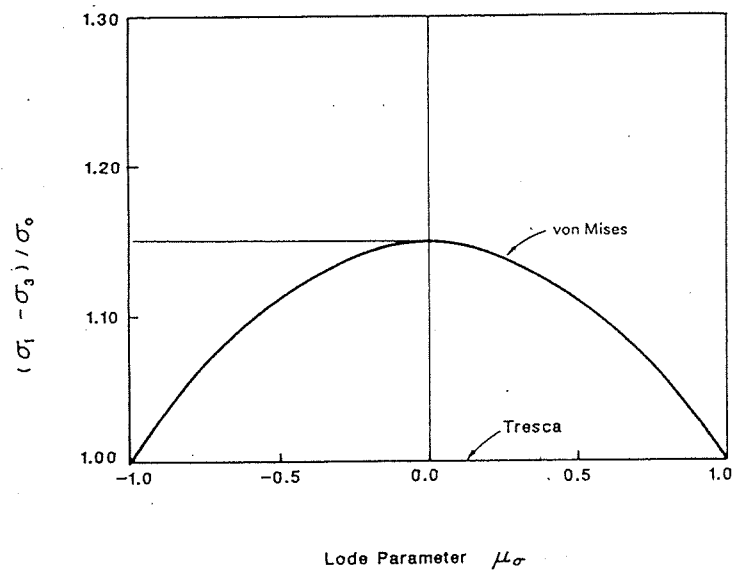


FIGURE S2.26. (c)

$$2.24. (a) (i) p_1 = p_y = \sqrt{\frac{3}{4r^2 - 6r + 3}} p_0$$

$$(ii) p_y = \begin{cases} \frac{p_0}{1-r}, & 0 \leq r \leq \frac{1}{2} \\ 2p_0, & \frac{1}{2} \leq r \leq 1 \\ \frac{p_0}{1-\frac{1}{2}}, & 1 \leq r \end{cases}$$

(b) Figure S2.24.

(c) $r = \frac{1}{2}$ and $r = 1$.

2.26. (c) Figure S2.26c.

3 Elastic Stress-Strain Relations

3.1. Strain

3.1.1. State of Strain at a Point

In the analysis of stress, a state of stress at a point can be found by making an infinite number of cuts through the point from which, for each cut, the associated *stress vector* is known. Similarly, the state of strain at a point is defined as the *totality* of all the changes in length of lines (fibers) of the material which pass through the point and also the *totality* of all the changes in angle between pairs of lines radiating from this point.

However, it will be shown later that the change in length of *any* line of the material which passes through the point and the change in angle between *any* two lines radiating from this point can be calculated once the changes in length and angle for the three lines parallel to a set of mutually perpendicular coordinate axes through this point are known.

Figure 3.1 shows an infinitesimal line element OP at point O in a body in its unstrained original position with length equal to unity. After deformation, the element is displaced to the new position $O'P'$, as shown in the figure. Notice that for a very small length of the line element, and for smooth variation of the deformations in the neighborhood of point O , the displaced element $O'P'$ remains straight. The *relative displacement vector* of point P with respect to point O is denoted by $\vec{\delta}'$, where the vector $O'P''$ is equal and parallel to the vector OP and the superscript n indicates the direction of the fiber element OP before deformation. Considering unit length fibers in the directions of the coordinate axes, x_1 , x_2 , and x_3 , the corresponding relative displacement vectors for these lines are denoted by $\vec{\delta}_1'$, $\vec{\delta}_2'$, and $\vec{\delta}_3'$, respectively. Alternatively, we can also use the dual notation $\vec{\delta}_1'$, $\vec{\delta}_2'$, and $\vec{\delta}_3'$, respectively. Both notations are used interchangeably in this chapter.

In order to find the relation between the relative displacement vector $\vec{\delta}'$ for any fiber with direction n and the relative displacement vectors $\vec{\delta}_1'$, $\vec{\delta}_2'$, and $\vec{\delta}_3'$ for the three coordinate axes, a two-dimensional picture is considered. This is because a two-dimensional picture is easier to visualize, and the

where a , and b are material constants. The stress-strain relationship of the material in uniaxial tension is given by

$$10^3 \epsilon = \frac{\sigma}{10} + \frac{1}{9} \left(\frac{\sigma}{10} \right)^3$$

where σ is in ksi.

- (a) Determine the constants a and b .
 - (b) Write the stress-strain relation of the material for a biaxial compression state.
 - (c) Write the stress-strain relation of the material for a pure shear state.
- 3.10. List and explain analytically and pictorially the restrictions imposed by Drucker's material stability postulate and their implications for an elastic material.

ANSWERS TO SELECTED PROBLEMS

3.1. (a) $\epsilon_{ij} = \begin{bmatrix} 0.1 & 0 & 0 \\ 0 & 0.25 & 0.075 \\ 0 & 0.075 & 0.3 \end{bmatrix}$

(b) $\omega_{ij} = \begin{bmatrix} 0 & 0.2 & -0.4 \\ -0.2 & 0 & -0.225 \\ 0.4 & 0.225 & 0 \end{bmatrix}$

(c) $\epsilon_1 = 0.354$, $\epsilon_2 = 0.196$, $\epsilon_3 = 0.10$; $n_i^{(1)} = (0, \pm 0.5847, \pm 0.8113)$, $n_i^{(2)} = (0, \pm 0.8113, \mp 0.5847)$, $n_i^{(3)} = (\pm 1, 0, 0)$.

(d) $\tilde{\delta} = (0.05, 0.178, 0.2496)$, $\tilde{\Omega} = (0.183, 0.259, -0.3125)$, $\tilde{\delta}' = (0.233, 0.437, -0.0629)$.

3.2. (a) $e_{ij} = \begin{bmatrix} -0.004 & -0.004 & 0 \\ -0.004 & 0.002 & 0 \\ 0 & 0 & 0.002 \end{bmatrix}$

(b) $J'_2 = 2.8 \times 10^{-5}$, $J'_3 = -4.8 \times 10^{-8}$.

(c) $\epsilon_v = -0.003$.

3.4. To satisfy the compatibility conditions, we must have $a_1 + b_1 - 2c_1 = 0$, $c_1 = 4$.

3.7. (a) $e_{ij} = 10^{-4} \times \begin{bmatrix} 0.867 & 0.433 & -3.466 \\ 0.433 & -6.066 & 2.6 \\ -3.466 & 2.6 & 5.2 \end{bmatrix}$

(b) $W = \Omega = 0.01311 \text{ in} \cdot \text{k/in}^3$.

(c) $\epsilon_1 = 8.511 \times 10^{-4}$, $\epsilon_2 = 0.4592 \times 10^{-4}$, $\epsilon_3 = -5.7701 \times 10^{-4}$.

3.8. (a) $\epsilon = 43.12 \times 10^{-3}$, $\gamma = -42.336 \times 10^{-3}$.

(b) At the end of Path 1, $\gamma (= \gamma_{xy}) = 2.352 \times 10^{-3}$, all other components = 0. At the end of Path (2); $\epsilon (= \epsilon_x) = 43.12 \times 10^{-3}$, $\epsilon_y = -20.38 \times 10^{-3}$, $\epsilon_z = -22.73 \times 10^{-3}$, $\gamma (= \gamma_{xy}) = 42.366 \times 10^{-3}$, $\gamma_{yz} = \gamma_{zx} = 0$.

(c) In principal stress space (σ_1, σ_2), Path 1 is from (0, 0) to (100,000, -10,000) psi. At the end of this path; $\epsilon_1 = 1.176 \times 10^{-3}$, $\epsilon_3 = 0$, $\epsilon_2 = -1.176 \times 10^{-3}$.

(f) Paths 1 and 4.

Part II: Plastic Stress-Strain Relations

in which σ_{ij} and ϵ_{kl} are the stress and strain increment tensors, respectively, and F_{ij} are tensor functions. For isotropic time-independent materials, it can be shown that the expression on the right-hand side of Eq. (3.174) is a linear function of the components $d\epsilon_{kl}$ of the strain increment tensor [see the books by Chen (1982) and Chen and Saleeb (1982) for details]. Then the constitutive relations of Eq. (3.174) may be written in the incrementally linear form

$$d\sigma_{ij} = C_{ijkl}(\sigma_{mn}) d\epsilon_{kl} \quad (3.175)$$

in which the material response tensor $C_{ijkl}(\sigma_{mn})$ is a function of the components of the stress tensor. The behavior described by Eqs. (3.175) is *infinitesimally* (or *incrementally*) *reversible*. This justifies the use of the prefix *hypo* in the term *hypoelastic* (or minimum elastic) to describe the constitutive relations (3.175).

The behavior of a hypoelastic material is in general path dependent (stress or strain history dependent). The integration of the differential equations (3.175) for different stress paths and initial conditions obviously leads to different stress-strain relations.

The tensor C_{ijkl} is often called the *tangential stiffness tensor* of the material. The most general form of C_{ijkl} for isotropic time-independent materials has been obtained as a polynomial function of the stress invariants with twelve material coefficients [see Chen (1982) and Chen and Saleeb (1982)]. An important characteristic exhibited is the *stress- or strain-induced anisotropy*. The initial isotropy of the material is destroyed, resulting in a generally anisotropic incremental stiffness. As a result of the induced anisotropy, there is a coupling between the volumetric response and deviatoric action. Also, the principal directions for the incremental stress and strain tensors do not coincide. The stress-induced anisotropy and the coupling effects are important features in modeling the behavior of real materials, such as concrete and soils, for which inelastic dilatation or compaction are dominant effects.

Recently, various special classes of incremental constitutive relations have been extensively used in modeling the nonlinear response of different engineering materials. Mainly, these models are developed on the basis of curve-fitting techniques. Examples of these can be found in the books by Chen (1982) and Chen and Saleeb (1982).

3.8. Summary

This chapter is concerned with the stress-strain relations for an elastic isotropic solid. The linear stress-strain relations are represented by the generalized Hooke's law, which is simple and most familiar to us, while the nonlinear elastic stress-strain relations, which are much more compli-

cated, are in general categorized as *total* and *incremental* stress-strain relations.

There are two types of total stress-strain relations: *Cauchy type* and *Green type*. Cauchy elastic stress-strain relations take the form

$$\sigma_{ij} = F_{ij}(\epsilon_{kl})$$

which represents a one-to-one correspondence between stress σ_{ij} and strain ϵ_{ij} . Thus, the stress and strain are reversible and path independent. The most commonly used models of this type are formulated by simple modifications of the isotropic elastic stress-strain relations based on *variable secant moduli* (e.g., E_s , ν_s , K_{ss} and G_s). Often, the material parameters in these models have well-defined physical relations to the observed stress-strain behavior of the material, and they can be easily determined from experimental data. However, *reversibility* and *path-independency* of the strain energy and complementary energy density functions, W and Ω , are not in general guaranteed. That is, thermodynamic laws may be violated since the models may generate energy for some load-unload stress paths. In order to satisfy thermodynamic laws, additional conditions must be imposed.

Green elastic stress-strain relations take the form

$$\sigma_{ij} = \frac{\partial W}{\partial \epsilon_{ij}} \quad \text{or} \quad \epsilon_{ij} = \frac{\partial \Omega}{\partial \sigma_{ij}}$$

Models of this type satisfy the laws of thermodynamics since the functions W and Ω are *path independent*. Also, the stresses σ_{ij} and strains ϵ_{ij} are reversible and path independent. Further, the *uniqueness* of stresses and strains in a boundary-value problem is satisfied if we impose the restriction of *convexity* (i.e., *positive definiteness*) on the energy functions W and Ω . Various functional forms for W and Ω can be chosen to achieve the desired phenomena of the behavior of materials.

The incremental stress-strain relations of a *hypoelastic* material take the form

$$d\sigma_{ij} = C_{ijkl}(\sigma_{mn}) d\epsilon_{kl}$$

The stresses and strains defined by these relations are incrementally reversible. However, the state of stress and the state of strain are load path dependent. In general, a hypoelastic model may violate the laws of thermodynamics in some load-unload cycles since it may generate energy.

References

- Chen, W.F., 1982. *Plasticity in Reinforced Concrete*, McGraw-Hill, New York.
- Chen, W.F., and A.F. Saleeb, 1982. *Constitutive Equations for Engineering Materials, Volume 1: Elasticity and Modeling*, Wiley-Interscience, New York.

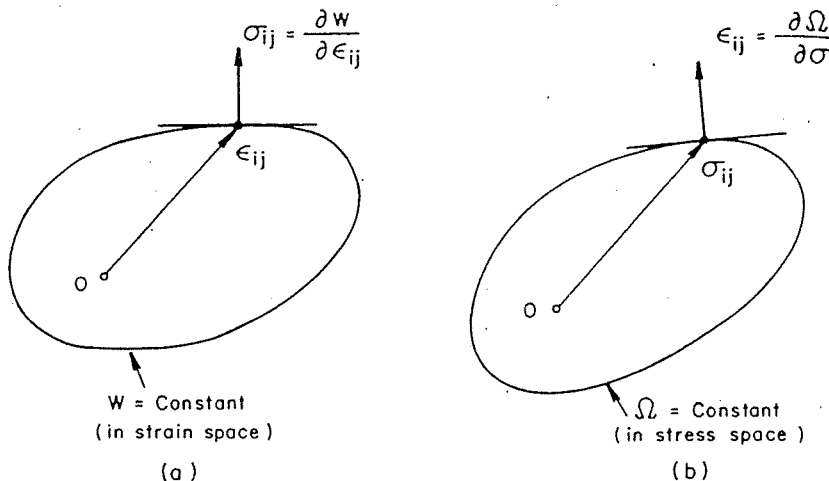


FIGURE 3.15. Normality of (a) σ_{ij} to the surface $W = \text{const.}$ and (b) ϵ_{ij} to the surface $\Omega = \text{const.}$

3.6.3. Convexity

As discussed earlier, for elastic materials, the second stability postulate implies that the constitutive relations are always of the Green (hyperelastic) type described by Eqs. (3.117) and (3.118). Moreover, these relations must satisfy the first stability requirement, inequality (3.160), which imposes additional conditions on the general form of the constitutive equations.

Consider the constitutive relations given by Eq. (3.117). The incremental stress components $\dot{\sigma}_{ij}$ can be expressed in terms of the incremental strains $\dot{\epsilon}_{ij}$ by differentiation; that is,

$$\dot{\sigma}_{ij} = \frac{\partial \sigma_{ij}}{\partial \epsilon_{kl}} \dot{\epsilon}_{kl} = \frac{\partial^2 W}{\partial \epsilon_{ij} \partial \epsilon_{kl}} \dot{\epsilon}_{kl} \quad (3.163)$$

Substituting for $\dot{\sigma}_{ij}$ from this equation into the stability condition (3.160), one obtains

$$\frac{\partial^2 W}{\partial \epsilon_{ij} \partial \epsilon_{kl}} \dot{\epsilon}_{ij} \dot{\epsilon}_{kl} > 0 \quad (3.164a)$$

That is, the quadratic form $(\partial^2 W / \partial \epsilon_{ij} \partial \epsilon_{kl}) \dot{\epsilon}_{ij} \dot{\epsilon}_{kl}$ must be positive definite for arbitrary values of the components $\dot{\epsilon}_{ij}$. The inequality (3.164a) may be rewritten in another convenient form as

$$H'_{ijkl} \dot{\epsilon}_{ij} \dot{\epsilon}_{kl} > 0 \quad (3.164b)$$

where H'_{ijkl} is a fourth-order tensor given by

$$H'_{ijkl} = \frac{\partial^2 W}{\partial \epsilon_{ij} \partial \epsilon_{kl}} \quad (3.165)$$

As can be easily seen from Eq. (3.165), tensor H'_{ijkl} satisfies the symmetry conditions (ϵ_{ij} is symmetric):

$$H'_{ijkl} = H'_{jikl} = H'_{ijlk} = H'_{jilk} = H'_{klij}$$

Hence, there will be only 21 independent elements in H'_{ijkl} .

Mathematically, the matrix of the components of $H'_{ijkl} = \partial^2 W / \partial \epsilon_{ij} \partial \epsilon_{kl}$ is known as the *Hessian matrix* of the function W . When ϵ_{ij} is expressed in a vector form with six components, as defined in Eq. (3.98), then the elements of the Hessian matrix for W are written as

$$[H] = \begin{vmatrix} \frac{\partial^2 W}{\partial \epsilon_x^2} & \frac{\partial^2 W}{\partial \epsilon_x \partial \epsilon_y} & \frac{\partial^2 W}{\partial \epsilon_x \partial \epsilon_z} & \frac{\partial^2 W}{\partial \epsilon_x \partial \gamma_{xy}} & \frac{\partial^2 W}{\partial \epsilon_x \partial \gamma_{yz}} & \frac{\partial^2 W}{\partial \epsilon_x \partial \gamma_{zx}} \\ \frac{\partial^2 W}{\partial \epsilon_y^2} & \frac{\partial^2 W}{\partial \epsilon_y \partial \epsilon_z} & \frac{\partial^2 W}{\partial \epsilon_y \partial \gamma_{xy}} & \frac{\partial^2 W}{\partial \epsilon_y \partial \gamma_{yz}} & \frac{\partial^2 W}{\partial \epsilon_y \partial \gamma_{zx}} & \frac{\partial^2 W}{\partial \epsilon_x \partial \gamma_{zx}} \\ \frac{\partial^2 W}{\partial \epsilon_z^2} & \frac{\partial^2 W}{\partial \epsilon_z \partial \epsilon_x} & \frac{\partial^2 W}{\partial \epsilon_z \partial \gamma_{xy}} & \frac{\partial^2 W}{\partial \epsilon_z \partial \gamma_{yz}} & \frac{\partial^2 W}{\partial \epsilon_z \partial \gamma_{zx}} & \frac{\partial^2 W}{\partial \epsilon_y \partial \gamma_{zx}} \\ \frac{\partial^2 W}{\partial \gamma_{xy}^2} & \frac{\partial^2 W}{\partial \gamma_{xy} \partial \gamma_{yz}} & \frac{\partial^2 W}{\partial \gamma_{xy} \partial \gamma_{zx}} & \frac{\partial^2 W}{\partial \gamma_{yz}^2} & \frac{\partial^2 W}{\partial \gamma_{yz} \partial \gamma_{zx}} & \frac{\partial^2 W}{\partial \gamma_{zx}^2} \\ \text{sym.} & & & & & \end{vmatrix} \quad (3.166)$$

and condition (3.164b) requires that $[H]$ be positive definite.

Alternatively, inequality (3.160) can be written in terms of Ω and σ_{ij} . Thus, using Eqs. (3.118) and following a similar procedure as outlined above, we finally get

$$H'_{ijkl} \dot{\sigma}_{ij} \dot{\sigma}_{kl} > 0 \quad (3.167)$$

where

$$H'_{ijkl} = \frac{\partial^2 \Omega}{\partial \sigma_{ij} \partial \sigma_{kl}} \quad (3.168)$$

and the elements of the Hessian matrix $[H']$ for Ω are exactly of the same form as those for W in Eq. (3.166) with W , ϵ , and γ being replaced by Ω , $\dot{\sigma}$, and τ , respectively.

From Eqs. (3.164) and (3.167), we conclude that the surfaces corresponding to constant W and Ω in strain and stress space, respectively, are *convex*. This can be proved mathematically as follows. Consider two different stress

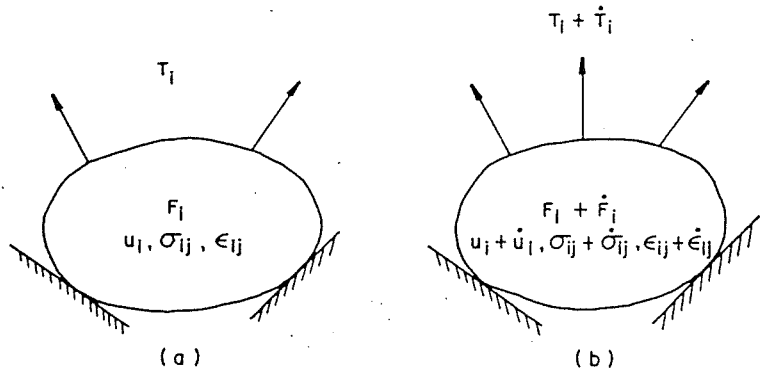


FIGURE 3.13. External agency and Drucker's stability postulate. (a) Existing system; (b) existing system and external agency.

A *stable material* is defined to be the one that satisfies the following conditions (now known as Drucker's stability postulates):

1. During the application of the added set of forces, the work done by the *external agency* on the changes in displacements it produces is positive.
2. Over the cycle of application and removal of the added set of forces, the new work performed by the *external agency* on the changes in displacements it produces is non-negative.

It is emphasized that the work referred to is only the work done by the added set of forces, \dot{T}_i, \dot{F}_i , on the *change* in displacements \dot{u}_i it produces, not the work done by the total forces on \dot{u}_i . Mathematically, the two stability requirements can be stated as

$$\int_A \dot{T}_i \dot{u}_i dA + \int_V \dot{F}_i \dot{u}_i dV > 0 \quad (3.158)$$

$$\oint_A \dot{T}_i \dot{u}_i dA + \oint_V \dot{F}_i \dot{u}_i dV \geq 0 \quad (3.159)$$

in which \oint indicates integration over a cycle of addition and removal of the additional set of forces and stresses.

The first postulate, Eq. (3.158), is called *stability in small*, while the second, Eq. (3.159), is termed *stability in cycle*. Note that these stability requirements are more restrictive than the laws of thermodynamics, which require only that the work done by the total (existing) forces F_i and T_i on \dot{u}_i be non-negative.

Applying the principle of virtual work to the "added" equilibrium set, \dot{F}_i , \dot{T}_i , and $\dot{\sigma}_{ij}$, and the corresponding compatible set, \dot{u}_i and $\dot{\epsilon}_{ij}$, the stability conditions in Eqs. (3.158) and (3.159) can be reduced to the following

inequalities (V is an arbitrary volume):

$$\dot{\sigma}_{ij} \dot{\epsilon}_{ij} > 0 \quad \text{stability in small} \quad (3.160)$$

$$\oint \dot{\sigma}_{ij} \dot{\epsilon}_{ij} \geq 0 \quad \text{stability in cycle} \quad (3.161)$$

where \oint is the integral taken over a cycle of applying and removing the added stress set $\dot{\sigma}_{ij}$.

Stability conditions (3.160) may be illustrated by the uniaxial σ - ϵ curves shown in Fig. 3.14. In panels a and b of the figure, an additional stress $\dot{\sigma} > 0$ gives rise to an additional strain $\dot{\epsilon} > 0$, with the product $\dot{\sigma}\dot{\epsilon} > 0$. That is, the additional stress $\dot{\sigma}$ does positive work, which is represented by the shaded triangles in the diagram. For the *unstable material* shown in panels c and d of Fig. 3.14, however, the work done by the additional stress $\dot{\sigma}$ is always negative.

Figure 3.14 also shows that the stability postulate assures the existence of a unique inverse of the stress-strain relation. For the stable behavior shown in panels a and b, the stress is determined uniquely by a given value of strain, and vice versa. For the unstable material, however, these two strains correspond to a single value of stress (Fig. 3.14c) or two stresses correspond to a single value of strain (Fig. 3.14d).

3.6. Normality, Convexity, and Uniqueness for an Elastic Solid

3.6.1. Existence of the Potential Functions W and Ω

According to the concept of stable materials, useful net energy cannot be extracted from a stable material in a cycle of application and removal of the added set of forces and displacements. Furthermore, energy must be put in if only irrecoverable (permanent or plastic) deformation is to take place. For elastic materials, all deformations are recoverable and stability requires that the work done by the external agency in such a cycle be zero: that is, the integral of inequality (3.161) is always zero for elastic materials. It can be shown that this provides a *necessary and sufficient condition* for the *existence* of strain energy and complementary energy functions, W and Ω , respectively.

For example, let the existing states of stress and strain in an elastic material body be denoted by σ_{ij}^* and ϵ_{ij}^* , respectively. Consider an external agency which applies and then releases a set of stresses additional to the existing state of stress. For an elastic material, when the stress state returns back to σ_{ij}^* , the strain state also returns to ϵ_{ij}^* ; a strain cycle is thus completed starting and ending at ϵ_{ij}^* . Over such a cycle, the second postulate requires

$K_s(I'_1, J'_2, J'_3)$ and $G_s(I'_1, J'_2, J'_3)$. The expression for W in this case is

$$W = \int_0^{\epsilon_{ij}} \sigma_{ij} d\epsilon_{ij} = \int_0^{J'_2} 2G_s(I'_1, J'_2, J'_3) dJ'_2 + \int_0^{I'_1} \frac{1}{2} K_s(I'_1, J'_2, J'_3) d(I'_1)^2 \quad (3.147)$$

in which $d(I'_1)^2 = 2I'_1 dI'_1$.

Similarly, if K_s and G_s are taken as functions of the stress invariants I_1 , J_2 , and J_3 , it can be shown that Ω is given by

$$\Omega = \int_0^{\epsilon_{ij}} \epsilon_{ij} d\sigma_{ij} = \int_0^{J'_2} \frac{dJ'_2}{2G_s(I_1, J_2, J_3)} + \int_0^{I'_1} \frac{d(I'_1)^2}{18K_s(I_1, J_2, J_3)} \quad (3.148)$$

As can be seen, in order for W to be independent of path, the integrals in Eq. (3.147) must depend only on the current values of I'_1 and J'_2 . This can always be satisfied if the moduli K_s and G_s are expressed as

$$\begin{aligned} K_s &= K_s(I'_1) \\ G_s &= G_s(J'_2) \end{aligned} \quad (3.149a)$$

But since I'_1 and J'_2 are related to ϵ_{oct} and γ_{oct} , Eqs. (3.149a) may be expressed in the alternative forms

$$K_s = K_s(\epsilon_{oct}) \quad (3.149b)$$

$$G_s = G_s(\gamma_{oct})$$

Similarly, in order to satisfy the path independence requirement for Ω in Eq. (3.148), K_s and G_s are taken to be functions of only I_1 and J_2 , respectively; that is,

$$\begin{aligned} K_s &= K_s(I_1) \\ G_s &= G_s(J_2) \end{aligned} \quad (3.150a)$$

or, in terms of octahedral stress components,

$$\begin{aligned} K_s &= K_s(\sigma_{oct}) \\ G_s &= G_s(\tau_{oct}) \end{aligned} \quad (3.150b)$$

Furthermore, K_s and G_s must, of course, be positive. Consequently, the integrals in Eqs. (3.147) and (3.148) are always positive (since I_1^2 and J_2 are positive). This confirms that W and Ω are *always positive definite*. The path independence for potential functions W and Ω is due to the reversibility of elastic behavior, while the positive definiteness of W and Ω results from the stability requirement of the material. This will be discussed in the following section.

3.4. Principle of Virtual Work

The principle of virtual work has proved very powerful as a technique in solving problems and in providing proofs for general theorems in solid mechanics. In the following, the virtual work equation is derived. This equation is needed for subsequent considerations of stability and uniqueness of general stress-strain relations, which may be irreversible and path dependent. In the derivation, the following assumption is made: the displacements are sufficiently *small* so that the changes in the geometry of the body are negligible and the original undeformed configuration can be used in setting up the equations for the system. This implies that nonlinear contributions in the compatibility of strains and displacement are neglected. It follows that equilibrium equations (3.70) and compatibility relations (3.71) are applicable here.

The equation of virtual work deals with two separate and unrelated sets: the *equilibrium set* and the *compatible set*. The equilibrium set and the compatible (or geometry) set are brought together, side by side but independently, in the equation of virtual work (Fig. 3.12).

equilibrium set

$$\int_A T_i u_i^* dA + \int_V F_i u_i^* dV = \int_V \sigma_{ij} \epsilon_{ij}^* dV \quad (3.151)$$

compatible set

Here integration is over the whole area, A , or volume, V , of the body. The quantities T_i and F_i are external surface and body forces, respectively. The stress field σ_{ij} is any set of stresses, *real* or *otherwise*, in equilibrium with

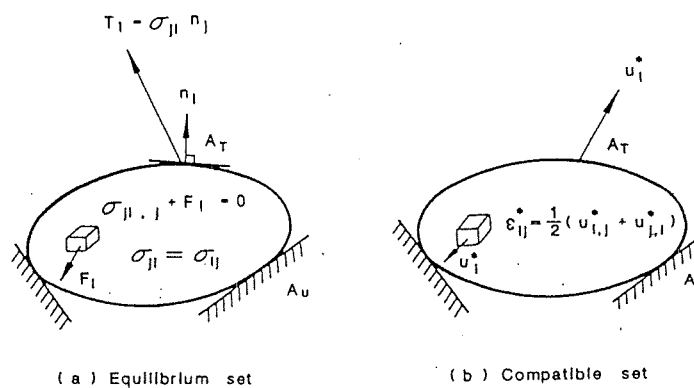
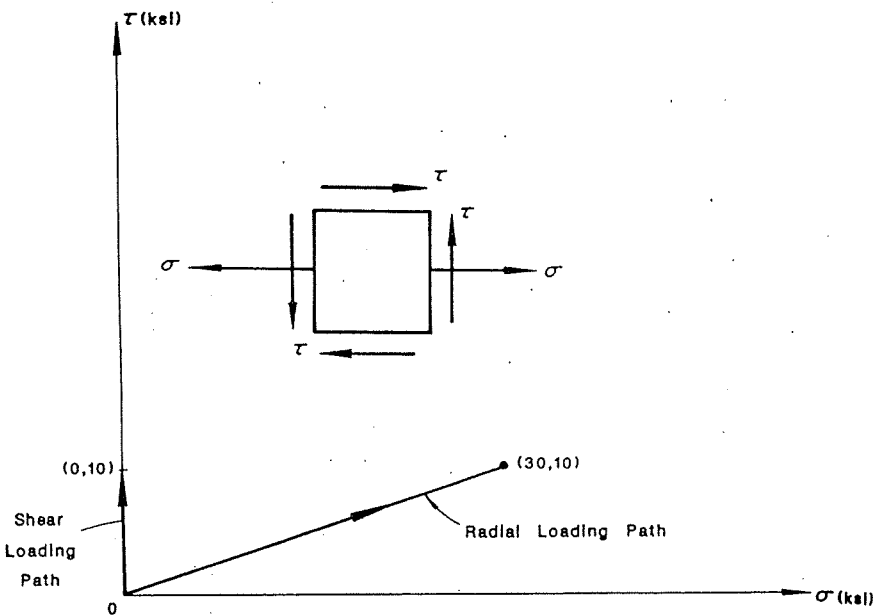


FIGURE 3.12. Two independent sets in the equation of virtual work.

FIGURE 3.11. Loading paths in (σ, τ) space (Example 3.6).

- Determine the constants a and b in Eq. (3.137).
- Find all the components of the normal and shear strains at the end of the given stress path.
- Consider a shearing stress path from $(0, 0)$ to $(0, 10)$ ksi, and calculate the resulting shear strain component γ_{xy} , where the $x-y$ plane coincides with the plane of stress components σ and τ . What is the value of the volume change ϵ_{kk} in this case?

SOLUTION. (a) From the given expression for Ω in Eq. (3.137), we have

$$\frac{\partial \Omega}{\partial I_1} = bJ_2 \quad \text{and} \quad \frac{\partial \Omega}{\partial J_2} = (a + bI_1)$$

Since $I_1 = \sigma_{kk}$ and $J_2 = \frac{1}{2}s_{mn}s_{mm}$ (Chapter 2), then

$$\begin{aligned} \frac{\partial I_1}{\partial \sigma_{ij}} &= \delta_{ij} \\ \frac{\partial J_2}{\partial \sigma_{ij}} &= s_{mn} \frac{\partial s_{mn}}{\partial \sigma_{ij}} = s_{mn} \frac{\partial(\sigma_{mn} - \frac{1}{3}\sigma_{kk}\delta_{mn})}{\partial \sigma_{ij}} \end{aligned} \quad (3.139a)$$

or

$$\begin{aligned} \frac{\partial J_2}{\partial \sigma_{ij}} &= s_{mn}(\delta_{im}\delta_{jn} - \frac{1}{3}\delta_{mn}\delta_{ij}) \\ &= s_{ij} - \frac{1}{3}\delta_{ij}s_{mm} \\ &= s_{ij} \quad (\text{since } s_{mm} = 0) \end{aligned} \quad (3.139b)$$

Therefore, the constitutive equations can be written as

$$\epsilon_{ij} = \frac{\partial \Omega}{\partial \sigma_{ij}} = (bJ_2)\delta_{ij} + (a + bI_1)s_{ij} \quad (3.140)$$

In simple tension, $\sigma_{11} = \sigma$ and all other components of stress are zero. Thus,

$$I_1 = \sigma, \quad J_2 = \frac{1}{3}\sigma^2, \quad s_{11} = \frac{2}{3}\sigma$$

and the stress-strain relation of Eq. (3.140) reduces to

$$\epsilon = \frac{2a}{3}\sigma + b\sigma^2$$

Comparing this equation with the stress-strain relation given in Eq. (3.138), we can easily obtain the constants a and b . The results are

$$a = \frac{3}{2} \times 10^{-4} \quad \text{and} \quad b = 1 \times 10^{-5}$$

(b) Substituting the above values of a and b into Eq. (3.140), it becomes

$$\epsilon_{ij} = (1 \times 10^{-5})J_2\delta_{ij} + (\frac{3}{2} \times 10^{-4} + 10^{-5}I_1)s_{ij} \quad (3.141)$$

The values of I_1 and J_2 at the end of the given radial path are calculated from the final values $\sigma = 30$ ksi and $\tau = 10$ ksi. Therefore, we get

$$I_1 = 30$$

$$J_2 = \frac{1}{6}[(30)^2 + (30)^2] + (10)^2 = 400$$

Substituting these values into Eq. (3.141), we find that

$$\epsilon_{ij} = (40 \times 10^{-4})\delta_{ij} + (4.5 \times 10^{-4})s_{ij}$$

which can be used to calculate the strain components ϵ_{ij} . The results are given by

$$\epsilon_{ii} = \begin{bmatrix} 130 & 45 & 0 \\ 45 & -5 & 0 \\ 0 & 0 & -5 \end{bmatrix} \times 10^{-4}$$

(c) For the shear loading path from $(0, 0)$ to $(0, 10)$ ksi, the values of I_1 and J_2 are

$$I_1 = 0, \quad J_2 = 100$$

The constitutive equation (3.141) then becomes

$$\epsilon_{ij} = 10^{-3}\delta_{ij} + 1.5 \times 10^{-4}s_{ij}$$

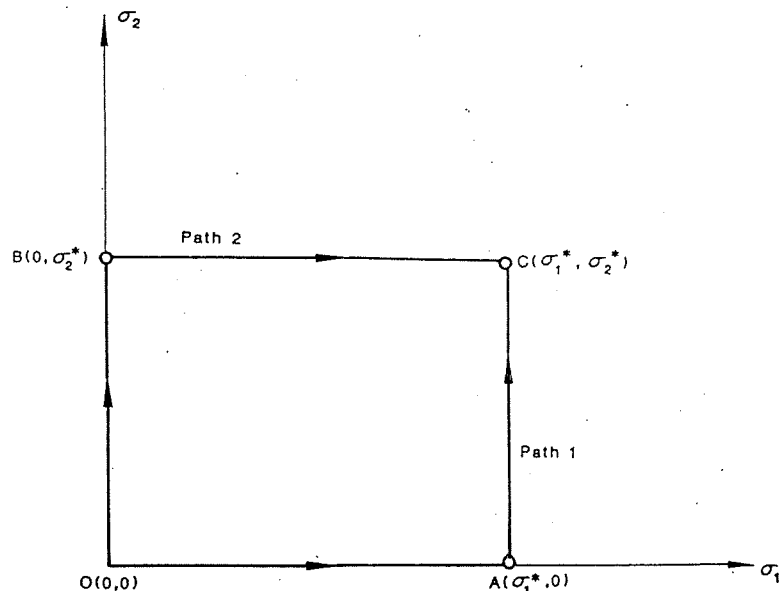


FIGURE 3.10. Two different loading paths to same final state (Example 3.5).

SOLUTION. Along Path 1, the expression for Ω in Eq. (3.114) can be written as

$$\Omega^{(1)} = \int_{(0,0)}^{(\sigma_1^*, 0)} (\epsilon_1 d\sigma_1 + \epsilon_2 d\sigma_2) + \int_{(\sigma_1^*, 0)}^{(\sigma_1^*, \sigma_2^*)} (\epsilon_1 d\sigma_1 + \epsilon_2 d\sigma_2)$$

Substituting for ϵ_1 and ϵ_2 from Eq. (3.123), and noting that $d\sigma_2 = 0$ and $d\sigma_1 = 0$ in the first and second integrands, respectively, we have

$$\Omega^{(1)} = \int_0^{\sigma_1^*} a_{11} \sigma_1 d\sigma_1 + \int_0^{\sigma_2^*} (a_{21} \sigma_1^* + a_{22} \sigma_2) d\sigma_2$$

Carrying out the indicated integrations,

$$\Omega^{(1)} = \frac{1}{2} a_{11} \sigma_1^{*2} + a_{21} \sigma_1^* \sigma_2^* + \frac{1}{2} a_{22} \sigma_2^{*2} \quad (3.124)$$

Similarly, for Path 2, it can be shown that $\Omega^{(2)}$ is given by

$$\Omega^{(2)} = \frac{1}{2} a_{11} \sigma_1^{*2} + a_{12} \sigma_1^* \sigma_2^* + \frac{1}{2} a_{22} \sigma_2^{*2} \quad (3.125)$$

Consequently, for $a_{12} \neq a_{21}$, the complementary energy density $\Omega^{(1)} \neq \Omega^{(2)}$. Thus, Ω is not unique, but depends on the loading path. Only when $a_{12} = a_{21}$ are the expressions for $\Omega^{(1)}$ and $\Omega^{(2)}$ identical. The condition $a_{12} = a_{21}$ makes the matrix of elastic coefficients in Eq. (3.123) symmetric. It is shown later

that the condition of symmetry of the matrix of elastic coefficients is similar to imposing the restriction (3.117) for Green elastic material.

For the stress cycle $OACBO$, Ω is given by

$$\Omega = \int (\epsilon_1 d\sigma_1 + \epsilon_2 d\sigma_2) \quad (3.126)$$

where the integration is extended over the complete cycle. This equation can be written as

$$\begin{aligned} \Omega &= \int_{(0,0)}^{(\sigma_1^*, \sigma_2^*)} (\epsilon_1 d\sigma_1 + \epsilon_2 d\sigma_2) && \text{along Path 1} \\ &+ \int_{(\sigma_1^*, \sigma_2^*)}^{(0,0)} (\epsilon_1 d\sigma_1 + \epsilon_2 d\sigma_2) && \text{along Path 2} \end{aligned}$$

The first part yields the same expression as $\Omega^{(1)}$ in Eq. (3.124). The second part gives the expression for $\Omega^{(2)}$ in Eq. (3.125) with a negative sign. The net value of Ω for the complete cycle is

$$\Omega = \Omega^{(1)} - \Omega^{(2)} = (a_{21} - a_{12}) \sigma_1^* \sigma_2^* \quad (3.127)$$

Depending on the values of a_{12} and a_{21} , the net complementary energy may be positive or negative (note that the term $\epsilon_{ij} d\sigma_{ij}$ in the definition of Ω may be viewed as the rate of work done by stress increments $d\sigma_{ij}$ on strains ϵ_{ij} , and this work is regarded as energy stored in the body). Thus, during the deformation process in the complete stress cycle, the material model described by the stress-strain relations (3.123) may dissipate or generate energy, the latter in violation of the laws of thermodynamics. For a symmetric elastic coefficients matrix ($a_{12} = a_{21}$), the net value of Ω for the complete cycle is zero, and full recovery of complementary energy upon complete unloading is ensured. For isotropic linear elastic material, the matrix $[C]$ in Eqs. (3.99) and (3.101) is symmetric, and thus Ω in this case is path independent.

3.3.2. Nonlinear Elastic Isotropic Stress-Strain Relationships Based on Functions W and Ω

For an isotropic elastic material, the strain energy density W [Eq. (3.112)] can be expressed in terms of any three independent invariants of the strain tensor ϵ_{ij} . Choosing the three invariants \bar{I}_1' , \bar{I}_2' , and \bar{I}_3' defined below, W is written as

$$W = W(\bar{I}_1', \bar{I}_2', \bar{I}_3') \quad (3.128)$$

where \bar{I}_1' , \bar{I}_2' , and \bar{I}_3' are given by

$$\begin{aligned} \bar{I}_1' &= \epsilon_{kk} \\ \bar{I}_2' &= \frac{1}{2} \epsilon_{km} \epsilon_{km} \\ \bar{I}_3' &= \frac{1}{3} \epsilon_{km} \epsilon_{kn} \epsilon_{mn} \end{aligned} \quad (3.129)$$

forms ($\tau_{z\theta} = \tau_{\theta r} = \gamma_{z\theta} = \gamma_{\theta r} = 0$):

$$\begin{Bmatrix} \sigma_r \\ \sigma_z \\ \sigma_\theta \\ \tau_{rz} \end{Bmatrix} = \frac{E}{(1+\nu)(1-2\nu)} \begin{bmatrix} (1-\nu) & \nu & \nu & 0 \\ \nu & (1-\nu) & \nu & 0 \\ \nu & \nu & (1-\nu) & 0 \\ 0 & 0 & 0 & (1-2\nu)/2 \end{bmatrix} \begin{Bmatrix} \epsilon_r \\ \epsilon_z \\ \epsilon_\theta \\ \gamma_{rz} \end{Bmatrix} \quad (3.109)$$

and

$$\begin{Bmatrix} \epsilon_r \\ \epsilon_z \\ \epsilon_\theta \\ \gamma_{rz} \end{Bmatrix} = \frac{1}{E} \begin{bmatrix} 1 & -\nu & -\nu & 0 \\ -\nu & 1 & -\nu & 0 \\ -\nu & -\nu & 1 & 0 \\ 0 & 0 & 0 & 2(1+\nu) \end{bmatrix} \begin{Bmatrix} \sigma_r \\ \sigma_z \\ \sigma_\theta \\ \tau_{rz} \end{Bmatrix} \quad (3.110)$$

3.3. Nonlinear Elastic Isotropic Stress-Strain Relation

3.3.1. Introduction

An elastic material is characterized by its total *reversibility*. In the uniaxial case (Fig. 3.9), this means that upon loading and subsequent unloading, the material follows the same stress-strain curve, i.e., from O to A and subsequently from A to O . Therefore, following a loading cycle OAQ , the state of the material is identical with that before loading. Reloading will follow the same loading path OA .

Such a reversibility implies that the mechanical work done by external loading will be regained if the load is removed statically. Thus, the work may be regarded as being stored in the deformed body in the form of energy. This stored energy is called *strain energy*.

In the uniaxial case, the *strain energy per unit volume* or the *strain energy density*, W , is represented by the area under the σ - ϵ curve shown in Fig. 3.9 and is expressed as

$$W(\epsilon) = \int_0^\epsilon \sigma d\epsilon \quad (3.111)$$

In the multiaxial case, the strain energy density is the sum of the contributions by all the stress components, i.e.,

$$W(\epsilon_{ij}) = \int_0^{\epsilon_{ij}} \sigma_{ij} d\epsilon_{ij} \quad (3.112)$$

Alternatively, the area above the σ - ϵ curve shown in Fig. 3.9, representing the *complementary energy density* (or the *complementary energy per unit*

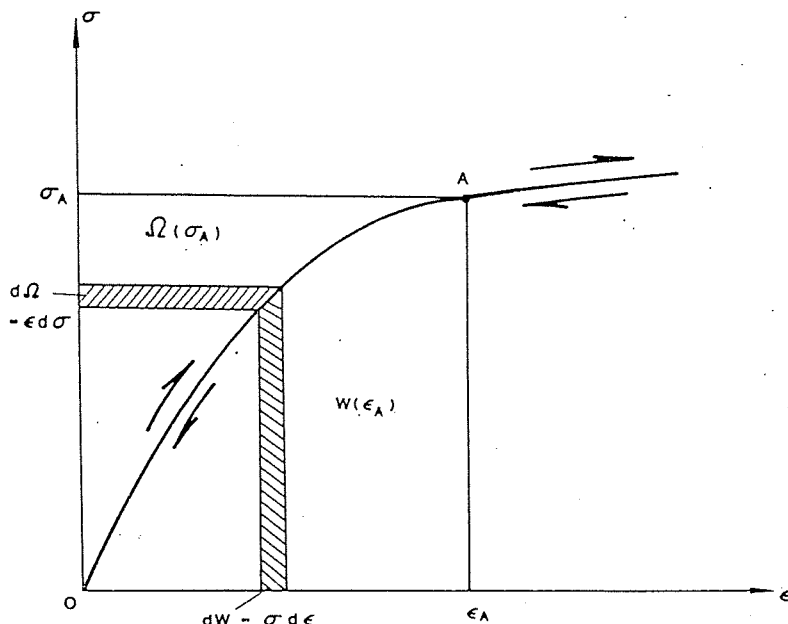


FIGURE 3.9. Strain energy density function W and complementary energy density function Ω .

volume) for the uniaxial case, is expressed as

$$\Omega(\sigma) = \int_0^\sigma \epsilon d\sigma \quad (3.113)$$

In the multiaxial case, it takes the form

$$\Omega(\sigma_{ij}) = \int_0^{\sigma_{ij}} \epsilon_{ij} d\sigma_{ij} \quad (3.114)$$

The strain energy density W and the complementary energy density Ω are functions of strain, ϵ_{ij} , and stress, σ_{ij} , respectively. It is evident that the energy functions W and Ω are related by

$$W + \Omega = \sigma_{ij} \epsilon_{ij} \quad (3.115)$$

Regarding the stress-strain relationships, there are two approaches to describing the reversible behavior of elastic materials. First, we may assume that there is a one-to-one correspondence between stress and strain, or in other words, the stress σ_{ij} is determined uniquely from the current strain

and

$$\lambda = \frac{\nu E}{(1+\nu)(1-2\nu)} \quad (3.86b)$$

or, conversely, Young's modulus E and Poisson's ratio ν can be expressed in terms of μ and λ as

$$E = \frac{\mu(3\lambda+2\mu)}{\lambda+\mu} \quad (3.87a)$$

$$\nu = \frac{\lambda}{2(\lambda+\mu)} \quad (3.87b)$$

By using Eqs. (3.86a) and (3.86b) in Eq. (3.75), the tensor of elastic moduli, C_{ijkl} , can be expressed in terms of E and ν :

$$C_{ijkl} = \frac{E}{2(1+\nu)} \left[\frac{2\nu}{(1-2\nu)} \delta_{ij}\delta_{kl} + \delta_{ik}\delta_{jl} + \delta_{il}\delta_{jk} \right] \quad (3.88)$$

Note that Eq. (3.84) may be written in a compact form:

$$\epsilon_{ij} = D_{ijkl}\sigma_{kl} \quad (3.89a)$$

and

$$D_{ijkl} = \frac{(1+\nu)}{2E} \left[-\frac{2\nu}{1+\nu} \delta_{ij}\delta_{kl} + \delta_{ik}\delta_{jl} + \delta_{il}\delta_{jk} \right] \quad (3.89b)$$

where D_{ijkl} is the inverse of C_{ijkl} and is called the compliance tensor.

Another modulus of elasticity discussed here is the so-called *bulk modulus* K , which is introduced by a hydrostatic compression test as shown in Fig. 3.8d. In this case, $\sigma_{11} = \sigma_{22} = \sigma_{33} = p = \sigma_{kk}/3$. The bulk modulus K is defined for this case as the ratio between the hydrostatic pressure p and the corresponding volume change ϵ_{kk} , i.e.,

$$K = \frac{p}{\epsilon_{kk}} \quad (3.90)$$

From Eq. (3.77), one gets

$$K = \lambda + \frac{1}{3}\mu \quad (3.91)$$

Substituting Eqs. (3.86) and (3.87) into Eq. (3.91) results in

$$K = \frac{E}{3(1-2\nu)} \quad (3.92)$$

3.2.4. Decomposition of Stress-Strain Relation

A neat and logical separation exists between the mean (hydrostatic or volumetric) and the shear (deviatoric) response components in an isotropic linear material. The hydrostatic response can be derived directly from Eq. (3.90) as

$$\sigma_{oct} = p = K\epsilon_{kk} \quad (3.93)$$

To derive the deviatoric response relations, we use the relation $s_{ij} = \sigma_{ij} - p\delta_{ij}$ and substitute for σ_{ij} and p from Eqs. (3.85) and (3.93), respectively, and note Eq. (3.92). This leads to

$$s_{ij} = \frac{E}{(1+\nu)} \epsilon_{ij} + \frac{\nu E}{(1+\nu)(1-2\nu)} \epsilon_{kk}\delta_{ij} - \frac{E}{3(1-2\nu)} \epsilon_{kk}\delta_{ij}$$

Substituting for $\epsilon_{ij} = e_{ij} + \frac{1}{3}\epsilon_{kk}\delta_{ij}$ and simplifying, we have the relation

$$s_{ij} = \frac{E}{1+\nu} e_{ij} = 2Ge_{ij} \quad (3.94)$$

Equations (3.93) and (3.94) give the required separation of the hydrostatic and deviatoric relations. Combining these two equations, we can write the total elastic strains ϵ_{ij} in terms of the hydrostatic and deviatoric stresses as

$$\epsilon_{ij} = \frac{1}{3} \epsilon_{kk}\delta_{ij} + e_{ij} = \frac{1}{3K} p\delta_{ij} + \frac{1}{2G} s_{ij} \quad (3.95)$$

or

$$\epsilon_{ij} = \frac{1}{9K} I_1 \delta_{ij} + \frac{1}{2G} s_{ij} \quad (3.96)$$

Similarly, σ_{ij} can be expressed in terms of the volumetric and deviatoric strains in the following form:

$$\sigma_{ij} = K\epsilon_{kk}\delta_{ij} + 2Ge_{ij} \quad (3.97)$$

3.2.5. Isotropic Linear Elastic Stress-Strain Relations in Matrix Form

The stress-strain relationships discussed above can be conveniently expressed in matrix form. These forms are suitable for use in solutions by numerical methods (e.g., finite-element method). In the following, matrix forms are given for various cases.

3.2.5.1. THREE-DIMENSIONAL CASE

The stress and strain components are defined by the two vectors $\{\sigma\}$ and $\{\epsilon\}$, respectively, which are given by

$$\{\sigma\} = \begin{pmatrix} \sigma_x \\ \sigma_y \\ \sigma_z \\ \tau_{xy} \\ \tau_{yz} \\ \tau_{zx} \end{pmatrix}, \quad \{\epsilon\} = \begin{pmatrix} \epsilon_x \\ \epsilon_y \\ \epsilon_z \\ \gamma_{xy} \\ \gamma_{yz} \\ \gamma_{zx} \end{pmatrix} \quad (3.98)$$

Now Eq. (3.85) can be written in matrix form as

$$\{\sigma\} = [C]\{\epsilon\} \quad (3.99)$$

displacements, Eq. (3.71a), represent a total of nine equations involving fifteen unknowns (six stresses, six strains, and three displacements). The insufficiency in the total number of available equations is made up for by a set of six material-dependent relationships which connect stresses with strains. These additional six equations or relationships are referred to as the *constitutive equations or relations* of materials. Once the constitutive relation for a material is established, the general formulation for the solution of a solid mechanics problem can be completed. The interrelations of variables (σ_{ij} , ϵ_{ij} , and u_i) can best be illustrated schematically as in Fig. 3.7b for the case of a static analysis.

An *elastic* material is one that recovers completely its original shape and size upon the removal of applied forces. For many materials at the *working* load level, the elastic range also includes a region throughout which stress and strain have a *linear* relationship, as we have shown previously in Chapter 1. This linear portion of the stress-strain relation ends at the proportional limit, and its general form is given by

$$\sigma_{ij} = C_{ijkl}\epsilon_{kl} \quad (3.72)$$

where C_{ijkl} is the *material elastic constant tensor*. It may also be remarked here that Eq. (3.72) is the simplest generalization of the linear dependence of stress on strain observed in the familiar Hooke's experiment in a simple tension test, and consequently Eq. (3.72) is often referred to as the *generalized Hooke's law*.

Since both σ_{ij} and ϵ_{kl} are second-order tensors, it follows that C_{ijkl} is a fourth-order tensor. In general, there are $(3)^4 = 81$ constants for such a tensor C_{ijkl} . However, since σ_{ij} and ϵ_{kl} are both *symmetric*, one has the following symmetry conditions:

$$C_{ijkl} = C_{jikl} = C_{ijlk} = C_{jilk} \quad (3.73)$$

Hence, the maximum number of independent constant is reduced to 36.

For a *Green elastic* material, it is shown later that the four subscripts of the elastic constants can be considered as pairs $C_{(ij)(kl)}$. As a result, the number of independent constants needed is reduced from 36 to 21. That is, if we know these 21 constants, we know all 81 constants. If, in addition, we have a plane of elastic symmetry, the number of elastic constants is reduced further from 21 to 13. If there is a second plane of elastic symmetry orthogonal to the first, the number of elastic constants is reduced still further. The second plane of symmetry implies also symmetry about the third orthogonal plane (*orthotropic symmetry*) and the number of elastic constants is reduced to 9. For a *transversely isotropic* material, the number is reduced to 5. Further, if we specify *cubic symmetry*, that is, the properties along the x -, y -, and z -directions are identical, then we cannot distinguish between directions x , y , and z . It follows that it takes only three independent constants to describe the elastic behavior of such a material. Finally, if we have a solid whose elastic properties are *not* a function of direction at all, then we need only *two* independent elastic constants to describe its behavior.

3.2.2. Isotropic Linear Elastic Stress-Strain Relations

For an *isotropic* material, the elastic constants in Eq. (3.72) must be the same for all directions. Thus, tensor C_{ijkl} must be an isotropic fourth-order tensor. It can be shown that the most general form for the isotropic tensor C_{ijkl} is given by (Section 1.5.6)

$$C_{ijkl} = \lambda\delta_{ij}\delta_{kl} - \mu(\delta_{ik}\delta_{jl} + \delta_{il}\delta_{jk}) + \alpha(\delta_{ik}\delta_{jl} - \delta_{il}\delta_{jk}) \quad (3.74)$$

where λ , μ , and α are scalar constants. Now, since C_{ijkl} must satisfy the symmetry conditions in Eqs. (3.73), we have $\alpha = 0$ in Eq. (3.74). Thus, Eq. (3.74) must take the form

$$C_{ijkl} = \lambda\delta_{ij}\delta_{kl} + \mu(\delta_{ik}\delta_{jl} + \delta_{il}\delta_{jk}) \quad (3.75)$$

From Eqs. (3.72) and (3.75), we get

$$\sigma_{ij} = \lambda\delta_{ii}\delta_{kk}\epsilon_{kk} + \mu(\delta_{ik}\delta_{jl} + \delta_{il}\delta_{jk})\epsilon_{kl}$$

or

$$\sigma_{ij} = \lambda\epsilon_{kk}\delta_{ij} + 2\mu\epsilon_{ij} \quad (3.76)$$

Hence, for an isotropic linear elastic material, there are only *two* independent material constants, λ and μ , which are called *Lamé's constants*.

Conversely, strains ϵ_{ij} can be expressed in terms of stresses in the constitutive relation of Eq. (3.76). For Eq. (3.76), one has

$$\sigma_{kk} = (3\lambda + 2\mu)\epsilon_{kk}$$

or

$$\epsilon_{kk} = \frac{\sigma_{kk}}{3\lambda + 2\mu} \quad (3.77)$$

Substituting this value of ϵ_{kk} into Eq. (3.76) and solving for ϵ_{ij} , we get

$$\epsilon_{ij} = \frac{-\lambda\delta_{ij}}{2\mu(3\lambda + 2\mu)}\sigma_{kk} + \frac{1}{2\mu}\sigma_{ij} \quad (3.78)$$

Equations (3.76) and (3.78) are the general forms of the constitutive relation for an isotropic linear elastic material. An important consequence of these equations is that for an isotropic material, the *principal directions* of the stress and strain tensors *coincide*.

3.2.3. Generalized Isotropic Hooke's Law Based on Experimental Evidence

Consider a simple tension test as shown in Fig. 3.8a. The only nonzero stress component, $\sigma_x = \sigma$, causes axial strain ϵ_x according to

$$\epsilon_x = \frac{\sigma_x}{E} \quad (3.79)$$

or in matrix notation,

$$\omega_{ij} = \begin{bmatrix} 0 & -\frac{1}{2}\left(\frac{\partial u}{\partial y} - \frac{\partial v}{\partial x}\right) & -\frac{1}{2}\left(\frac{\partial u}{\partial z} - \frac{\partial w}{\partial x}\right) \\ \frac{1}{2}\left(\frac{\partial u}{\partial y} - \frac{\partial v}{\partial x}\right) & 0 & -\frac{1}{2}\left(\frac{\partial v}{\partial z} - \frac{\partial w}{\partial y}\right) \\ \frac{1}{2}\left(\frac{\partial u}{\partial z} - \frac{\partial w}{\partial x}\right) & \frac{1}{2}\left(\frac{\partial v}{\partial z} - \frac{\partial w}{\partial y}\right) & 0 \end{bmatrix} \quad (3.64)$$

3.1.9. Physical Interpretation for Small Strains

For small deformation, there is a simple physical interpretation for the components of strain ϵ_{ij} . For example, the normal strain component ϵ_{11} can be interpreted as follows. Consider the line element dx_i , which lies along the x_1 -axis before deformation as shown in Fig. 3.6a. After deformation, the element is denoted by $d\xi_i$. Thus, we have

$$dx_i = (ds_0, 0, 0)$$

Substituting for dx_i in Eq. (3.58), we get

$$ds^2 - ds_0^2 = 2\epsilon_{ij} dx_i dx_j = 2\epsilon_{11} dx_1 dx_1 = 2\epsilon_{11} ds_0^2$$

or

$$(ds + ds_0)(ds - ds_0) = 2\epsilon_{11} ds_0^2$$

which can be written as

$$\frac{ds - ds_0}{ds_0} = \left(\frac{2ds_0}{ds + ds_0} \right) \epsilon_{11}$$

But for small deformation, ds is nearly equal to ds_0 ; therefore,

$$\epsilon_{11} = \frac{ds - ds_0}{ds_0} \quad (3.65)$$

Thus, ϵ_{11} represents the extension or change in length per unit length of a line element which before deformation is parallel to the x_1 -axis. Strain components ϵ_{22} and ϵ_{33} have similar interpretations.

The shear component ϵ_{12} can also be interpreted by considering the two line elements $dx_i^{(1)}$ and $dx_i^{(2)}$ originally parallel to the x_1 and x_2 axes, respectively, as shown in Fig. 3.6b. Denote the total decrease in the right angle between the two lines after deformation by ϕ_{12} . Thus, we have

$$\cos\left(\frac{\pi}{2} - \phi_{12}\right) = \frac{d\xi_i^{(1)} d\xi_i^{(2)}}{|d\xi_i^{(1)}||d\xi_i^{(2)}|}$$

Using Eq. (3.56), we get

$$\begin{aligned} \cos\left(\frac{\pi}{2} - \phi_{12}\right) &= \frac{(dx_i^{(1)} + u_{i,k} dx_k^{(1)})(dx_i^{(2)} + u_{i,l} dx_l^{(2)})}{|d\xi_i^{(1)}||d\xi_i^{(2)}|} \\ &= \frac{dx_i^{(1)} dx_i^{(2)} + (u_{i,k} + u_{k,i} + u_{r,i} u_{r,k}) dx_i^{(1)} dx_k^{(2)}}{|d\xi_i^{(1)}||d\xi_i^{(2)}|} \end{aligned}$$

But $dx_i^{(1)} dx_i^{(2)} = 0$ (two orthogonal vectors); then

$$\cos\left(\frac{\pi}{2} - \phi_{12}\right) = \frac{2\epsilon_{ik} dx_i^{(1)} dx_k^{(2)}}{|d\xi_i^{(1)}||d\xi_i^{(2)}|} = \frac{2\epsilon_{12}}{(1 + \epsilon_{11})(1 + \epsilon_{22})}$$

which for small deformation reduces to

$$\cos\left(\frac{\pi}{2} - \phi_{12}\right) = 2\epsilon_{12} \quad (3.66)$$

But $\cos(\pi/2 - \phi_{12}) \approx \phi_{12}$; hence, ϵ_{12} represents one-half the decrease in the right angle between two line elements that before deformation are parallel to the x_1 - and x_2 -axis. Similar derivations can be made for the components ϵ_{13} and ϵ_{23} . Consequently, the off-diagonal terms in Eq. (3.61) represent shear deformation. Physical visualization of the meaning of the partial derivatives in Eq. (3.61) leads to the same interpretation in terms of fractional elongations and angle changes previously obtained more generally.

3.1.10. Equations of Strain Compatibility

In the analysis of stress, it has been pointed out that we must establish the equilibrium equations to ensure that the body is always in an equilibrium state. In the analysis of strain, however, there must be some conditions to be imposed on the strain components so that the deformed body remains continuous. This can be illustrated by considering, for example, Eq. (3.60); namely,

$$u_{i,j} + u_{j,i} = 2\epsilon_{ij} \quad (3.67)$$

For given displacements, u_i , the strain components, ϵ_{ij} , can be determined from Eq. (3.67). On the other hand, for prescribed strain components ϵ_{ij} , Eq. (3.67) represents a system of partial differential equations for the determination of the displacement components u_i . Since there are six equations for three unknown functions u_i , we cannot expect in general that the system of Eqs. (3.67) will have a solution if the strain components ϵ_{ij} are arbitrarily chosen. Therefore, in order to have *single-valued* continuous displacement function u_i , some restrictions must be imposed on the strain components ϵ_{ij} . Such restrictions are called *compatibility conditions*. It can be shown that the compatibility equations for a simply connected region may be written in the form

$$\epsilon_{ij,kl} + \epsilon_{kl,ij} - \epsilon_{ik,jl} - \epsilon_{jl,ik} = 0 \quad (3.68)$$

$$J'_3 = \frac{1}{3} e_{ij} e_{jk} e_{ki} = \begin{vmatrix} e_x & e_{xy} & e_{xz} \\ e_{yx} & e_y & e_{yz} \\ e_{zx} & e_{zy} & e_z \end{vmatrix} = \frac{1}{3} (e_1^3 + e_2^3 + e_3^3) = e_1 e_2 e_3 \quad (3.50)$$

in which e_1 , e_2 , and e_3 are the principal values of the deviatoric strain tensor. Also it can be shown that the invariants J'_1 , J'_2 , and J'_3 are related to the strain invariants, I'_1 , I'_2 , and I'_3 , through the following relations:

$$\begin{aligned} J'_1 &= 0 \\ J'_2 &= \frac{1}{3} (I'^2 - 3I'_3) \\ J'_3 &= \frac{1}{27} (2I'^3 - 9I'_1 I'_2 + 27I'_3) \end{aligned} \quad (3.51)$$

Finally, it can be seen that the octahedral shear strain γ_{oct} is related to the second invariant of the deviatoric strain tensor, J'_2 , as was the case for stresses:

$$\gamma_{\text{oct}} = 2\sqrt{\frac{2}{3}} J'_2 \quad (3.52)$$

3.1.8. Strain-Displacement Relationships

Let the coordinates of a material particle P in a body in the initial (undeformed) position be denoted by $x_i(x_1, x_2, x_3)$ referred to the fixed axes x_1 , x_2 , and x_3 , as shown in Fig. 3.5. The coordinates of the same particle after deformation are denoted by $\xi_i(\xi_1, \xi_2, \xi_3)$ with respect to axes x_1 , x_2 , and x_3 . Figure 3.5 shows two neighboring points P and Q with coordinates x_i and $x_i + dx_i$, respectively, before deformation, and the length of element PQ is denoted by ds_0 . After deformation, the two points are deformed to points P' and Q' with coordinates ξ_i and $\xi_i + d\xi_i$, respectively, and the length of element $P'Q'$ becomes ds . The displacement vector of P is denoted by u_i , as shown. Thus, we have

$$ds_0^2 = dx_i x_i \quad (3.53)$$

$$ds^2 = d\xi_i d\xi_i \quad (3.54)$$

and

$$\xi_i = x_i + u_i \quad (3.55)$$

Then

$$d\xi_i = dx_i + u_{i,j} dx_j \quad (3.56)$$

or

$$d\xi_i = (\delta_{ij} + u_{i,j}) dx_j \quad (3.57)$$

where $u_{i,j} = \partial u_i / \partial x_j$.

It is evident that the equality of ds^2 and ds_0^2 is the necessary and sufficient condition for rigid-body motion; hence, the difference $ds^2 - ds_0^2$ can be taken

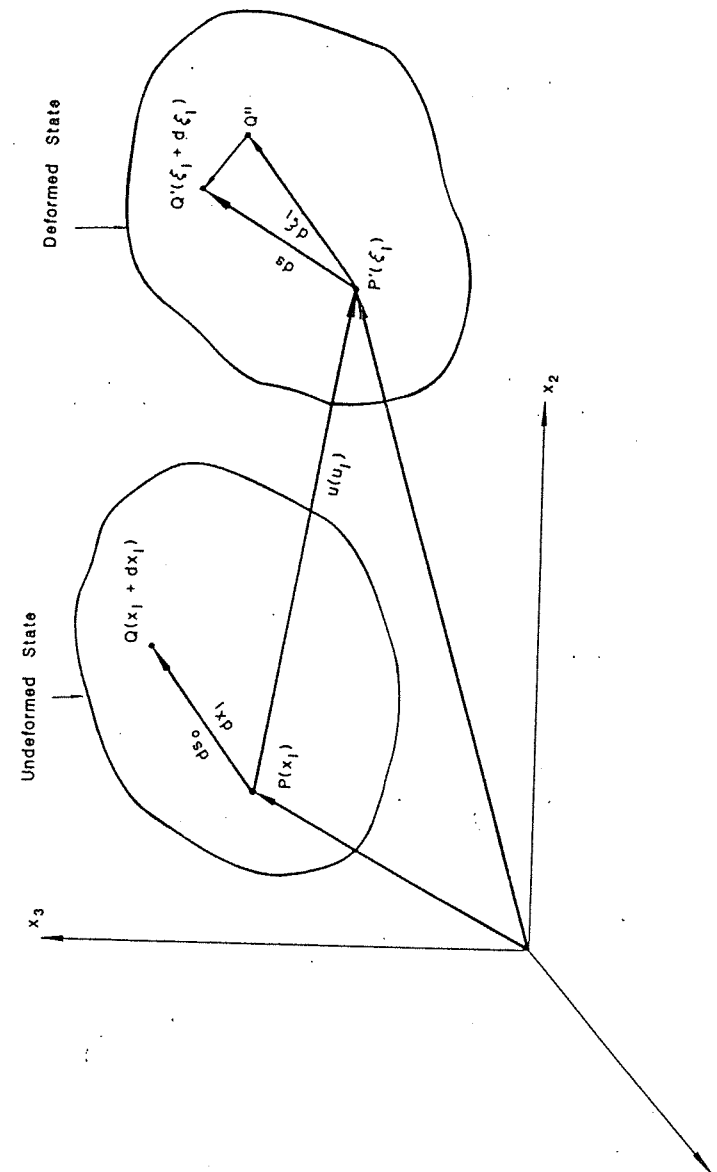


FIGURE 3.5. Deformation of a particle.

the cubic Eq. (3.28), into Eq. (3.25), the principal directions $n^{(1)}$, $n^{(2)}$, and $n^{(3)}$ can be obtained, just as was done for the case of the stress tensor. Following the same procedures as in the analysis of stress, it can be shown that the principal strains assume the stationary values.

3.1.5. Principal Shear Strains

Definitions. The shear strains for some fibers at a point that assume stationary values are called the *principal shear strains*. To find the directions of such fibers, a similar procedure as for stresses is followed. Consider a line fiber at point P with direction n and strain vector δ referred to principal strain axes. The normal strain component for this fiber is ϵ_n and the magnitude of the resultant shear strain component is denoted by θ_n (tensorial shear strain). Thus,

$$\theta_n^2 = \delta_i \delta_i - \epsilon_n^2$$

Substituting for δ_i and ϵ_n from Eqs. (3.14) and (3.18), respectively, in terms of the components ϵ_{ij} referred to the principal strain axes, we get

$$\theta_n^2 = (\epsilon_{ji} \epsilon_{ki} n_j n_k) - (\epsilon_1 n_1^2 + \epsilon_2 n_2^2 + \epsilon_3 n_3^2)^2$$

or

$$\theta_n^2 = (\epsilon_1^2 n_1^2 + \epsilon_2^2 n_2^2 + \epsilon_3^2 n_3^2) - (\epsilon_1 n_1^2 + \epsilon_2 n_2^2 + \epsilon_3 n_3^2)^2 \quad (3.33)$$

Comparing Eq. (3.33) with Eq. (2.43), it is seen that they are of identical form, with S_n replaced by θ_n and the principal stresses by the principal strains. The principal shear strains and the corresponding directions can therefore be obtained in exactly the same manner as for stresses. Thus, designating the tensorial principal shear strains by θ_1 , θ_2 , and θ_3 , we can write

$$\begin{aligned} \theta_1 &= \frac{1}{2} |\epsilon_2 - \epsilon_3| \\ \theta_2 &= \frac{1}{2} |\epsilon_1 - \epsilon_3| \\ \theta_3 &= \frac{1}{2} |\epsilon_1 - \epsilon_2| \end{aligned} \quad (3.34)$$

and the engineering principal shear strains γ_1 , γ_2 , and γ_3 are given by

$$\begin{aligned} \gamma_1 &= |\epsilon_2 - \epsilon_3| \\ \gamma_2 &= |\epsilon_1 - \epsilon_3| \\ \gamma_3 &= |\epsilon_1 - \epsilon_2| \end{aligned} \quad (3.35)$$

The *maximum shear strain* is the largest value of the principal shear strains. Hence, for $\epsilon_1 > \epsilon_2 > \epsilon_3$, the maximum shear strain is given by

$$\gamma_{\max} = 2\theta_{\max} = |\epsilon_1 - \epsilon_3| \quad (3.36)$$

3.1.6. Octahedral Strains

The octahedral normal and shear strains of the octahedral fiber, that is, of a material fiber which before deformation is equally inclined with respect to the three principal strain axes 1, 2, and 3, are denoted by ϵ_{oct} and γ_{oct} , respectively. For an octahedral fiber, the unit vector n has the components $(1/\sqrt{3}, 1/\sqrt{3}, 1/\sqrt{3})$. Thus, from Eq. (3.18), the octahedral normal strain ϵ_{oct} is given by

$$\epsilon_{\text{oct}} = \frac{1}{3} (\epsilon_1 + \epsilon_2 + \epsilon_3) = \frac{I'_1}{3} \quad (3.37)$$

which represents the mean of the three principal strains.

The *octahedral shear strain*, γ_{oct} , with the engineering definition of shear strain, can be obtained from Eq. (3.33), with $\gamma_{\text{oct}} = 2\theta_{\text{oct}}$. Thus,

$$\gamma_{\text{oct}} = \frac{2}{3} [(\epsilon_1 - \epsilon_2)^2 + (\epsilon_2 - \epsilon_3)^2 + (\epsilon_3 - \epsilon_1)^2]^{1/2} \quad (3.38)$$

In terms of strain invariants, the octahedral shear strain can be written as

$$\gamma_{\text{oct}} = \frac{2\sqrt{2}}{3} (I'^2 - 3I'_2)^{1/2} \quad (3.39)$$

and in terms of general nonprincipal strains, it becomes

$$\gamma_{\text{oct}} = \frac{2}{3} [(\epsilon_x - \epsilon_y)^2 + (\epsilon_y - \epsilon_z)^2 + (\epsilon_z - \epsilon_x)^2 + 6(\epsilon_{xy}^2 + \epsilon_{yz}^2 + \epsilon_{zx}^2)]^{1/2} \quad (3.40)$$

which expresses the octahedral shear strain in terms of the strain components referred to an arbitrary set of axes x , y , and z .

EXAMPLE 3.2. The strain tensor ϵ_{ij} at a point is given by

$$\epsilon_{ij} = \begin{bmatrix} -0.00100 & 0 & 0 \\ 0 & -0.00100 & 0.000785 \\ 0 & 0.000785 & 0.00200 \end{bmatrix} \quad (3.41)$$

Calculate:

- The principal strains ϵ_1 , ϵ_2 , and ϵ_3 .
- The maximum shear strain γ_{\max} .
- The octahedral strains.

SOLUTION. (a) Calculate the strain invariants I'_1 , I'_2 , and I'_3 from Eqs. (3.29) to (3.31):

$$I'_1 = (-0.00100) + (-0.00100) + (0.00200) = 0$$

$$I'_2 = (-0.00100)(0.00200) - (0.000785)^2$$

$$+ (-0.00100)(0.00200) + (-0.00100)^2 = -3.62 \times 10^{-6}$$

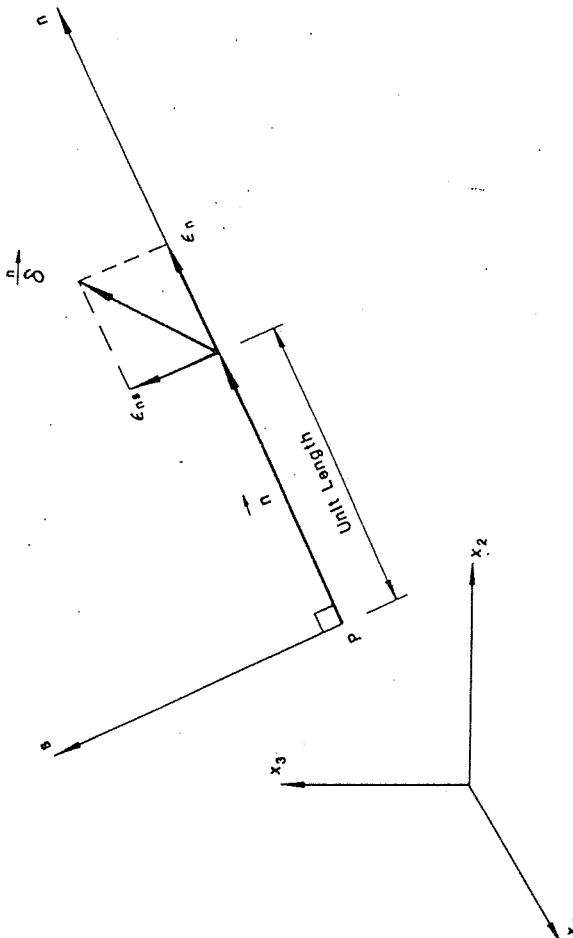


FIGURE 3.4. Normal and shear strain components of strain vector at a point for a fiber.

For a fiber with direction $n = (0, -1/\sqrt{5}, -2/\sqrt{5})$, calculate:

- The normal strain ϵ_n for the fiber.
- The magnitude of the strain vector δ .
- The magnitude of the shear strain ϵ_{ns} , where unit vector s has the components $(-1, 0, 0)$.

SOLUTION. (a) Substituting for the components of n and ϵ_{ij} in Eq. (3.18), we get

$$\epsilon_n = \frac{0.00100}{5} - \frac{0.00150(4)}{5} - \frac{0.00250(2)}{5} = -0.00200$$

(b) From Eq. (3.14), the components δ_i are calculated:

$$\delta_1 = (0.00183)\left(-\frac{1}{\sqrt{5}}\right) + (-0.00025)\left(-\frac{2}{\sqrt{5}}\right) = -0.00059$$

$$\delta_2 = (0.0010)\left(-\frac{1}{\sqrt{5}}\right) + (-0.00125)\left(-\frac{2}{\sqrt{5}}\right) = 0.00067$$

$$\delta_3 = (-0.00125)\left(-\frac{1}{\sqrt{5}}\right) + (-0.00150)\left(-\frac{2}{\sqrt{5}}\right) = 0.00190$$

Thus,

$$|\delta| = [(-0.00059)^2 + (0.00067)^2 + (0.00190)^2]^{1/2} = 0.00210$$

or $|\delta|$ may be calculated directly from the relation

$$|\delta|^2 = \delta_i \delta_i = \epsilon_{ij} \epsilon_{ik} n_j n_k = 4.41 \times 10^{-6}$$

(c) The magnitude of shear strain ϵ_{ns} is calculated using Eq. (3.19):

$$\begin{aligned} \epsilon_{ns} &= \epsilon_{11} n_1 s_1 + \epsilon_{22} n_2 s_2 + \epsilon_{33} n_3 s_3 \\ &\quad + \epsilon_{12}(n_2 s_1 + n_1 s_2) + \epsilon_{23}(n_3 s_2 + n_2 s_3) + \epsilon_{31}(n_1 s_3 + n_3 s_1) \\ &= (0.00183)\left(-\frac{1}{\sqrt{5}}\right)(-1) + (-0.00025)\left(-\frac{2}{\sqrt{5}}\right)(-1) = 0.00060 \end{aligned}$$

Note that the shear strain ϵ_{ns} so calculated represents the projection of the resultant shear strain θ in the s direction. The resultant shear strain θ at this point for the fiber n must be calculated by the relation

$$\theta^2 = |\delta|^2 - \epsilon_n^2 = 0.41 \times 10^{-6}, \quad \text{or } |\theta| = 0.00064$$

three relative displacement vectors $\overset{\text{h}}{\delta}'$, $\overset{\text{2}}{\delta}'$, and $\overset{\text{3}}{\delta}'$. We still have to separate the rigid-body displacements (translations and/or rotations of the body as a whole), if any, from these relative displacement vectors since the rigid-body displacements are of no interest in the analysis of strain. The separation procedure is given in the following for the case of infinitesimal deformations.

The relative displacement vectors associated with the three fibers in the direction of the coordinate axes x_1 , x_2 , and x_3 can be decomposed into components in the direction of the three coordinate axes. For example, the relative displacement vector $\overset{\text{1}}{\delta}'$, associated with the x_1 direction, has the three components ϵ'_{11} , ϵ'_{12} , and ϵ'_{13} in the direction of the three coordinate axes x_1 , x_2 , and x_3 , respectively. Thus, Eq. (3.2) can be written in the component form

$$\overset{\text{h}}{\delta}' = \epsilon'_{ji} n_j \quad (3.3)$$

where the nine scalar quantities ϵ'_{ij} needed to define the three relative displacement vectors $\overset{\text{1}}{\delta}'$, $\overset{\text{2}}{\delta}'$, and $\overset{\text{3}}{\delta}'$ constitute a tensor. This tensor, called the *relative displacement tensor*, defines completely the relative displacement vector $\overset{\text{h}}{\delta}'$ of fiber n . Using dual notations, this tensor is written as

$$\epsilon'_{ij} = \begin{bmatrix} \epsilon'_{11} & \epsilon'_{12} & \epsilon'_{13} \\ \epsilon'_{21} & \epsilon'_{22} & \epsilon'_{23} \\ \epsilon'_{31} & \epsilon'_{32} & \epsilon'_{33} \end{bmatrix} = \begin{bmatrix} \epsilon'_x & \epsilon'_{xy} & \epsilon'_{xz} \\ \epsilon'_{yx} & \epsilon'_y & \epsilon'_{yz} \\ \epsilon'_{zx} & \epsilon'_{zy} & \epsilon'_z \end{bmatrix} \quad (3.4)$$

In general, as can be seen from Eq. (3.4), the relative displacement tensor ϵ'_{ij} is *not* symmetric.

A rigid-body motion, as mentioned earlier, is characterized by the fact that the length of any line element joining any two points remains unchanged. In the following, the conditions on the coefficients ϵ'_{ij} that satisfy this requirement for rigid-body motion are derived. Consider the line element $OP =$ unit vector n , as shown in Fig. 3.1, and assume that after pure rigid-body motion, the element assumes the new position $O'P'$ as shown. Then,

$$|n|^2 = |n + \overset{\text{h}}{\delta}'|^2 = |n|^2 + 2|n|\overset{\text{h}}{\delta}'$$

or

$$n_i n_i = (n_i + \overset{\text{h}}{\delta}'_i)(n_i + \overset{\text{h}}{\delta}'_i) = n_i n_i + 2n_i \overset{\text{h}}{\delta}'_i$$

where the higher-order terms in $\overset{\text{h}}{\delta}'$ are neglected since only infinitesimal deformations are considered. Substituting for $\overset{\text{h}}{\delta}'$ from Eq. (3.3), we get

$$n \cdot \overset{\text{h}}{\delta}' = n_i \overset{\text{h}}{\delta}'_i = n_i (\epsilon'_{ji} n_j) = 0$$

or, when written out in full,

$$\begin{aligned} \epsilon'_{ji} n_i n_j &= \epsilon'_{11} n_1^2 + \epsilon'_{22} n_2^2 \\ &\quad + \epsilon'_{33} n_3^2 + (\epsilon'_{12} + \epsilon'_{21}) n_1 n_2 + (\epsilon'_{23} + \epsilon'_{32}) n_2 n_3 + (\epsilon'_{31} + \epsilon'_{13}) n_3 n_1 = 0 \end{aligned} \quad (3.5)$$

Since Eq. (3.5) must be true for all values of n_1 , n_2 , and n_3 , the necessary and sufficient condition for the tensor ϵ'_{ij} to represent a rigid-body rotation is given by

$$\epsilon'_{11} = \epsilon'_{22} = \epsilon'_{33} = \epsilon'_{12} + \epsilon'_{21} = \epsilon'_{23} + \epsilon'_{32} = \epsilon'_{31} + \epsilon'_{13} = 0$$

or

$$\epsilon'_{ij} = -\epsilon'_{ji} \quad (3.6)$$

That is, for rigid-body rotation, the relative displacement tensor ϵ'_{ij} of Eq. (3.4) is *skew-symmetric*.

Now, every second-order tensor can be decomposed into the sum of a symmetric tensor and a skew-symmetric tensor. It follows, therefore, that if we decompose the tensor ϵ'_{ij} into symmetric and skew-symmetric parts, the skew-symmetric part represents rigid-body rotation, whereas the symmetric part represents *pure deformation*. Thus, we can write

$$\epsilon'_{ij} = \frac{1}{2}(\epsilon'_{ij} + \epsilon'_{ji}) + \frac{1}{2}(\epsilon'_{ij} - \epsilon'_{ji}) \quad (3.7)$$

$$\text{where } \epsilon'_{ij} = \epsilon_{ij} + \omega_{ij} \quad (3.8)$$

$$\epsilon_{ij} = \frac{1}{2}(\epsilon'_{ij} + \epsilon'_{ji}) \quad (3.9)$$

$$\omega_{ij} = \frac{1}{2}(\epsilon'_{ij} - \epsilon'_{ji}) \quad (3.10)$$

Expanding both ϵ_{ij} and ω_{ij} , we get

$$\epsilon_{ij} = \begin{bmatrix} \epsilon'_{11} & \frac{1}{2}(\epsilon'_{12} + \epsilon'_{21}) & \frac{1}{2}(\epsilon'_{13} + \epsilon'_{31}) \\ \frac{1}{2}(\epsilon'_{12} + \epsilon'_{21}) & \epsilon'_{22} & \frac{1}{2}(\epsilon'_{23} + \epsilon'_{32}) \\ \frac{1}{2}(\epsilon'_{13} + \epsilon'_{31}) & \frac{1}{2}(\epsilon'_{23} + \epsilon'_{32}) & \epsilon'_{33} \end{bmatrix} \quad (3.11)$$

$$\omega_{ij} = \begin{bmatrix} 0 & \frac{1}{2}(\epsilon'_{12} - \epsilon'_{21}) & \frac{1}{2}(\epsilon'_{13} - \epsilon'_{31}) \\ \frac{1}{2}(\epsilon'_{21} - \epsilon'_{12}) & 0 & \frac{1}{2}(\epsilon'_{23} - \epsilon'_{32}) \\ \frac{1}{2}(\epsilon'_{31} - \epsilon'_{13}) & \frac{1}{2}(\epsilon'_{32} - \epsilon'_{23}) & 0 \end{bmatrix} \quad (3.12)$$

The symmetric tensor ϵ_{ij} is called the *strain tensor* and the skew-symmetric tensor ω_{ij} is known as the *rotation tensor*. Now, if we substitute for ϵ'_{ij} from Eq. (3.8) into Eq. (3.3), we obtain

$$\overset{\text{h}}{\delta}' = \epsilon_{ji} n_j + \omega_{ji} n_j \quad (3.13)$$

The second part of Eq. (3.13) represents the rigid-body rotation whereas the first part represents the pure deformations.

The relative displacement vector corresponding to pure deformation is called the *strain vector*. The strain vector is denoted by $\overset{\text{h}}{\delta}$ and is given by

$$\overset{\text{h}}{\delta}_i = \epsilon_{ji} n_j = \epsilon_{ij} n_j \quad (3.14)$$

4

Stress-Strain Relations for Perfectly Plastic Materials

4.1. Introduction

For many practical applications, a material may be idealized and assumed to have a negligible strain-hardening effect, i.e., its uniaxial stress-strain diagram beyond the yield point can be approximated by a horizontal straight line, with the constant stress level σ_0 (Fig. 4.1a). Thus, plastic deformation is assumed to occur under a constant flow stress. This behavior is called *perfectly* or *ideally plastic* behavior.

Perfectly plastic idealization can lead to a drastic simplification of the analysis of a complex structural problem. In particular, for a perfectly plastic material, the powerful upper- and lower-bound theorems of limit analysis can be established, from which simple, direct, and realistic methods for estimating the load-carrying capacity of structures in a direct manner can be developed. These bounding theorems and their applications to structural engineering problems will be given in Chapters 8 and 9. This chapter deals only with the stress-strain relations of a perfectly plastic material.

The stress-strain relation in the uniaxial case as shown in Fig. 4.1a is rather simple. However, the general behavior of the material under a complex stress state is not so straightforward, because it involves six stress and six strain components. The question therefore arises as to how the simple stress-strain relationships observed from a uniaxial stress test can be generalized to predict the behavior of the material under any general combined stress state.

This chapter is divided into three parts. The first part, Sections 4.2 through 4.6, is devoted to the classical flow theory of plasticity. The basic concepts of the flow rule and the convexity, normality, and uniqueness for elastic-perfectly plastic materials are discussed in detail. The second part, Section 4.7, provides a simple example and introduces some features of elastic-plastic behavior of a structure. The final part, Sections 4.8 through 4.11, deals with the constitutive relations for elastic-perfectly plastic materials. Specific forms of incremental stress-strain relations for different material models are presented.

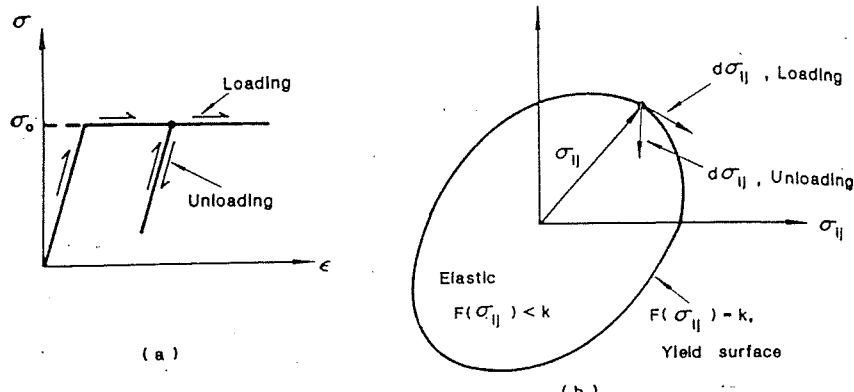


FIGURE 4.1. An elastic-perfectly plastic material. (a) Uniaxial stress-strain relation; (b) geometric representation of yield surface and criterion of loading and unloading.

4.1.1. Elastic Limit and Yield Function

Generalization of the *elastic limit* has been discussed previously in Chapter 2, where the elastic limit of a material under all possible combinations of stresses was defined as a yield function in terms of stress σ_{ij} in the form

$$f(\sigma_{ij}) = F(\sigma_{ij}) - k = 0 \quad (4.1)$$

The significance of this yield function can best be interpreted geometrically as a surface in stress space. For a perfectly plastic material, the yield function is assumed to remain unchanged. Thus, the parameter k in Eq. (4.1) is a constant, and the yield surface is therefore fixed in stress space (Fig. 4.1b).

4.1.2. Criterion for Loading and Unloading

Plastic deformation occurs as long as the stress point is on the yield surface. For the plastic flow to continue, the state of stress must remain on the yield surface. This condition is termed "loading." Otherwise, the stress state must drop below the yield value; in this case, no further plastic deformation occurs and all incremental deformations are elastic. This condition is termed "unloading."

The concept of loading and unloading for a complex stress state is clearest when f is interpreted geometrically as a surface and σ_{ij} and $d\sigma_{ij}$ as stress and stress increment vectors in stress space (Fig. 4.1b). Consider, for example, a material element in a plastic state, characterized by the stress vector σ_{ij} . If we add to the current stress state σ_{ij} an infinitesimal increment

of stress $d\sigma_{ij}$ (additional loading), will this additional stress cause further plastic deformation? For a perfectly plastic material, the stress point cannot move outside the yield surface. Plastic flow can occur only when the stress point is on the yield surface, and the additional loading $d\sigma_{ij}$ must therefore move along the tangential direction. Thus, the condition for a continuation or further plastic flow, or the criterion for loading, is

$$f(\sigma_{ij}, k) = 0 \quad \text{and} \quad df = \frac{\partial f}{\partial \sigma_{ij}} d\sigma_{ij} = 0 \quad (4.2)$$

and the criterion for unloading is

$$f(\sigma_{ij}, k) = 0 \quad \text{and} \quad df = \frac{\partial f}{\partial \sigma_{ij}} d\sigma_{ij} < 0 \quad (4.3)$$

As a result, the yield function $f(\sigma_{ij})$ also serves as the *criterion of loading* for further plastic deformation, or as the *criterion of unloading* for elastic deformation. The yield function or surface $f(\sigma_{ij})$ is also called the *loading function or surface*.

4.1.3. Elastic and Plastic Strain Increment Tensors

Since the magnitude of the plastic strain ϵ_{ij}^p is unlimited during flow, we must think therefore in terms of the strain rates $\dot{\epsilon}_{ij}$ or of infinitesimal changes of strain, or strain increments, $d\epsilon_{ij}$. The total strain increment tensor is assumed to be the sum of the elastic and plastic strain increment tensors:

$$d\epsilon_{ij} = d\epsilon_{ij}^e + d\epsilon_{ij}^p \quad (4.4)$$

Since Hooke's law or any other nonlinear elastic model (see Chapter 3) can be assumed to provide the necessary relationship between the incremental changes of stress and elastic strain, the stress-strain relation for a plastic material reduces essentially to a relation involving the current state and the incremental changes of stress and plastic strain. This latter relationship for a perfectly plastic material will be derived in detail in this chapter.

4.2. Plastic Potential and Flow Rule

The flow rule is the necessary kinematic assumption postulated for plastic deformation or *plastic flow*. It gives the ratio or the relative magnitudes of the components of the plastic strain increment tensor $d\epsilon_{ij}^p$. Since the increment $d\epsilon_{ij}^p$ may be represented geometrically by a vector with nine components in strain space, as shown in Fig. 4.2, the flow rule therefore also defines the direction of the plastic strain increment vector $d\epsilon_{ij}^p$ in the strain space.

We have seen in Chapter 3 that the elastic strain can be derived directly by differentiating the *elastic potential function* or complementary energy

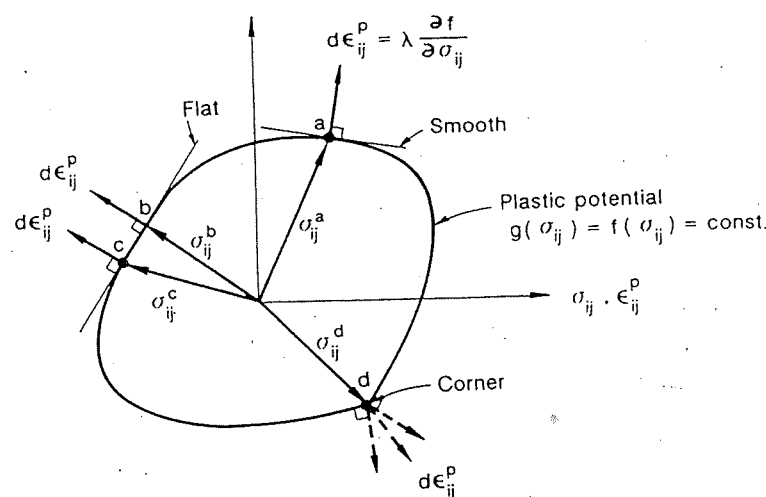


FIGURE 4.2. Geometric illustration of associated flow rule.

density function with respect to stresses σ_{ij} [see Eq. (3.118)]. In 1928, von Mises proposed the similar concept of the *plastic potential function*, which is a scalar function of the stresses, $g(\sigma_{ij})$. Then the plastic flow equations can be written in the form

$$d\epsilon_{ij}^P = d\lambda \frac{\partial g}{\partial \sigma_{ij}} \quad (4.5)$$

where $d\lambda$ is a *positive scalar factor of proportionality*, which is nonzero only when plastic deformations occur. The equation $g(\sigma_{ij}) = \text{constant}$ defines a surface (*hypersurface*) of plastic potential in nine-dimensional stress space. The direction cosines of the normal vector to this surface at the point σ_{ij} on the surface are proportional to the gradient $\partial g / \partial \sigma_{ij}$. The relation (4.5) implies that the plastic flow vector $d\epsilon_{ij}^P$, if plotted as a free vector in stress space, is directed along the normal to the surface of plastic potential (Fig. 4.2).

Of great importance is the simplest case when the yield function and the plastic potential function coincide, $f = g$. Thus,

$$d\epsilon_{ij}^P = d\lambda \frac{\partial f}{\partial \sigma_{ij}} \quad (4.6)$$

and plastic flow develops along the normal to the yield surface $\partial f / \partial \sigma_{ij}$ (see Fig. 4.2). Equation (4.6) is called the *associated flow rule* because the plastic flow is connected or associated with the yield criterion, while relation (4.5) with $f \neq g$ is called a *nonassociated flow rule*.

von Mises used the associated flow rule for the development of his plastic stress-strain relations for metals. It will be shown later that (1) the associated flow rule (4.6) is valid for irreversible plastic materials where work expended on plastic deformation cannot be reclaimed; (2) the stress-strain law of a material based on the associated flow rule will result in a *unique* solution of a boundary-value problem; and (3) the associated flow rule makes it possible and convenient to formulate various generalizations of the plasticity equations by considering yield and loading surfaces of more complex form.

4.3. Flow Rule Associated with von Mises Yield Function

We shall now take the von Mises yield function

$$f(\sigma_{ij}) = J_2 - k^2 = 0 \quad (4.7)$$

as the plastic potential. Then the flow rule has the simple form:

$$d\epsilon_{ij}^P = d\lambda \frac{\partial f}{\partial \sigma_{ij}} = d\lambda s_{ij} \quad (4.8)$$

where s_{ij} is the deviatoric stress tensor and $d\lambda$ is a factor of proportionality with the value

$$d\lambda \begin{cases} = 0 & \text{wherever } J_2 < k^2 \text{ or } J_2 = k^2, \text{ but } dJ_2 < 0 \\ > 0 & \text{wherever } J_2 = k^2 \text{ and } dJ_2 = 0 \end{cases}$$

Equation (4.8) can also be expressed in terms of the components of the strain increments and stresses as

$$\frac{d\epsilon_x^P}{s_x} = \frac{d\epsilon_y^P}{s_y} = \frac{d\epsilon_z^P}{s_z} = \frac{d\gamma_{yz}^P}{2\tau_{xz}} = \frac{d\gamma_{zx}^P}{2\tau_{xy}} = \frac{d\gamma_{xy}^P}{2\tau_{yx}} = d\lambda \quad (4.9)$$

Relations (4.9) are known as the *Prandtl-Reuss equations*. It was Prandtl, in 1924, who extended the earlier Levy-von Mises equations [see Eq. (4.15)] and first proposed the stress-strain relation in the plane strain case for an elastic-perfectly plastic material. Reuss, in 1930, extended the Prandtl equations to the three-dimensional case and gave the general form of Eq. (4.9).

The relationship between the plastic strain increment $d\epsilon_{ij}^P$ and the von Mises yield function $f = J_2$ as given by Eqs. (4.8) or (4.9), or the flow rule associated with the von Mises yield condition can be shown graphically in the three-dimensional principal stress space. However, the three-dimension picture is difficult to draw and instead it is best shown by a cross section on the hydrostatic plane and by a cross section on the deviatoric plane of the three-dimensional surface as in Fig. 4.3. The normal to the yield surface as viewed along the hydrostatic axis is a radial line (Fig. 4.3b) that is parallel

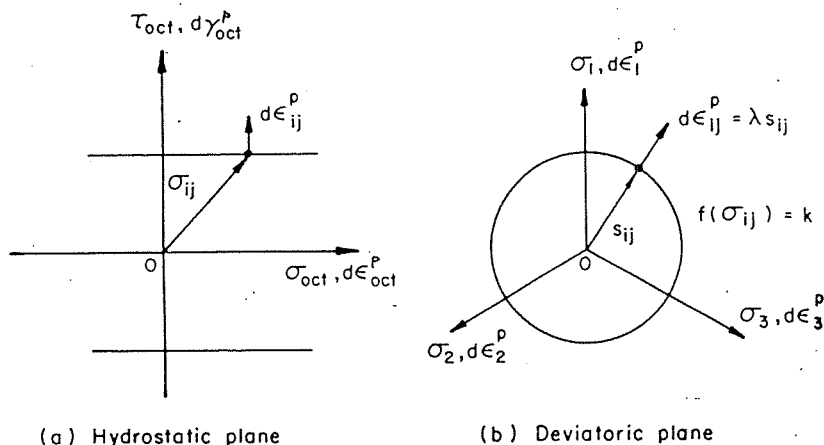


FIGURE 4.3. Flow rule associated with von Mises yield function.

to the π -plane. Its direction is therefore parallel to the direction of the projection of the appropriate stress vector σ_{ij} onto the π -plane, which is, of course, precisely its deviatoric stress component vector s_{ij} .

Equation (4.8) or (4.9) states that a small increment of plastic strain $d\epsilon_{ij}^p$ depends only on the current state of deviatoric stress s_{ij} , not on the stress increment $d\sigma_{ij}$ which is required to maintain the plastic flow. Also, the principal axes of stress σ_{ij} or s_{ij} and the plastic strain increment $d\epsilon_{ij}^p$ coincide. Note that these equations are only statements about the ratio or the relative magnitudes of the components of the plastic strain increment tensor; they give no direct information about its absolute magnitude.

According to Eq. (4.8), there is no plastic volumetric deformation; that is,

$$d\epsilon_{ii}^p = d\lambda \ s_{ii} = 0 \quad (4.10)$$

This can also be seen in Fig. 4.3a where the plastic strain increment vector $d\epsilon_{ij}^p$ is normal to the hydrostatic axis, and the hydrostatic strain component, $d\epsilon_{opt}^p$, is therefore zero.

The total strain increment $d\epsilon_{ij}$ is the sum of the elastic and plastic strain increments (Eq. 4.4). If Hooke's law [Eqs. (3.84) or (3.96)] is applied for the elastic component $d\epsilon_{ij}^e$ and the flow rule [Eq. (4.8)] for the plastic component $d\epsilon_{ij}^p$, we have

$$d\epsilon_{ij} = \frac{1+\nu}{E} d\sigma_{ij} - \frac{\nu}{E} d\sigma_{kk} \delta_{ij} + d\lambda s_{ij} \\ = \frac{d\sigma_{kk}}{9K} \delta_{ij} + \frac{ds_{ij}}{2G} + d\lambda s_{ij} \quad (4.11)$$

Equation (4.11) may also be separated into expressions for the volumetric and deviatoric or shear strain increments of the forms:

$$d\epsilon_{ii} = \frac{1}{3K} d\sigma_{kk}$$

$$de_{ij} = \frac{1}{2G} ds_{ij} + d\lambda s_{ij} \quad (4.12)$$

In practical applications, we expand Eq. (4.11) explicitly in terms of stress and strain components, giving rise to three equations for the normal strains of the form:

$$d\epsilon_x = \frac{1}{E} [d\sigma_x - \nu(d\sigma_y + d\sigma_z)] + \frac{2}{3} d\lambda \left[\sigma_x - \frac{1}{2} (\sigma_y + \sigma_z) \right], \text{ etc.} \quad (4.13)$$

and three equations for the shear strains of the form:

$$d\gamma_{yz} = \frac{1}{G} d\tau_{yz} + 2 d\lambda \tau_{yz}, \text{ etc.} \quad (4.14)$$

In problems of large plastic flow, the elastic strain may be neglected. In such a case, the material can be idealized as rigid-perfectly plastic, and the total strain increment $d\epsilon_{ij}$ and the plastic strain increment $d\epsilon_{ij}''$ are identical. The stress-strain relations for such a material may be written as

$$\frac{d\epsilon_x}{s_x} = \frac{d\epsilon_y}{s_y} = \frac{d\epsilon_z}{s_z} = \frac{d\gamma_{yz}}{2\tau_{yz}} = \frac{d\gamma_{zx}}{2\tau_{zx}} = \frac{d\gamma_{xy}}{2\tau_{xy}} = d\lambda \quad (4.15)$$

in which the superscript, p , of Eqs. (4.8) and (4.9) has been dropped. Equations (4.15) are known as the *Levy-von Mises equations*. In their historical development, it was St. Venant, in 1870, who first proposed that the principal axes of strain increment coincided with the principal axes of stress. These general stress-strain relations were obtained later by Levy in 1871 and independently by von Mises in 1913.

Expanding the Levy-von Mises relation in terms of stress components gives three equations for normal plastic strain increments of the form

$$d\epsilon_x = \frac{2}{3} d\lambda [\sigma_x - \frac{1}{2}(\sigma_+ + \sigma_-)], \text{ etc.} \quad (4.16)$$

and three equations for shear plastic strain increments of the form

$$d\gamma_{\nu\nu} = 2\tau_{\nu\nu} d\lambda, \text{ etc.} \quad (4.17)$$

4.4. Flow Rule Associated with Tresca Yield Function

Now, take the Tresca yield function as the plastic potential, which in principal stress space is a right hexagonal prism consisting of six planes. The deviatoric section of the prism is shown in Fig. 4.4a. Suppose that the

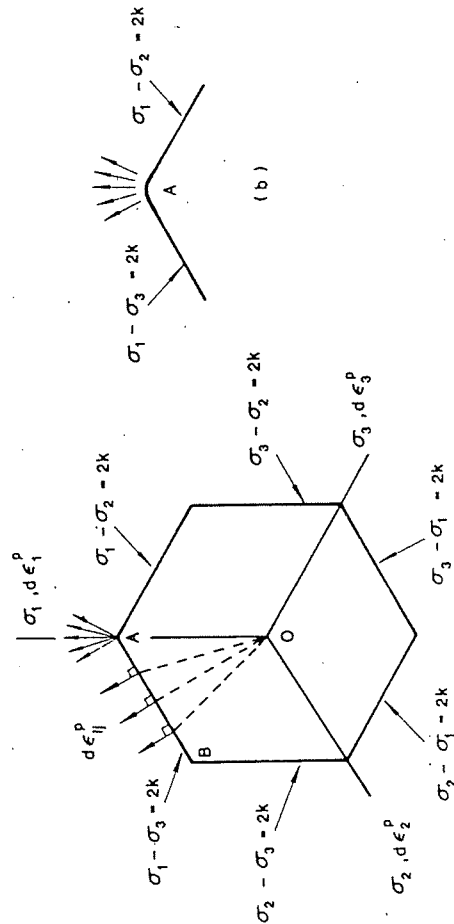


FIGURE 4.4. Flow rule associated with Tresca yield function. (a) Normality of the plastic strain increment vector; (b) vertex A as a limit of a smooth surface.

ordering in magnitude of the principal stresses is $\sigma_1 > \sigma_2 > \sigma_3$; we can then write the corresponding yield function or plastic potential function in the form

$$f = F(\sigma_{ij}) - 2k = \sigma_1 - \sigma_3 - 2k = 0 \quad (4.18)$$

According to the associated flow rule, the principal plastic strain increments, $d\epsilon_1^p$, $d\epsilon_2^p$, $d\epsilon_3^p$, satisfy the following relations:

$$d\epsilon_1^p = d\lambda \frac{\partial f}{\partial \sigma_1} = d\lambda$$

$$d\epsilon_2^p = d\lambda \frac{\partial f}{\partial \sigma_2} = 0$$

$$d\epsilon_3^p = d\lambda \frac{\partial f}{\partial \sigma_3} = -d\lambda$$

or, in a more compact form,

$$(d\epsilon_1^p, d\epsilon_2^p, d\epsilon_3^p) = d\lambda (1, 0, -1), \quad d\lambda \geq 0 \quad (4.19)$$

Similar results can be derived for the other five possible combinations of algebraic orders of magnitude of the principal stresses σ_1 , σ_2 , and σ_3 .

The plastic strain increments can therefore be illustrated geometrically in a combined principal stress/principal strain increment space as shown in Fig. 4.4a. It is seen that anywhere on the plane AB where $\sigma_1 > \sigma_2 > \sigma_3$, the directions of the plastic strain increments are parallel to each other and perpendicular to the plane AB of the Tresca hexagon. Similar relationships can be developed for other planes of the hexagon.

In the special case where, for example, $\sigma_1 > \sigma_2 = \sigma_3$, the situation is more involved, because the maximum shear stress is equal to the yield value k not only on the 45° shear planes parallel to the x_2 -axis but also on the 45° planes parallel to the x_3 -axis. We have therefore the freedom to assume that the shear slip may occur along either of the two possible maximum shear planes:

$$(i) \quad \sigma_{\max} = \sigma_1, \quad \sigma_{\min} = \sigma_3$$

$$(d\epsilon_1^p, d\epsilon_2^p, d\epsilon_3^p) = d\lambda (1, 0, -1), \quad \text{for } d\lambda \geq 0$$

$$(ii) \quad \sigma_{\max} = \sigma_1, \quad \sigma_{\min} = \sigma_2$$

$$(d\epsilon_1^p, d\epsilon_2^p, d\epsilon_3^p) = d\mu (1, -1, 0), \quad \text{for } d\mu \geq 0$$

In this case, we shall assume that the resulting plastic strain increment vector is a linear combination of the two increments given above, i.e.,

$$(d\epsilon_1^p, d\epsilon_2^p, d\epsilon_3^p) = d\lambda (1, 0, -1) + d\mu (1, -1, 0), \quad \text{for } d\lambda \geq 0, d\mu \geq 0 \quad (4.20)$$

This situation corresponds to the special case where the current stress state σ_{ij} lies on a vertex of the hexagon. As a result, the plastic strain increment vector must lie between the directions of the normals to the two adjacent sides of the hexagon (Fig. 4.4a). This vertex or *singular point* at a potential surface can also be viewed as a limiting case of a smooth surface, and the flow rule can still be applied for a smooth surface at this corner point (Fig. 4.4b).

In general, at a singular point where several smooth yield surfaces intersect, the strain increments can generally be expressed as a linear combination of those increments given by the normals of the respective surfaces intersecting at the point, i.e.,

$$d\epsilon_{ij}^p = \sum_{k=1}^n d\lambda_k \frac{\partial f_k}{\partial \sigma_{ij}} \quad (4.21)$$

As a result, at the vertex, the direction of the strain increment vector cannot be determined uniquely. Further, if the yield surface contains a flat part (Fig. 4.2 or Fig. 4.4a), there also exists no unique relationship between the stress and the strain increment. In general, the correspondence between the plastic strain increment vector $d\epsilon_{ij}^p$ and the stress vector σ_{ij} is not always one to one. However, it will be shown in the following example that the incremental plastic work dW_p done or the rate of dissipation of energy is always uniquely determined by the magnitude of the plastic strain rate as given by

$$dW_p = \sigma_1 d\epsilon_1^p + \sigma_2 d\epsilon_2^p + \sigma_3 d\epsilon_3^p = 2k \max|d\epsilon^p| \quad (4.22)$$

where $\max|d\epsilon^p|$ denotes the absolute value of the numerically largest principal component of the plastic strain increment vector.

EXAMPLE 4.1. Using the flow rule associated with the Tresca yield condition,

- (a) show that the plastic work increment is given by expression (4.22);
- (b) assuming that a material element yields at a biaxial stress state, $\sigma_1 = \sigma_0/\sqrt{3}$, $\sigma_2 = -\sigma_0/\sqrt{3}$, where σ_0 is the yield stress in uniaxial tension, and also given $d\epsilon_1^p = c$, where c is a constant, find the plastic strain increments and plastic work increment.

SOLUTION. (a) For a stress point on the side AB with the equation $\sigma_1 - \sigma_3 = 2k$, the components of the strain increment vector are $d\epsilon_2^p = 0$ and $d\epsilon_3^p = -d\epsilon_1^p$. The plastic work increment is therefore given by

$$\begin{aligned} dW_p &= \sigma_1 d\epsilon_1^p + \sigma_2 d\epsilon_2^p + \sigma_3 d\epsilon_3^p \\ &= (\sigma_1 - \sigma_3) d\epsilon_1^p = 2k d\epsilon_1^p \end{aligned} \quad (4.23)$$

since $\sigma_1 = \sigma_3 + 2k$ on AB . Note that $\max|d\epsilon^p| = d\epsilon_1^p$ in this case, so that $2k d\epsilon_1^p$ can be written in the form of Eq. (4.22).

If the stress point coincides with the vertex A , then, $\sigma_1 = \sigma_3 + 2k$ and $\sigma_2 = \sigma_3$, and therefore we have

$$dW_p = (\sigma_3 + 2k) d\epsilon_1^p + \sigma_3 d\epsilon_2^p + \sigma_3 d\epsilon_3^p \quad (4.24)$$

Using the *incompressibility condition*,

$$d\epsilon_1^p + d\epsilon_2^p + d\epsilon_3^p = 0$$

Equation (4.24) yields

$$dW_p = 2k d\epsilon_1^p \quad (4.25)$$

Since $d\epsilon_1^p$ is the numerically largest principal component in this case, Eq. (4.25) can also be written in the form of Eq. (4.22). In a similar manner, it can be shown that Eq. (4.22) holds for every stress point on the hexagon.

(b) According to the Tresca yield condition, we have

$$\tau_{\max} = \frac{\sigma_{\max} - \sigma_{\min}}{2} = \frac{1}{2} \left(\frac{\sigma_0}{\sqrt{3}} + \frac{\sigma_0}{\sqrt{3}} \right) = k$$

Thus, $k = \sigma_0/\sqrt{3}$. The flow rule associated with this yield condition defines the increments of the plastic strain components in the σ_1 and σ_2 directions as

$$(d\epsilon_1^p, d\epsilon_2^p) = d\lambda (1, -1) = (c, -c)$$

Thus, c is the largest plastic strain component and the plastic work increment is obtained as

$$dW_p = 2k \max|d\epsilon^p| = 2kc = \frac{2\sigma_0 c}{\sqrt{3}}$$

4.5. Flow Rule Associated with Mohr-Coulomb Yield Function

In the applications of limit analysis, some frictional materials such as concretes or soils are idealized as elastic-perfectly plastic materials obeying the Mohr-Coulomb yield criterion. The Mohr-Coulomb yield surface is an irregular hexagonal pyramid. Its deviatoric sections are *irregular hexagons* as shown in Fig. 4.5. The yield function takes the following form [see Eq. (2.174)]:

$$\sigma_1 \frac{1 + \sin \phi}{2c \cos \phi} - \sigma_3 \frac{1 - \sin \phi}{2c \cos \phi} = 1 \quad (4.26)$$

where ϕ is the *angle of internal friction* and c the *cohesion*. Equation (4.26) can also be written in compact form as [see Eq. (2.179)]

$$m\sigma_1 - \sigma_3 = f'_c \quad \text{for } \sigma_1 \geq \sigma_2 \geq \sigma_3 \quad (4.27)$$

where f'_c is the *uniaxial compressive strength* and m is the strength ratio between f'_c and f'_t , the uniaxial tensile strength (see Section 2.3.3). To obtain

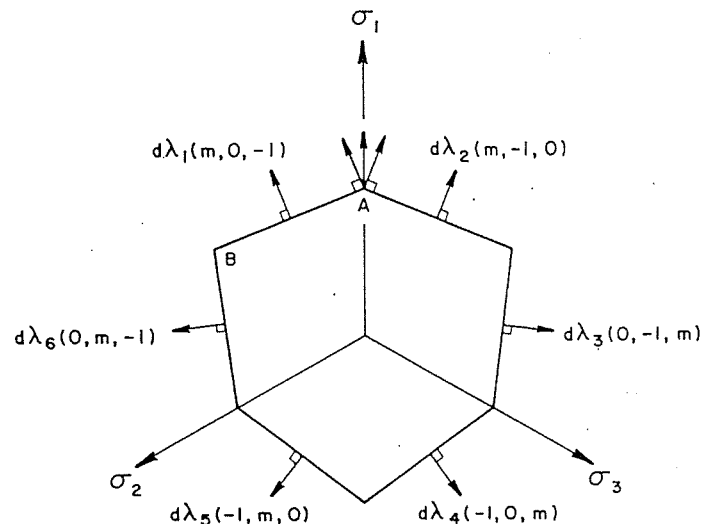


FIGURE 4.5. Flow rule associated with Mohr-Coulomb yield surface.

the expression for the plastic strain increment ($d\epsilon_1^p$, $d\epsilon_2^p$, $d\epsilon_3^p$), the following three cases must be considered separately.

Case 1. The yield stress point lies on the surface plane of the pyramid, say, for example, on face AB (Fig. 4.5), where $\sigma_1 > \sigma_2 > \sigma_3$ and Eq. (4.27) holds. According to the associated flow rule, we have the following plastic strain increments:

$$d\epsilon_1^p = m d\lambda, \quad d\epsilon_2^p = 0, \quad d\epsilon_3^p = -d\lambda \quad \text{for } d\lambda \geq 0 \quad (4.28)$$

or, in compact form,

$$(d\epsilon_1^p, d\epsilon_2^p, d\epsilon_3^p) = d\lambda (m, 0, -1), \quad \text{for } d\lambda \geq 0 \quad (4.29)$$

Similar results can be obtained for the other five possible algebraic orderings of the principal stresses σ_1 , σ_2 , and σ_3 . These results are summarized and shown graphically in Fig. 4.5.

Notice that the plastic volumetric strain increment is

$$d\epsilon_v^p = d\epsilon_1^p + d\epsilon_2^p + d\epsilon_3^p = d\lambda (m - 1) \quad (4.30)$$

Since $m = f'_c/f'_t \geq 1$, it follows that the Mohr-Coulomb material model with the associated flow rule always predicts volume dilatation except in the special case $m = 1$, which reduces to the case of the Tresca material model.

From Eq. (4.30), we can separate the sum of the principal plastic strain increments into two parts: the compressive part

$$\sum |d\epsilon_i^p| = d\lambda \quad (4.31)$$

and the tensile part

$$\sum d\epsilon_i^p = m d\lambda \quad (4.32)$$

Such a separation can be done as well for the other five planes of the pyramid. Then we have

$$\frac{\sum d\epsilon_i^p}{\sum |d\epsilon_i^p|} = m \quad (4.33)$$

and

$$d\epsilon_v^p = \sum d\epsilon_i^p - \sum |d\epsilon_i^p| \quad (4.34)$$

Now, consider further the plastic work increment dW_p . By definition, we have

$$dW_p = \sigma_1 d\epsilon_1^p + \sigma_2 d\epsilon_2^p + \sigma_3 d\epsilon_3^p = (\sigma_1 m - \sigma_3) d\lambda \quad (4.35)$$

Using Eqs. (4.27) and (4.31), Eq. (4.35) becomes

$$dW_p = f'_c \sum |d\epsilon_i^p| \quad (4.36)$$

or

$$dW_p = \frac{f'_c}{m} \sum d\epsilon_i^p \quad (4.37)$$

Case 2. The yield stress point lies on the edges of the pyramid, say, along the edge A (Fig. 4.5), where $\sigma_1 > \sigma_2 = \sigma_3$ and the two surfaces

$$m\sigma_1 - \sigma_3 = f'_c$$

and

$$m\sigma_1 - \sigma_2 = f'_c$$

intersect. In this case, Eq. (4.21) can be applied. Thus, the corresponding plastic strain increments are expressed as

$$(d\epsilon_1^p, d\epsilon_2^p, d\epsilon_3^p) = d\lambda_1(m, 0, -1) + d\lambda_2(m, -1, 0) \\ = [(d\lambda_1 + d\lambda_2)m, -d\lambda_2, -d\lambda_1] \quad (4.38)$$

This strain vector lies between the directions of the normals to the two adjacent surfaces. Similar relations can be obtained for the other five edges.

The plastic volume change is obtained from Eq. (4.38) as

$$d\epsilon_v^p = m(d\lambda_1 + d\lambda_2) - (d\lambda_1 + d\lambda_2)$$

which is the sum of two parts: the compressive part

$$\sum |d\epsilon_i^p| = d\lambda_1 + d\lambda_2$$

and the tensile part

$$\sum |d\epsilon_i^p| = m(d\lambda_1 + d\lambda_2)$$

and we can see that

$$d\epsilon_v^p = \sum d\epsilon_i^p - \sum |d\epsilon_i^p| \quad (4.39)$$

It can be seen that $d\epsilon_p^r > 0$ for $m > 1$, and that Eqs. (4.33) and (4.34) are still valid. By a similar derivation to that of Eq. (4.35), we can obtain the plastic work increment expression dW_p in the following form:

$$\begin{aligned} dW_p &= (\sigma_1 m - \sigma_3) d\lambda_1 + (\sigma_1 m - \sigma_2) d\lambda_2 \\ &= f'_c(d\lambda_1 + d\lambda_2) = f'_c \sum |d\epsilon_p^r| \end{aligned} \quad (4.40)$$

Case 3. The yield stress point coincides with the apex of the pyramid, where six surfaces intersect. Following the same procedure, a similar expression to Eq. (4.38) for the plastic strain $d\epsilon_p^r$ can be obtained. We can also show that Eqs. (4.34) and (4.36) are still valid. Derivations of this will be left to the reader as an exercise.

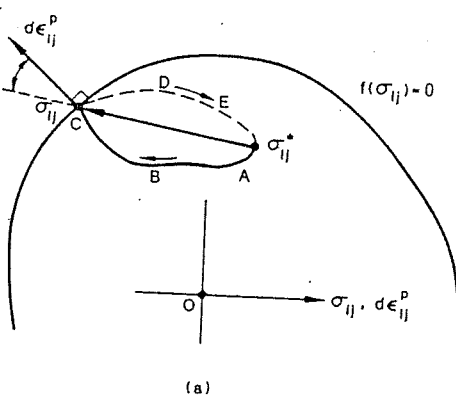
4.6. Convexity, Normality, and Uniqueness for Elastic-Perfectly Plastic Materials

The associated flow rule or *normality rule* discussed before has been established firmly in the mathematical theory of *metal plasticity*. It will be shown in what follows that since the condition of irreversibility of plastic deformation implies that work expended on plastic deformation in a cycle is positive, the positive plastic work leads to convexity of the yield surface and normality of the plastic flow, and that the normality condition, or the associated flow rule, guarantees the uniqueness of the solution of an elastic-plastic boundary-value problem. The normality of the plastic flow and the convexity of the yield surface are of very general nature for elastic-perfectly plastic materials as well as for materials that harden.

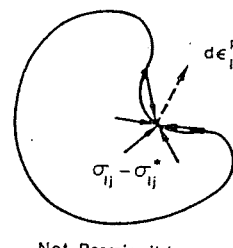
4.6.1. Convexity of the Yield Surface and Normality of the Plastic Flow

Because of the irreversible character of plastic deformation, work expended on plastic deformation cannot be reclaimed. This means that the work of the stresses on the change of plastic strain is positive whenever a change of plastic strain occurs. In this section, we shall investigate what restrictions this *irreversibility condition* imposes on the plastic stress-strain relationship.

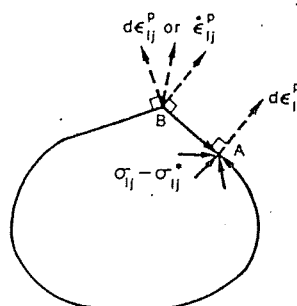
Consider a unit volume of material in which there is a homogeneous state of stress σ_{ij}^* on or inside the yield surface (Fig. 4.6a). Suppose an external agency adds stresses along a path ABC lying inside the surface until σ_{ij} on the yield surface is just reached. Only elastic work has taken place so far. Now suppose that the external agency keeps the stress state σ_{ij} on the yield surface for a short time. Plastic flow must occur, and only plastic work takes place during the flow. The external agency then releases σ_{ij} and returns the state of stress to σ_{ij}^* along an elastic path DE . As all purely elastic changes are completely reversible and independent of the



(a)



(b)



(c)

FIGURE 4.6. Convexity of the yield surface and normality of the plastic flow.

path from σ_{ij}^* to σ_{ij} and back to σ_{ij}^* , all the elastic energy is recovered. The plastic work done by the external agency on this loading and unloading cycle is the scalar product of the stress vector $\sigma_{ij} - \sigma_{ij}^*$ and the plastic strain increment vector $d\epsilon_{ij}^p$. The requirement that this work be positive for plastic deformation leads to

$$(\sigma_{ij} - \sigma_{ij}^*) d\epsilon_{ij}^p \geq 0 \quad (4.41)$$

The geometric interpretation of expression (4.41) is given below. If plastic strain coordinates are superimposed upon stress coordinates, as in Fig. 4.6, the positive scalar product requires an acute angle between the stress vector $\sigma_{ij} - \sigma_{ij}^*$ and the strain increment vector $d\epsilon_{ij}^p$. Since all possible stress vectors, $\sigma_{ij} - \sigma_{ij}^*$, must satisfy Eq. (4.41), this leads inevitably to the following consequences:

- (i) Convexity: The yield surface must be convex. If not convex as shown in Fig. 4.6b, the possible directions of $d\sigma_{ij}$ cover more than 180° for some planes through $d\epsilon_{ij}^p$. Thus, the angle between $\sigma_{ij} - \sigma_{ij}^*$ and $d\epsilon_{ij}^p$ may be greater than 90° . However, Eq. (4.41) requires the angle between them to be less than 90° . Hence, the surface must be convex.
- (ii) Normality: The plastic strain increment vector $d\epsilon_{ij}^p$ must be normal to the yield surface at a smooth point and lie between adjacent normals at a corner. As shown in Fig. 4.6c, if the surface is convex and smooth at point A, $d\epsilon_{ij}^p$ must be normal to the surface so that it makes a right angle or less with all possible $\sigma_{ij} - \sigma_{ij}^*$, and condition (4.41) is satisfied. If the surface has a corner at point B, there is some freedom in the direction of $d\epsilon_{ij}^p$ but the vector must lie between the normals at an adjacent point to the corner so that Eq. (4.41) is satisfied.

The irreversible character of plastic deformation requires the increment of plastic work to be positive

$$dW_p = \sigma_{ij} d\epsilon_{ij}^p = d\lambda \sigma_{ij} \frac{\partial f}{\partial \sigma_{ij}} \geq 0 \quad (4.42)$$

Since the scalar product of the radius vector σ_{ij} on the yield surface and the exterior normal of the yield surface $\partial f / \partial \sigma_{ij}$ is non-negative (Fig. 4.2), they must make an acute angle for a convex surface. The multiplier $d\lambda$ in Eq. (4.6) is seen to be related to the magnitude of the increment of plastic work dW_p , and this factor $d\lambda$ must always be positive when plastic flow occurs in order to assure the irreversible nature of plastic deformation. Note that the yield function is $f = F - k = 0$; thus, $\partial f / \partial \sigma_{ij} = \partial F / \partial \sigma_{ij}$, and Eq. (4.42) can be reduced to

$$dW_p = d\lambda \sigma_{ij} \frac{\partial F}{\partial \sigma_{ij}} = d\lambda nF \quad (4.43)$$

when F is a homogeneous function of degree n in the stresses, as it is for most theories in metal plasticity.

4.6.2. Uniqueness of Solution and Normality Condition of Flow

Uniqueness of solution of a boundary-value problem for an elastic material was discussed in Section 3.6.4. In this section, we shall see that the uniqueness requirement is also satisfied for an elastic-perfectly plastic material if the normality condition is imposed on the stress-strain relation.

Let us assume that our boundary-value problem admits two solutions: $d\sigma_{ij}^{(a)}$, $d\epsilon_{ij}^{(a)}$ and $d\sigma_{ij}^{(b)}$, $d\epsilon_{ij}^{(b)}$, both corresponding to dT_i on A_T , du_i on A_u , and dF_i in V . The equation of virtual work then is employed, assuming continuous u_i throughout V ,

$$\int_{A_T} dT_i^* du_i dA + \int_{A_u} dT_i^* du_i dA + \int_V dF_i^* du_i dV = \int_V d\sigma_{ij}^* d\epsilon_{ij} dV \quad (4.44)$$

where the starred quantities are related through equilibrium and the unstarred ones are compatible. There need be no relation between the two sets of increments. Therefore, the difference between the two assumed states a and b can be substituted into Eq. (4.44) although $d\sigma_{ij}^{(b)} - d\sigma_{ij}^{(a)}$ need not and often does not produce $d\epsilon_{ij}^{(b)} - d\epsilon_{ij}^{(a)}$. Substitution gives

$$0 = \int_V (d\sigma_{ij}^{(b)} - d\sigma_{ij}^{(a)}) (d\epsilon_{ij}^{(b)} - d\epsilon_{ij}^{(a)}) dV \quad (4.45)$$

because $dT_i^{(a)} = dT_i^{(b)}$ on A_T , $du_i^a = du_i^b$ on A_u , and $dF_i^{(a)} = dF_i^{(b)}$ in V .

Using the geometrical representation of the preceding section, we represent the difference of the two stress increments at a given point of the body in Eq. (4.45) by $\Delta d\sigma_{ij} = d\sigma_{ij}^{(b)} - d\sigma_{ij}^{(a)}$, the difference of the increments of elastic strain by $\Delta d\epsilon_{ij}^e$, and the difference of the increments of plastic strain by $\Delta d\epsilon_{ij}^p$. Now the integrand of the scalar product in Eq. (4.45) must vanish, i.e.,

$$dI = \Delta d\sigma_{ij} \Delta d\epsilon_{ij} = \Delta d\sigma_{ij} (\Delta d\epsilon_{ij}^e + \Delta d\epsilon_{ij}^p) = 0 \quad (4.46)$$

Applying a stress-strain relation to Eq. (4.46), dI can be expressed in a quadratic form. If we can show that dI is positive definite, Eq. (4.46) would lead to $\Delta d\epsilon_{ij} = 0$ and $\Delta d\sigma_{ij} = 0$, the uniqueness is satisfied. In other words, any incremental stress-strain relation which assures that the integrand dI is positive definite will therefore satisfy the condition of uniqueness.

Now $\Delta d\epsilon_{ij}^e$ is related to $\Delta d\sigma_{ij}$ by the generalized Hooke's law, and the scalar product $\Delta d\sigma_{ij} \Delta d\epsilon_{ij}^e$ is positive definite. For the scalar product $\Delta d\sigma_{ij} \Delta d\epsilon_{ij}^p$, three cases must be discussed separately:

Case 1. Both solutions constitute loading at the point under consideration.

In this case, $\Delta d\sigma_{ij}$ must lie in the tangent plane to the perfectly plastic yield surface (Fig. 4.1b). It is easily seen that if the plastic strain vector $d\epsilon_{ij}^p$ is normal to the yield surface, the product $\Delta d\sigma_{ij} \Delta d\epsilon_{ij}^p$ will be non-negative for all vectors $\Delta d\sigma_{ij}$ which are tangent to this surface.

Case 2. Both solutions constitute unloading. In this case, $\Delta d\epsilon_{ij}^p = 0$, so that dI is positive definite because $\Delta d\sigma_{ij} \Delta d\epsilon_{ij}^e$ is.

Case 3. One solution constitutes loading, the other unloading. If we take $d\sigma_{ij}^{(b)}$ as loading with $d\epsilon_{ij}^{p(b)}$ and $d\sigma_{ij}^{(a)}$ as unloading with $d\epsilon_{ij}^{p(a)} = 0$, the product $\Delta d\sigma_{ij} \Delta d\epsilon_{ij}^p$ has the form

$$(d\sigma_{ij}^{(b)} - d\sigma_{ij}^{(a)}) d\epsilon_{ij}^{p(b)} = d\sigma_{ij}^{(b)} d\epsilon_{ij}^{p(b)} - d\sigma_{ij}^{(a)} d\epsilon_{ij}^{p(b)} \quad (4.47)$$

Since $d\sigma_{ij}^{(b)}$ constitutes loading, the stress increment vector $d\sigma_{ij}^{(b)}$ must lie in the tangent plane. If the plastic strain vector $d\epsilon_{ij}^{p(b)}$ is in the direction along the exterior normal of the yield surface (Fig. 4.2), the product $d\sigma_{ij}^{(b)} d\epsilon_{ij}^{p(b)}$, the first term on the right-hand side of Eq. (4.47), is zero because $d\sigma_{ij}^{(b)}$ is orthogonal to $d\epsilon_{ij}^{p(b)}$. The other stress increment vector $d\sigma_{ij}^{(a)}$ must point toward the interior of the yield surface because it constitutes unloading (Fig. 4.1b). If the plastic strain increment vector $d\epsilon_{ij}^{p(b)}$ is normal to the convex yield surface f , the stress increment vector $d\sigma_{ij}^{(a)}$ will always make an obtuse angle with $d\epsilon_{ij}^{p(b)}$. Thus, the second term on the right-hand side of Eq. (4.47) is made non-negative. In the present case, the order in which the two solutions are taken does not affect the sign of the product $\Delta d\sigma_{ij} \Delta d\epsilon_{ij}^p$ because both $\Delta d\sigma_{ij}$ and $\Delta d\epsilon_{ij}^p$ change sign when this order is reversed. We can therefore conclude that the associated flow rule satisfies the condition of uniqueness.

It should be noted here that although the plastic term in Eq. (4.46), $\Delta d\sigma_{ij} \Delta d\epsilon_{ij}^p$, may be zero, the elastic term, $\Delta d\sigma_{ij} \Delta d\epsilon_{ij}^e$, is always positive definite unless $\Delta d\sigma_{ij} = 0$. Uniqueness, in this sense, is established for the elastic-plastic case but not for the rigid-plastic case where the elastic term is identically zero at all times.

We are now in a position to state that the simple relation $g = f$ has a special significance in the mathematical theory of plasticity. Two immediate consequences of this are now evident. (1) The plastic strain increment vector $d\epsilon_{ij}^p$ must be normal to the yield or loading surface $f(\sigma_{ij}) = 0$. This is now known as the *normality condition*. (2) This type of plastic stress-strain relations leads to the uniqueness of the solution of a boundary-value problem. As will be seen later, the normality relation (4.6) also leads rather directly to the establishment of the powerful theorems of limit analysis of perfect plasticity (Chapter 8).

This type of normality condition is of a very general nature. In Chapter 5, it is shown that this relation is also valid for materials which work harden. The normality condition imposed on the plastic stress-strain law has strong implications with respect to uniqueness of solution for work hardening and perfectly plastic bodies. It also leads to the formulations of the variational and absolute-minimum principles as well.

4.7. A Simple Elastic-Plastic Problem: The Expansion of a Thick-Walled Cylinder

In this section, we shall discuss in some detail the behavior of a simple structure made of elastic-perfectly plastic material. This discussion will help us understand some basic features and useful concepts of elastic-plastic deformation of a structure. The example selected for analysis is the thick-walled tube, with closed ends, under internal pressure. The tube has inner radius a and outer radius b (Fig. 4.7). We shall assume that the tube is sufficiently long for end effects not to be felt in the zone which we study.

For this problem, it is best to work in cylindrical coordinates (r, θ, z) ; r is the radial distance measured perpendicularly from the axis of the tube, θ is an angular circumferential coordinate measured from an arbitrary datum, and z is the axial distance from an arbitrary datum plane parallel to the axis.

4.7.1. Basic Equations

The only nontrivial *equilibrium* equation is the radial one

$$\frac{d\sigma_r}{dr} - \frac{\sigma_\theta - \sigma_r}{r} = 0 \quad (4.48)$$

The *compatibility* equations express the geometrical relationships between strain and displacement. The displacement is still assumed to be small, and if u is a radial displacement of a point originally at radius r ,

$$\epsilon_r = \frac{du}{dr} \quad (4.49)$$

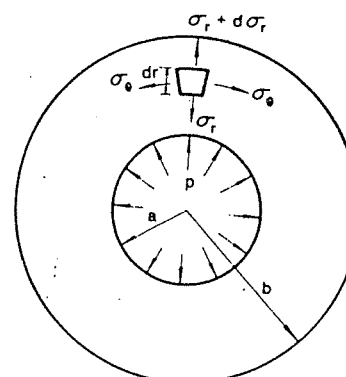


FIGURE 4.7. Transverse section of a thick-walled tube subject to interior pressure.

and, assuming symmetrical deformation,

$$\epsilon_\theta = \frac{u}{r} \quad (4.50)$$

In the axial direction, we can at present only state the "long tube" condition for the extension of the tube without bending:

$$\epsilon_z = \text{constant} = C \quad (4.51)$$

These relations are purely geometric, and thus hold irrespective of whether the strain is elastic or plastic.

The material of the tube is assumed to be elastic-perfectly plastic. In the elastic range, the behavior is described in terms of two elastic constants, Young's modulus E and Poisson's ratio ν . Because r , θ , and z are, by symmetry, the principal stress directions, we may write the elastic constitutive relations:

$$\begin{aligned} E\epsilon_r &= \sigma_r - \nu(\sigma_\theta + \sigma_z) \\ E\epsilon_\theta &= \sigma_\theta - \nu(\sigma_r + \sigma_z) \\ E\epsilon_z &= \sigma_z - \nu(\sigma_r + \sigma_\theta) \end{aligned} \quad (4.52)$$

The yield condition is that of Tresca, and the flow rule is associated with it by means of the normality condition.

The boundary conditions are especially simple:

$$\sigma_r = 0 \quad \text{at } r = b \quad (4.53)$$

$$\sigma_r = -p \quad \text{at } r = a \quad (4.54)$$

where p is the interior gauge pressure. Lastly, in the axial direction, overall equilibrium requires

$$p\pi a^2 = \int_a^b 2\pi\sigma_z r dr \quad (4.55)$$

4.7.2. Elastic Solution

Elastic analysis of this problem is straightforward. First use Eq. (4.51) to eliminate σ_z from Eq. (4.52). Then eliminate u from Eqs. (4.49) and (4.50) to give a compatibility relation

$$\epsilon_r = \frac{d}{dr}(r\epsilon_\theta) \quad (4.56)$$

Into this, substitute for ϵ_r and ϵ_θ in terms of σ_θ , σ_r , and C [Eq. (4.51)], using the relations just derived. This gives a first-order linear differential equation in σ_θ , σ_r , $(d\sigma_r/dr)$ and $(d\sigma_\theta/dr)$, but not in fact involving C . Eliminate σ_θ and $d\sigma_\theta/dr$ using this equation and Eq. (4.48) to give a

second-order differential equation in σ_r . Solve this subject to Eqs. (4.53) and (4.54) to give:

$$\sigma_r = p \left(-\frac{b^2}{r^2} + 1 \right) / \left(\frac{b^2}{a^2} - 1 \right) = \frac{pa^2(r^2 - b^2)}{r^2(b^2 - a^2)} \quad (4.57)$$

Substitution into Eq. (4.48) gives

$$\sigma_\theta = p \left(\frac{b^2}{r^2} + 1 \right) / \left(\frac{b^2}{a^2} - 1 \right) = \frac{pa^2(r^2 + b^2)}{r^2(b^2 - a^2)} \quad (4.58)$$

To find the stress σ_z , we use these results in the third relation of Eqs. (4.52) and note Eq. (4.51). This yields

$$\sigma_z = \nu(\sigma_r + \sigma_\theta) + EC = 2\nu \frac{pa^2}{b^2 - a^2} + EC \quad (4.59)$$

Substitution of σ_z in Eq. (4.55) yields $\epsilon_z = C = (1 - 2\nu)pa^2/[E(b^2 - a^2)]$. If we assume plane strain, i.e., $\epsilon_z = 0$, then we have

$$\nu = 0.5 \quad \text{and} \quad \sigma_z = \frac{1}{2}(\sigma_r + \sigma_\theta) \quad (4.60)$$

Equation (4.60) implies that for the problem to satisfy both $\epsilon_z = 0$ and Eq. (4.55), ν must take the special value 0.5.

The radial displacement, u , is obtained from Eqs. (4.50) and the second relation of (4.52):

$$u = r\epsilon_\theta = \frac{(1 + \nu)a^2 p}{E(b^2 - a^2)} \left[\frac{(1 - 2\nu)r}{(1 + \nu)} + \frac{b^2}{r} \right] \quad (4.61)$$

This elastic stress distribution only applies, of course, if p is sufficiently small for the stress point $(\sigma_r, \sigma_\theta, \sigma_z)$ at all radii within the wall of the tube to lie within the yield locus.

Note that, from Eq. (4.60), σ_z always takes a value such that it is the intermediate principal stress, i.e.,

$$\sigma_\theta > \sigma_z > \sigma_r$$

Hence, the yield condition of Tresca is

$$\sigma_\theta - \sigma_r = \sigma_0 \quad (4.62)$$

where σ_0 is the yield stress in simple tension. Substitution of Eqs. (4.57) and (4.58) in Eq. (4.62) gives

$$\sigma_\theta - \sigma_r = 2p \left(\frac{b^2}{r^2} \right) / \left(\frac{b^2}{a^2} - 1 \right) = \sigma_0 \quad (4.63)$$

It is clear from Eq. (4.63) that if the pressure is increased steadily, the yield stress is first reached at the inner surface, $r = a$. Thus, using Eq. (4.63) with $r = a$, we find that the pressure at which the yield point is first reached is given by

$$p = p_c = \frac{\sigma_0}{2} \left(1 - \frac{a^2}{b^2} \right) \quad (4.64)$$

Notice that the pressure for first yield at $r = a$ is a function of the ratio b/a and not of the absolute size of the tube.

4.7.3. Elastic-Plastic Expansion

If the pressure is increased above the value for first yield, an enlarging plastic zone spreads outwards from the inner surface.

To analyze this partly elastic, partly plastic state of affairs, suppose that at some stage in the expansion of the tube, the elastic-plastic boundary is at radius c , where $a \leq c \leq b$, as shown in Fig. 4.8. At $r = c$, let $\sigma_r = -q$; i.e., call the radial pressure q at this radius. The outer elastic zone cannot differentiate, so to speak, between pressure q exerted by the plastic zone or q provided by a fluid. It follows therefore that because the outer surface is not loaded, the equations we have already derived apply in the elastic region, provided the symbol a is replaced throughout by c . In particular, because the stress must be at the yield point at $r = c$, Eq. (4.64) gives

$$q = \frac{\sigma_0}{2} \left(1 - \frac{c^2}{b^2} \right) \quad (4.65)$$

Turning now to the plastic zone, we find that the key to the situation is the *yield condition* (4.62). Substituting (4.62) into the equilibrium equation (4.48), we can integrate directly to obtain

$$\sigma_r = \sigma_0 \ln r + \text{constant} \quad (4.66)$$

The constant is determined by the boundary condition $\sigma_r = -q$ at $r = c$; using this, we find

$$\sigma_r = -q + \sigma_0 \ln \frac{r}{c}$$

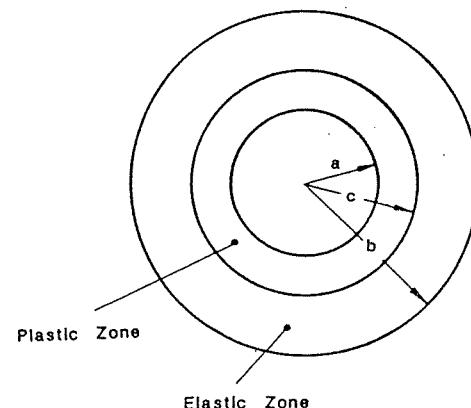


FIGURE 4.8. Plastic zone contained within an elastic zone.

Substituting (4.65) for q and using the yield condition (4.62) gives the stresses in the yield zone as

$$\begin{aligned} \sigma_r &= \sigma_0 \left[\ln \frac{r}{c} - \frac{1}{2} \left(1 - \frac{c^2}{b^2} \right) \right] \\ \sigma_\theta &= \sigma_0 \left[\ln \frac{r}{c} + \frac{1}{2} \left(1 + \frac{c^2}{b^2} \right) \right] \end{aligned} \quad (4.67)$$

We can now use the boundary condition $\sigma_r = -p$ at $r = a$ to obtain

$$\begin{aligned} p &= q + \sigma_0 \ln \left(\frac{c}{a} \right) \\ &= \frac{\sigma_0}{2} \left(1 - \frac{c^2}{b^2} \right) + \sigma_0 \ln \frac{c}{a} \end{aligned} \quad (4.68)$$

Hence, for any value of c between a and b , the corresponding pressure may be calculated. Also for any value of c , σ_θ and σ_r are determined throughout the tube. Figure 4.9 shows the results for a tube with $b/a = 2$ for various values of c/a . It is interesting to note that in the plastic zone the stresses are *statically determinate*, and, given the pressure at one boundary, the pressure at the other boundary is determined. Thus, the equations in the plastic zone, besides being simpler than those in the elastic zone, are of a different *kind*. The fact that the equilibrium equation and the yield condition can be solved directly without reference to deformation—i.e., that the situation is statically determinate—is a consequence of the *uncoupling* of stress and strain which follows from the special nonhardening form of our idealized plastic material.

4.7.4. Elastic-Plastic Deformation

It is noted that the radial expansion of the plastic zone is controlled by the elastic deformation of the elastic zone which entirely surrounds it. The elastic zone can be regarded as sustaining a pressure q exactly as if the inner portion of the tube were filled with fluid. It follows that the pattern of strain within the tube in the elastic-plastic condition is a very simple one—there is no axial elongation, and since the material is incompressible in both the elastic and plastic ranges, the deformation may readily be expressed in terms of a single parameter. A convenient index of the deformation is the radial enlargement of the tube, u_b , at $r = b$.

At $r = b$, using Eq. (4.61) with c substituted for a and q for p , and substituting for q from Eq. (4.65), noting $\nu = \frac{1}{2}$, we have

$$\frac{u_b}{b} = \frac{3}{4} \frac{\sigma_0}{E} \left(\frac{c}{b} \right)^2 \quad (4.69)$$

Using this in Eq. (4.68) and rearranging, we find

$$\frac{2p}{\sigma_0} = 1 - \frac{4}{3} \frac{E}{\sigma_0} \frac{u_b}{b} + \ln \left(\frac{4}{3} \frac{E}{\sigma_0} \frac{u_b}{b} \right) + 2 \ln \frac{b}{a} \quad (4.70)$$

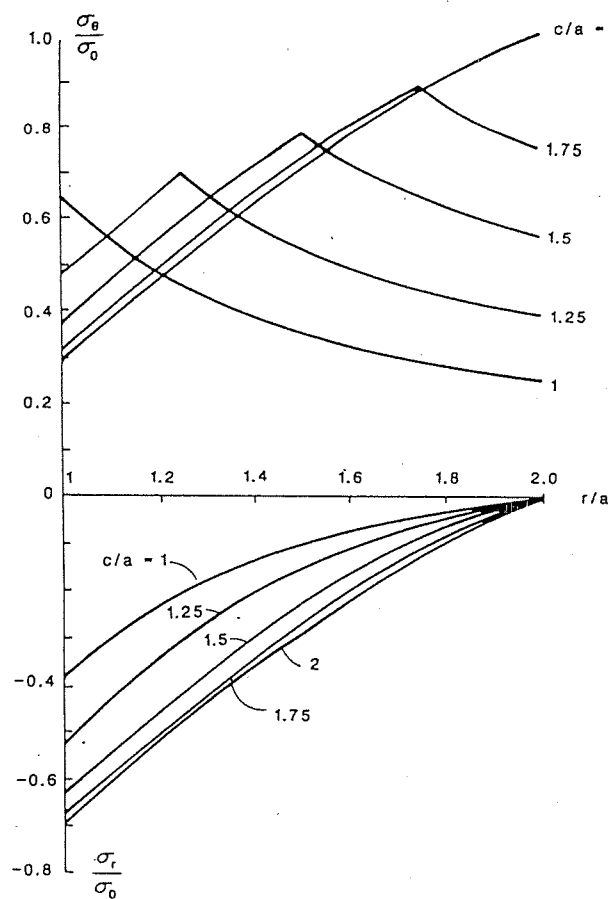


FIGURE 4.9. Successive distributions of circumferential and radial stress in the elastic-plastic expansion of a tube: $b/a = 2$.

This relationship between pressure and radial enlargement applies provided $a \leq c \leq b$, from which, using Eq. (4.69), we obtain

$$\frac{a^2}{b^2} \leq \frac{4}{3} \frac{E}{\sigma_0} \frac{u_b}{b} \leq 1 \quad (4.71)$$

When the behavior is entirely elastic, the corresponding equation is

$$\frac{2p}{\sigma_0} = \left(\frac{b^2}{a^2} - 1 \right) \left(\frac{4}{3} \frac{E}{\sigma_0} \frac{u_b}{b} \right) \quad (4.72)$$

When the elastic-plastic boundary reaches the outer surface, $c = b$, and Eq. (4.68) becomes

$$\frac{2p_c}{\sigma_0} = 2 \ln \frac{b}{a} \quad (4.73)$$

The "full plastic" pressure $p_c = \sigma_0 \ln(b/a)$ is maintained if the tube expands further. According to the elastic-perfectly plastic assumption, it is possible for indefinitely large strains to take place in the absence of a surrounding elastic ring.

These results are plotted for $b/a = 2$ as curve ORST in Fig. 4.10.

In conclusion, there are three phases of behavior for an initially stress-free tube with closed ends, made of elastic-perfectly plastic material and subject to a steadily increasing interior pressure:

- (i) An *elastic* phase, in which all the material is in the elastic range.
- (ii) An *elastic-plastic* phase in which an inner plastic zone is contained within an elastic zone. The plastic zone spreads as the pressure increases, but the deflections—which are controlled by the elastic zone—are of the same order as those in the elastic phase.

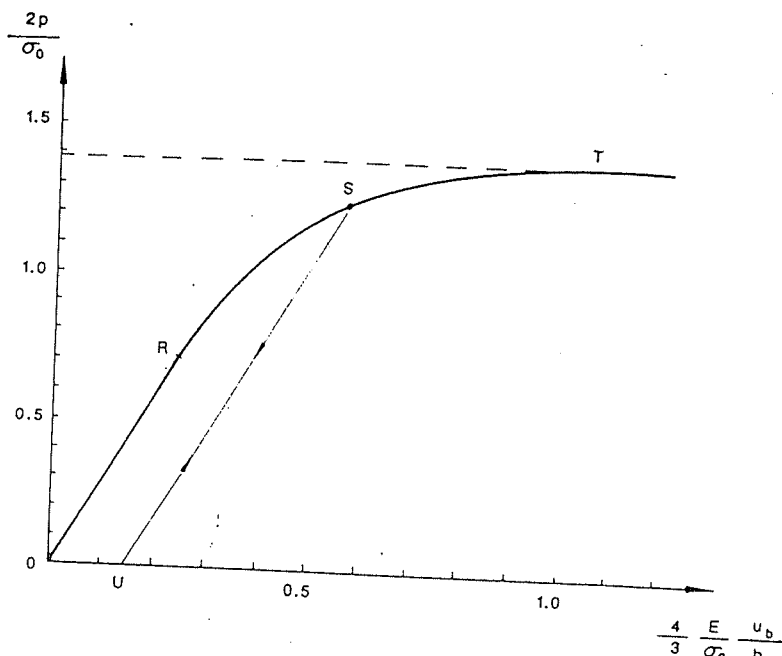


FIGURE 4.10. Elastic-plastic pressure-expansion curve showing unloading behavior.

- (iii) A full-plastic phase in which, the outer elastic zone having vanished, the tube is free to expand by plastic deformation and achieves much larger deflections than in the elastic range. Apart from second-order effects, plastic expansion takes place at a constant pressure called the *plastic collapse pressure*. At this pressure, we predict, the tube will bulge considerably, and may burst.

4.7.5. Unloading

Suppose now that the pressure, having been raised into the elastic-plastic range, is steadily reduced until the pressure is again zero. What happens to the stresses in the tube?

For definiteness, we consider a particular case, $b = 2a$, with the pressure (applied to the stress-free tube) having risen to the value corresponding to $c = 1.5a$, i.e., by Eq. (4.68), $p = \sigma_0 [7/32 + \ln(1.5)] = 0.624\sigma_0$. The distributions of the principal stresses under these conditions are shown in Fig. 4.11 (full curves). When the pressure begins to fall, it seems likely that the material which was at the yield stress will have its stress "level" reduced, and will thus immediately reenter the elastic range. Because we now have some permanent plastic deformation in the contained plastic zone, we must regard the elastic relations (4.52) as referring to *changes* of stress and strain. As all the material is now behaving elastically, we can use results (4.57) to (4.59) to work out the *changes* in σ_r , σ_θ , and σ_z for negative pressure increments. For a complete removal of pressure, for example, we must subtract from the elastic-plastic stress distribution in Fig. 4.11 a stress distribution which would have occurred at the same pressure if the material had remained elastic. This is shown in Fig. 4.11 (broken curves). We must, of course, now check that the material is nowhere stressed to yield. This is easily done in the present case because— σ_z being the intermediate principal stress—we simply have to verify that $|\sigma_\theta - \sigma_r| < \sigma_0$ everywhere; in Fig. 4.11 this is clearly so.

It is instructive to plot the stress trajectories in the π -plane, shown in Fig. 4.12. Since $\sigma_z = (\sigma_\theta + \sigma_r)/2$ everywhere (this includes the *assumption* that such is the case in the plastic zone on first loading), all points lie on a line through the origin perpendicular to the projection of the σ_z -axis. Points A , B , and C correspond to the radii a , b , and c , respectively, when $p = 0.624\sigma_0$, and A' , B' , and C' to the same radii when the pressure has been released. It is clear that the yield condition is not violated in the unloaded state. Having loaded the tube into the partially plastic range and then unloaded, we are thus left with a *residual stress distribution*.

If we now increase the pressure again, the stress points in Fig. 4.12 will retrace their paths between A' , B' , C' and A , B , C ; yielding will recommence at $p = 0.624\sigma_0$, and at higher pressures the behavior will be exactly as if the pressure had been increased beyond this point in the first loading. The pressure-radial displacement behavior under this program of loading is

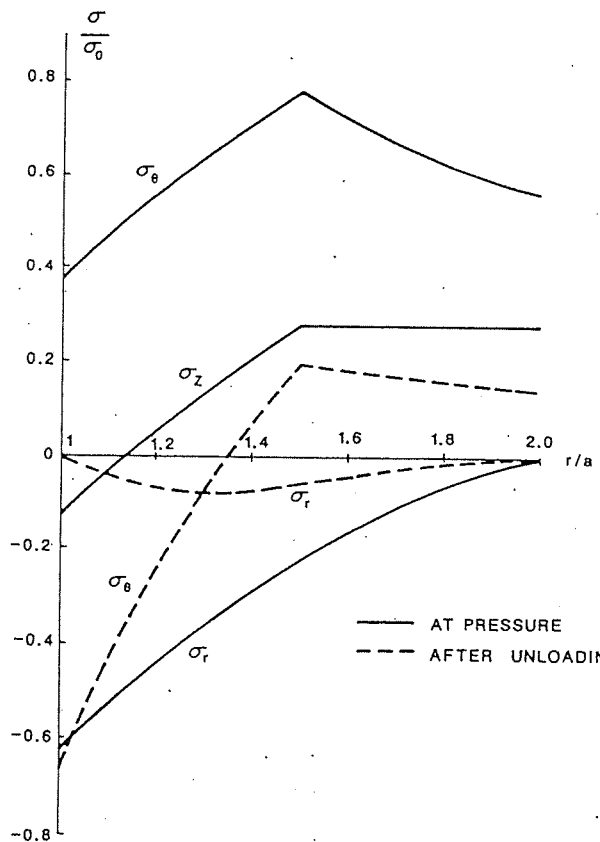


FIGURE 4.11. Distribution of circumferential, radial, and axial stress at a particular stage in the elastic-plastic expansion of a tube and after release of pressure.

shown by curve $ORSU$ in Fig. 4.10; it is closely analogous to the load-extension behavior in a tensile test of a hardening material.

4.7.6. "Shakedown"

Another important aspect of the phenomenon of readjustment of stress distributions in structures by limited plastic flow of the ductile material is seen in structures which carry repeatedly applied and alternating loads. A possible mode of failure under these circumstances is low-cycle *fatigue* of part of the structure through cyclic plastic deformation. What tends to happen in many structures is that in the course of the first few applications

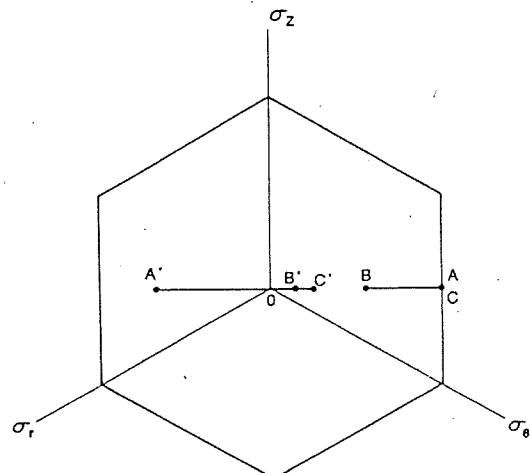


FIGURE 4.12. Stress trajectories for partly plastic tube at pressure and after release of pressure (cf. Fig. 4.11).

of loads, the structure "does its best," by means of limited plastic flow, to set up residual stress distributions that will minimize the plastic fatigue strains in subsequent cycles.

To provide a simple illustration of this, consider a pressure $p = 0.624\sigma_0$ repeatedly applied to our tube ($b/a = 2$). Supposing that the tube was initially stress-free, first yield would be reached at $p = 0.375\sigma_0$ [see Eq. (4.64)]: it might thus be thought—at least, by anyone unfamiliar with plastic analysis—that this would be the pressure limit for avoidance of repeated plasticity in repeated pressure loading. However, the analysis we have already done shows that a single application of $p = 0.624\sigma_0$ induces a residual stress pattern which enables the structure to respond to repeated pressure application up to this level by purely elastic action. We say that the structure will *shake down* to elastic behavior for repeated pressurization between $p = 0$ and $p = 0.624\sigma_0$; we draw an analogy with the behavior of a feather-filled cushion which "shakes down" when repeatedly sat upon.

Figure 4.12 suggests that our particular tube will shake down for even higher pressures: in fact, it may easily be shown that shakedown will occur for all pressures up to the plastic collapse pressure. This result however is, in a sense, a special one for sufficiently small values of b/a . For values of this ratio greater than about 2.2, shakedown is possible only for pressures lower than the plastic collapse pressure (Problem 4.6).

It must be admitted that the preceding example of shakedown has been extremely simple: a simple structure subject to only one kind of loading whose sign never changed. Clearly, a full discussion of shakedown should

involve multiple independent loading systems with the possibility of variation of sign. This is, however, beyond the scope of the present book.

A practical application of shakedown in thick tubes is the "autofrettage" process, which has been used for many years in the manufacture of gun barrels. It is clearly desirable that the inner bore of the barrel should retain its dimensional accuracy on repeated pressurization due to firing. By subjecting the barrel to an *overpressure* before the final surface machining is done, a residual stress system is set up in the barrel which ensures that the bore never goes into the plastic range subsequently, under normal conditions.

4.8. Incremental Stress-Strain Relationships

In an elastoplastic analysis by a numerical approach, the most common technique is the incremental method using tangent stiffness. The constitutive relations given in Sections 4.2 to 4.5 cannot be directly applied. An incremental relationship between stress and strain is needed in forming the tangent stiffness matrix. These types of constitutive relations are studied here in this section.

As discussed before, multiaxial perfectly plastic behavior requires that the stress increment vector be tangent to the yield surface and the plastic strain increment vector be normal to the loading surface. According to the concept of perfect plasticity, the magnitude of the plastic strain increment cannot be uniquely determined by the given current stresses σ_{ij} and stress increments $d\sigma_{ij}$. However, for given current stresses σ_{ij} and a given plastic strain increment $d\epsilon_{ij}^p$ satisfying the flow rule, the stress increment $d\sigma_{ij}$ can be determined by the so-called *consistency condition* which ensures that the stress state remains on the yield surface.

4.8.1. Constitutive Relation in General Form

According to Section 4.1, the total strain increment is assumed to be the sum of the elastic strain increment and the plastic strain increment [Eq. (4.4)]:

$$d\epsilon_{ij} = d\epsilon_{ij}^e + d\epsilon_{ij}^p \quad (4.74)$$

The elastic strain increment can be obtained from Hooke's law [see Eqs. (3.89) and (3.96)]:

$$d\epsilon_{ij}^e = D_{ijkl} d\sigma_{kl} \quad (4.75a)$$

or

$$d\epsilon_{ij}^e = \frac{dI_1}{9K} \delta_{ij} + \frac{ds_{ij}}{2G} \quad (4.75b)$$

and the plastic strain increment is obtained from the flow rule, Eq. (4.6). Then the complete strain-stress relations for an elastic-perfectly plastic material are expressed as

$$d\epsilon_{ij} = D_{ijkl} d\sigma_{kl} + d\lambda \frac{\partial f}{\partial \sigma_{ij}} \quad (4.76a)$$

or

$$d\epsilon_{ij} = \frac{dI_1}{9K} \delta_{ij} + \frac{ds_{ij}}{2G} + d\lambda \frac{\partial f}{\partial \sigma_{ij}} \quad (4.76b)$$

where $d\lambda$ is an as yet undetermined factor with the value

$$d\lambda \begin{cases} = 0 & \text{whenever } f < 0 \text{ or } f = 0 \text{ but } df < 0 \\ > 0 & \text{whenever } f = 0 \text{ and } df = 0 \end{cases} \quad (4.77)$$

We shall determine the form of the factor $d\lambda$ below. This can be accomplished by combining the stress-strain relations (4.76) with the *consistency condition*

$$df = \frac{\partial f}{\partial \sigma_{ij}} d\sigma_{ij} = 0 \quad (4.78)$$

which ensures that the stress state $(\sigma_{ij} + d\sigma_{ij})$ existing after the incremental change $d\sigma_{ij}$ has taken place still satisfies the yield criterion f

$$f(\sigma_{ij} + d\sigma_{ij}) = f(\sigma_{ij}) + df = f(\sigma_{ij}) \quad (4.79)$$

Solving Eq. (4.76) for $d\sigma_{ij}$, or directly using Hooke's law [Eq. (3.72)], the flow rule [Eq. (4.6)], and Eq. (4.74), we can determine the stress increment tensor

$$d\sigma_{ij} = C_{ijkl} (d\epsilon_{kl} - d\epsilon_{kl}^p) = C_{ijkl} d\epsilon_{kl} - d\lambda C_{ijkl} \frac{\partial f}{\partial \sigma_{kl}} \quad (4.80)$$

Substitute Eq. (4.80) into Eq. (4.78) and solve for $d\lambda$:

$$d\lambda = \frac{\frac{\partial f}{\partial \sigma_{ij}} C_{ijkl} d\epsilon_{kl}}{\frac{\partial f}{\partial \sigma_{rs}} C_{rstu} \frac{\partial f}{\partial \sigma_{tu}}} \quad (4.81)$$

All indices in Eq. (4.81) are dummy indices, indicating the scalar character of $d\lambda$. Therefore, if f is defined for a particular material of interest and strain increments $d\epsilon_{ij}$ are prescribed, the factor $d\lambda$ is determined uniquely.

Equation (4.81) is now substituted into Eq. (4.80); then the incremental stress-strain relation can be expressed explicitly in the following form

$$d\sigma_{ij} = \left[C_{ijkl} - \frac{C_{ijmn} \frac{\partial f}{\partial \sigma_{mn}} \frac{\partial f}{\partial \sigma_{pq}} C_{pqkl}}{\frac{\partial f}{\partial \sigma_{rs}} C_{rstu} \frac{\partial f}{\partial \sigma_{tu}}} \right] d\epsilon_{kl} \quad (4.82a)$$

in which some dummy subscripts have been properly altered. The coefficient tensor in the parentheses represents the elastic-plastic tensor of tangent moduli for an elastic-perfectly plastic material:

$$C_{ijkl}^{ep} = C_{ijkl} - \frac{C_{ijmn} \frac{\partial f}{\partial \sigma_{mn}} \frac{\partial f}{\partial \sigma_{pq}} C_{pqkl}}{\frac{\partial f}{\partial \sigma_{rs}} C_{rstu} \frac{\partial f}{\partial \sigma_{tu}}} \quad (4.82b)$$

Equation (4.82) is the most general formulation of the constitutive relation for an elastic-perfectly plastic material. It is seen that the stress increments can be determined uniquely by the yield function $f(\sigma_{ij})$ and the strain increments $d\epsilon_{ij}$. In other words, if the current stress state σ_{ij} is known and the increments of strain $d\epsilon_{ij}$ are prescribed, the corresponding stress increments $d\sigma_{ij}$ can be found from Eq. (4.82). In general, however, if the current stress state is known and the stress increments are prescribed, the corresponding strain increments cannot be uniquely determined because the plastic strain increments can be defined only to within the indeterminate factor $d\lambda$ [see Eq. (4.76)].

4.8.2. Constitutive Relation in Terms of Elastic Moduli E and ν or G and K

Now we need to express the elastic tensor, C_{ijkl} , in the constitutive equation explicitly in terms of the elastic moduli E and ν or G and K . To this end, we substitute Eq. (3.88) for C_{ijkl} into Eq. (4.81) to obtain an expression for the factor $d\lambda$:

$$d\lambda = \frac{\frac{\partial f}{\partial \sigma_{ij}} d\epsilon_{ij} + \frac{\nu}{1-2\nu} d\epsilon_{kk} \frac{\partial f}{\partial \sigma_{ij}} \delta_{ij}}{\frac{\partial f}{\partial \sigma_{rs}} \frac{\partial f}{\partial \sigma_{rs}} + \frac{\nu}{1-2\nu} \left(\frac{\partial f}{\partial \sigma_{rs}} \delta_{rs} \right)^2} \quad (4.83a)$$

Note that $\nu = \frac{1}{2}(3K - 2G)/(3K + G)$. Thus, the above expression can be rewritten as

$$d\lambda = \frac{\frac{\partial f}{\partial \sigma_{ij}} d\epsilon_{ij} + \frac{3K - 2G}{6G} d\epsilon_{kk} \frac{\partial f}{\partial \sigma_{ij}} \delta_{ij}}{\frac{\partial f}{\partial \sigma_{rs}} \frac{\partial f}{\partial \sigma_{rs}} + \frac{3K - 2G}{6G} \left(\frac{\partial f}{\partial \sigma_{rs}} \delta_{rs} \right)^2} \quad (4.83b)$$

Also, we can substitute Eq. (3.88) for C_{ijkl} into Eq. (4.80) to obtain an expression for $d\sigma_{ij}$ in terms of E and ν as

$$d\sigma_{ij} = \frac{E}{1+\nu} d\epsilon_{ij} + \frac{\nu E}{(1+\nu)(1-2\nu)} d\epsilon_{kk} \delta_{ij} - d\lambda \left[\frac{E}{1+\nu} \frac{\partial f}{\partial \sigma_{ii}} + \frac{\nu E}{(1+\nu)(1-2\nu)} \frac{\partial f}{\partial \sigma_{mm}} \delta_{mm} \delta_{ij} \right] \quad (4.84a)$$

or in terms of G and K as

$$d\sigma_{ij} = 2G d\epsilon_{ij} + K d\epsilon_{kk} \delta_{ij} - d\lambda \left[\left(K - \frac{2}{3} G \right) \frac{\partial f}{\partial \sigma_{mn}} \delta_{mn} \delta_{ij} + 2G \frac{\partial f}{\partial \sigma_{ij}} \right] \quad (4.84b)$$

For a number of materials, the yield function is generally expressed in terms of the stress invariants I_1 and J_2 in the form

$$f(\sigma_{ij}) = F(I_1, \sqrt{J_2}) - k = 0 \quad (4.85)$$

It follows that

$$\frac{\partial f}{\partial \sigma_{ij}} = \frac{\partial f}{\partial I_1} \frac{\partial I_1}{\partial \sigma_{ij}} + \frac{\partial f}{\partial \sqrt{J_2}} \frac{\partial \sqrt{J_2}}{\partial \sigma_{ij}} \quad (4.86)$$

which reduces to

$$\frac{\partial f}{\partial \sigma_{ij}} = \frac{\partial f}{\partial I_1} \delta_{ij} + \frac{1}{2\sqrt{J_2}} \frac{\partial f}{\partial \sqrt{J_2}} s_{ij} \quad (4.87)$$

With this expression, Eq. (4.84b) becomes

$$d\sigma_{ij} = 2G d\epsilon_{ij} + K d\epsilon_{kk} \delta_{ij} - d\lambda \left(3K \frac{\partial f}{\partial I_1} \delta_{ij} + \frac{G}{\sqrt{J_2}} \frac{\partial f}{\partial \sqrt{J_2}} s_{ij} \right) \quad (4.88)$$

where $d\lambda$ has the form

$$d\lambda = \frac{3K d\epsilon_{kk} (\partial f / \partial I_1) + (G/\sqrt{J_2})(\partial f / \partial \sqrt{J_2}) s_{mn} de_{mn}}{9K(\partial f / \partial I_1)^2 + G(\partial f / \partial \sqrt{J_2})^2} \quad (4.89)$$

In the next two sections, we shall discuss how these equations can be used for specified yield functions.

4.9. Prandtl-Reuss Material Model (J_2 Theory)

Most of the essential features of the incremental theory of plasticity can be illustrated by the most elementary form, $F = F(J_2)$. The simplest form of $F(J_2)$ is $\sqrt{J_2}$, now known as the von Mises yield criterion. The elastic-perfectly plastic stress-strain relations derived on the basis of the von Mises yield criterion

$$f = \sqrt{J_2} - k = 0 \quad (4.90)$$

and its associated flow rule are now known as the *Prandtl-Reuss material model*. This model is probably the most widely used and perhaps the simplest elastic-perfectly plastic material model.

To find the complete stress-strain relations of Prandtl-Reuss material, we simply substitute Eq. (4.90) for the yield function f into Eq. (4.89) to

obtain $d\lambda$ and then substitute $d\lambda$ into Eqs. (4.76b) and (4.88) to obtain

$$d\epsilon_{ij} = \frac{ds_{ij}}{2G} + \frac{dI_1}{9K} \delta_{ij} + \frac{s_{mn} de_{mn}}{2k^2} s_{ij} \quad (4.91)$$

$$d\sigma_{ij} = 2G d\epsilon_{ij} + K d\epsilon_{kk} \delta_{ij} - \frac{Gs_{mn} de_{mn}}{k^2} s_{ij} \quad (4.92)$$

When the conditions for the occurrence of plastic flow are satisfied,

$$J_2 = k^2 \quad \text{and} \quad df = \frac{\partial f}{\partial \sigma_{ij}} d\sigma_{ij} = s_{ij} ds_{ij} = 0 \quad (4.93)$$

The quantity $s_{mn} de_{mn}$ in the third term of Eqs. (4.91) and (4.92) is recognized as the rate of work due to distortion. Expanding this quantity in terms of the plastic and elastic strain increments, we obtain

$$s_{mn} de_{mn} = s_{mn} (de_{mn}^e + de_{mn}^p) \quad (4.94)$$

When we note that

$$de_{mn}^e = \frac{ds_{mn}}{2G} \quad (4.95)$$

and use the fact that

$$dJ_2 = s_{mn} ds_{mn} = 0 \quad (4.96)$$

Eq. (4.94) reduces to

$$s_{mn} de_{mn} = s_{mn} de_{mn}^p \quad (4.97)$$

indicating that the rate of distortional work in the plastic range is due solely to plastic deformation. Further, from Eqs. (4.91) and (4.92) we have

$$d\epsilon_{kk} = \frac{dI_1}{3K} = d\epsilon_{kk}^e \quad (4.98)$$

which implies that

$$de_{kk}^p = d\epsilon_{kk} - d\epsilon_{kk}^e = 0 \quad (4.99)$$

The volume change is purely elastic and no *plastic* volume change can occur for the Prandtl-Reuss material model. The plastic strain rate has only a deviatoric component, which is defined by the flow rule [see Eq. (4.8)]:

$$de_{ij}^p = d\lambda \frac{\partial f}{\partial \sigma_{ij}} = d\lambda \frac{\partial J_2}{\partial \sigma_{ij}} = d\lambda s_{ij} \quad (4.100)$$

The rate of plastic work can be simply derived:

$$dW_p = \sigma_{ij} de_{ij}^p = d\lambda \sigma_{ij} s_{ij} = 2 d\lambda J_2 = 2 d\lambda k^2 \quad (4.101)$$

From this, we determine the factor $d\lambda$

$$d\lambda = \frac{dW_p}{2k^2} = \frac{s_{mn} de_{mn}^p}{2k^2} = \frac{s_{mn} de_{mn}}{2k^2} \quad (4.102)$$

When $d\lambda = 0$, Eqs. (4.91) and (4.92) reduce to Hooke's law in differential form. Since the quantity $d\lambda$ is proportional to the increment $s_{mn} de_{mn}$, it is evident that the strain increments de_{ij} in Eq. (4.91) are not uniquely determined for a given stress state σ_{ij} ; but if the strain increments de_{ij} and the current stress state σ_{ij} are given, the corresponding stress increments $d\sigma_{ij}$ are uniquely determined by Eq. (4.92).

In conclusion, the characteristics of the Prandtl-Reuss material may be summarized as follows:

1. The increments of plastic strain depend on the current values of the deviatoric stress state, not on the stress increment required to reach this state.
2. The principal axes of the stress and the plastic strain increment tensors coincide.
3. No plastic volume change can occur during plastic flow.
4. The ratios of plastic strain increments in the different directions are specified, but the actual magnitudes of the increments are determined by $d\lambda$, which is related to the amount of actual increment in the work of plastic deformation dW_p .

EXAMPLE 4.2. Examine the behavior of Prandtl-Reuss material under conditions of uniaxial strain.

SOLUTION. Under uniaxial strain conditions, the strain increments and stresses are given as

$$\begin{aligned} de_{ij} &= [de_1, 0, 0]; \quad de_{ij} = \frac{1}{3}de_1[2, -1, -1] \\ \sigma_{ij} &= [\sigma_1, \sigma_2, \sigma_2]; \quad s_{ij} = [s_1, s_2, s_2] \end{aligned} \quad (4.103)$$

and the von Mises yield criterion has the simple form

$$\sqrt{J_2} = \frac{1}{\sqrt{3}} |\sigma_1 - \sigma_2| = k \quad (4.104)$$

In the elastic range, the incremental stress-strain relations are given by

$$d\sigma_1 = \left(K + \frac{4}{3}G \right) de_1 = B de_1 = \frac{3K + 4G}{9K} dI_1 \quad (4.105a)$$

and

$$d\sigma_1 - d\sigma_2 = 2G de_1 = \frac{2G}{3K} dI_1 \quad (4.105b)$$

By substituting the yield criterion (4.104) into Eqs. (4.105), the value of the vertical stress σ_1 at yield is obtained:

$$|\sigma_1| = \frac{\sqrt{3}(3K + 4G)}{6G} k = \frac{\sqrt{3}B}{2G} k \quad (4.106)$$

where $B = K + \frac{4}{3}G$ is known as the *constrained modulus*. Thus, when σ_1 reaches the value given by Eq. (4.106), the material yields, and further increase of vertical stress results in both plastic and elastic strains as the stress state moves along the perfectly plastic yield surface. In the plastic range, the stress-strain relations (4.92) for the shear components have the form

$$ds_1 = 2G de_1 - \frac{G(s_1 de_1 + 2s_2 de_2)}{k^2} s_1 \quad (4.107)$$

When we use the fact that $ds_{ii} = de_{ii} = 0$ and $de_1 = 2 de_1/3$, Eq. (4.107) becomes

$$ds_1 = \frac{4G}{3} de_1 - \frac{Gs_1^2}{k^2} de_1 = 0 \quad (4.108)$$

since $k^2 = J_2 = \frac{3}{4}s_1^2$ in the plastic range. Equation (4.108) indicates that $ds_2 = 0$ also because $ds_{ii} = 0$.

Thus, in the uniaxial strain test, the stress changes beyond the initial yield are purely of the hydrostatic pressure type:

$$d\sigma_1 = ds_1 + \frac{1}{3}dI_1 = \frac{1}{3}dI_1 \quad (4.109a)$$

$$d\sigma_2 = ds_2 + \frac{1}{3}dI_1 = \frac{1}{3}dI_1 \quad (4.109b)$$

The material behaves as though it were a fluid once it has reached its limiting shear resistance, and the corresponding volume changes are purely elastic

$$\frac{1}{3}dI_1 = K de_1 \quad (4.110)$$

Substitution of Eq. (4.110) into Eq. (4.109a) leads to the vertical stress-strain relation in the plastic range

$$d\sigma_1 = K de_1 \quad (4.111)$$

Figure 4.13 depicts schematically the behavior of Prandtl-Reuss material in a uniaxial strain test. The slope of the σ_1 vs. ϵ_1 curve (Fig. 4.13a) breaks, or softens, when yielding occurs and becomes equal to the bulk modulus. Accordingly, the loading slopes of the $(\sigma_1 - \sigma_2)$ vs. $(\epsilon_1 - \epsilon_2)$ curve and the $(\sigma_1 - \sigma_2)$ vs. $I_1/3$ curve become zero (Fig. 4.13b and d). Since $de_{kk} = 0$, the slope of the $I_1/3$ vs. ϵ_{kk} curve remains constant (Fig. 4.13c). Once the material unloads, it follows the linear elastic relations (4.105) until it reaches the yield surface again on the opposite side of the yield surface, corresponding to

$$\frac{1}{\sqrt{3}} (\sigma_1 - \sigma_2) = -k \quad (4.112)$$

and then the material flows plastically again, according to Eqs. (4.92). This unloading behavior is also shown in Fig. 4.13.

EXAMPLE 4.3. Examine the behavior of Prandtl-Reuss material under a plane stress condition defined by $\sigma_{ij} = [\sigma_1, 0, \sigma_3]$.

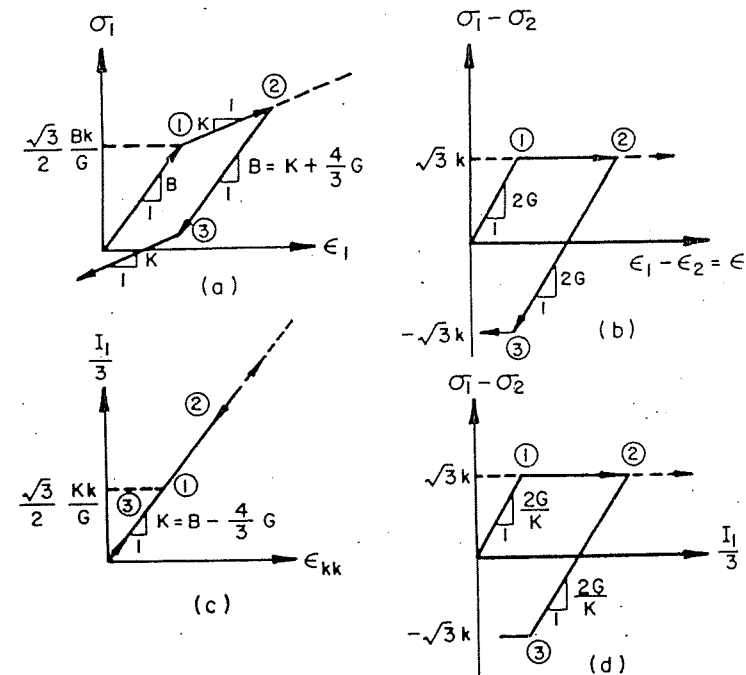


FIGURE 4.13. Behavior of Prandtl-Reuss material under conditions of uniaxial strain. (a) vertical stress-strain relation; (b) principal stress difference-strain relation; (c) pressure-volumetric-strain relation; and (d) principal stress difference-pressure relation (stress path).

SOLUTION. For this stress state, the material will yield when

$$J_2 = \frac{1}{3}(\sigma_1^2 + \sigma_3^2 - \sigma_1\sigma_3) = k^2 \quad (4.113)$$

Equation (4.113) describes an ellipse in (σ_1, σ_3) stress space (Fig. 4.14). We now consider a biaxial tension-tension test where the lateral stress σ_3 is held constant at the k value while the vertical stress is increased from point A to point B. Before reaching the yield point B, the behavior of the material is linearly elastic with

$$\begin{aligned} d\sigma_1 &= \frac{9KG}{3K+G} d\epsilon_1 = E d\epsilon_1 \\ d\epsilon_3 &= -\frac{3K-2G}{6K+2G} d\epsilon_1 = -\nu d\epsilon_1 \end{aligned} \quad (4.114)$$

$$d\epsilon_2 = d\epsilon_3$$

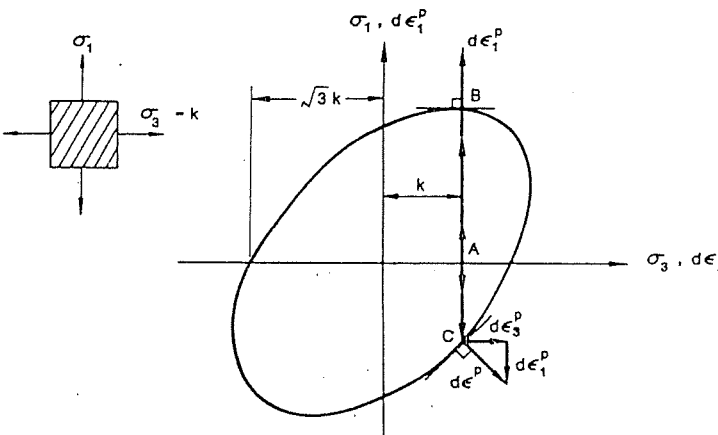


FIGURE 4.14. von Mises yield curve for special plane stress condition; AB and AC are stress paths; $d\epsilon^p$ = plastic strain increment vector.

At point B, the material yields, and unlimited plastic deformation takes place at $\sigma_1 = 2k$, $\sigma_3 = k$; the corresponding components of the plastic strain increments are

$$\begin{aligned} d\epsilon_3^p &= d\lambda \frac{\partial J_2}{\partial \sigma_3} = \frac{d\lambda}{3} (2\sigma_3 - \sigma_1) = 0 \\ d\epsilon_2^p &= -d\epsilon_1^p = -k d\lambda \text{ due to incompressibility} \end{aligned} \quad (4.115)$$

Note that we cannot obtain $d\epsilon_2^p$ by differentiating the yield condition (4.113) because it is a form given in (σ_1, σ_3) subspace only. However, we can differentiate J_2 in the original form $\frac{1}{6}[(\sigma_1 - \sigma_2)^2 + (\sigma_2 - \sigma_3)^2 + (\sigma_3 - \sigma_1)^2]$ to obtain $d\epsilon_2^p = -d\lambda (\sigma_1 + \sigma_3)/3 = -k d\lambda$. If we repeat the same test and change the direction of σ_1 (a biaxial tension-compression test), we find that the material yields when $\sigma_1 = -k$ and $\sigma_3 = k$ (point C in Fig. 4.14). At point C, the unlimited plastic flow has the value

$$d\epsilon_2^p = 0, \quad d\epsilon_1^p = -d\epsilon_3^p = -k d\lambda \quad (4.116)$$

If the plastic strain increment coordinates are superimposed on the stress coordinates, as shown in Fig. 4.14, the concept of normality or the associated flow rule can be demonstrated clearly from this simple example. In the biaxial tension-tension test, $d\epsilon_3^p = 0$, and the plastic strain increment vector $d\epsilon_1^p$ is perpendicular to the yield surface at point B. In the biaxial tension-compression test, on the other hand, $d\epsilon_1^p = -d\epsilon_3^p$, indicating that the plastic strain increment vector is perpendicular to the yield surface at point C.

4.10. Drucker-Prager Material Model

The Drucker-Prager yield criterion f takes the form (see Section 2.3.4)

$$f \doteq \sqrt{J_2} + \alpha I_1 - k = 0 \quad (4.117)$$

where α and k are positive material constants. As described in Chapter 2, the yield surface, $f=0$, in principal stress space is a right-circular cone with its axis equally inclined with respect to each of the coordinate axes and its apex in the tension octant.

According to Eqs. (4.76) and (4.89), the stress-strain relation corresponding to the yield function (4.117) is

$$d\epsilon_{ij} = \frac{ds_{ij}}{2G} + \frac{dI_1}{9K} \delta_{ij} + d\lambda \left(\frac{s_{ij}}{2\sqrt{J_2}} + \alpha \delta_{ij} \right) \quad (4.118)$$

where

$$d\lambda = \frac{(G/\sqrt{J_2})s_{mn} de_{mn} + 3K\alpha de_{kk}}{G+9K\alpha^2} \quad (4.119)$$

A very important feature of Eq. (4.118) is that the plastic rate of cubic dilatation as given by the third term on the right-hand side of this equation is

$$de_{kk}^p = 3\alpha d\lambda \quad (4.120)$$

Equation (4.120) shows that plastic deformation must be accompanied by an increase in volume if $\alpha \neq 0$. This property is known as *dilatancy*; it is the consequence of the dependency of the yield function on hydrostatic pressure. For any yield surface open in the direction of the negative hydrostatic axis, a plastic volume expansion takes place at yield with an associated flow rule. This is perhaps easier to see from the following geometric arguments.

The meridians of the yield surface are the intersection curves between the yield surface and a plane (the meridian plane) containing the hydrostatic axis; that is, $\theta = \text{const.}$ in a general yield function. Figure 4.15 shows such a typical meridian of a Drucker-Prager yield surface open in the direction of the negative hydrostatic axis. The normality condition or associated flow rule requires that the plastic strain increment vector de_{ij}^p be perpendicular to the yield surface at the actual yield point P . It is therefore also perpendicular to the meridian through P . The vector de_{ij}^p is now decomposed into the vertical and horizontal components de_{ij}^{pa} and de_{ij}^{ph} parallel to the ρ and ξ axes, respectively. The horizontal component de_{ij}^{pb} represents the plastic volume change, which is always positive when the yield surface opens in the direction of the negative hydrostatic axis (Fig. 4.15). This implies that plastic flow must always be accompanied by an *increase* in volume.

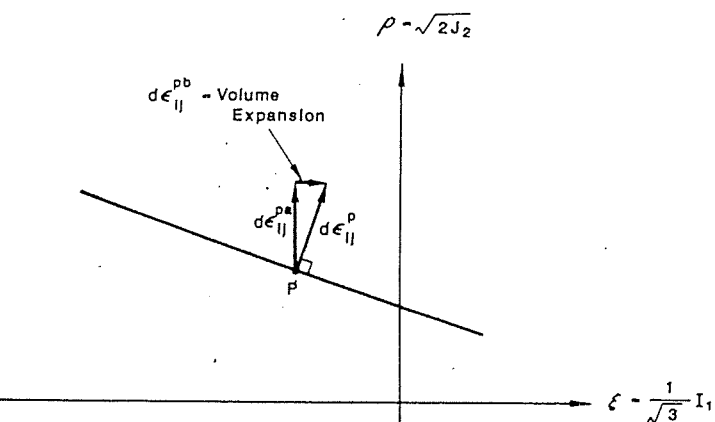


FIGURE 4.15. Plastic volume expansion associated with Drucker-Prager yield surface.

The increment of total volumetric strain $de_{kk} = de_{kk}^e + de_{kk}^p$ can be determined from Eq. (4.118) and $d\lambda$ from (4.119). From Eq. (4.118), we have

$$de_{kk} = \frac{dI_1}{3K} + 3\alpha \frac{(G/\sqrt{J_2})[\sigma_{mn} de_{mn} - I_1(d\epsilon_{kk}/3)] + 3K\alpha de_{kk}}{G+9K\alpha^2} \quad (4.121)$$

Solving for de_{kk} and using Eq. (4.117), we obtain

$$de_{kk} = \frac{\sqrt{J_2} dI_1}{3KGk} (G+9K\alpha^2) + \frac{3\alpha}{k} \sigma_{mn} de_{mn} \quad (4.122)$$

Substituting the yield function (4.117) into Eqs. (4.88) and (4.89), we obtain the following relationship for the stress increment tensor for the Drucker-Prager material

$$d\sigma_{ij} = 2G de_{ij} + K de_{kk} \delta_{ij} - d\lambda \left(\frac{G}{\sqrt{J_2}} s_{ij} + 3K\alpha \delta_{ij} \right) \quad (4.123)$$

where $d\lambda$ is already given by Eq. (4.119). Equation (4.123) can be rewritten in the preferable form

$$d\sigma_{ij} = C_{ijmn}^p de_{mn} \quad (4.124)$$

for direct use in a finite-element formulation, where

$$\begin{aligned} C_{ijmn}^p &= 2G\delta_{im}\delta_{jn} + \left(K - \frac{2}{3}G \right) \delta_{ij}\delta_{mn} \\ &\quad - \frac{(G/\sqrt{J_2})s_{ij} + 3K\alpha\delta_{ij}}{G+9K\alpha^2} \left(\frac{G}{\sqrt{J_2}} s_{mn} + 3K\alpha\delta_{mn} \right) \end{aligned} \quad (4.125)$$

The tensor C_{ijmn}^{ep} is a specific form of the elastic-plastic tensor of tangent moduli for the Drucker-Prager material model. The general form of C_{ijmn}^{sp} is given by Eq. (4.82b).

EXAMPLE 4.4. Write explicitly the plane strain constitutive matrix for Drucker-Prager material.

SOLUTION. For the plane strain case ($\gamma_{yz} = \gamma_{xz} = \epsilon_z = 0$), we can write in matrix form

$$\begin{bmatrix} d\sigma_x \\ d\sigma_y \\ d\tau_{xy} \\ d\sigma_z \end{bmatrix} = [C^{ep}] \begin{bmatrix} d\epsilon_x \\ d\epsilon_y \\ d\gamma_{xy} \\ d\gamma_{xz} \end{bmatrix} \quad (4.126)$$

where the z -axis is normal to the plane and $d\gamma_{xy}$ is the so-called engineering shear strain increment

$$d\gamma_{xy} = 2 d\epsilon_{xy} \quad (4.127)$$

and

$$[C^{ep}] = [C] + [C']$$

in which

$$[C] = \begin{bmatrix} K + \frac{4}{3}G & K - \frac{2}{3}G & 0 \\ K - \frac{2}{3}G & K + \frac{4}{3}G & 0 \\ 0 & 0 & G \\ K - \frac{2}{3}G & K - \frac{2}{3}G & 0 \end{bmatrix} \quad (4.128)$$

$$[C'] = \frac{-1}{G + 9K\alpha^2} \begin{bmatrix} H_1^2 & H_1H_2 & H_1H_3 \\ H_2H_1 & H_2^2 & H_2H_3 \\ H_3H_1 & H_3H_2 & H_3^2 \\ H_4H_1 & H_4H_2 & H_4H_3 \end{bmatrix} \quad (4.129)$$

and

$$H_1 = 3K\alpha + \frac{G}{\sqrt{J_2}} s_x, \quad H_2 = 3K\alpha + \frac{G}{\sqrt{J_2}} s_y$$

$$H_3 = \frac{G}{\sqrt{J_2}} \tau_{xy}, \quad H_4 = 3K\alpha + \frac{G}{\sqrt{J_2}} s_z$$

EXAMPLE 4.5. Examine the behavior of Drucker-Prager material under a uniaxial state-of-strain test:

$$\begin{aligned} d\epsilon_{ij} &= [d\epsilon_1, 0, 0] \\ d\epsilon_{ij} &= \frac{1}{3}d\epsilon_1[2, -1, -1] \\ \sigma_{ij} &= [\sigma_1, \sigma_2, \sigma_2] \end{aligned} \quad (4.130)$$

SOLUTION. The elastic behavior of the material is governed by Eqs. (4.105), which can be rewritten as

$$\sigma_1 = \frac{3K + 4G}{9K} I_1 \quad (4.131a)$$

and

$$\sigma_1 - \sigma_2 = \frac{2G}{3K} I_1 \quad (4.131b)$$

By using Eq. (4.131a), Eq. (4.131b) can be written as

$$\sigma_1 - \sigma_2 = \frac{6G}{3K + 4G} \sigma_1 \quad (4.131c)$$

The Drucker-Prager yield condition in the case of uniaxial strain becomes

$$\alpha I_1 + \sqrt{J_2} = \alpha(\sigma_1 + 2\sigma_2) + \frac{1}{\sqrt{3}} |\sigma_1 - \sigma_2| = k \quad (4.132)$$

Substituting Eq. (4.131a) for I_1 and Eq. (4.131c) for $\sqrt{J_2}$ or $|\sigma_1 - \sigma_2|$ into Eq. (4.132) leads to

$$|\sigma_1| = \frac{\sqrt{3}(3K + 4G)k}{6G \pm 9\sqrt{3}K\alpha} = \frac{\sqrt{3}Bk}{2G \pm 3\sqrt{3}K\alpha} \quad (4.133)$$

in which the upper sign corresponds to the case of $\sigma_1 > 0$ and the lower sign to $\sigma_1 < 0$. When α is equal to zero, Eq. (4.133) reduces to Eq. (4.106), corresponding to Prandtl-Reuss material. The effect of α in this case is to decrease the value of the vertical stress σ_1 at yield for a uniaxial tension test (upper sign) and to increase the value σ_1 at yield for a uniaxial compression test (lower sign). Further increase of the vertical stress σ_1 results in the stress state in the material moving along the yield surface undergoing both elastic and plastic deformation. The incremental relation between vertical stress and vertical strain is obtained for Eq. (4.123) in the elastoplastic range

$$d\sigma_1 = \left(K + \frac{4}{3}G \right) d\epsilon_1 - \frac{(3K\alpha \pm 2G/\sqrt{3})^2}{9K\alpha^2 + G} d\epsilon_1 \quad (4.134)$$

in which the upper sign is for the case $d\sigma_1 > 0$ while the lower sign is for $d\sigma_1 < 0$. Again, it is noted that when α is set equal to zero, Eq. (4.134) reduces to the corresponding equation (4.111) for Prandtl-Reuss material.

From Eq. (4.134), the slope of the σ_1 vs. ϵ_1 curve during plastic flow can be obtained as

$$\frac{d\sigma_1}{d\epsilon_1} = K \frac{(1 \pm 2\sqrt{3}\alpha)^2}{1 + 9\alpha^2 K/G} \quad (4.135)$$

in which the upper sign is for the case $d\sigma_1 < 0$ while the lower sign is for $d\sigma_1 > 0$.

The stress-strain relation in a uniaxial strain-compression test is shown in Fig. 4.16 for both Prandtl-Reuss and Drucker-Prager material models. For the Prandtl-Reuss model (Fig. 4.16a), the curve is elastic until the yield condition is reached at a stress proportional to k [Eq. (4.106)]. In the plastic region, the slope is simply the bulk modulus K . Unloading is elastic until the opposite side of the yield surface is reached and then plastic again with slope K . At the completion of the compressive stress cycle, a permanent (compressive) strain remains.

The case of Drucker-Prager model loaded not too far beyond the elastic range is similar (Fig. 4.16b). To see this, let's examine the slope of the σ_1 vs. ϵ_1 curve in the plastic region. Since in order for the uniaxial strain-stress path to reach the yield surface in the compression test, the following condition must hold [see Eq. (4.133)]:

$$\frac{2G}{\sqrt{3}K} > 3\alpha \quad (4.136)$$

thus from Eq. (4.135) the slope of the σ_1 vs. ϵ_1 curve during the plastic flow

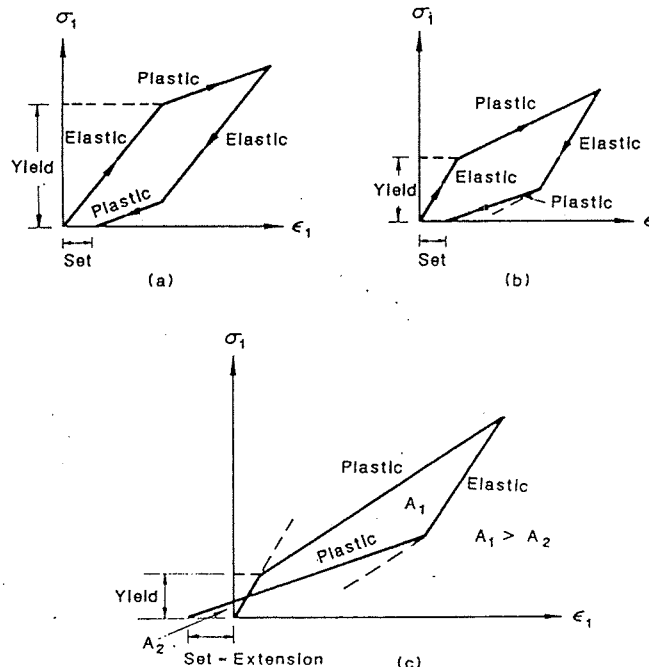


FIGURE 4.16. Uniaxial strain for Prandtl-Reuss and Drucker-Prager models. (a) Prandtl-Reuss, elastoplastic, k large; (b) Drucker-Prager, stress small; (c) Drucker-Prager, stress large.

is larger than K in compression loading (upper sign, for $d\sigma_1 < 0$) and smaller in unloading or reversed tension loading (lower sign, for $d\sigma_1 > 0$). The permanent strain at the end of a load-unload cycle is still compressive if the material is loaded not too far beyond yield and then unloaded, as shown in Fig. 4.16b. However, when this material is loaded well beyond the elastic range (Fig. 4.16c), the permanent set becomes an extension. This can be considered the one-dimensional analogue of the three-dimensional phenomenon of dilatancy.

To examine the volumetric strain increment under compressive loading, letting $i=j$ in Eq. (4.123) and noting that $d\lambda = d\epsilon_1 (2G/\sqrt{3} - 3K\alpha)/(G + 9K\alpha^2)$ for the case of $\sigma_1 < 0$, we can obtain the incremental relation between hydrostatic pressure and compressive volumetric strain for uniaxial strain tests as

$$dI_1 = \frac{9K\alpha \{[(2\sqrt{3})/3]G - 3K\alpha\}}{G + 9K\alpha^2} d\epsilon_{kk} + 3K d\epsilon_{kk} \quad (4.137)$$

When α is set equal to zero, Eq. (4.137) reduces to the corresponding expression for elastic material. The volumetric strain increment $d\epsilon_{kk}$ can be found from Eq. (4.137); then the increment of plastic volumetric strain is obtained by subtracting the elastic part, $d\epsilon''_{kk} = dI_1/K$, from $d\epsilon_{kk}$:

$$d\epsilon''_{kk} = \frac{\alpha(2\sqrt{3}G - 9K\alpha)}{3KG(1 + 2\sqrt{3}\alpha)} dI_1 \quad (4.138)$$

Noting Eq. (4.136), we see that the increment of plastic volumetric strain is positive (expansion) as expected.

4.11. General Isotropic Material

The yield surfaces considered in the previous sections are defined in terms of only the stress invariants I_1 and J_2 , and are independent of the stress invariant J_3 , or the angle of similarity θ . However, for a general isotropic material, the yield surface is a function of I_1 , J_2 , and J_3 , expressed by

$$f(I_1, J_2, J_3) = 0 \quad (4.139)$$

The gradient $\partial f / \partial \sigma_{ij}$ in this case can be written as

$$\frac{\partial f}{\partial \sigma_{ij}} = \frac{\partial f}{\partial I_1} \frac{\partial I_1}{\partial \sigma_{ij}} + \frac{\partial f}{\partial J_2} \frac{\partial J_2}{\partial \sigma_{ij}} + \frac{\partial f}{\partial J_3} \frac{\partial J_3}{\partial \sigma_{ij}} \quad (4.140a)$$

or

$$\frac{\partial f}{\partial \sigma_{ij}} = B_0 \delta_{ij} + B_1 s_{ij} + B_2 t_{ij} \quad (4.140b)$$

where B_0 , B_1 , and B_2 denote the derivatives $\partial f/\partial J_1$, $\partial f/\partial J_2$, and $\partial f/\partial J_3$, respectively, and δ_{ij} is the Kronecker delta, s_{ij} the deviatoric stress tensor, and t_{ij} the deviation of the square of the stress deviation s_{ij} :

$$t_{ij} = \frac{\partial J_3}{\partial \sigma_{ij}} = s_{ik}s_{kj} - \frac{2}{3}J_2\delta_{ij} \quad (4.141)$$

In fact, the most commonly used yield criteria of Tresca and Mohr-Coulomb belong to this type. As an illustration, recall Eq. (2.180), which is an alternative expression of the Mohr-Coulomb criterion:

$$f(\sigma_{ij}) = \frac{1}{3}I_1 \sin \phi + \sqrt{J_2} \sin \left(\theta + \frac{\pi}{3} \right) + \frac{\sqrt{J_2}}{\sqrt{3}} \cos \left(\theta + \frac{\pi}{3} \right) \sin \phi - c \cos \phi = 0 \quad (4.142)$$

and note that

$$\cos 3\theta = \frac{3\sqrt{3}}{2} \frac{J_3}{J_2^{3/2}} \quad (4.143)$$

Hence, we have:

$$\begin{aligned} \frac{\partial \theta}{\partial J_2} &= \frac{3\sqrt{3}}{4 \sin 3\theta} \frac{J_3}{J_2^{5/2}} = \frac{\cot 3\theta}{2J_2} \\ \frac{\partial \theta}{\partial J_3} &= -\frac{\sqrt{3}}{2 \sin 3\theta} \frac{1}{J_2^{3/2}} = -\frac{\cot 3\theta}{3J_3} \end{aligned} \quad (4.144)$$

Taking the derivatives of Eq. (4.142) with respect to I_1 , J_2 , and J_3 , we obtain

$$\begin{aligned} B_0 &= \frac{\partial f}{\partial I_1} = \frac{\sin \phi}{3} \\ B_1 &= \frac{\partial f}{\partial J_2} = \frac{\sin(\theta + \pi/3)}{2\sqrt{J_2}} \left\{ \left[1 + \cot \left(\theta + \frac{\pi}{3} \right) \cot 3\theta \right] \right. \\ &\quad \left. + \frac{\sin \phi}{\sqrt{3}} \left[\cot \left(\theta + \frac{\pi}{3} \right) - \cot 3\theta \right] \right\} \\ B_2 &= \frac{\partial f}{\partial J_3} = \frac{\sin \left(\theta + \frac{\pi}{3} \right) \sin \phi - \sqrt{3} \cos \left(\theta + \frac{\pi}{3} \right)}{2J_2 \sin 3\theta} \end{aligned} \quad (4.145)$$

It can be seen from Eq. (4.140) that only the constants B_i need be defined by the yield surface. In other words, only these three quantities have to be varied between one yield surface and the other. The constants B_i are given in Table 4.1 for the four yield criteria considered in this section. Other yield functions can be expressed in the same form with equal ease.

TABLE 4.1. Constants B_i defined by different yield surfaces.

Yield surface	B_0	B_1	B_2
von Mises [Eq. (2.143)]	0	1	0
Tresca [Eq. (2.138)]	0	$\left[\sin \left(\theta + \frac{\pi}{3} \right) / \sqrt{J_2} \right] \left[1 + \cot \left(\theta + \frac{\pi}{3} \right) \cot 3\theta \right]$	$\left[-\sqrt{3} \cos \left(\theta + \frac{\pi}{3} \right) / J_2 \sin 3\theta \right]$
Mohr-Coulomb [Eq. (2.180)]	$\frac{\sin \phi}{3}$	$\left[\sin \left(\theta + \frac{\pi}{3} \right) / 2\sqrt{J_2} \right] \left\{ \left[1 + \cot \left(\theta + \frac{\pi}{3} \right) \cot 3\theta \right] \right.$ $\left. + \sin \phi \left[\cot \left(\theta + \frac{\pi}{3} \right) - \cot 3\theta \right] \right\} / \sqrt{3}$	$\frac{1}{2J_2 \sin 3\theta} \left[\sin \left(\theta + \frac{\pi}{3} \right) \sin \phi - \sqrt{3} \cos \left(\theta + \frac{\pi}{3} \right) \right]$
Drucker-Prager [Eq. (2.185)]	α	$\frac{1}{2\sqrt{J_2}}$	0

In finite-element applications, the constitutive relation of a material is reflected by the material stiffness matrix C_{ijkl}^{ep} , which is used in forming the tangent stiffness. This stiffness matrix relates the strain increment with the stress increment as given by Eq. (4.82a):

$$d\sigma_{ij} = C_{ijkl}^{ep} d\epsilon_{kl} \quad (4.146)$$

To obtain a general form of tensor C_{ijkl}^{ep} , we rewrite Eq. (4.82b) as

$$C_{ijkl}^{ep} = C_{ijkl} + C_{ijkl}^p \quad (4.147)$$

in which C_{ijkl} is the elastic tensor given by Eq. (3.88) as

$$C_{ijkl} = \frac{E}{2(1+\nu)} \left[\frac{2\nu}{(1-2\nu)} \delta_{ij}\delta_{kl} + \delta_{ik}\delta_{jl} + \delta_{il}\delta_{jk} \right] \quad (4.148)$$

while C_{ijkl}^p is the plastic tensor expressed as

$$C_{ijkl}^p = -\frac{H_{ij}H_{kl}}{h} \quad (4.149)$$

where

$$h = \frac{\partial f}{\partial \sigma_{rs}} C_{rstu} \frac{\partial f}{\partial \sigma_{tu}} \quad (4.150)$$

and

$$H_{ij} = C_{ijmn} \frac{\partial f}{\partial \sigma_{mn}} \quad (4.151)$$

Substituting Eqs. (4.148) for C_{ijkl} and (4.140) for $\partial f / \partial \sigma_{ij}$ into Eqs. (4.150) and (4.151), after a lengthy but straightforward derivation [see Problem 4.13], we come up with the following expressions for h and H_{ij} in terms of the elastic constants G and ν and the coefficients B_0 , B_1 , and B_2 :

$$h = 2G \left(3B_0^2 \frac{1+\nu}{1-2\nu} + 2B_1^2 J_2 + \frac{2}{3} B_2^2 J_2^2 + 6B_1 B_2 J_3 \right) \quad (4.152)$$

$$H_{ij} = 2G \left(B_0 \frac{1+\nu}{1-2\nu} \delta_{ij} + B_1 s_{ij} + B_2 t_{ij} \right) \quad (4.153)$$

If the stress increment tensor $d\sigma_{ij}$ and the strain increment tensor $d\epsilon_{ij}$ are expressed explicitly in vector forms as

$$\{d\sigma_{ij}\} = \{d\sigma_x, d\sigma_y, d\sigma_z, d\tau_{yz}, d\tau_{zx}, d\tau_{xy}\} \quad (4.154)$$

$$\{d\epsilon_{ij}\} = \{d\epsilon_x, d\epsilon_y, d\epsilon_z, d\gamma_{yz}, d\gamma_{zx}, d\gamma_{xy}\}$$

where $d\gamma_{xy} = 2d\epsilon_{xy}$, etc., are the engineering shear strains, the corresponding vector for tensor H_{ij} has the form

$$\{H_{ij}\} = \{H_x, H_y, H_z, H_{yz}, H_{zx}, H_{xy}\} \quad (4.155)$$

where

$$H_x = 2G \left[B_0 \frac{1+\nu}{1-2\nu} + B_1 s_x + B_2 \left(s_x^2 + s_{xy}^2 + s_{xz}^2 - \frac{2}{3} J_2 \right) \right], \text{ etc.}$$

and

$$H_{yz} = 2G [B_1 s_{yz} + B_2 (s_{xy}s_{xz} + s_y s_{yz} + s_{yz}s_z)], \text{ etc.}$$

Thus, the tensor C_{ijkl}^{ep} can be expressed in a matrix form as

$$[C^{ep}] = [C] + [C^p] \quad (4.156)$$

where

$$[C] = \begin{bmatrix} K + \frac{4}{3}G & K - \frac{2}{3}G & K - \frac{2}{3}G & 0 & 0 & 0 \\ K - \frac{2}{3}G & K + \frac{4}{3}G & K - \frac{2}{3}G & 0 & 0 & 0 \\ K - \frac{2}{3}G & K - \frac{2}{3}G & K + \frac{4}{3}G & 0 & 0 & 0 \\ 0 & 0 & 0 & G & 0 & 0 \\ 0 & 0 & 0 & 0 & G & 0 \\ 0 & 0 & 0 & 0 & 0 & G \end{bmatrix} \quad (4.157)$$

and

$$[C^p] = -\frac{1}{h} \begin{bmatrix} H_x^2 & H_x H_y & H_x H_z & H_x H_{yz} & H_x H_{zx} & H_x H_{xy} \\ H_y^2 & H_y H_z & H_y H_{yz} & H_y H_{zx} & H_y H_{xy} & \\ & H_z^2 & H_z H_{yz} & H_z H_{zx} & H_z H_{xy} & \\ & & H_{yz}^2 & H_{yz} H_{zx} & H_{yz} H_{xy} & \\ & & & H_{zx}^2 & H_{zx} H_{xy} & \\ & & & & H_{xy}^2 & \end{bmatrix} \quad (4.158)$$

References

- Chen, W.F., 1975. *Limit Analysis and Soil Plasticity*, Elsevier, Amsterdam.
- Chen, W.F., 1982. *Plasticity in Reinforced Concrete*, McGraw-Hill, New York.
- Chen, W.F., and G.Y. Baladi, 1985. *Soil Plasticity: Theory and Implementation*, Elsevier, Amsterdam.
- Drucker, D.C., 1956. "On Uniqueness in the Theory of Plasticity," *Quarterly of Applied Mathematics*, 14: 35-42.
- Hill, R., 1950. *The Mathematical Theory of Plasticity*, Oxford University Press, London.
- Hoffman, O., and G. Sachs, 1953. *Introduction to the Theory of Plasticity*, McGraw-Hill, New York.
- Nielsen, M.P., 1984. *Limit Analysis and Concrete Plasticity*, Prentice-Hall, Englewood Cliffs, NJ.
- Owen, D.R.J., and E. Hinton, 1980. *Finite Elements in Plasticity: Theory and Practice*, Pineridge Press Limited, Swansea, U.K.

Prager, W., 1949. "Recent Developments in the Mathematical Theory of Plasticity," *Journal of Applied Physics*, 20: 235-241.

PROBLEMS

4.1. A long circular thin-walled pressure vessel is subjected to an interior pressure p and yielded. Find the ratio of the plastic strain increments in three principal directions according to the Prandtl-Reuss equation.

4.2. A thin-walled tube is subjected to a constant axial tension and a variable torsion. The axial stress is $\sigma_z = \frac{1}{2}\sigma_0$. According to the von Mises criterion, find the magnitude of the shear stress τ such that the tube begins to yield. Also find the ratio of the plastic strain increments $d\epsilon_{ij}^p$ when the tube is yielded.

4.3. A material element is subjected to three proportional loadings. The ratios of the principal stresses for the three loading cases are given as (1) $(2\sigma, \sigma, 0)$; (2) $(\sigma, \sigma, 0)$; (3) $(0, -\sigma, -\sigma)$. According to

(a) the von Mises yield criterion: $J_2 = k^2$;

(b) the Tresca yield criterion: $\tau_{\max} = \frac{\sigma_{\max} - \sigma_{\min}}{2} = k$;

(c) the Drucker-Prager criterion: $\alpha I_1 + \sqrt{J_2} = k$;

(d) the Mohr-Coulomb criterion: $\frac{m\sigma_{\max} - \sigma_{\min}}{2} = k$,

find the magnitude of σ for each of the above three loading cases such that the material begins to yield. Also find the principal plastic strain increment vector $(d\epsilon_1^p, d\epsilon_2^p, d\epsilon_3^p)$ during yielding based on the associated flow rule.

4.4. Show that the plastic strain increment at the apex of the Mohr-Coulomb hexagonal pyramid can be expressed as

$$d\epsilon_1^p = (d\lambda_1 + d\lambda_2)m - (d\lambda_4 + d\lambda_5)$$

$$d\epsilon_2^p = (d\lambda_5 + d\lambda_6)m - (d\lambda_2 + d\lambda_3)$$

$$d\epsilon_3^p = (d\lambda_3 + d\lambda_4)m - (d\lambda_1 + d\lambda_6)$$

Show also that Eqs. (4.34) and (4.36) are still valid in this case (see Fig. 4.5).

4.5. The modified Mohr-Coulomb yield surface is a Mohr-Coulomb surface

$$m\sigma_{\max} - \sigma_{\min} = f'_c$$

combined with a tension cutoff plane:

$$\sigma_{\max} = f'_t$$

This yield surface consists of nine flat planes, nine edges, and seven apices. Discuss the plastic strain increment at the cutoff planes and at their relevant edges and apices. Show that

(a) the plastic strain increments satisfy

$$\frac{\sum d\epsilon_i^p}{\sum |d\epsilon_i^p|} > m$$

(b) the plastic work increment can be expressed by

$$dW_p = f'_c \sum |d\epsilon_i^p| + f'_t (\sum d\epsilon_i^p - m \sum d\epsilon_i^p)$$

4.6. A thick-walled tube is first loaded into the elastic-plastic range with an internal pressure p , $p_e \leq p \leq p_c$, and then completely unloaded.

(a) Find the residual stresses.

(b) Determine the highest pressure for which the material of the tube would not yield again upon unloading.

(c) Show that if the ratio of outer and inner radii of the tube, b/a , is less than about 2.2, the material will shake down to elastic behavior for repeated pressurization between $p=0$ and $p=p_c$.

4.7. A thick-walled tube of perfectly plastic material sustains the full plastic internal pressure given by Eq. (4.73). Examine the location on the Tresca yield surface of stress points for different radii, apply the normality rule to obtain information about possible plastic deformation, and verify that such deformation is compatible with a mode of collapse for the tube.

4.8. A composite tube is composed of n tubes made of the same material, one inside the other. The inner and outer radii of the n tubes are $(r_1, r_1), (r_1, r_2), \dots, (r_{n-1}, r_n)$, respectively. The composite tube is subjected to an internal pressure p . The material obeys the Tresca yield condition. Assume that yield occurs simultaneously at the inner surfaces of each tube. Show that

(a) The inner pressure for the initial yielding is given by

$$p = \frac{\sigma_0}{2} \left\{ n - \left[\left(\frac{r_1}{r_1} \right)^2 + \left(\frac{r_1}{r_2} \right)^2 + \dots + \left(\frac{r_{n-1}}{r_n} \right)^2 \right] \right\}$$

in which σ_0 is the yield stress in simple tension.

(b) If the ratio of the outer and inner radii of each tube is

$$\frac{r_k}{r_{k-1}} = \left(\frac{r_c}{r_i} \right)^{1/n} \quad k = 1, 2, \dots, n; \quad r_0 = r_i, r_n = r_c$$

the pressure p takes the maximum value for the initial yielding, and

$$(p_c)_{\max} = \frac{n\sigma_0}{2} \left[1 - \left(\frac{r_i}{r_c} \right)^{2/n} \right].$$

(c) The full plastic pressure p is given by

$$p_c = \sigma_0 \ln \frac{r_c}{r_i}$$

4.9. Consider a hollow sphere of internal radius a and external radius b . Discuss the behavior of the sphere under an internal pressure.

(a) Find the elastic stresses and displacements. Determine the maximum pressure p_a for which this elastic solution is valid.

(b) Find the elastic-plastic solution and the maximum pressure p_c for which it is valid.

(c) What simplifications, if any, result if the material is assumed to be incompressible in both elastic and plastic ranges?

- (d) Find the residual stresses after a complete unloading and determine the highest pressure for which shakedown occurs.
 (e) Find the stresses and strain rates for uncontained plastic flow.

4.10. In a combined tension/torsion test on a thin-wall tube of circular cross section, let σ and ϵ be the axial stress and axial strain and τ and γ be the shear stress and shear strain, respectively. Assume that the tube is made of Prandtl-Reuss material with $\nu = \frac{1}{2}$. Calculate the stresses σ and τ corresponding to the strain state $(\epsilon, \gamma) = (\sigma_y/E, \sigma_y/\sqrt{3}G)$ for the following three loading paths (Fig. P4.6):

- (a) The axial strain ϵ is first increased up to the yield value $\epsilon = \sigma_y/E$, then kept unchanged, while the shear strain γ is increased up to its final value $\gamma = \sigma_y/\sqrt{3}G$.
 (b) Reverse of the above loading path: the shear strain γ is first increased up to its final value $\gamma = \sigma_y/\sqrt{3}G$, then held constant, while the axial strain ϵ is increased up to its final value σ_y/E .
 (c) Both strains ϵ and γ are increased proportionately with a ratio of $\epsilon/\gamma = \sqrt{3}G/E = 1/\sqrt{3}$, until their final values are reached.

Hint: Noting that $\sigma_{mn} d\epsilon_{mn} = \sigma_{mn} d\epsilon_{mn}$, $d\lambda$ can thus be obtained in terms of k , σ , $d\epsilon$, τ , and $d\gamma$. Because of the incompressibility condition, Eqs. (4.91) or (4.92) will lead to a group of differential equations with respect to $\sigma(\epsilon, \gamma)$ and $\tau(\epsilon, \gamma)$. Let $d\epsilon = 0$ or $d\gamma = 0$; the differential equations can be integrated for cases (a) and (b).

4.11. Follow Example 4.3 to examine the behavior of Drucker-Prager material under a plane stress condition. Compare the results with that for Prandtl-Reuss material.

4.12. Prove Eqs. (4.145).

4.13. Prove Eqs. (4.152) and (4.153).

4.14. A long thick-walled concrete tube with open end ($\sigma_2 = 0$) is subjected to internal pressure p . The inner radius and outer radius are a and b , respectively.

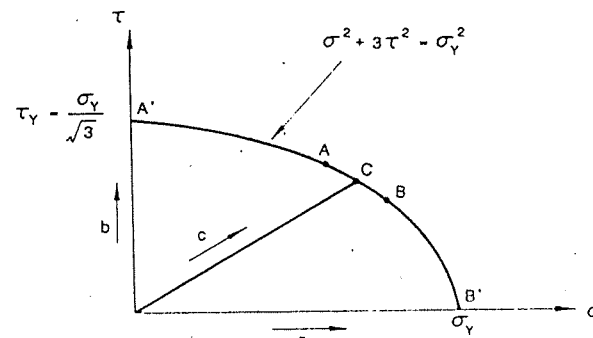


FIGURE P4.6.

Assume the concrete material follows the Rankine criterion with uniaxial tensile strength f'_t .

- (a) Determine the elastic limit internal pressure p_e .
 (b) Determine the relationship between the elastic-plastic boundary $r = c$ and the internal pressure p for $p > p_e$.
 (c) Determine the plastic limit internal pressure p_p .
 (d) For the case of $b/a = 2$, plot σ_r and σ_θ vs. r curves for the elastic-plastic boundary at $c = a$, $c = \frac{1}{2}(a+b)$, and $c = b$, respectively.

4.15. A long vertical circular hole with internal radius a in a half-space of rock is subjected to an internal pressure p as shown in Fig. P4.15. Assume the rock material follows the Rankine criterion, with uniaxial tensile strength f'_t . Determine the relationship between the radius of the plastic zone and the internal pressure.

4.16. Resolve Problem 4.15 using the Tresca yield criterion. Show that the relationship between the radius of the plastic zone and the internal pressure can be obtained by letting $b \rightarrow \infty$ in Eq. (4.68).

4.17. Assuming the concrete material follows the Mohr-Coulomb criterion, resolve Problem 4.14. The uniaxial tensile and compressive strengths of the material are f'_t and f'_c , respectively. Plot σ_r and σ_θ vs. r curves using $f'_c/f'_t = 10$.

4.18. Resolve Problem 4.15 using the Mohr-Coulomb criterion. Assume the uniaxial tensile and compressive strengths of the rock material are f'_t and f'_c , respectively.

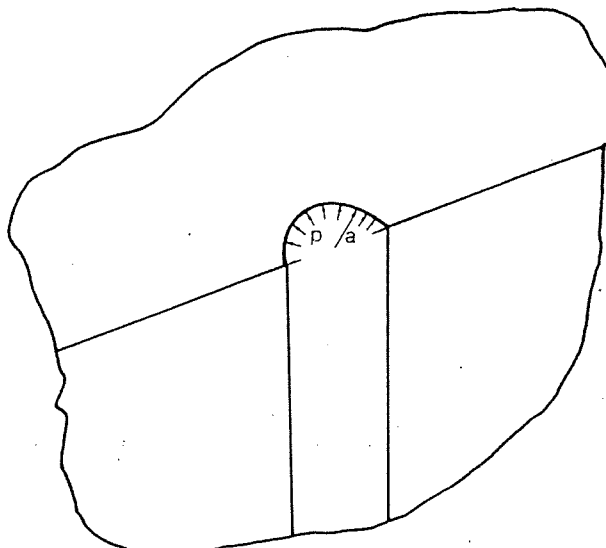


FIGURE P4.15.

- 4.19. Noting that the Tresca criterion and the Rankine criterion are special cases of the Mohr-Coulomb criterion, show that
- the elastic-plastic solutions of the thick-walled cylinder described in Section 4.7 and Problem 4.14 are special cases of the solution of Problem 4.17.
 - the elastic-plastic solutions of the vertical circular hole in a half-space described in Problems 4.15 and 4.16 are special cases of the solution of Problem 4.18.
- 4.20. Derive the expression of the scalar factor $d\lambda$ for a general elastic-perfectly plastic material using the associated flow rule, such that

$$d\epsilon_{ij}^p = d\lambda \frac{\partial f}{\partial \sigma_{ij}}$$

where $f = f(\sigma_{ij})$ is the yield function. Assuming the elastic behavior of the material is linear and isotropic, express the scalar factor $d\lambda$ in terms of the two elastic constants K and G .

- 4.21. Develop a Fortran code to calculate the material stiffness matrix $[C^{ep}]$ of Eq. (4.156) for the four yield criteria given in Table 4.1.

ANSWERS TO SELECTED PROBLEMS

- 4.1. $(d\epsilon_y^p, d\epsilon_z^p, d\epsilon_r^p) = d\lambda(s_y, s_z, s_r) = d\lambda(1, 0, -1)$.
 4.2. $\tau_r = \sigma_u/2; d\epsilon_y^p : d\epsilon_z^p : d\epsilon_r^p : d\gamma_{yz}^p = s_r : s_y : s_z : 2s_{yz} = (-1) : (-1) : (2) : (6)$.
 4.3. (1a) $\sigma_y = k, d\epsilon_y^p = d\lambda(1, 0, -1);$ (1b) $\sigma_y = k, d\epsilon_y^p = d\lambda(1, 0, -1);$
 (1c) $\sigma_y = k/(1+3\alpha), d\epsilon_y^p = d\lambda(\alpha+\frac{1}{3}, \alpha, \alpha-\frac{1}{3});$
 (1d) $\sigma_y = k/m, d\epsilon_y^p = d\lambda(m, 0, -1);$ (2a) $\sigma_y = \sqrt{3}k, d\epsilon_y^p = d\lambda(1, 1, -2);$
 (2b) $\sigma_y = 2k, d\epsilon_y^p = d\lambda_1(1, 0, -1) + d\lambda_2(0, 1, -1);$
 (2c) $\sigma_y = \sqrt{3}k/(1+2\sqrt{3}\alpha), d\epsilon_y^p = d\lambda(\alpha+1/2\sqrt{3}, \alpha+1/2\sqrt{3}, \alpha-1/\sqrt{3});$
 (2d) $\sigma_y = 2k/m, d\epsilon_y^p = d\lambda_1(m, 0, -1) + d\lambda_2(0, m, -1);$
 (3a) $\sigma_y = \sqrt{3}k, d\epsilon_y^p = d\lambda(2, -1, -1);$
 (3b) $\sigma_y = 2k, d\epsilon_y^p = d\lambda_1(1, 0, -1) + d\lambda_2(1, -1, 0);$
 (3c) $\sigma_y = \sqrt{3}k/(1-2\sqrt{3}\alpha), d\epsilon_y^p = d\lambda(\alpha+1/\sqrt{3}, \alpha-1/2\sqrt{3}, \alpha-1/2\sqrt{3});$
 (3d) $\sigma_y = 2k, d\epsilon_y^p = d\lambda_1(m, 0, -1) + d\lambda_2(m, -1, 0).$

- 4.6. (a)

$$\begin{aligned} \sigma_r^r &= \begin{cases} \sigma_0 \ln \frac{r}{a} - p - \frac{pa^2}{b^2 - a^2} \left(1 - \frac{b^2}{r^2} \right), & a \leq r \leq c \\ \frac{\sigma_0 c^2}{2b^2} \left(1 - \frac{b^2}{r^2} \right) - \frac{pa^2}{b^2 - a^2} \left(1 - \frac{b^2}{r^2} \right), & c \leq r \leq b \end{cases} \\ \sigma_\theta^r &= \begin{cases} \sigma_0 \left(1 + \ln \frac{r}{a} \right) - p - \frac{pa^2}{b^2 - a^2} \left(1 + \frac{b^2}{r^2} \right), & a \leq r \leq c \\ \frac{\sigma_0 c^2}{2b^2} \left(1 + \frac{b^2}{r^2} \right) - \frac{pa^2}{b^2 - a^2} \left(1 + \frac{b^2}{r^2} \right), & c \leq r \leq b \end{cases} \\ \sigma_z^r &= \nu(\sigma_r^r + \sigma_\theta^r) \end{aligned}$$

$$(b) p \leq \sigma_0 \left(1 - \frac{a^2}{b^2} \right) = 2p_c.$$

- 4.10. (a) $\sigma = 0.648\sigma_y$

$$\tau = 0.440\sigma_y$$

- (b) $\sigma = 0.762\sigma_y$

$$\tau = 0.374\sigma_y$$

- (c) $\sigma = 0.707\sigma_y$

$$\tau = 0.408\sigma_y$$

- 4.13. The following formulas are provided for later use:

$$t_{ij} = s_{ik} s_{kj} - \frac{2}{3} J_2 \delta_{ij}$$

$$t_{ii} = s_{ik} s_{ki} - 2J_2 = 0$$

$$t_{ij} s_{ij} = (s_{ik} s_{kj} - \frac{2}{3} J_2 \delta_{ij}) s_{ij} = s_{ii} s_{jk} s_{ki} = 3J_3$$

$$t_{ii} t_{ii} = s_{ik} s_{kj} s_{il} s_{li} - \frac{2}{3} J_2 s_{ik} s_{ki} + \frac{4}{9} J_2^2 \delta_{ii} \delta_{ii}$$

$$= 2J_2^2 - \frac{8}{3} J_2^2 + \frac{4}{9} J_2^2 = \frac{2}{3} J_2^2$$

Equations (4.153) and (4.152) are derived as follows:

$$\begin{aligned} H_{ij} &= C_{ijmn} \frac{\partial f}{\partial \sigma_{mn}} \\ &= \frac{E}{2(1+\nu)} \left[\frac{2\nu}{(1-2\nu)} \delta_{ij} \delta_{mn} + \delta_{im} \delta_{jn} + \delta_{in} \delta_{jm} \right] (B_0 \delta_{mn} + B_1 s_{mn} + B_2 t_{mn}) \\ &= 2G \left(\frac{\nu}{1-2\nu} \delta_{ij} \delta_{mn} + \delta_{im} \delta_{jn} \right) (B_0 \delta_{mn} + B_1 s_{mn} + B_2 t_{mn}) \\ &= 2G \left(\frac{\nu B_0}{1-2\nu} \delta_{ij} \delta_{mn} \delta_{mn} + B_0 \delta_{im} \delta_{jn} \delta_{mn} + \frac{\nu B_1}{1-2\nu} \delta_{ij} \delta_{mn} s_{mn} + B_1 \delta_{im} \delta_{jn} s_{mn} \right. \\ &\quad \left. + \frac{\nu B_2}{1-2\nu} \delta_{ij} \delta_{mn} t_{mn} + B_2 \delta_{im} \delta_{jn} t_{mn} \right) \\ &= 2G \left(\frac{3\nu B_0}{1-2\nu} \delta_{ij} + B_0 \delta_{ij} + 0 + B_1 s_{ij} + 0 + B_2 t_{ij} \right) \\ &= 2G \left(B_0 \frac{1+\nu}{1-2\nu} \delta_{ij} + B_1 s_{ij} + B_2 t_{ij} \right) \\ h &= \frac{\partial f}{\partial \sigma_{ii}} C_{ijmn} \frac{\partial f}{\partial \sigma_{nn}} = \frac{\partial f}{\partial \sigma_{ii}} (2G) \left(B_0 \frac{1+\nu}{1-2\nu} \delta_{ii} + B_1 s_{ii} + B_2 t_{ii} \right) \\ &= 2G(B_0 \delta_{ii} + B_1 s_{ii} + B_2 t_{ii}) \left(B_0 \frac{1+\nu}{1-2\nu} \delta_{ii} + B_1 s_{ii} + B_2 t_{ii} \right) \\ &= 2G \left(B_0^2 \frac{1+\nu}{1-2\nu} \delta_{ii} \delta_{ii} + B_1^2 s_{ii} s_{ii} + B_2^2 t_{ii} t_{ii} + 2B_1 B_2 s_{ii} t_{ii} \right) \\ &= 2G \left(3B_0^2 \frac{1+\nu}{1-2\nu} + 2B_1^2 J_2 + \frac{2}{3} B_2^2 J_2^2 + 6B_1 B_2 J_3 \right) \end{aligned}$$

Stress-Strain Relations for Work-Hardening Materials

5.1. Introduction

Engineering material usually exhibits a work-hardening behavior. Increasing the stress beyond the initial yield surface and into the work-hardening range (loading) produces both plastic and elastic deformations. At each stage of plastic deformation, a new yield surface, called the *subsequent loading surface*, is established. If the state of stress is now changed such that the stress point representing it in a stress space moves inside the new yield surface (unloading), the behavior of the material is again elastic, and no plastic deformation will take place. The stress-strain behavior related to loading or unloading from new yield surface is *loading path dependent* or *loading history dependent*.

In developing constitutive equations for work-hardening materials, two basic approaches have been used. The first type of formulation is the *deformation theory* in the form of the total stress-strain relation. This theory assumes that the state of stress determines the state of strain uniquely as long as the plastic deformation continues. This is identical with the nonlinear elastic stress-strain relation of Chapter 3 as long as unloading does not occur. Thus, the most general form of this theory during loading may be written as

$$\epsilon_{ij}^p = \epsilon_{ij} - \epsilon_{ij}^e = f(\sigma_{ij}) \quad (5.1)$$

where ϵ_{ij}^p and ϵ_{ij}^e are the plastic and elastic components of the total strain ϵ_{ij} , respectively. Equation (5.1) indicates a *loading-path-independent* behavior. It cannot adequately describe the phenomena associated with loading and unloading near the yield surface along a neutral loading path. Nevertheless, such theories have been used extensively in practice for the solution of elastic-plastic problems because of their comparative simplicity. However, the total stress-strain relation based on deformation theory is only valid in the case of *proportional loading*.

The other type of theory is the *incremental theory* or *flow theory*. This type of formulation relates the increment of plastic strain components $d\epsilon_{ij}^p$ to the state of stress, σ_{ij} , and the stress increment, $d\sigma_{ij}$. The simplest type of flow theory, as already discussed in Chapter 4, is the *theory of perfect*

plasticity. A large number of the techniques used in the previous discussion on perfect plasticity carry through here with little change for work-hardening plasticity. The fundamental difference is that the yield surface is now not fixed in stress space, but rather the stress point σ_{ij} is permitted to move outside the yield surface. The response of the material after initial yielding is described by specifying a new yield surface called the *subsequent yield surface*, and the rule that specifies this post-yield response is called the *hardening rule*.

Basic assumptions used in the development of the incremental theory of work-hardening plasticity include:

- (a) The *existence* of an initial yield surface which defines the elastic limit of the material in a multiaxial state of stress. The concept of yield surface has been discussed in Chapter 2.
- (b) The *hardening rule* which describes the evolution of subsequent yield surfaces. Several hardening rules have been proposed in the past and will be discussed later in this chapter.
- (c) The *flow rule* which is related to a plastic potential function and defines the direction of the incremental plastic strain vector in strain space. The concept of flow rule has been discussed in some detail in Chapter 4 for perfectly plastic materials. For work-hardening materials, the associated flow rule represents a result of *Drucker's stability postulate*. This will be studied in the later part of this chapter.

This chapter is concerned with the development of the constitutive relations of work-hardening materials. The deformation theory is first introduced in Section 5.2. Then the basic concepts of the incremental theory are discussed. This later theory accounts for loading, unloading, and reloading and is suitable for describing the complete stress-history-dependent behavior of a work-hardening plastic solid. This is the main subject of the present chapter.

5.2. Deformation Theory of Plasticity

5.2.1. Deformation Theory for J_2 -Material

The simplest and most popular deformation theory is the *J_2 deformation theory*. The theory is based upon the following four assumptions: (i) the material is initially isotropic; (ii) the plastic strain involves only a change in shape but no change in volume, and the elastic strain is related to the stress by Hooke's law; (iii) the principal axes of the plastic strain and the stress coincide; (iv) the principal values of the plastic strain have the same ratios to each other as the principal values of the stress deviator.

In the development of the stress-strain relation, the total strain ϵ_{ij} is decomposed into elastic and plastic components ϵ_{ij}^e and ϵ_{ij}^p by the simple

superposition:

$$\epsilon_{ij} = \epsilon_{ij}^e + \epsilon_{ij}^p \quad (5.2)$$

According to assumption (ii), the elastic strain ϵ_{ij}^e is related to the stress σ_{ij} by Hooke's law [see Eq. (3.96) of Chapter 3]

$$\epsilon_{ij}^e = \frac{s_{ij}}{2G} + \frac{\sigma_{kk}}{9K} \delta_{ij} \quad (5.3)$$

and the plastic strain ϵ_{ij}^p consists only of the component of deviatoric strain ϵ_{ij}^p . Assumptions (iii) and (iv) relate this plastic strain ϵ_{ij}^p to the stress deviator s_{ij} as

$$\epsilon_{ij}^p = \epsilon_{ij}^p = \phi s_{ij} \quad (5.4)$$

in which ϕ is a scalar, which may be considered a function of the invariant J_2 :

$$\phi = \phi(J_2) \quad (5.5)$$

The scalar function $\phi(J_2)$ is a material property determined by experiment.

In order to calibrate the function $\phi(J_2)$ with the experimental uniaxial stress-strain curve, we introduce a stress variable called the *effective stress* σ_e , defined as

$$\sigma_e = \sqrt{3J_2} = \sqrt{\frac{3}{2}s_{ij}s_{ij}} \quad (5.6)$$

and a strain variable called the *effective plastic strain*, defined as

$$\epsilon_p = \sqrt{\frac{3}{2}\epsilon_{ij}^p\epsilon_{ij}^p} \quad (5.7)$$

It can be seen that in the uniaxial tension case with $\sigma_1 > 0$, $\sigma_2 = \sigma_3 = 0$, the effective stress σ_e reduces to the stress σ_1 . On the other hand, due to the *plastic-incompressibility condition*, in the case of uniaxial tension, we have

$$\epsilon_2^p = \epsilon_3^p = -\frac{1}{2}\epsilon_1^p \quad (5.8)$$

Substituting Eq. (5.8) into Eq. (5.7), we recognize that the effective strain ϵ_p reduces to the uniaxial strain ϵ_1^p .

Now, we can define a single *effective stress-effective strain curve*, whose shape is governed by the simple uniaxial tension test, taking the following form

$$\sigma_e = \sigma_e(\epsilon_p) \quad (5.9)$$

Multiplying Eq. (5.4) by itself yields

$$\sqrt{\epsilon_{ij}^p\epsilon_{ij}^p} = \phi \sqrt{s_{ij}s_{ij}}$$

Using the definitions of effective stress σ_e and effective strain ϵ_p leads to an expression for the parameter ϕ :

$$\phi = \frac{3}{2} \frac{\epsilon_p}{\sigma_e} \quad (5.10)$$

or

$$\phi = \frac{\sqrt{3}}{2} \frac{\epsilon_p}{\sqrt{J_2}} \quad (5.11)$$

Since the effective strain ϵ_p is related to the effective stress σ_e or the stress invariant J_2 through the uniaxial stress-strain relation (5.9), ϕ can be obtained as a function of J_2 .

Using Eq. (5.10) for ϕ , the constitutive equation (5.4) is now rewritten in terms of the stress and strain components explicitly as

$$\begin{aligned} \epsilon_x^p &= \frac{\epsilon_p}{\sigma_e} \left[\sigma_x - \frac{1}{2}(\sigma_y + \sigma_z) \right] \\ \epsilon_y^p &= \frac{\epsilon_p}{\sigma_e} \left[\sigma_y - \frac{1}{2}(\sigma_x + \sigma_z) \right] \\ \epsilon_z^p &= \frac{\epsilon_p}{\sigma_e} \left[\sigma_z - \frac{1}{2}(\sigma_x + \sigma_y) \right] \\ \gamma_{xz}^p &= \frac{3\epsilon_p}{\sigma_e} \tau_{xz} \\ \gamma_{yz}^p &= \frac{3\epsilon_p}{\sigma_e} \tau_{yz} \\ \gamma_{xy}^p &= \frac{3\epsilon_p}{\sigma_e} \tau_{xy} \end{aligned} \quad (5.12)$$

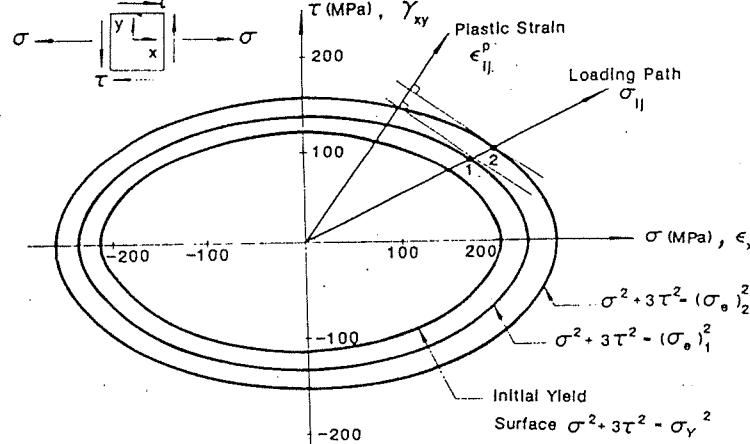
The stress-strain relationships of the deformational type for J_2 -material were first formulated by Hencky in 1924 to describe a perfectly plastic behavior, and then by Nadai in 1931 to represent the behavior of a work-hardening material.

Equations (5.4) and (5.12) express the stress-strain behavior of a work-hardening material with a continuous transition from an elastic state to a plastic state, as long as the loading condition

$$dJ_2 > 0 \quad (5.13)$$

is satisfied. Otherwise, Hooke's law must be used and the plastic strain remains unchanged. In view of this, the total stress-strain relation of the deformational type is strictly valid only for or near a proportional loading path. In this case, the stress components increase in a constant ratio to each other, so that the strains can be expressed in terms of the final state of stress along this proportional loading path.

The validity of the deformation theory for loading paths other than the proportional loading path has been studied by Budiansky (1959). Assuming Drucker's postulate to constitute a criterion for physical soundness, Budiansky has shown that deformation theories are consistent with this postulate for a range of loading paths in the vicinity of proportional loading.

FIGURE 5.1. An illustration of J_2 deformation theory (Example 5.1).

EXAMPLE 5.1. An element of J_2 -material is subjected to a proportional loading path with a stress ratio $\sigma/\tau = 2$ as shown in Fig. 5.1. The stress-strain relation in simple tension of the material is given by

$$\epsilon = \begin{cases} \frac{\sigma}{E} & (\sigma \leq \sigma_y) \\ \frac{\sigma}{E} + \frac{\sigma - \sigma_y}{m} & (\sigma > \sigma_y) \end{cases} \quad (5.14)$$

with Young's modulus $E = 207$ GPa, yield stress $\sigma_y = 207$ MPa, constant $m = 25$ GPa, and Poisson's ratio $\nu = 0.3$. Find all the components of the normal and shear strains corresponding to the two states of stress with: (i) $\sigma = 180$ MPa, $\tau = 90$ MPa and (ii) $\sigma = 200$ MPa, $\tau = 100$ MPa.

SOLUTION. The yield condition for J_2 -material subjected to stresses σ and τ is expressed as

$$\sigma^2 + 3\tau^2 = \sigma_y^2 \quad (5.15)$$

Substituting $\sigma = 180$ MPa and $\tau = 90$ MPa in Eq. (5.15) leads to

$$\sigma^2 + 3\tau^2 = (180)^2 + 3(90)^2 = (238.1)^2 > \sigma_y^2$$

Thus, the element has yielded under the stress states (i) and (ii), and its strain included elastic and plastic parts. The elastic strain is determined by

Hooke's law [see Eqs. (3.101) and (3.102)]. At stress state (i):

$$(\epsilon_e^e)_1 = \frac{\sigma}{E} = \frac{180}{207 \times 10^3} = 8.69 \times 10^{-4}$$

$$(\epsilon_z^e)_1 = (\epsilon_z^e)_1 = -\frac{\nu}{E} \sigma = -\frac{(0.3)(180)}{207 \times 10^3} = -2.609 \times 10^{-4}$$

$$(\gamma_{xy}^e)_1 = \frac{2(1+\nu)\tau}{E} = \frac{2(1+0.3)(90)}{207 \times 10^3} = 1.130 \times 10^{-3}$$

$$(\gamma_{xz}^e)_1 = (\gamma_{yz}^e)_1 = 0$$

At stress state (ii):

$$(\epsilon_e^e)_2 = \frac{200}{207 \times 10^3} = 9.662 \times 10^{-4}$$

$$(\epsilon_z^e)_2 = (\epsilon_z^e)_2 = -\frac{(0.3)(200)}{207 \times 10^3} = -2.899 \times 10^{-4}$$

$$(\gamma_{xy}^e)_2 = \frac{2(1+0.3)(100)}{207 \times 10^3} = 1.256 \times 10^{-3}$$

$$(\gamma_{xz}^e)_2 = (\gamma_{yz}^e)_2 = 0$$

The plastic strains are calculated from Eq. (5.12), with the effective stress σ_e obtained from Eq. (5.6):

$$\sigma_e = \sqrt{3J_2} = \sqrt{\sigma^2 + 3\tau^2}$$

For stress state (i),

$$(\sigma_e)_1 = \sqrt{(180)^2 + 3(90)^2} = 238.1 \text{ MPa}$$

For stress state (ii),

$$(\sigma_e)_2 = \sqrt{(200)^2 + 3(100)^2} = 264.6 \text{ MPa}$$

According to the given stress-strain relation (5.14), the effective strain can be expressed in terms of effective stress σ_e as

$$\epsilon^p = \frac{\sigma_e - \sigma_y}{m}$$

and the ratio ϵ_p/σ_e in Eq. (5.12) is calculated for these two stress states as

$$\left(\frac{\epsilon_p}{\sigma_e}\right)_1 = \frac{(\sigma_e)_1 - \sigma_y}{m(\sigma_e)_1} = \frac{238.1 - 207}{(25,000)(238.1)} = 5.225 \times 10^{-6} \frac{1}{\text{MPa}}$$

and

$$\left(\frac{\epsilon_p}{\sigma_e}\right)_2 = \frac{(\sigma_e)_2 - \sigma_y}{m(\sigma_e)_2} = \frac{264.6 - 207}{(25,000)(264.6)} = 8.707 \times 10^{-6} \frac{1}{\text{MPa}}$$

respectively. Now the plastic strains can be obtained from Eq. (5.12).

$$(\epsilon_x^p)_1 = \left(\frac{\epsilon_p}{\sigma_e} \right)_1 \sigma = (5.225 \times 10^{-6})(180) = 9.405 \times 10^{-4}$$

$$(\epsilon_y^p)_1 = (\epsilon_z^p)_1 = \left(\frac{\epsilon_p}{\sigma_e} \right)_1 \left(-\frac{\sigma}{2} \right) = (5.225 \times 10^{-6})(-90) = -4.702 \times 10^{-4}$$

$$(\gamma_{xy}^p)_1 = 3 \left(\frac{\epsilon_p}{\sigma_e} \right)_1 \tau = 3(5.225 \times 10^{-6})(90) = 1.411 \times 10^{-3}$$

$$(\gamma_{yz}^p)_1 = (\gamma_{xz}^p)_1 = 0$$

Similarly, for stress state (ii), we have

$$(\epsilon_x^p)_2 = (8.707 \times 10^{-6})(200) = 1.741 \times 10^{-3}$$

$$(\epsilon_y^p)_2 = (\epsilon_z^p)_2 = -8.707 \times 10^{-4}$$

$$(\gamma_{xy}^p)_2 = 3(8.707 \times 10^{-6})(100) = 2.612 \times 10^{-3}$$

$$(\gamma_{yz}^p)_2 = (\gamma_{xz}^p)_2 = 0$$

Finally, the total strain ϵ_{ij} is given as the sum of the elastic strain ϵ_{ij}^e and the plastic strain ϵ_{ij}^p :

$$\begin{aligned} [\epsilon_{ij}]_1 &= \begin{bmatrix} (\epsilon_x^e)_1 + (\epsilon_x^p)_1 & \frac{1}{2}[(\gamma_{xy}^e)_1 + (\gamma_{xy}^p)_1] & 0 \\ \frac{1}{2}[(\gamma_{xy}^e)_1 + (\gamma_{xy}^p)_1] & (\epsilon_y^e)_1 + (\epsilon_y^p)_1 & 0 \\ 0 & 0 & (\epsilon_z^e)_1 + (\epsilon_z^p)_1 \end{bmatrix} \\ &= \begin{bmatrix} 1.810 & 1.271 & 0 \\ 1.271 & -0.731 & 0 \\ 0 & 0 & -0.731 \end{bmatrix} \times 10^{-3} \end{aligned}$$

and similarly

$$[\epsilon_{ij}]_2 = \begin{bmatrix} 2.707 & 1.934 & 0 \\ 1.934 & -1.160 & 0 \\ 0 & 0 & -1.160 \end{bmatrix} \times 10^{-3}$$

Figure 5.1 shows the loading path and the direction of the plastic strain vector. It can be seen that the plastic strain vector is normal to the yield surface at the stress points. This has been manifested by Eq. (5.4).

5.2.2. Generalization of J_2 -Theory

The stress-strain relation of Eqs. (5.4) and (5.5) is comparatively simple in structure. It involves only the stress invariant J_2 . More elaborate stress-strain relationships have been proposed in the past. For example, Prager has formulated the following relationship between the plastic strain and stress

for metals under the proportional loading condition:

$$\epsilon_{ij}^p = f(J_2, J_3)s_{ij} + g(J_2, J_3)t_{ij} \quad (5.16)$$

which includes also the third invariant of the stress deviator, J_3 , and its derivatives, t_{ij} :

$$t_{ij} = \frac{\partial J_3}{\partial \sigma_{ij}} = s_{ik}s_{kj} - \frac{2}{3}J_2\delta_{ij} \quad (5.17)$$

For the constitutive relations (5.16), assumptions (iii) and (iv) have been eliminated but assumption (i), concerning the initial isotropy, and assumption (ii) concerning the plastic incompressibility, are still maintained. The scalar functions $f(J_2, J_3)$ and $g(J_2, J_3)$ are material properties determined by experiments. In comparison to Eq. (5.4), Eq. (5.16) provides more flexibility in fitting the experimental data.

Furthermore, if the assumption of the plastic incompressibility condition is discarded, a more general form of the stress-strain relation applicable to nonmetallic materials may be expressed as

$$\epsilon_{ij}^p = P(I_1, J_2, J_3)\delta_{ij} + Q(I_1, J_2, J_3)s_{ij} + R(I_1, J_2, J_3)t_{ij} \quad (5.18)$$

in which δ_{ij} is the Kronecker delta. For some nonmetallic frictional materials such as soils, concretes, and rocks, the plastic volume change is usually appreciable, and thus the effect of the first stress invariant I_1 must be taken into account. Since the constitutive equations (5.18) involve all three stress invariants as variables in the three scalar functions P , Q , and R , it follows that they are suitable for description of such materials under proportional loading.

In the following sections, we shall discuss the basic concepts of the incremental theory of plasticity for work-hardening plastic solids. This is the main topic of the present chapter.

5.3. Loading Surface and Hardening Rules

5.3.1. Loading Surface and Loading Criterion

Loading surface is the subsequent yield surface for an elastoplastically deformed material, which defines the boundary of the current elastic region. If a stress point lies within this region, no additional plastic deformation takes place. On the other hand, if the state of stress is on the boundary of the elastic region and tends to move out of the current loading surface, additional plastic deformations will occur, accompanied by a configuration change of the current loading surface. In other words, the current loading surface or the subsequent yield surface will change its current configuration when plastic deformation takes place. Thus, the loading surface may be generally expressed as a function of the current state of stress (or strain)

and some hidden variables such that

$$f(\sigma_{ij}, \epsilon_{ij}^p, k) = 0 \quad (5.19)$$

in which the so-called hidden variables are expressed in terms of the plastic strain ϵ_{ij}^p and a *hardening parameter* k .

To determine the nature of the subsequent loading surfaces is one of the major problems in the work-hardening theory of plasticity. The response of a material after initial yielding differs considerably in various plasticity theories. This post-yield response, called the *hardening rule*, is described by specifying the rule for the evolution of the subsequent yield surfaces or loading surfaces. Several hardening rules have been proposed in the past for use in plastic analysis. Since the configuration change of the loading surface is closely related to the "plastic loading," we shall first discuss the loading criterion for a work-hardening material. This will then be followed by the study of the hardening rules.

For a uniaxial behavior, the concepts of "loading" and "unloading" are self-evident (see Fig. 5.2a). However, this is not the case under a multiaxial stress state, and load/unload must be clearly specified. The loading surface itself is, of course, an essential part of defining loading and unloading. We shall define further here that loading or plastic flow occurs only when the stress point is on the loading surface and the additional loading or stress incremental vector $d\sigma_{ij}$ is directed outward from the current elastic region. To express the above statement more precisely, we introduce a unit vector n^f normal to the loading surface in stress space (Fig. 5.2b) whose components are given by

$$n_{ij}^f = \frac{\partial f / \partial \sigma_{ij}}{\left(\frac{\partial f}{\partial \sigma_{11}} \frac{\partial f}{\partial \sigma_{22}} \right)^{1/2}} \quad (5.20)$$

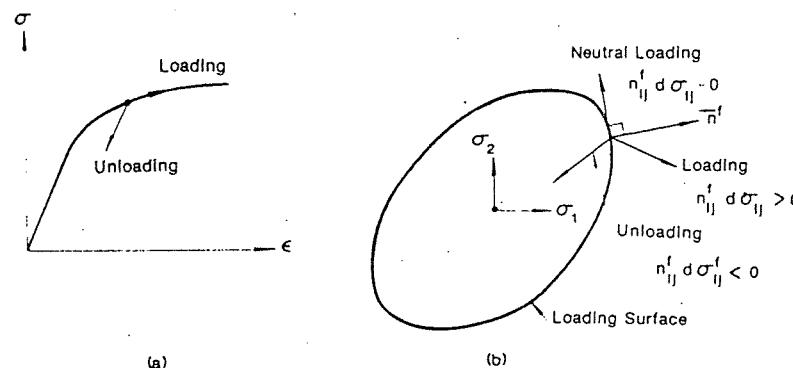


FIGURE 5.2. Loading criterion for a work-hardening material: (a) uniaxial case; (b) multiaxial case.

If the angle between the vector $d\sigma_{ij}$ and n_{ij}^f is acute (Fig. 5.2b), additional plastic deformation will occur. Thus, the criterion for loading is

$$\text{if } f = 0 \text{ and } n_{ij}^f d\sigma_{ij} > 0, \text{ then } d\epsilon_{ij}^p \neq 0 \quad (5.21)$$

On the other hand, if the two vectors $d\sigma_{ij}$ and n_{ij}^f form an obtuse angle, unloading will occur. Thus, the criterion for unloading is

$$\text{if } f = 0 \text{ and } n_{ij}^f d\sigma_{ij} < 0, \text{ then } d\epsilon_{ij}^p = 0 \quad (5.22)$$

In the *neutral loading* case, the additional load vector $d\sigma_{ij}$ is perpendicular to the normal vector n_{ij}^f , and no additional plastic deformation will occur. This condition is termed "*neutral loading*." The criterion for "*neutral loading*" is

$$\text{if } f = 0 \text{ and } n_{ij}^f d\sigma_{ij} = 0, \text{ then } d\epsilon_{ij}^p = 0 \quad (5.23)$$

Recall the loading criterion for an elastic-perfectly plastic material discussed in Chapter 4 [see Eqs. (4.2) and (4.5)]; in that case, the initial yield surface becomes the *limit surface* with plastic deformation taking place only when $f = 0$ and $d\sigma_{ij}$ is tangent to the yield surface. Thus, for a perfectly plastic material, there is no neutral loading case such as satisfied by Eq. (5.23).

5.3.2. Hardening Rules

When an initial yield surface is known, the rule of work hardening defines its modification during the process of plastic flow. A number of hardening rules have been proposed. The most widely used rules are those of *isotropic hardening*, *kinematic hardening*, and a combination of both, i.e., the so-called *mixed hardening*. In this section, we shall discuss these three simple rules in some detail.

For clarity, the general form of the loading function of Eq. (5.19) can be written as

$$f(\sigma_{ij}, \epsilon_{ij}^p, k) = F(\sigma_{ij}, \epsilon_{ij}^p) - k^2(\epsilon_p) = 0 \quad (5.24)$$

in which the hardening parameter k^2 represents the size of the yield surface, while the function $F(\sigma_{ij}, \epsilon_{ij}^p)$ defines the shape of that surface. Here, the parameter k^2 is expressed as a function of ϵ_p , called the *effective strain*, which is an integrated increasing function of the plastic strain increments but not the plastic strain itself (see Section 5.5). The value of ϵ_p depends on the loading history or the plastic strain path.

Since the work hardening of a material tends to introduce anisotropies in an initially isotropic material, it is not sufficient to represent an anisotropic yield surface in the space of principal stresses that has been used for an isotropic material. In the following, the yield surface will therefore be described in the nine-dimensional stress space of σ_{ij} . Diagrams will be drawn, however, in two dimensions, but the basic geometric ideas are readily extended to higher-dimensional spaces.

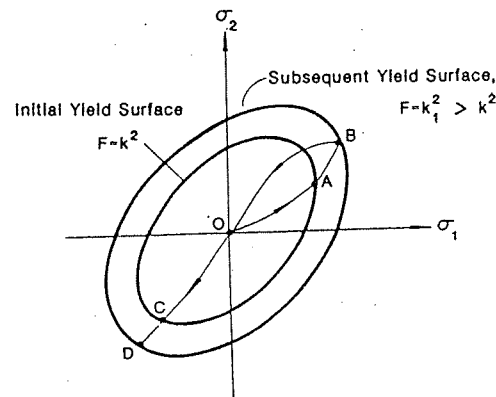


FIGURE 5.3. Subsequent yield surface for isotropic-hardening material.

5.3.3. Isotropic Hardening

For a perfectly plastic material, the equation for the fixed yield surface has the form $F(\sigma_{ij}) = k^2$, where k is a constant. The simplest work-hardening rule is based on the assumption that the initial yield surface expands uniformly without distortion and translation as plastic flow occurs, as shown schematically in Fig. 5.3. The size of the yield surface is now governed by the value k^2 , which depends upon plastic strain history. The equation for the subsequent yield surface or loading surface can be written in the general form

$$F(\sigma_{ij}) = k^2(\epsilon_p) \quad (5.25)$$

If, for example, the von Mises initial yield function, $F = J_2$, is used, Eq. (5.25) becomes

$$J_2 = \frac{1}{2} s_{ij} s_{ij} = k^2(\epsilon_p) \quad (5.26)$$

When the effective stress $\sigma_e = \sqrt{(3J_2)}$ is introduced into Eq. (5.26) as a hardening parameter, the isotropic-hardening von Mises model takes the form

$$f(\sigma_{ij}, k) = \frac{1}{2} s_{ij} s_{ij} - \sigma_e^2(\epsilon_p) = 0 \quad (5.27)$$

where the hardening parameter $\sigma_e(\epsilon_p)$ is related to the effective strain ϵ_p through an experimental uniaxial stress-strain curve. The effective strain ϵ_p will be defined later either as a scalar function of the work done by the plastic deformation or as the accumulated plastic strain (see Section 5.5).

5.3.3.1. AN ILLUSTRATIVE EXAMPLE

As an illustration, consider a material element subjected to uniaxial normal and shear stresses as shown in Fig. 5.4. Based on the von Mises yield

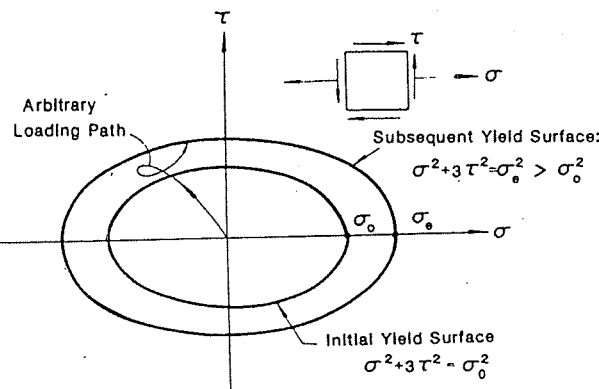


FIGURE 5.4. Hardening parameter for an element subject to normal and shear stresses.

criterion, the initial yield function is given by

$$f = \sigma^2 + 3\tau^2 - \sigma_0^2 = 0 \quad (5.28)$$

or

$$F = \sigma^2 + 3\tau^2 = \sigma_0^2 \quad (5.29)$$

in which σ_0 is the initial yield stress under uniaxial tension. After the initial yielding, if the material is subjected to a general loading path, according to the isotropic hardening rule, its subsequent loading surfaces are generally expressed as

$$\sigma^2 + 3\tau^2 = \sigma_e^2 \quad (5.30)$$

in which the hardening parameter σ_e^2 , characterizing the size of a loading surface, is the largest previous value of $(\sigma^2 + 3\tau^2)$ reached in the stress history. Since the recorded history of the material is represented by the hardening parameter, the material characterized by Eq. (5.30) may be regarded as a stress-hardening material.

5.3.3.2. THE BAUSCHINGER EFFECT

The isotropic hardening model is simple to use, but it applies mainly to monotonic loading without stress reversals. Because the loading surface expands uniformly (or isotropically) and remains self-similar with increasing plastic deformation (Fig. 5.3), it cannot account for the Bauschinger effect exhibited by most structural materials.

The term *Bauschinger effect* refers to a particular type of directional anisotropy induced by a plastic deformation; namely, an initial plastic deformation of one sign reduces the resistance of the material with respect to a subsequent plastic deformation of the opposite sign. The behavior

predicted by the isotropic hardening rule is, in fact, contrary to this observation. The rule implies that because of work hardening, the material will exhibit an increase in the compressive yield stress equal to the increase in the tension yield stress. This is illustrated in Fig. 5.3, where the yield limits in the first loading direction (OAB) and in the reversed loading direction (OCD) are equal in magnitude. Since plastic deformation is an anisotropic process, it cannot be expected that the theory of isotropic hardening will lead to a realistic result when complex loading paths with stress reversal are considered.

5.3.4. Kinematic Hardening

The *kinematic hardening rule* assumes that during plastic deformation, the loading surface translates as a rigid body in stress space, maintaining the size, shape, and orientation of the initial yield surface. This hardening rule, due to Prager (1955, 1956), provides a simple means of accounting for the Bauschinger effect.

This rule is illustrated schematically in Fig. 5.5. As the stress point moves along its loading path from point A to point B , the yield surface translates (no rotation) as a rigid body. Thus, the subsequent yield surface will wind up in the position indicated in Fig. 5.5 when the stress point has reached position B . The new position of the yield surface represents the most current yield function, whose center is denoted by α_{ij} . Note that if the stress is unloaded from point B along the initial path of loading, i.e., if B now traces out path BAO , the material behaves elastically from point B to point C .

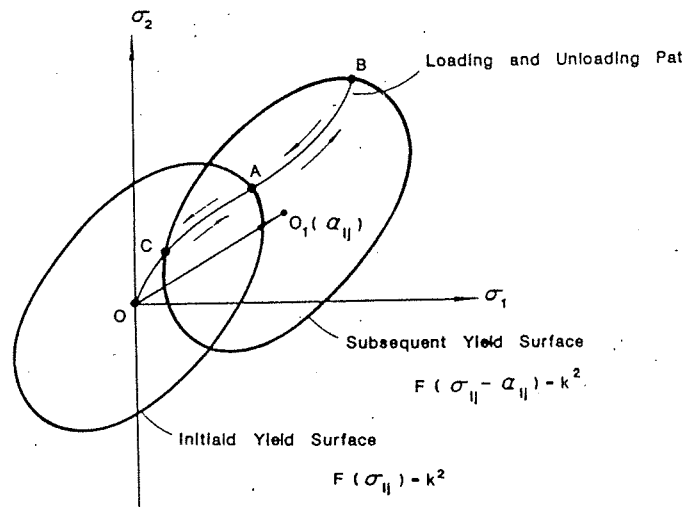


FIGURE 5.5. Subsequent yield surface for kinematic-hardening material.

but then begins to flow again before the stresses are completely relieved. In fact, the subsequent yield surface may or may not enclose the origin in stress space. As a consequence of assuming a rigid-body translation of the loading surface, the kinematic hardening rule predicts an ideal Bauschinger effect for a complete reversal of loading conditions.

For kinematic hardening, the equation of the loading surface has the general form

$$f(\sigma_{ij}, \epsilon_{ij}'') = F(\sigma_{ij} - \alpha_{ij}) - k^2 = 0 \quad (5.31)$$

where k is a constant and α_{ij} are the coordinates of the center of the loading surface (or the vector OO_1 in Fig. 5.5), which changes with the plastic deformation. As an illustration, let us consider the following simple example.

EXAMPLE 5.2. A yielded material element is subjected to a normal stress σ and a shear stress τ as shown in Fig. 5.6. Determine the coordinate change of the center of the loading surface $d\alpha_{ij}$ due to an additional load $d\sigma_{ij} = (d\sigma, d\tau)$ which satisfies the criterion of loading. Assume $d\alpha_{ij}$ is in the direction parallel to the normal vector to the loading surface at the current yield point A in the stress subspace (σ, τ) . Assume the material satisfies the von Mises criterion.

SOLUTION. Based on the von Mises criterion, the initial yield function is given by Eq. (5.28). Due to kinematic hardening, the subsequent yield function is expressed as

$$f = (\sigma - \bar{\sigma})^2 + 3(\tau - \bar{\tau})^2 - \sigma_0^2 = 0 \quad (5.32)$$

in which $(\bar{\sigma}, \bar{\tau})$ are the coordinates of the center of the current loading surface, and the hardening parameter σ_0^2 remains constant.

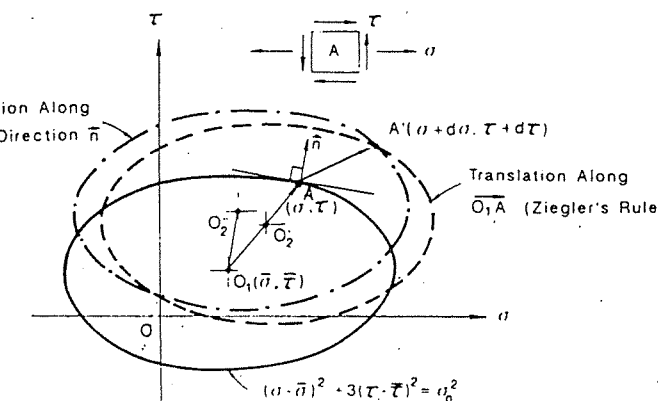


FIGURE 5.6. Subsequent yield surfaces due to different kinematic hardening rules (Examples 5.2 and 5.4).

Now, a stress increment $(d\sigma, d\tau)$ is imposed on the stress state $A(\sigma, \tau)$ which lies on the loading surface $f=0$ and satisfies the loading condition:

$$\frac{\partial f}{\partial \sigma} d\sigma + \frac{\partial f}{\partial \tau} d\tau > 0$$

Thus, plastic strain takes place, and according to the kinematic hardening rule, the loading surface translates in the stress space. To determine the incremental translation of the center, $d\alpha_{ij}$, due to the stress increments $(d\sigma, d\tau)$, we assume that the vector $d\alpha_{ij}$ is in the direction parallel to the normal vector \mathbf{n} at the contact or the current yield stress point A in the subspace of stress (σ, τ) . Therefore, $d\alpha_{ij}$ has only two nonzero elements, i.e.,

$$\{d\alpha_{ij}\} = \{d\tilde{\sigma}, d\tilde{\tau}\} \quad (5.33)$$

which satisfy

$$d\tilde{\sigma} = c \frac{\partial f}{\partial \sigma} = 2c(\sigma - \tilde{\sigma})$$

$$d\tilde{\tau} = c \frac{\partial f}{\partial \tau} = 6c(\tau - \tilde{\tau}) \quad (5.34)$$

where c is a constant. Since the stress point A' remains on the new yield surface during loading, the change in f , df must be zero:

$$df = 2(\sigma - \tilde{\sigma})(d\sigma - d\tilde{\sigma}) + 6(\tau - \tilde{\tau})(d\tau - d\tilde{\tau}) = 0 \quad (5.35)$$

Solving Eqs. (5.34) and (5.35) for $d\tilde{\sigma}$ and $d\tilde{\tau}$, we obtain the incremental translation of the center $(d\tilde{\sigma}, d\tilde{\tau})$ as

$$\begin{aligned} d\tilde{\sigma} &= (\sigma - \tilde{\sigma})[(\sigma - \tilde{\sigma})d\sigma + 3(\tau - \tilde{\tau})d\tau]/[\sigma_0^2 + 6(\tau - \tilde{\tau})^2] \\ d\tilde{\tau} &= 3(\tau - \tilde{\tau})[(\sigma - \tilde{\sigma})d\sigma + 3(\tau - \tilde{\tau})d\tau]/[\sigma_0^2 + 6(\tau - \tilde{\tau})^2] \end{aligned} \quad (5.36)$$

The translation $(d\tilde{\sigma}, d\tilde{\tau})$ is shown by the line O_1O_2' while the updated yield curve is shown by a dashed-dotted line in Fig. 5.6. For a given loading path, Eq. (5.36) can be integrated and the current position of the center can be determined.

5.3.4.1. PRAGER'S HARDENING RULE

It is seen that the key to a subsequent yield surface based on a kinematic hardening rule is the determination of the coordinates of the center, α_{ij} . The simplest version for determining the hardening parameter α_{ij} is to assume a linear dependence of $d\alpha_{ij}$ on $d\epsilon_{ij}^p$. This is known as *Prager's hardening rule*, which has the simple form

$$d\alpha_{ij} = c d\epsilon_{ij}^p \quad \text{or} \quad \alpha_{ij} = c \epsilon_{ij}^p \quad (5.37)$$

where c is the work-hardening constant, characteristic for a given material. Equation (5.37) may be taken as the definition of linear work hardening.

If we adopt the *associated flow rule*, Prager's hardening rule is equivalent to the assumption that the vector $d\alpha_{ij}$ moves in the direction parallel to the normal vector \mathbf{n} at the current stress state on the yield surface in stress space.

Some inconsistencies may arise when Prager's hardening rule is used in a subspace of stress. For example, if some of the stress components are set equal to zero in Eq. (5.31), say, $\sigma_{ij}'' = 0$ and $\sigma_{ij}' \neq 0$, Eq. (5.31) can be written

$$F(\sigma_{ij}' - \alpha_{ij}', -\alpha_{ij}'') - k^2 = 0 \quad (5.38)$$

Since $d\alpha_{ij}'' = c d\epsilon_{ij}^p$ is not necessarily zero, Eq. (5.38) no longer necessarily represents a surface which merely translates in the stress space; it may also deform as well, due to the changing values of α_{ij}'' . This can best be seen from Example 5.3 below.

It should be noted that in the last example, we have assumed that the vector $d\alpha_{ij}$ moves in the direction parallel to the normal to the yield surface at stress state A in subspace (σ_x, τ_{xy}) , i.e.,

$$d\alpha_{xx} = c \frac{\partial f}{\partial \sigma_x}, \quad d\alpha_{xy} = c \frac{\partial f}{\partial \tau_{xy}}, \quad \text{other components} = 0 \quad (5.39)$$

which is in the direction of the projection of the vector $\partial f / \partial \sigma_{ij}$ onto the $\sigma_x - \tau_{xy}$ plane. Based on this assumption, the subsequent yield function holds the same form as Eq. (5.32) during hardening. However, this is not the case if Prager's rule is used to determine the parameters α_{ij} .

EXAMPLE 5.3. Using Prager's rule, solve the same problem as in Example 5.2.

SOLUTION. Prager's rule is expressed as

$$d\alpha_{ij} = \bar{c} d\epsilon_{ij}^p = c \frac{\partial f}{\partial \sigma_{ij}} \quad (5.40)$$

in which the associated flow rule has been used. The general form of the subsequent yield surface of a J_2 -material is given by

$$f = \frac{1}{2}(s_{ij} - \alpha_{ij})(s_{ij} - \alpha_{ij}) - \sigma_0^2 = 0 \quad (5.41)$$

Substitution of Eq. (5.41) into Eq. (5.40) leads to

$$d\alpha_{ij} = c \frac{\partial f}{\partial \sigma_{ij}} = 3c(s_{ij} - \alpha_{ij}) \quad (5.42)$$

Now the material element is only subjected to the normal stress σ and the shear stress τ , i.e.,

$$\sigma_{xx} = \sigma, \quad \tau_{xy} = \tau, \quad \text{other components of } \sigma_{ij} = 0$$

and

$$\alpha_{xx} = \tilde{\sigma}, \quad \alpha_{xy} = \tilde{\tau}, \quad \text{other components of } \alpha_{ij} = 0 \quad (5.43)$$

Thus, Eq. (5.41) takes the form of Eq. (5.32):

$$f = (\sigma - \tilde{\sigma})^2 + 3(\tau - \tilde{\tau})^2 - \sigma_0^2 = 0 \quad (5.44)$$

and from Eq. (5.42), the changes of the coordinates of the center, $d\alpha_{ij}$, are

obtained as

$$\begin{aligned} d\alpha_{xx} &= 2c(\sigma - \tilde{\sigma}), & d\alpha_{yy} = d\alpha_{zz} &= -c(\sigma - \tilde{\sigma}) \\ d\alpha_{xy} = d\alpha_{yx} &= 3c(\tau - \tilde{\tau}), & d\alpha_{xz} = d\alpha_{zx} = d\alpha_{yz} = d\alpha_{zy} &= 0 \end{aligned} \quad (5.45)$$

It is seen that $d\alpha_{yy}$ and $d\alpha_{zz}$ are no longer equal to zero. Denote the updated value of the hardening parameter as

$$\tilde{\alpha}_{ij} = \alpha_{ij} + d\alpha_{ij}$$

Then the updated subsequent yield surface is expressed by

$$f = (\sigma - \tilde{\alpha}_{xx}^2) + 3(\tau - \tilde{\alpha}_{xy})^2 + (-\tilde{\alpha}_{yy})^2 + (-\tilde{\alpha}_{zz})^2 - \sigma_0^2 = 0 \quad (5.46)$$

Comparison of Eq. (5.46) to Eq. (5.44) indicates that Prager's hardening rule leads to a subsequent yield surface which not only translates but also changes its shape during the plastic flow caused by an additional loading. Equation (5.46) does not really represent a kinematic hardening rule as described earlier.

5.3.4.2. ZIEGLER'S HARDENING RULE

In order to obtain a kinematic hardening rule that is also valid in subspaces, Ziegler (1959) modified Prager's hardening rule and assumed that the rate of translation takes place in the direction of the reduced-stress vector $\tilde{\alpha}_{ij} = \sigma_{ij} - \alpha_{ij}$ in the form

$$d\alpha_{ij} = d\mu(\sigma_{ij} - \alpha_{ij}) \quad (5.47)$$

where $d\mu$ is a positive proportionality factor which depends on the history of the deformation. For simplicity, this factor can be assumed to have the simple form

$$d\mu = a d\epsilon_p \quad (5.48)$$

in which a is a positive constant, characteristic for a given material.

EXAMPLE 5.4. Using Ziegler's hardening rule, solve the same problem as in Example 5.2.

SOLUTION. In this case, Ziegler's rule of Eq. (5.47) is expressed as

$$\begin{aligned} d\tilde{\sigma} &= d\alpha_{xx} = d\mu(\sigma - \tilde{\sigma}) \\ d\tilde{\tau} &= d\alpha_{xy} = d\alpha_{yx} = d\mu(\tau - \tilde{\tau}) \\ \text{other components of } d\alpha_{ij} &= 0 \end{aligned} \quad (5.49)$$

Following the same procedure as in Example 5.2, and solving Eqs. (5.49) and (5.35) for $d\tilde{\sigma}$ and $d\tilde{\tau}$, we obtain

$$d\tilde{\sigma} = \frac{1}{\sigma_0^2} (\sigma - \tilde{\sigma}) [(\sigma - \tilde{\sigma}) d\sigma + 3(\tau - \tilde{\tau}) d\tau] \quad (5.50)$$

$$d\tilde{\tau} = \frac{1}{\sigma_0^2} (\tau - \tilde{\tau}) [(\sigma - \tilde{\sigma}) d\sigma + 3(\tau - \tilde{\tau}) d\tau]$$

The translation increment ($d\tilde{\sigma}, d\tilde{\tau}$) of the center is shown by $O_1O'_2$ in Fig. 5.6, which is along the direction of the reduced-stress vector $O_1A(\sigma - \tilde{\sigma}, \tau - \tilde{\tau})$, and the updated yield surface is shown by a dashed line in the figure.

5.3.5. Mixed Hardening

A combination of kinematic and isotropic hardening would lead to the more general *mixed hardening rule* (Hodge, 1957):

$$f(\sigma_{ij}, \epsilon_{ij}^p, k) = F(\sigma_{ij} - \alpha_{ij}) - k^2(\epsilon_p) = 0 \quad (5.51)$$

In this case, the loading surface experiences a translation defined by α_{ij} and a uniform expansion measured by k^2 ; but it still retains its original shape. With the mixed hardening rule, different degrees of the Bauschinger effect can be simulated, by simply adjusting the two hardening parameters, α_{ij} and k^2 .

For illustration, consider a J_2 -material subjected to a mixed hardening rule. The general form of the subsequent loading surface is

$$f = \frac{1}{2}(s_{ij} - \alpha_{ij})(s_{ij} - \alpha_{ij}) - k^2(\epsilon_p) = 0 \quad (5.52)$$

If Prager's hardening rule is employed, Eq. (5.52) can be rewritten as

$$f = \frac{1}{2}(s_{ij} - ce_{ij}^p)(s_{ij} - ce_{ij}^p) - k^2(\epsilon_p) = 0 \quad (5.53)$$

where c is a constant. In stress space, the surface moves around but does not simply expand outward, as in Fig. 5.3, or translate as in Fig. 5.5. The subsequent yield surfaces do not form a one-parameter family but intersect the previous ones, as shown in section by the dashed curve in Fig. 5.7. It is these surfaces in stress space that determine whether or not additional plastic deformations will occur in the subsequent loading.

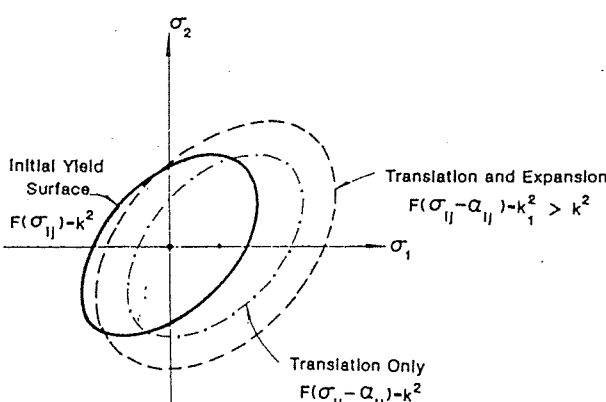


FIGURE 5.7. Subsequent yield surface for mixed-hardening J_2 -material.

5.4. Flow Rule and Drucker's Stability Postulate

5.4.1. Flow Rules

So far, the loading surface alone has been considered, and the shape of the subsequent loading surfaces in a given loading program can be determined by the choice of a specific hardening rule. The necessary connection between the loading function f and the stress-strain relation for a work-hardening material will be made here by means of a flow rule.

When the current yield surface f is reached, the material is in a state of plastic flow upon further loading. Introducing the concept of a *plastic potential function* $g(\sigma_{ij}, \epsilon_{ij}^p, k)$ in analogy with ideal-fluid-flow problems, we define the flow rule

$$d\epsilon_{ij}^p = d\lambda \frac{\partial g}{\partial \sigma_{ij}} \quad (5.54)$$

where $d\lambda > 0$ is a scalar function that will vary throughout the history of the straining process. The gradient of the plastic potential surface $\partial g / \partial \sigma_{ij}$ defines the direction of the plastic strain increment vector $d\epsilon_{ij}^p$, while the length or the magnitude of the vector is determined by the *loading parameter* $d\lambda$. Here, as in Chapter 4 for a perfectly plastic material, the flow rule is termed associated if the plastic potential surface has the same shape as the current yield or loading surface

$$g(\sigma_{ij}, \epsilon_{ij}^p, k) = f(\sigma_{ij}, \epsilon_{ij}^p, k)$$

and Eq. (5.54) takes the form

$$d\epsilon_{ij}^p = d\lambda \frac{\partial f}{\partial \sigma_{ij}} \quad (5.55)$$

i.e., the plastic flow develops along the normal to the loading surface. Relation (5.55) is called the *associated flow rule* because the plastic flow is associated with the current loading surface. Since there is, in general, very little experimental evidence on plastic potential functions for engineering materials the associated flow rule is applied predominantly to these materials for practical reasons. Apart from its simplicity, the *normality condition* of Eq. (5.55) assures a *unique* solution for a given boundary-value problem using any stress-strain relations developed on this basis. Perhaps the most fundamental development for the subject of this section is the fact that the basic *stability postulate* or *Drucker postulate* (1951) for the definition of stable, work-hardening materials leads, among other consequences, to the normality condition. The shape of the loading surfaces and the form of the stress-strain relations are all tied together to the basic definition or postulate of a work-hardening material, as discussed below.

5.4.2. Drucker's Stability Postulate

Drucker's stability postulate has been discussed previously in Chapter 3 for the definition of a general *stable material*, which is expressed in terms of an external agency that adds load to the already loaded body (see Fig. 3.13). The plastic work-hardening material is a special case of the general stable inelastic materials. It also satisfies the stability postulate as given by Eqs. (3.160) and (3.161) in Chapter 3. In the following, we see that the definition of a work-hardening material as formulated by Drucker is more restrictive than the law of thermodynamics requires.

If an external agency slowly applies additional forces to a work-hardening body which is already loaded and then removes them, then

1. positive work is done by the external agency during the application of the added loads;
2. the net work performed by the external agency over a cycle of application and removal of the added loads is positive if plastic deformation has occurred in the cycle.

The work done by the added set of forces \dot{T}_i, \dot{F}_i on the changes in displacement \dot{u} (see Fig. 3.13) is expressed as

$$dW = \int_A \dot{T}_i \dot{u}_i dA + \int_V \dot{F}_i \dot{u}_i dV$$

Thus, the two stability requirements are stated as

$$\int_A \dot{T}_i \dot{u}_i dA + \int_V \dot{F}_i \dot{u}_i dV > 0 \quad (5.56)$$

and

$$\oint_A \dot{T}_i \dot{u}_i dA + \oint_V \dot{F}_i \dot{u}_i dV > 0 \quad (5.57)$$

in which \oint indicates integration over a cycle of addition and removal of the additional set of forces, and plastic deformation is assumed to occur in this cycle.

Applying the principle of virtual work, the stability postulate can be expressed in terms of stresses and strains as follows.

$$\dot{\sigma}_{ij} \dot{\epsilon}_{ij} > 0 \quad \text{or} \quad d\sigma_{ij} d\epsilon_{ij}^p > 0 \quad \text{stability in small} \quad (5.58)$$

$$\oint \dot{\sigma}_{ij} \dot{\epsilon}_{ij} > 0 \quad \text{or} \quad \oint d\sigma_{ij} d\epsilon_{ij}^p > 0 \quad \text{stability in cycle in small} \quad (5.59)$$

These inequalities are illustrated geometrically in Fig. 5.8. We have assumed that the plastic strain $d\epsilon_{ij}^p \neq 0$ in Eq. (5.59). In general, we can write

$$\oint \dot{\sigma}_{ij} \dot{\epsilon}_{ij} \geq 0 \quad \text{or} \quad \oint d\sigma_{ij} d\epsilon_{ij}^p \geq 0 \quad (5.60)$$

The equal sign is valid if no plastic strain occurred in the cycle.

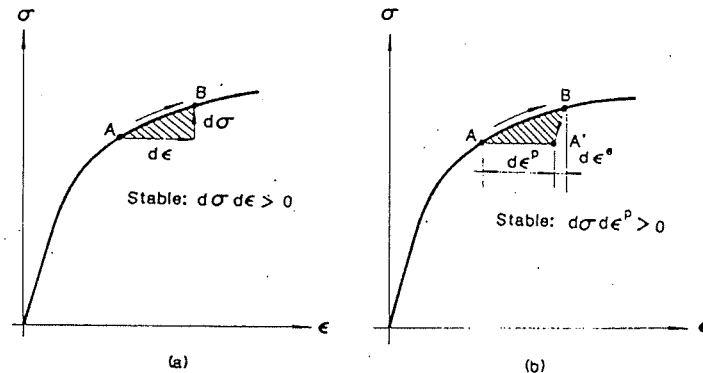


FIGURE 5.8. Stability postulate for work-hardening materials: (a) stability in small; (b) stability in cycle in small.

Consider a material element subjected to a homogeneous state of stress σ_{ij}^* which is either on or inside the yield surface (Fig. 5.9). Suppose an external agency adds stresses along a path ABC with AB lying inside the yield surface and point B just on it. The stresses continue to move outward and cause the yield surface to evolute until point C is reached. The external agency then releases and returns the state of stress back to σ_{ij}^* along an elastic path CDA . As the elastic deformations are fully reversible and independent of the path from σ_{ij}^* to σ_{ij} and back to σ_{ij}^* , all the elastic energy is recovered. The plastic work done by the external agency on this loading and unloading cycle is the scalar product of the stress vector $\sigma_{ij} - \sigma_{ij}^*$ and the plastic strain increment vector $d\epsilon_{ij}^p$. This stability requirement of Eq. (5.60) leads to

$$(\sigma_{ij} - \sigma_{ij}^*) d\epsilon_{ij}^p \geq 0 \quad (5.61)$$

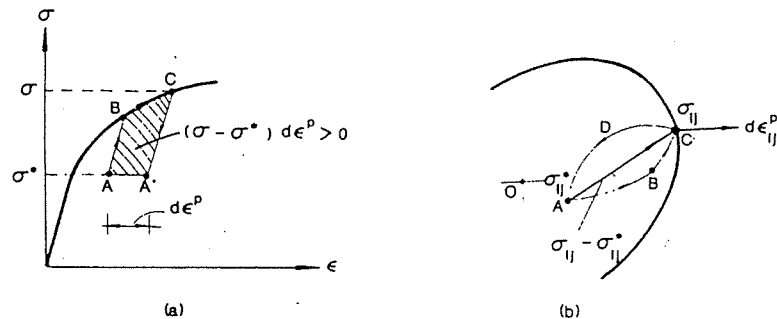


FIGURE 5.9. Stability in cycle: Existing state of stress inside the yield surface (point A); stress path ABC produced by external agency.

If plastic strain coordinates are superimposed upon stress coordinates, as in Fig. 5.9, Eq. (5.61) can be interpreted geometrically as the scalar product of the stress increment vector $(\sigma_{ij} - \sigma_{ij}^*)$ with the strain increment vector $d\epsilon_{ij}^p$. A positive scalar product requires an acute angle between these two vectors. The stability postulate leads therefore to the following consequences for work-hardening materials (Drucker, 1960):

Convexity: The initial yield and all the subsequent loading surfaces must be convex.

Normality: The plastic strain increment vector $d\epsilon_{ij}^p$ must be *normal* to the yield or loading surface $f(\sigma_{ij}, \epsilon_{ij}^p, k) = 0$ at a smooth point:

$$d\epsilon_{ij}^p = d\lambda \frac{\partial f}{\partial \sigma_{ij}} \quad (5.62)$$

and lie between adjacent normals at a corner.

Convexity and normality conditions for elastic-perfectly plastic materials have been discussed in Chapter 4. The reasoning is also sound here for work-hardening materials.

Linearity: The plastic strain increment must be *linear* in the stress increment. Equation (5.62) indicates that the ratio of the components of plastic strain increment, $d\epsilon_{ij}^p$, are independent of the ratios of the components of stress increment, $d\sigma_{ij}$, at any smooth point on the surface. However, the magnitude of $d\epsilon_{ij}^p$, characterized by the scalar $d\lambda$, is dependent only on the projection of the stress increment, $d\sigma_{ij}$, onto the direction of the normal $\partial f / \partial \sigma_{ij}$. That is,

$$d\lambda = \bar{G} \partial f = \bar{G} \frac{\partial f}{\partial \sigma_{mn}} d\sigma_{mn} \quad (5.63)$$

and

$$d\epsilon_{ij}^p = \bar{G} \partial f \frac{\partial f}{\partial \sigma_{ij}} = \bar{G} \frac{\partial f}{\partial \sigma_{ij}} \frac{\partial f}{\partial \sigma_{mn}} d\sigma_{mn} \quad (5.64)$$

where \bar{G} is a scalar function which may depend upon stress, strain, and the history of loading. But \bar{G} is independent of $d\sigma_{ij}$. Note that in Eq. (5.63), the increment ∂f is evaluated only with respect to increments in the stress components, i.e., with other variables unchanged [see Eq. (5.19)].

Continuity: The condition of *continuity* requires that for $d\sigma_{ij}$ tangential to the yield surface (neutral loading), no plastic increment is induced. This condition is satisfied by Eqs. (5.63) and (5.64) since for $d\sigma_{ij}$ tangential to the yield surface, we have $\partial f = (\partial f / \partial \sigma_{mn}) d\sigma_{mn} = 0$.

Uniqueness: Uniqueness of the solution of a boundary-value problem for a work-hardening material can be proved directly from the stability postulate (Drucker, 1956). Suppose a body is under the action of existing surface traction T_i , body forces F_i , displacements u_i , stresses σ_{ij} , and strains ϵ_{ij} (see Fig. 3.7a). If small changes of the applied forces and displacements, dT_i on A_T , dF_i in V , du_i on A_u , are now imposed on the

body, uniqueness requires that the stress and strain changes, $d\sigma_{ij}$ and $d\epsilon_{ij}$, be uniquely determined by the changes of applied forces and displacements.

This can be proved in the usual manner. Two solutions are assumed: $d\sigma_{ij}^a$, $d\epsilon_{ij}^a$ and $d\sigma_{ij}^b$, $d\epsilon_{ij}^b$, corresponding to the same applied load and displacement increments dT_i on A_T , du on A_u , and dF_i in V . Using the equation of virtual work, we have [Eq. (3.171)]

$$\int_V (d\sigma_{ij}^a - d\sigma_{ij}^b)(d\epsilon_{ij}^a - d\epsilon_{ij}^b) dV = 0 \quad (5.65)$$

If the integrand in Eq. (5.65) can be shown to be *positive definite*, uniqueness is proved. As a first step, the strain rates are decomposed into elastic and plastic parts, $d\epsilon_{ij} = d\epsilon_{ij}^e + d\epsilon_{ij}^p$, and the integrand is written

$$(d\sigma_{ij}^a - d\sigma_{ij}^b)(d\epsilon_{ij}^a - d\epsilon_{ij}^b) + (d\sigma_{ij}^a - d\sigma_{ij}^b)(d\epsilon_{ij}^p - d\epsilon_{ij}^p) \quad (5.66)$$

The first term is always positive definite for both linear and nonlinear elasticity (see Section 3.6, Chapter 3). Thus, if the second term can also be shown to be positive or zero, then the positive-definiteness of the integrand is proved.

To examine the second term of Eq. (5.66), consider three possibilities. If a and b are both elastic changes (Fig. 5.10a), both $d\epsilon_{ij}^p$ and $d\epsilon_{ij}^p$ vanish, so the second term is zero. If b is elastic, i.e., $d\epsilon_{ij}^p = 0$, and a is elastic-plastic (Fig. 5.10b), then the second term is positive because both $d\sigma_{ij}^a d\epsilon_{ij}^p$ and $-d\sigma_{ij}^b d\epsilon_{ij}^p$ are positive. When a and b both represent elastic-plastic changes (Fig. 5.10c), we first note that from Eq. (5.64), the incremental plastic strain-stress relation is linear and can therefore be written in the general form:

$$d\epsilon_{ij}^p = H_{ijkl} d\sigma_{kl} \quad (5.67)$$

in which the coefficients H_{ijkl} are functions of stress and may also depend upon the strain and the history of loading, but do not depend on the stress increment, $d\sigma_{ij}$. Now both $d\epsilon_{ij}^p$, $d\sigma_{ij}^a$ and $d\epsilon_{ij}^p$, $d\sigma_{ij}^b$ satisfy Eq. (5.67). Thus, the difference between a and b also satisfies Eq. (5.67). The stress difference $d\sigma_{ij}^a - d\sigma_{ij}^b$ may be considered then as applied by the external agency which produces the corresponding plastic strain

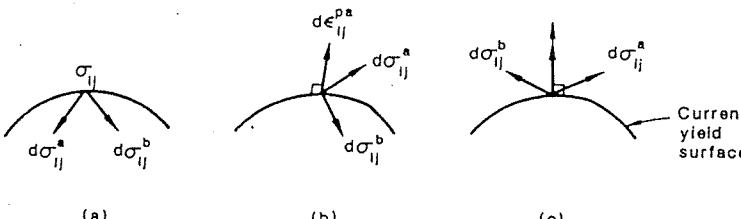


FIGURE 5.10. Proof of uniqueness: (a) both a and b are elastic; (b) b is elastic, a is elastic-plastic; (c) both a and b are elastic-plastic.

difference $d\epsilon_{ij}^{pa} - d\epsilon_{ij}^{pb}$. The stability postulate of Eq. (5.59) then gives

$$(d\sigma_{ij}^a - d\sigma_{ij}^b)(d\epsilon_{ij}^{pa} - d\epsilon_{ij}^{pb}) > 0 \quad (5.68)$$

Hence, Eq. (5.66) is positive definite, i.e.,

$$(d\sigma_{ij}^a - d\sigma_{ij}^b)(d\epsilon_{ij}^p - d\epsilon_{ij}^p) > 0 \quad (5.69)$$

and the uniqueness condition is therefore established.

5.4.3. Nonassociated Flow Rule

It has been shown that the associated flow (normality) rule and the convexity, continuity, and uniqueness conditions are all the consequences of Drucker's stability postulate. This is a fundamental unification of the theory of plasticity.

However, it is to be noted that the stability postulate is a *sufficient* but not a *necessary* criterion. In other words, this postulate may not be *necessarily* required in a general formulation of any flow rule for elastic-plastic materials (Mroz, 1963). It has been shown that for an elastic-work-hardening-plastic material, the uniqueness allows a nonassociated flow rule to occur which does not necessarily satisfy Drucker's stability postulate. Further, since when the uniqueness of stress and strain trajectories for a given loading history exists, the material can be regarded as locally stable, thus the condition of uniqueness rather than the stability postulate may be regarded as a basic criterion in establishing elastic-plastic stress-strain relationships. Based on uniqueness, certain conditions imposed on the plastic potential function have been derived by Mroz (1963).

The nonassociated flow rule can be expressed as

$$d\epsilon_{ij}^p = d\lambda \frac{\partial g}{\partial \sigma_{ij}} = \bar{G} \frac{\partial f}{\partial \sigma_{ij}} = \bar{G} \frac{\partial g}{\partial \sigma_{ij}} \frac{\partial f}{\partial \sigma_{mn}} d\sigma_{mn} \quad (5.70)$$

in which Eq. (5.63) has been used, and the plastic strain increment is *linear* in stress increment. The condition of continuity is also satisfied.

For some geotechnical materials, such as rocks, soils, and concretes, it has been found that the associated flow rule tends to overestimate the plastic volume expansion. The nonassociated flow rule is therefore adopted in establishing the constitutive relations. This will be discussed in Chapter 7 in the context of modeling the inelastic behavior of concrete materials.

When the plastic potential function g (or f for associated plastic flow) is of the most general isotropic form $g(I_1, J_2, J_3)$, Eq. (5.70) [or Eq. (5.64) using f as potential function instead of g] leads to

$$d\epsilon_{ij}^p = \bar{G} \left(\frac{\partial g}{\partial I_1} \frac{\partial I_1}{\partial \sigma_{ij}} + \frac{\partial g}{\partial J_2} \frac{\partial J_2}{\partial \sigma_{ij}} + \frac{\partial g}{\partial J_3} \frac{\partial J_3}{\partial \sigma_{ij}} \right) df \quad (5.71)$$

which can be written in the general form as

$$d\epsilon_{ij}^p = [P(I_1, J_2, J_3) \delta_{ij} + Q(I_1, J_2, J_3) s_{ij} + R(I_1, J_2, J_3) t_{ij}] df \quad (5.72)$$

where t_{ij} , defined in Eq. (5.17), is the deviation of the square of the stress deviator s_{ij} . A marked similarity can be seen between the *deformation theory* [Eq. (5.18)] and the *incremental theory* [Eq. (5.72)], but the difference is extremely important. Now, when $\partial f = 0$, that is when the stress change is on the current loading surface or a neutral loading, there is no change in any component of plastic strain (*condition of continuity*).

In a true sense, such a theory is isotropic because the principal stresses may have any orientation with respect to axes fixed in the material. However, it is anisotropic in that the principal directions of the increments in plastic strain will not coincide with the stress increments. The *anisotropy* is introduced by the state of stress, but it is not *intrinsic*. Removal of the stress leaves a material isotropic in the usual sense. Similarly, rotation of the state of stress with respect to the material rotates the anisotropy. This can clearly be seen if the components of the stress-strain relation (5.72) are written out; with the stress increments appearing explicitly, they look like a highly anisotropic incremental generalized Hooke's law of the form

$$d\epsilon_x = G_1 d\sigma_x + G_2 d\sigma_y + G_3 d\sigma_z + G_4 d\tau_{xy} + G_5 d\tau_{yz} + G_6 d\tau_{zx} \quad (5.73)$$

where the G 's are functions of the state of stress and include both the elastic and the plastic behavior. An increment of shearing stress may produce an elongation or contraction, and similarly, an increment of normal stress may cause a shearing strain. However, as previously stated, the anisotropy is produced by the existing state of stress and is not intrinsic.

5.5. Effective Stress and Effective Strain

For the work-hardening theory of plasticity to be of any practical use, we must relate the hardening parameters in the loading function to the experimental uniaxial stress-strain curve. To this end, we are looking for some stress variable, called *effective stress*, that is a function of the stresses and some strain variable, called *effective strain*, that is a function of the plastic strains, so that they can be plotted against each other and used to correlate the test results obtained by different loading programs. The single effective stress-effective strain curve should preferably be reduced to a uniaxial stress-strain curve for the uniaxial stress test.

5.5.1. Effective Stress

Since the loading function, $f(\sigma_{ij}, \epsilon_{ij}^p, k) = 0$ by definition, determines whether additional plastic flow takes place or not and is also a positively increasing function, it can be used as a truly significant stress variable to define the *effective stress*.

Consider the case of *isotropic* hardening in which the loading function takes the form of Eq. (5.25) or

$$f(\sigma_{ij}, k) = F(\sigma_{ij}) - k^2(\epsilon_p) = 0$$

The function $F(\sigma_{ij})$ is used to define the effective stress. Since the effective stress should reduce to the stress σ_1 in the uniaxial test, it follows that the loading function $F(\sigma_{ij})$ must be some constant C times the effective stress σ_e to some power

$$F(\sigma_{ij}) = C\sigma_e^n \quad (5.74)$$

For example, if we assume von Mises material, $F(\sigma_{ij}) = J_2$, then

$$J_2 = C\sigma_e^n \quad (5.75)$$

or

$$J_2 = \frac{1}{6}[(\sigma_1 - \sigma_2)^2 + (\sigma_2 - \sigma_3)^2 + (\sigma_3 - \sigma_1)^2] = C\sigma_e^n \quad (5.76)$$

and for the uniaxial test, $\sigma_e = \sigma_1$ and $\sigma_2 = \sigma_3 = 0$. Therefore

$$n = 2, \quad C = \frac{1}{3}, \quad \sigma_e = \sqrt{3J_2} \quad (5.77)$$

Similarly, for Drucker-Prager material, $F(\sigma_{ij}) = \alpha I_1 + \sqrt{J_2}$,

$$\alpha I_1 + \sqrt{J_2} = C\sigma_e^n \quad (5.78)$$

and for the uniaxial test, we have

$$\alpha\sigma_e + \frac{1}{\sqrt{3}}\sigma_e = C\sigma_e^n$$

Therefore,

$$n = 1, \quad C = \alpha + \frac{1}{\sqrt{3}}, \quad \sigma_e = \frac{\sqrt{3}\alpha I_1 + \sqrt{3}J_2}{1 + \sqrt{3}\alpha} \quad (5.79)$$

For the cases of *kinematic* hardening or *mixed* hardening, the loading function is written in the general form as Eq. (5.51)

$$f(\sigma_{ij}, \epsilon_{ij}^p, k) = F(\sigma_{ij} - \alpha_{ij}) - k^2(\epsilon_p) = 0 \quad (5.80)$$

We denote

$$\bar{\sigma}_{ij} = \sigma_{ij} - \alpha_{ij} \quad (5.81)$$

as the *reduced-stress tensor*, measured from an origin at the center of the translated yield surface. Then, the *reduced effective stress* $\bar{\sigma}_e$ is defined by the following relation similar to Eq. (5.74):

$$F(\bar{\sigma}_{ij}) = C\bar{\sigma}_e^n \quad (5.82)$$

Equations (5.77) and (5.79) are still valid for definitions of the reduced effective stress of von Mises and Drucker-Prager materials, respectively. Note that a reduced effective stress is associated with an expansion of the loading surface.

5.5.2. Effective Strain

The definition of *effective plastic strain*, ϵ_p , is not quite as simple. Two methods are generally used. One defines the effective plastic strain increment intuitively as some simple combination of plastic strain increments which is always positive and increasing. The simplest combination of this type with the correct "dimension" is

$$d\epsilon_p = C \sqrt{d\epsilon_{ij}^p d\epsilon_{ij}^p} \quad (5.83)$$

For example, if we assume an $f(J_2, J_3)$ type of pressure-independent material which satisfies the plastic-incompressibility condition

$$d\epsilon_1^p + d\epsilon_2^p + d\epsilon_3^p = 0 \quad (5.84)$$

then to make the definition (5.83) agree for the uniaxial stress test, we must have

$$\begin{aligned} d\epsilon_1^p = d\epsilon_p &= C \sqrt{[(d\epsilon_1^p)^2 + (\frac{1}{2}d\epsilon_2^p)^2 + (\frac{1}{2}d\epsilon_3^p)^2]} \\ &= C \sqrt{\frac{3}{2}} d\epsilon_1^p \end{aligned} \quad (5.85)$$

which leads to

$$C = \sqrt{\frac{2}{3}}, \quad d\epsilon_p = \sqrt{\frac{2}{3}} d\epsilon_{ij}^p d\epsilon_{ij}^p \quad (5.86)$$

The second method defines the effective plastic strain increment in terms of the *plastic work* per unit volume in the form

$$dW_p = \sigma_e d\epsilon_p \quad (5.87)$$

By definition, the increment of the plastic work is

$$dW_p = \sigma_{ij} d\epsilon_{ij}^p = d\lambda \sigma_{ij} \frac{\partial f}{\partial \sigma_{ij}} = d\lambda \sigma_{ij} \frac{\partial F}{\partial \sigma_{ij}} \quad (5.88)$$

in which the plastic strain increment $d\epsilon_{ij}^p$ has been related to the stresses by the flow rule of Eq. (5.62). If the function F is homogeneous of degree n in the stresses, as it is for many cases in metal plasticity theories, Eq. (5.88) can be further reduced to

$$dW_p = d\lambda nF \quad (5.89)$$

The scalar function $d\lambda$ can be obtained by squaring each of the terms in Eq. (5.62) and adding:

$$d\epsilon_{ij}^p d\epsilon_{ij}^p = (d\lambda)^2 \frac{\partial F}{\partial \sigma_{ij}} \frac{\partial F}{\partial \sigma_{ij}} \quad (5.90)$$

Taking the square root of both sides and substituting $d\lambda$ into Eq. (5.89) shows that dW_p must be a function of F and $\sqrt{(d\epsilon_{ij}^p d\epsilon_{ij}^p)}$

$$dW_p = \frac{\sqrt{d\epsilon_{ij}^p d\epsilon_{ij}^p} nF}{\sqrt{\partial F / \partial \sigma_{mn} \partial F / \partial \sigma_{mn}}} = \sigma_e d\epsilon_p \quad (5.91)$$

where we have used Eq. (5.87) to determine the effective plastic strain ϵ_p .

If, for example, the Drucker-Prager $F = \alpha I_1 + \sqrt{J_2}$ is used, the plastic work equation (5.91) becomes

$$\begin{aligned} dW_p &= \frac{\sqrt{d\epsilon_{ij}^p d\epsilon_{ij}^p} (1)(\alpha I_1 + \sqrt{J_2})}{\sqrt{3\alpha^2 + \frac{1}{2}}} \\ &= \frac{\sqrt{3}(\alpha I_1 + \sqrt{J_2})}{1 + \sqrt{3}\alpha} d\epsilon_p \end{aligned} \quad (5.92)$$

where $(\partial F / \partial \sigma_{ij})(\partial F / \partial \sigma_{ij}) = 3\alpha^2 + \frac{1}{2}$, $n = 1$, and σ_e of Eq. (5.79) have been used. From Eq. (5.92), it can readily be shown that

$$d\epsilon_p = \frac{\alpha + 1/\sqrt{3}}{\sqrt{3\alpha^2 + \frac{1}{2}}} \sqrt{d\epsilon_{ij}^p d\epsilon_{ij}^p} \quad (5.93)$$

As for the von Mises material, for which $\alpha = 0$, Eq. (5.93) reduces to Eq. (5.86), where the effective plastic strain ϵ_p is defined by an alternative method which is rather intuitive. In general, the two definitions of effective plastic strain ϵ_p —in terms of the plastic work [Eq. (5.87)] or in terms of the accumulated plastic strain [Eq. (5.83)]—will result in different scalar functions depending on the loading function. They are the same only for $F = J_2$. However, the effective plastic strain ϵ_p , as defined by Eq. (5.86) for $F = J_2$ material, is found to be reasonably correct for almost any $F(J_2, J_3)$ material that is pressure independent.

5.5.3. Effective Stress-Effective Strain Relation

The effective stress-effective strain relation, characterizing the hardening processes of a material, is now calibrated on the uniaxial stress test, which has the general form

$$\sigma_e = \sigma_e(\epsilon_p) \quad (5.94)$$

Differentiation gives the incremental relation

$$d\sigma_e = H_p(\sigma_e) d\epsilon_p \quad (5.95)$$

where $H_p(\sigma_e)$ is a *plastic modulus* associated with the rate of expansion of the yield or loading surface

$$H_p = \frac{d\sigma_e}{d\epsilon_p} \quad (5.96)$$

with H_p the slope of the uniaxial stress-plastic strain curve at the current value of σ_e .

The *strain history* for the material as recorded by the *length of the effective plastic strain path*

$$\epsilon_p = \int d\epsilon_p = \int \frac{d\sigma_e}{H_p(\sigma_e)} \quad (5.97)$$

must be a function of effective stress only. There will be a unique inverse for a work-hardening material, so that σ_e or F is a function of $\epsilon_p = \int d\epsilon_p$.

5.5.3.1. MIXED HARDENING

A combination of isotropic and kinematic hardening allows the yield surface to expand and to translate simultaneously in stress space. The yield and loading function takes the form of Eq. (5.80). We have defined the reduced effective stress by Eq. (5.82). Since the strain ϵ_p in Eq. (5.80) governs the isotropic expansion of the yield surface, it can be considered the *reduced effective plastic strain* and denoted by $\bar{\epsilon}_p$. Then, the loading surface of Eq. (5.80) is rewritten as

$$f = F(\bar{\sigma}_{ij}) - k^2(\bar{\epsilon}_p) = 0 \quad (5.98)$$

which is a measure of the expansion of the yield surface from an origin at the center of this surface. The rate of expansion of the yield surface is governed by the *reduced effective stress-strain relation*

$$\dot{\sigma}_e = \dot{\sigma}_e(\bar{\epsilon}_p) \quad (5.99)$$

determined by the experimental uniaxial stress-strain relation.

The total increment of plastic strain is now simply split into two collinear components

$$d\epsilon_{ij}^p = d\epsilon_{ij}^i + d\epsilon_{ij}^k \quad (5.100)$$

where $d\epsilon_{ij}^i$ is associated with the expansion of the yield surface and $d\epsilon_{ij}^k$ is associated with the translation of the yield surface. These two strain components can be written as

$$d\epsilon_{ij}^i = M d\epsilon_{ij}^p \quad (5.101)$$

$$d\epsilon_{ij}^k = (1 - M) d\epsilon_{ij}^p \quad (5.102)$$

where M is the *parameter of mixed hardening*, with the range $0 < M \leq 1$.

The share of the plastic strain increment $d\epsilon_{ij}^i$ associated with the expansion of the yield surface is now used to define the *reduced effective strain* $d\bar{\epsilon}_p$ as

$$d\bar{\epsilon}_p = C \sqrt{d\epsilon_{ij}^i d\epsilon_{ij}^i} \quad (5.103)$$

It follows from Eq. (5.101) that the *reduced effective plastic strain* $\bar{\epsilon}_p$ associated with isotropic hardening is now related to the effective plastic strain ϵ_p by the simple relation

$$\bar{\epsilon}_p = M \int C \sqrt{d\epsilon_{ij}^p d\epsilon_{ij}^p} = M \epsilon_p \quad (5.104)$$

Differentiation of Eq. (5.99) gives the rate of expansion of the yield surface

$$d\bar{\sigma}_e = \bar{H}_p d\bar{\epsilon}_p = M \bar{H}_p d\epsilon_p \quad (5.105)$$

where \bar{H}_p is the *plastic modulus* associated with the expansion of the yield surface.

The rate of translation of the yield surface, $d\alpha_{ij}$, as given by Eq. (5.37) or Eqs. (5.47) and (5.48), is related to the share of the plastic strain increment $d\epsilon_{ij}^k = (1 - M) d\epsilon_{ij}^p$ that is associated with the translation. Hence, in the case of mixed hardening, $d\epsilon_{ij}^k$ and $d\epsilon_p = (1 - M) \epsilon_p$ must replace $d\epsilon_{ij}^p$ in Eq. (5.37) and $d\epsilon_p$ in Eq. (5.48) in calculating the translation rate $d\alpha_{ij}$

$$d\alpha_{ij} = c d\epsilon_{ij}^k = c(1 - M) d\epsilon_{ij}^p \quad \text{for Prager's rule} \quad (5.106)$$

or

$$d\alpha_{ij} = a(1 - M) d\epsilon_p (\sigma_{ij} - \alpha_{ij}) \quad \text{for Ziegler's rule} \quad (5.107)$$

5.6. Illustrative Examples

We have discussed the hardening rules and the flow rules. Based on these important assumptions, the general stress-strain relations can now be established for a work-hardening material. The concepts of the effective stress and the effective strain allow us to calibrate the multiaxial stress-strain relation on the uniaxial stress test data. In the following, we shall present some illustrative examples.

EXAMPLE 5.5. (a) Given the uniaxial stress-plastic strain relation $\sigma_e = \sigma(\epsilon_p)$, find the hardening function \tilde{G} in the general stress-strain formulation of Eq. (5.64) for an isotropic-hardening von Mises material with a loading surface of the form

$$f = J_2 - k^2(\epsilon_p) = 0 \quad (5.108)$$

(b) If the uniaxial stress-strain relation is given by the Ramberg-Osgood relation

$$\epsilon_1 = \epsilon_i^e + \epsilon_i^n = \frac{\sigma_1}{E} + a \left(\frac{\sigma_1}{b} \right)^{2n+1} \quad (5.109)$$

in which E is the initial elastic modulus and a, b , and n are constants, find the incremental plastic strain-stress relation.

SOLUTION. (a) For the simplest and most commonly used isotropic-hardening von Mises model of Eq. (5.108), $\partial f / \partial \sigma_{ij} = \partial J_2 / \partial \sigma_{ij} = s_{ij}$, $\partial f = dJ_2$, Eq. (5.64) takes the form:

$$d\epsilon_{ij}^p = \tilde{G} s_{ij} dJ_2 \quad (5.110)$$

Squaring each of the terms represented by Eq. (5.110) and adding, we have

$$d\epsilon_{ij}^p d\epsilon_{ij}^p = \tilde{G}^2 2J_2 (dJ_2)^2$$

Taking the square root of both sides and noting the definitions of effective stress $\sigma_e = \sqrt{(3J_2)}$ and effective strain $d\epsilon_p = \sqrt{\frac{2}{3} d\epsilon_{ij}^p d\epsilon_{ij}^p}$ yields

$$d\epsilon_p = \frac{2}{3} \tilde{G} \sigma_e dJ_2 = \frac{4}{9} \tilde{G} \sigma_e^2 d\sigma_e \quad (5.111)$$

in which the relation $dJ_2 = \frac{2}{3}\sigma_e d\sigma_e$ has been used. For a given $\sigma_e - \epsilon_p$ relationship, the plastic modulus $H_p = d\sigma_e/d\epsilon_p$ is known, and the hardening function \bar{G} is now found to be

$$\bar{G} = \frac{9}{4} \frac{1}{H_p \sigma_e^2} = \frac{3}{4H_p J_2} \quad (5.112)$$

(b) Now, the uniaxial stress-strain relation is given by Eq. (5.109) in which

$$\epsilon^p = a \left(\frac{\sigma_1}{b} \right)^{2n+1}$$

Hence,

$$H_p = \frac{d\sigma_e}{d\epsilon_p} = \frac{d\sigma}{d\epsilon^p} = \frac{d\sigma_1}{d\epsilon_1^p} = \frac{1}{2n+1} \left(\frac{b}{a} \right) \left(\frac{b}{\sigma_e} \right)^{2n} \quad (5.113)$$

Substitution of Eqs. (5.113) and (5.112) into Eq. (5.110) leads to the plastic strain-stress relation

$$d\epsilon_{ij}^p = \frac{3(2n+1)}{4} \left(\frac{a}{b} \right) \left(\frac{3J_2}{b^2} \right)^n s_{ij} \left(\frac{dJ_2}{J_2} \right) \quad \text{for } J_2 = k^2 \text{ and } dJ_2 > 0$$

in which dJ_2 is linear in stress increment. This constitutive equation can be written out in component form like Eq. (5.73).

EXAMPLE 5.6. An initially unstressed and unstrained thin-walled circular tube is subjected to a combined axial-tension and twisting-moment loading history which produces the successive straight-line paths in (σ, τ) space shown in Fig. 5.11a. Assume that the material is elastic-plastic, and the elastic response is linear with Young's modulus $E = 210$ GPa and $\nu = 0.3$, while the plastic response is of the von Mises isotropic stress-hardening type. The stress-strain curve in simple tension is given by

$$\epsilon = \epsilon^e + \epsilon^p = \frac{\sigma}{2.1 \times 10^5} + \frac{1}{3 \times 10^6} \left(\frac{\sigma}{7} \right)^3 \quad (5.114)$$

where σ is in MPa. Note that the plastic strain represented by the second term takes place at the beginning of loading.

- (a) Write the stress-strain relation in component form explicitly in terms of σ , τ , $d\sigma$, and $d\tau$.
- (b) Find the elastic and plastic components of strain at the end of each loading path.

SOLUTION. (a) For the isotropic-hardening von Mises model, from Example 5.5, we have

$$d\epsilon_{ij}^p = \bar{G}(J_2) s_{ij} dJ_2 \quad (5.115)$$

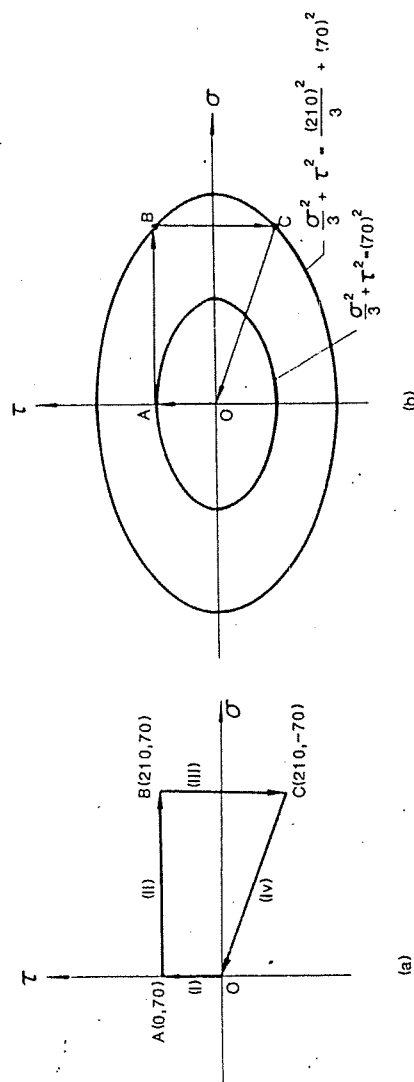


FIGURE 5.11. A von Mises isotropic material subject to loading path O-A-B-C-O (units: MPa).

For the elastic strain, based on Hooke's law, we have

$$d\epsilon_{ij}^e = \frac{1+\nu}{E} ds_{ij} + \frac{1-2\nu}{3E} d\sigma_{kk} \delta_{ij} \quad (5.116)$$

Adding up the elastic and plastic strains leads to

$$d\epsilon_{ij} = \frac{1+\nu}{E} ds_{ij} + \frac{1-2\nu}{3E} d\sigma_{kk} \delta_{ij} + \bar{G} s_{ij} dJ_2 \quad (5.117)$$

Since in $\sigma-\tau$ space, $\sigma_x = \sigma$, $\tau_{xy} = \tau$, other components = 0; we have

$$J_2 = \frac{1}{3}\sigma^2 + \tau^2$$

$$dJ_2 = \frac{2}{3}\sigma d\sigma + 2\tau d\tau$$

and

$$d\sigma_{kk} = d\sigma$$

Equation (5.117) can be expressed in component form as

$$\begin{aligned} d\epsilon_x &= d\epsilon = \frac{d\sigma}{E} + \frac{2}{3} \bar{G}\sigma \left(\frac{2}{3}\sigma d\sigma + 2\tau d\tau \right) \\ d\epsilon_y &= d\epsilon_z = -\nu \frac{d\sigma}{E} - \frac{1}{3} \bar{G}\sigma \left(\frac{2}{3}\sigma d\sigma + 2\tau d\tau \right) \\ d\gamma_{xy} &= d\gamma = \frac{2(1+\nu)}{E} d\tau + 2\bar{G}\tau \left(\frac{2}{3}\sigma d\sigma + 2\tau d\tau \right) \\ d\gamma_{xz} &= d\gamma_{yz} = 0 \end{aligned} \quad (5.118)$$

From the given simple tension data, the hardening function $\bar{G}(J_2)$ in Eq. (5.115) can be calculated by using Eqs. (5.112) and (5.113) with $a = 10^{-6}/3$, $b = 7$, and $n = 1$ as

$$\bar{G} = \frac{9}{4} \frac{1}{H_p \sigma_e^2} = \frac{9}{4} \frac{1}{\sigma_e^2 (d\sigma_e/d\epsilon_p)} = \frac{9}{4} \frac{\sigma_e^2}{\sigma_e^2 (7^3)(10^6)} = 6.56 \times 10^{-9} \quad (5.119)$$

Substituting Eq. (5.119) into (5.118) yields the formulas for the calculation of all strain increments in the plastic loading cases:

$$\begin{aligned} d\epsilon_x &= d\epsilon = \left(\frac{1}{E} + 2.92 \times 10^{-9} \sigma^2 \right) d\sigma + (8.75 \times 10^{-9} \sigma \tau) d\tau \\ d\epsilon_y &= d\epsilon_z = -\left(\frac{\nu}{E} + 1.46 \times 10^{-9} \sigma^2 \right) d\sigma - (4.38 \times 10^{-9} \sigma \tau) d\tau \\ d\gamma_{xy} &= d\gamma = (8.75 \times 10^{-9} \tau \sigma) d\sigma + [1.24 \times 10^{-5} + 26.25 \times 10^{-9} \tau^2] d\tau \end{aligned} \quad (5.120)$$

(b) The elastic and plastic strain components at the end of each loading path (Fig. 5.11b) are found as follows.

(i) For path OA, plastic loading occurs. Since $\sigma = 0$, $d\sigma = 0$, we obtain the strain components from Eq. (5.120) as

$$\epsilon_{xA} = \epsilon_{yA} = \epsilon_{zA} = 0$$

and

$$\gamma_A^e = \frac{2(1+\nu)}{E} \int_0^{\tau_A} d\tau = \frac{(2)(1.3)(70)}{2.1 \times 10^5} = 8.67 \times 10^{-4}$$

$$\gamma_A^p = 26.25 \times 10^{-9} \int_0^{\tau_A} \tau^2 d\tau = (26.25 \times 10^{-9}) \left(\frac{1}{3} \right) (70)^3 = 3 \times 10^{-3}$$

At the end of Path OA, the elastic and plastic strain tensors are now obtained as

$$\epsilon_A^e = \begin{bmatrix} 0 & 0.867/2 & 0 \\ 0.867/2 & 0 & 0 \\ 0 & 0 & 0 \end{bmatrix} \times 10^{-3}, \quad \epsilon_A^p = \begin{bmatrix} 0 & \frac{3}{2} & 0 \\ \frac{3}{2} & 0 & 0 \\ 0 & 0 & 0 \end{bmatrix} \times 10^{-3}$$

and the subsequent yield surface is given as

$$J_2 = \frac{\sigma_2}{3} + \tau^2 = (70)^2 \quad (5.121)$$

which is shown in Fig. 5.11b.

(ii) Path AB is also a plastic loading path (see Fig. 5.11b). Since along path AB, $\tau = 70$ MPa, $d\tau = 0$, the elastic plastic strain components at the end of this path are obtained from Eq. (5.120) as follows:

$$\epsilon_{xB}^e = \epsilon_{xA}^e + \int_A^B d\epsilon_x^e = 0 + \int_0^{210} \frac{d\sigma}{E} = \frac{210}{2.1 \times 10^5} = 10^{-3}$$

$$\epsilon_{yB}^e = \epsilon_{yA}^e + \int_A^B d\epsilon_y^e = 0 - \nu \int_0^{210} \frac{d\sigma}{E} = -0.3 \times 10^{-3}$$

$$\epsilon_{zB}^e = \epsilon_{yB}^e = -0.3 \times 10^{-3}$$

$$\gamma_B^e = \gamma_A^e = 8.67 \times 10^{-4}$$

$$\epsilon_{xB}^p = \epsilon_{xA}^p + \int_A^B d\epsilon_x^p = 0 + \int_0^{210} (2.92 \times 10^{-9}) \sigma^2 d\sigma = 9.01 \times 10^{-3}$$

$$\epsilon_{yB}^p = -\frac{1}{2} \epsilon_{xB}^p = -4.5 \times 10^{-3}$$

$$\epsilon_{zB}^p = \epsilon_{yB}^p = -4.5 \times 10^{-3}$$

$$\gamma_B^p = \gamma_A^p + \int_A^B d\gamma^p = 3 \times 10^{-3} + \int_0^{210} (8.75 \times 10^{-9})(70) \sigma d\sigma = 16.5 \times 10^{-3}$$

which can be expressed in matrix form as

$$\epsilon_B^e = \begin{bmatrix} 1 & 0.867/2 & 0 \\ 0.867/2 & -0.3 & 0 \\ 0 & 0 & -0.3 \end{bmatrix} \times 10^{-3}$$

$$\epsilon_B^p = \begin{bmatrix} 9.01 & 16.5/2 & 0 \\ 16.5/2 & -4.5 & 0 \\ 0 & 0 & -4.5 \end{bmatrix} \times 10^{-3}$$

During loading, the yield surface expands and at point B , we have

$$J_2 = \frac{\sigma^2}{3} + \tau^2 = \frac{(210)^2}{3} + (70)^2 \quad (5.122)$$

which is the current yield surface as shown in Fig. 5.11b.

(iii) It can be seen from Fig. 5.11b that along path BC , elastic unloading occurs and the strain changes in path BC are purely elastic and can be obtained by Hooke's law. Since along BC , $\sigma = 210$ MPa, $d\sigma = 0$, we have

$$d\epsilon_x^e = d\epsilon_y^e = d\epsilon_z^e = 0$$

and

$$\int_B^C d\gamma^e = \int_{70}^{-70} \frac{2(1+\nu)}{E} d\tau = -1.73 \times 10^{-3}$$

At the end of this path, the strain tensors are given by

$$\epsilon_C^e = \begin{bmatrix} 1 & -0.867/2 & 0 \\ -0.867/2 & -0.3 & 0 \\ 0 & 0 & -0.3 \end{bmatrix} \times 10^{-3}$$

$$\epsilon_C^p = \epsilon_B^p = \begin{bmatrix} 9.01 & 16.5/2 & 0 \\ 16.5/2 & -4.5 & 0 \\ 0 & 0 & -4.5 \end{bmatrix} \times 10^{-3}$$

(iv) Path CO is also an elastic unloading path. The changes of the elastic strains are found by Hooke's law as

$$\int_C^0 d\epsilon_x^e = \int_{210}^0 \frac{d\sigma}{E} = -10^{-3}$$

$$\int_C^0 d\epsilon_y^e = -\nu \int_{210}^0 \frac{d\sigma}{E} = 0.3 \times 10^{-3}$$

$$\int_C^0 d\gamma^e = \int_{-70}^0 \frac{2(1+\nu)}{E} d\tau = 0.867 \times 10^{-3}$$

$$\int_C^0 d\epsilon_z^e = 0.3 \times 10^{-3}$$

As can be seen, the elastic strain changes during loading path CO just offset the elastic strain ϵ_C^e at point C , and the total elastic strains for the complete cycle $O-A-B-O$ are zero, while the plastic strains are irrecoverable. These plastic strains are induced at the end of loading path AB and remain unchanged. At the end of this loading program, we have

$$\epsilon_O^e = 0; \quad \epsilon_O^p = \epsilon_C^p = \epsilon_B^p = \begin{bmatrix} 9.01 & 16.5/2 & 0 \\ 16.5/2 & -4.5 & 0 \\ 0 & 0 & -4.5 \end{bmatrix} \times 10^{-3}$$

Also, we have the subsequent loading surface as given by Eq. (5.122), which is a record for the complete load history of the material.

5.7. Incremental Stress-Strain Relationships

In the previous sections, we have discussed the basic assumptions and equations used in the development of the incremental theory of work-hardening plasticity. Based on these basic equations, a general constitutive equation for an elastic-plastic work-hardening material will be derived in this section in the form of

$$d\sigma_{ij} = C_{ijkl}^{ep} d\epsilon_{kl} \quad (5.123)$$

where C_{ijkl}^{ep} is the *elastic-plastic stiffness tensor of tangent modulus*, which is a function of stress state and loading history. For a given stress state and loading history, Eq. (5.123) gives the stress increment $d\sigma_{ij}$ for a given strain increment $d\epsilon_{ij}$ which constitutes a plastic loading. This equation is needed in a numerical analysis of plasticity, such as finite-element analysis.

5.7.1. Constitutive Relation for a General Work-Hardening Material

The general expression of a yield surface or loading surface for a work-hardening material as discussed in Section 5.3 has the form

$$f(\sigma_{ij}, \epsilon_{ij}^p, k) = 0 \quad (5.124)$$

where $k = k(\epsilon_p)$ is an isotropic hardening parameter. The strain increment $d\epsilon_{ij}$ is decomposed into two parts,

$$d\epsilon_{ij} = d\epsilon_{ij}^e + d\epsilon_{ij}^p \quad (5.125)$$

in which the elastic strain increment, $d\epsilon_{ij}^e$, is related to the stress increment, $d\sigma_{ij}$, by the generalized Hooke's law as

$$d\sigma_{ij} = C_{ijkl} d\epsilon_{kl}^e \quad (5.126)$$

where C_{ijkl} is the tensor of elastic modulus, as discussed in Chapter 3; the

plastic strain increment, $d\epsilon_{ij}^p$, can be generally expressed by a nonassociated flow rule in the form

$$d\epsilon_{ij}^p = d\lambda \frac{\partial g}{\partial \sigma_{ij}} \quad (5.127)$$

where $g = g(\sigma_{ij}, \epsilon_{ij}^p, k)$, as for $f(\sigma_{ij}, \epsilon_{ij}^p, k)$, is a known plastic potential function as discussed in Section 5.4, and $d\lambda$ is a scalar function to be determined later by the consistency condition $df = 0$. Substituting the elastic strain increment, $d\epsilon_{ij}^e$, from Eq. (5.125) and the plastic strain increment, $d\epsilon_{ij}^p$, from Eq. (5.127) into Hooke's law, Eq. (5.126), we have

$$d\sigma_{ij} = C_{ijkl} \left(d\epsilon_{kl} - d\lambda \frac{\partial g}{\partial \sigma_{kl}} \right) \quad (5.128)$$

From the above equation, we see that if we know the scalar function $d\lambda$, the constitutive relation is fully determined. To obtain $d\lambda$, consider a plastic loading process. At the current state, we know the current stress state σ_{ij} and the current plastic deformation state ϵ_{ij}^p and $k(\epsilon_p)$, and they must satisfy the current yield function, Eq. (5.124),

$$f(\sigma_{ij}, \epsilon_{ij}^p, k) = 0$$

After a small increment in total strain, $d\epsilon_{ij}$, which constitutes a plastic loading, the current state is changed to the new subsequent state, $\sigma_{ij} + d\sigma_{ij}$, $\epsilon_{ij}^p + d\epsilon_{ij}^p$, $k + dk$, and the new state must satisfy the subsequent yield function, Eq. (5.124), in the mathematical form

$$f(\sigma_{ij} + d\sigma_{ij}, \epsilon_{ij}^p + d\epsilon_{ij}^p, k + dk) = f(\sigma_{ij}, \epsilon_{ij}^p, k) + df = 0$$

or

$$df = \frac{\partial f}{\partial \sigma_{ij}} d\sigma_{ij} + \frac{\partial f}{\partial \epsilon_{ij}^p} d\epsilon_{ij}^p + \frac{\partial f}{\partial k} dk = 0 \quad (5.129)$$

This is known as the *consistency condition* for a general work-hardening material and imposes the restriction on the increments between $d\sigma_{ij}$, $d\epsilon_{ij}^p$, and dk . This condition assures that in a plastic loading process, the subsequent stress and deformation states remain on the subsequent yield surface. The scalar function $d\lambda$ in Eq. (5.128) can be determined directly from this condition. This is described in the following.

Consider first the increment of the isotropic hardening parameter, dk , in Eq. (5.129). The isotropic hardening parameter k is a function of the effective plastic strain ϵ_p , which can be expressed in the simple form of Eq. (5.83).

$$d\epsilon_p = C \sqrt{d\epsilon_{ij}^p d\epsilon_{ij}^p}$$

Using Eq. (5.83) for $d\epsilon_p$ and the flow rule, Eq. (5.127), we obtain

$$dk = \frac{dk}{d\epsilon_p} d\epsilon_p = \frac{dk}{d\epsilon_p} C \sqrt{\frac{\partial g}{\partial \sigma_{ij}} \frac{\partial g}{\partial \sigma_{ij}}} d\lambda \quad (5.130)$$

Substituting Eqs. (5.127) for $d\epsilon_{ij}^p$, (5.128) for $d\sigma_{ij}$, and (5.130) for dk into the consistency condition (5.129), we have

$$df = \frac{\partial f}{\partial \sigma_{ij}} C_{ijkl} d\epsilon_{kl} - h d\lambda = 0 \quad (5.131)$$

where

$$h = \frac{\partial f}{\partial \sigma_{ij}} C_{ijkl} \frac{\partial g}{\partial \sigma_{kl}} - \frac{\partial f}{\partial \epsilon_{ij}^p} \frac{\partial g}{\partial \sigma_{ij}} - \frac{\partial f}{\partial k} \frac{dk}{d\epsilon_p} C \sqrt{\frac{\partial g}{\partial \sigma_{ij}} \frac{\partial g}{\partial \sigma_{ij}}} \quad (5.132)$$

From Eq. (5.131), the scalar function $d\lambda$ can be solved as

$$d\lambda = \frac{1}{h} \frac{\partial f}{\partial \sigma_{ij}} C_{ijkl} d\epsilon_{kl} = \frac{1}{h} H_{kl} d\epsilon_{kl} \quad (5.133)$$

where the second-order tensor H_{kl} associated with the yield function, f , is defined as

$$H_{kl} = \frac{\partial f}{\partial \sigma_{ij}} C_{ijkl} \quad (5.134)$$

Similarly, we shall define the second-order tensor H_{kl}^* associated with the potential function, g , as

$$H_{kl}^* = \frac{\partial g}{\partial \sigma_{ij}} C_{ijkl} \quad (5.135)$$

This second-order tensor will be utilized later in connection with the development of the elastic-plastic tangent stiffness tensor C_{ijkl}^T below.

In Eq. (5.133), we have expressed the scalar function $d\lambda$ in terms of a given strain increment $d\epsilon_{ij}$. In the following, we shall show that the scalar function $d\lambda$ can also be expressed in terms of a given stress increment $d\sigma_{ij}$. To this end, we write the nonassociated flow rule (5.70) in the form

$$d\epsilon_{ij}^p = d\lambda \frac{\partial g}{\partial \sigma_{ij}} = \bar{G} \frac{\partial g}{\partial \sigma_{ij}} \frac{\partial f}{\partial \sigma_{kl}} d\sigma_{kl} = \frac{1}{\kappa} \frac{\partial g}{\partial \sigma_{ij}} \frac{\partial f}{\partial \sigma_{kl}} d\sigma_{kl} \quad (5.136)$$

in which κ is known as the *hardening modulus* and is related to the hardening function \bar{G} and the scalar function $d\lambda$ by

$$\kappa = \frac{1}{\bar{G}} \quad (5.137)$$

$$d\lambda = \frac{1}{\kappa} \frac{\partial f}{\partial \sigma_{kl}} = \frac{1}{\kappa} \frac{\partial f}{\partial \sigma_{kl}} d\sigma_{kl} \quad (5.138)$$

respectively. Since $(\partial f / \partial \sigma_{ij}) d\sigma_{ij} = df$, $d\epsilon_{ij}^p = (\partial f / \kappa) (\partial g / \partial \sigma_{ij})$, $dk = (dk / d\epsilon_p) d\epsilon_p$, and

$$d\epsilon_p = C d\lambda \sqrt{(\partial g / \partial \sigma_{ij}) / (\partial g / \partial \sigma_{ij})} = (C \partial f / \kappa) \sqrt{(\partial g / \partial \sigma_{ij}) / (\partial g / \partial \sigma_{ij})}$$

the consistency condition (5.129) can be written as

$$df = df + \frac{\partial f}{\partial \epsilon_{ij}^p} \frac{\partial f}{\partial \sigma_{ij}} \frac{\partial g}{\partial \sigma_{ij}} + \frac{\partial f}{\partial k} \frac{dk}{d\epsilon_p} \frac{C \partial f}{\kappa} \sqrt{\frac{\partial g}{\partial \sigma_{ij}} \frac{\partial g}{\partial \sigma_{ij}}} = 0 \quad (5.139)$$

From this, the scalar function κ can be solved as

$$\kappa = -\frac{\partial f}{\partial \epsilon_{ij}^p} \frac{\partial g}{\partial \sigma_{ij}} - \frac{\partial f}{\partial k} \frac{dk}{d\epsilon_p} C \sqrt{\frac{\partial g}{\partial \sigma_{ij}} \frac{\partial g}{\partial \sigma_{ij}}} \quad (5.140)$$

As can be seen, the hardening modulus κ is determined from the isotropic hardening rule. For the special case of an elastic-perfectly plastic material, the yield surface does not change during loading, i.e., $\partial f / \partial \epsilon_{ij}^p = 0$ and $dk / d\epsilon_p = 0$; hence, we have $\kappa = 0$. Using Eq. (5.140), we can also express the scalar function h in Eq. (5.132) in terms of the hardening modulus κ by

$$h = \kappa + \frac{\partial f}{\partial \sigma_{ij}} C_{ijkl} \frac{\partial g}{\partial \sigma_{kl}} = \kappa + H_{st} \frac{\partial g}{\partial \sigma_{st}} \quad (5.141)$$

Once the scalar function $d\lambda$ is determined, the plastic strain increment, $d\epsilon_{ij}^p$, is known from the flow rule (5.127)

$$d\epsilon_{ij}^p = d\lambda \frac{\partial g}{\partial \sigma_{ij}} = \frac{1}{h} \frac{\partial f}{\partial \sigma_{mn}} C_{mnst} \frac{\partial g}{\partial \sigma_{ij}} d\epsilon_{st} = \frac{1}{h} H_{st} \frac{\partial g}{\partial \sigma_{ij}} d\epsilon_{st} \quad (5.142)$$

and the corresponding stress increment, $d\sigma_{ij}$, can be determined from Eq. (5.128) using Eq. (5.142)

$$\begin{aligned} d\sigma_{ij} &= C_{ijkl} \left(d\epsilon_{kl} - \frac{1}{h} \frac{\partial f}{\partial \sigma_{mn}} C_{mnst} \frac{\partial g}{\partial \sigma_{kl}} d\epsilon_{st} \right) \\ &= C_{ijkl} \left(\delta_{sk} \delta_{tl} - \frac{1}{h} \frac{\partial f}{\partial \sigma_{mn}} C_{mnst} \frac{\partial g}{\partial \sigma_{kl}} \right) d\epsilon_{st} \\ &= \left(C_{ijst} - \frac{1}{h} \frac{\partial f}{\partial \sigma_{mn}} C_{mnst} C_{ijkl} \frac{\partial g}{\partial \sigma_{kl}} \right) d\epsilon_{st} \\ &= C_{ijst}^{ep} d\epsilon_{st} \end{aligned} \quad (5.143)$$

or

$$d\sigma_{ij} = C_{ijkl}^{ep} d\epsilon_{kl} \quad (5.144)$$

Thus, the elastic-plastic tangent stiffness tensor can be written in the form

$$C_{ijkl}^{ep} = C_{ijkl} + C_{ijkl}^p \quad (5.145)$$

with

$$C_{ijkl}^p = -\frac{1}{h} \frac{\partial f}{\partial \sigma_{mn}} C_{mnkl} C_{ijst} \frac{\partial g}{\partial \sigma_{st}} = -\frac{1}{h} H_{kl} H_{ij}^* \quad (5.146)$$

where C_{ijkl}^p is called the *plastic tangent stiffness tensor* and represents the degradation of the stiffness of the material due to plastic flow. It is obvious from Eq. (5.146) that the tensor C_{ijkl}^p lacks symmetry, and so does C_{ijkl}^{ep} if a nonassociated flow rule is used, i.e.,

$$\text{if } g \neq f, \text{ then } C_{ijkl}^{ep} \neq C_{klji}^{ep} \quad (5.147)$$

Furthermore, in this case, the elastic-plastic tangent stiffness C_{ijkl}^{ep} may not be positive definite. In contrast, if the associated flow rule is adopted, the positive-definiteness of the tensor C_{ijkl}^{ep} can be ensured.

The incremental elastic-plastic stress-strain relationship (5.144) is valid only for the case of plastic loading. Thus, before using this relationship to calculate the corresponding stress increment, $d\sigma_{ij}$, for a given strain increment, $d\epsilon_{ij}$, one must check first whether the material is in a plastic loading state corresponding to the given strain increment $d\epsilon_{ij}$. If not, the elastic stress-strain relationship

$$d\sigma_{ij} = C_{ijkl} d\epsilon_{kl} \quad (5.148)$$

should be used instead of the elastic-plastic stress-strain relationship. To this end, a proper loading criterion is needed. In Section 5.3, we have expressed the loading criterion in terms of stress increment. However, here we need to express the loading criterion in terms of the given strain increment, because the stress increment is unknown and is yet to be determined from the strain increment. This is probably true in most numerical analysis methods of plasticity for structures, for example, the popular finite-element method.

Refer now to the consistency condition (5.131). It can be shown that the scalar function h as defined in Eq. (5.132) is always positive for a work-hardening material as well as for a strain-softening material. This will be described later in Chapter 7. The proof of this statement is outside the scope of this book. Using this fact, we shall derive the loading criterion in terms of strain increments $d\epsilon_{ij}$ as follows.

For a plastic loading, $d\lambda$ is a non-negative factor and $h d\lambda$ is always positive. It then follows from the consistency condition (5.131) that

$$\frac{\partial f}{\partial \sigma_{ij}} C_{ijkl} d\epsilon_{kl} > 0 \quad (5.149)$$

For a neutral loading, we have $d\epsilon_{ij}^p = 0$, or $d\lambda = 0$, and the consistency condition (5.131) leads to

$$\frac{\partial f}{\partial \sigma_{ij}} C_{ijkl} d\epsilon_{kl} = 0 \quad (5.150)$$

For an unloading from an elastic-plastic state, the stress state on the surface is moved inward, resulting in $df < 0$. Further, for this case, we have $d\lambda = 0$. Using the condition $df < 0$ and $d\lambda = 0$ in Eq. (5.131), we have

$$\frac{\partial f}{\partial \sigma_{ij}} C_{ijkl} d\epsilon_{kl} < 0 \quad (5.151)$$

In summary, the loading criterion for a given strain increment $d\epsilon_{ij}$ can be expressed as

$$\frac{\partial f}{\partial \sigma_{ij}} C_{ijkl} d\epsilon_{kl} \begin{cases} > 0, & \text{loading} \\ = 0, & \text{neutral loading} \\ < 0, & \text{unloading} \end{cases} \quad (5.152)$$

In conclusion, the complete stress-strain relationship for an elastic-plastic work-hardening material can be expressed in the general form as follows.

For $f(\sigma_{ij}, \epsilon_{ij}^p, k) = 0$, and $(\partial f / \partial \sigma_{ij}) C_{ijkl} d\epsilon_{kl} > 0$, we have

$$d\sigma_{ij} = C_{ijkl}^{sp} d\epsilon_{kl} \quad (5.153)$$

where C_{ijkl}^{sp} is given in Eqs. (5.145) and (5.146).

For $f(\sigma_{ij}, \epsilon_{ij}^p, k) < 0$, or $f(\sigma_{ij}, \epsilon_{ij}^p, k) = 0$ and $(\partial f / \partial \sigma_{ij}) C_{ijkl} d\epsilon_{kl} \leq 0$, we have

$$d\sigma_{ij} = C_{ijkl} d\epsilon_{kl} \quad (5.154)$$

where the elastic tangent stiffness tensor C_{ijkl} is given in Chapter 3.

5.7.2. Constitutive Relation for a Mixed-Hardening Material

The general expression of a yield surface for a mixed-hardening material has the form

$$f(\bar{\sigma}_{ij}, k) = f(\sigma_{ij} - \alpha_{ij}, k) = 0 \quad (5.155)$$

Here, the yield surface is expressed in terms of α_{ij} instead of ϵ_{ij}^p explicitly. We shall derive the incremental stress-strain relationships for a mixed-hardening material directly from the basic plasticity equations. In this development, we shall assume that the plastic strain increments $d\epsilon_{ij}^p$ can be further split into two parts, the isotropic hardening part $d\epsilon_{ij}^i$ and the kinematic hardening part $d\epsilon_{ij}^k$:

$$d\epsilon_{ij}^p = d\epsilon_{ij}^i + d\epsilon_{ij}^k \quad (5.156)$$

in which we take

$$d\epsilon_{ij}^i = M d\epsilon_{ij}^p, \quad d\epsilon_{ij}^k = (1 - M) d\epsilon_{ij}^p \quad (5.157)$$

where $0 \leq M \leq 1$ represents the degree of mixture between the isotropic hardening and the kinematic hardening. In this case, the consistency condition becomes

$$df = \frac{\partial f}{\partial \sigma_{ij}} d\sigma_{ij} + \frac{\partial f}{\partial \alpha_{ij}} d\alpha_{ij} + \frac{\partial f}{\partial k} dk = 0 \quad (5.158)$$

If Prager's hardening rule, Eq. (5.106), is used, we have

$$d\alpha_{ij} = c d\epsilon_{ij}^k = c(1 - M) d\epsilon_{ij}^p = c(1 - M) \frac{\partial g}{\partial \sigma_{ij}} d\lambda \quad (5.159)$$

or if Ziegler's hardening rule, Eq. (5.107), is used, we have

$$\begin{aligned} d\alpha_{ij} &= a(1 - M)(\sigma_{ij} - \alpha_{ij}) d\epsilon_p \\ &= a(1 - M)(\sigma_{ij} - \alpha_{ij}) C \sqrt{\frac{\partial g}{\partial \sigma_{kl}} \frac{\partial g}{\partial \sigma_{kl}}} d\lambda \end{aligned} \quad (5.160)$$

or writing these hardening rules in a general form,

$$d\alpha_{ij} = A_{ij} d\lambda \quad (5.161)$$

where for Prager's rule

$$A_{ij} = c(1 - M) \frac{\partial g}{\partial \sigma_{ij}} \quad (5.162)$$

and for Ziegler's rule

$$A_{ij} = a(1 - M)(\sigma_{ij} - \alpha_{ij}) C \sqrt{\frac{\partial g}{\partial \sigma_{kl}} \frac{\partial g}{\partial \sigma_{kl}}} \quad (5.163)$$

and the effective plastic strain definition

$$d\epsilon_p = C \sqrt{d\epsilon_{ij}^p d\epsilon_{ij}^p} = C \sqrt{\frac{\partial g}{\partial \sigma_{ij}} \frac{\partial g}{\partial \sigma_{ij}}} d\lambda \quad (5.164)$$

has been used in the derivation, and the parameters a and c have been discussed in Section 5.5. The isotropic hardening parameter k is a function of the reduced effective plastic strain, $\bar{\epsilon}_p$, defined as

$$\bar{\epsilon}^p = C \int \sqrt{d\epsilon_{ij}^i d\epsilon_{ij}^i} = MC \int \sqrt{d\epsilon_{ij}^p d\epsilon_{ij}^p} = M \int d\epsilon_p = M\epsilon_p \quad (5.165)$$

$$d\bar{\epsilon}_p = M d\epsilon_p = MC \sqrt{\frac{\partial g}{\partial \sigma_{ij}} \frac{\partial g}{\partial \sigma_{ij}}} d\lambda \quad (5.166)$$

Thus, we have the relationship

$$dk = \frac{dk}{d\bar{\epsilon}_p} d\bar{\epsilon}_p = \frac{dk}{d\epsilon_p} MC \sqrt{\frac{\partial g}{\partial \sigma_{kl}} \frac{\partial g}{\partial \sigma_{kl}}} d\lambda \quad (5.167)$$

Noting that

$$\frac{\partial f}{\partial \sigma_{ij}} = \frac{\partial f}{\partial \bar{\sigma}_{kl}} \frac{\partial \bar{\sigma}_{kl}}{\partial \sigma_{ij}} = \frac{\partial f}{\partial \bar{\sigma}_{kl}} \delta_{ik} \delta_{jl} = \frac{\partial f}{\partial \bar{\sigma}_{ij}} \quad (5.168)$$

$$\frac{\partial f}{\partial \alpha_{ij}} = \frac{\partial f}{\partial \bar{\sigma}_{kl}} \frac{\partial \bar{\sigma}_{kl}}{\partial \alpha_{ij}} = \frac{\partial f}{\partial \bar{\sigma}_{kl}} (-\delta_{ik} \delta_{jl}) = -\frac{\partial f}{\partial \bar{\sigma}_{ij}} = -\frac{\partial f}{\partial \sigma_{ij}} \quad (5.169)$$

the consistency condition (5.131) can then be rewritten as

$$df = \frac{\partial f}{\partial \sigma_{ij}} C_{ijkl} d\epsilon_{kl} - \bar{h} d\lambda = 0 \quad (5.170)$$

where

$$\bar{h} = H_{kl} \frac{\partial g}{\partial \sigma_{kl}} + A_{kl} \frac{\partial f}{\partial \sigma_{kl}} - \frac{\partial f}{\partial k} \frac{dk}{d\bar{\epsilon}_p} MC \sqrt{\frac{\partial g}{\partial \sigma_{kl}} \frac{\partial g}{\partial \sigma_{kl}}} \quad (5.171)$$

in which the tensor H_{kl} is defined in Eq. (5.134). The scalar function $d\lambda$ for the mixed-hardening material is now solved from Eq. (5.170) as

$$d\lambda = \frac{1}{\bar{h}} \frac{\partial f}{\partial \sigma_{ij}} C_{ijkl} d\epsilon_{kl} = \frac{1}{\bar{h}} H_{kl} d\epsilon_{kl} \quad (5.172)$$

and the elastic-plastic tangent stiffness tensor is obtained for a mixed-hardening material as

$$C_{ijkl}^{ep} = C_{ijkl} + C_{ijkl}^p = C_{ijkl} - \frac{1}{\bar{h}} H_{kl} H_{ij}^* \quad (5.173)$$

The general loading criterion, Eq. (5.152), is, of course, valid for the special mixed-hardening material. In summary, the complete stress-strain relationship for a mixed-hardening material can be expressed as follows.

For $f(\sigma_{ij} - \alpha_{ij}, k) = 0$, and $(\partial f / \partial \sigma_{ij}) C_{ijkl} d\epsilon_{kl} > 0$, we have

$$d\sigma_{ij} = C_{ijkl}^{ep} d\epsilon_{kl} \quad (5.174)$$

where the elastic-plastic tangent stiffness C_{ijkl}^{ep} is given in Eq. (5.173).

For $f(\sigma_{ij} - \alpha_{ij}, k) < 0$, or $f(\sigma_{ij} - \alpha_{ij}, k) = 0$, $(\partial f / \partial \sigma_{ij}) C_{ijkl} d\epsilon_{kl} \leq 0$, we have

$$d\sigma_{ij} = C_{ijkl} d\epsilon_{kl} \quad (5.175)$$

where the elastic tangent stiffness C_{ijkl} is given in Chapter 3.

5.7.3. Illustrative Examples

The incremental stress-strain relations for a general work-hardening material and for a special mixed-hardening material have been established in the preceding sections. In the following, we shall derive the two most commonly used material models, namely, the von Mises and Drucker-Prager materials, as illustrative examples.

EXAMPLE 5.7. Derive the stress-strain equations for von Mises material with the associated mixed-hardening rule.

SOLUTION. The loading function of von Mises material corresponding to the mixed-hardening rule can be expressed as

$$f(\sigma_{ij} - \alpha_{ij}, k) = \frac{3}{2} \tilde{\sigma}_{ij} \tilde{\sigma}_{ij} - \tilde{\sigma}_e^2 (\tilde{\epsilon}_p) = 0 \quad (5.176)$$

Here, $\tilde{\sigma}_{ij}$ denotes the deviatoric reduced stress tensor

$$\tilde{\sigma}_{ij} = \sigma_{ij} - \frac{1}{3} \tilde{\sigma}_{kk} \delta_{ij} \quad (5.177)$$

and $\tilde{\sigma}_{ij} = \sigma_{ij} - \alpha_{ij}$ is the reduced-stress tensor; the reduced effective stress, $\tilde{\sigma}_e$, which replaces the usual hardening parameter k , is defined by Eqs. (5.77) and (5.82); and the reduced effective plastic strain, $\tilde{\epsilon}_p$, is defined by Eq. (5.103) with the constant $C = \sqrt{\frac{2}{3}}$.

Using the associated flow rule, $g = f$, the derivatives of g and f are found as

$$\frac{\partial f}{\partial \sigma_{ij}} = \frac{\partial g}{\partial \sigma_{ij}} = 3 \tilde{\sigma}_{ij} \quad (5.178)$$

For a linear-elastic isotropic material, we have the following form of Hooke's law expressed in terms of the two elastic constants G and ν :

$$C_{ijkl} = 2G \left(\delta_{ik} \delta_{jl} + \frac{\nu}{1-2\nu} \delta_{ij} \delta_{kl} \right) \quad (5.179)$$

where G is the shear modulus and ν is Poisson's ratio. The tensors H_{kl} and H_{kl}^* as defined in Eqs. (5.134) and (5.135) are now obtained as

$$H_{kl} = H_{kl}^* = \frac{\partial f}{\partial \sigma_{ij}} C_{ijkl} = 6G \tilde{\sigma}_{kl} \quad (5.180)$$

Consider first Prager's hardening rule. Using Eq. (5.162) for the tensor A_{ij} , Eq. (5.178) for $\partial f / \partial \sigma_{ij}$ and $\partial g / \partial \sigma_{ij}$, and Eq. (5.180) for H_{kl} and H_{kl}^* , the scalar function \bar{h} as defined in Eq. (5.171) can be written as

$$\bar{h} = 18G \tilde{\sigma}_{kk} \tilde{\sigma}_{kk} + 9c(1-M) \tilde{\sigma}_{kk} \tilde{\sigma}_{kk} + 2\tilde{\sigma}_e \frac{d\tilde{\sigma}_e}{d\tilde{\epsilon}_p} M \sqrt{6\tilde{\sigma}_{kk} \tilde{\sigma}_{kk}} \quad (5.181)$$

where we have replaced k by $\tilde{\sigma}_e$ in Eq. (5.171) and have used the yielding function of Eq. (5.176). Using the definition for the slope or the stiffness of the reduced effective stress-strain relation, $\tilde{H} = d\tilde{\sigma}_e / d\tilde{\epsilon}_p$, the scalar function \bar{h} can be reduced to the simple form

$$\bar{h} = [12G + 6c(1-M) + 4M\tilde{H}_p] \tilde{\sigma}_e^2 \quad (5.182)$$

In this equation, the parameter c is related to the component of the kinematic hardening part and the parameter \tilde{H}_p is related to the component of the isotropic hardening part of the mixed-hardening model. These two parameters will be determined from a uniaxial stress-strain curve. For the uniaxial stress state, the reduced-stress tensor $\tilde{\sigma}_{ij}$ can be expressed as

$$\begin{aligned} \tilde{\sigma}_{11} &= \sigma_{11} - \alpha_{11}, & \tilde{\sigma}_{22} &= \tilde{\sigma}_{33} = 0 - \alpha_{22} = \frac{1}{2}\alpha_{11} \\ \tilde{\sigma}_{ij} &= 0 \quad \text{for } i \neq j \end{aligned} \quad (5.183)$$

where $\alpha_{22} = \alpha_{33} = -\alpha_{11}/2$ follows directly from Prager's hardening rule, Eq. (5.106), and the plastic-incompressibility condition of J_2 -material. Hence, the reduced effective stress $\tilde{\sigma}_e$ in the uniaxial case is obtained as

$$\begin{aligned} \tilde{\sigma}_e^2 &= 3\tilde{J}_2 = \frac{1}{2}[(\tilde{\sigma}_{11} - \tilde{\sigma}_{22})^2 + (\tilde{\sigma}_{22} - \tilde{\sigma}_{33})^2 + (\tilde{\sigma}_{33} - \tilde{\sigma}_{11})^2] \\ &= (\sigma_{11} - \frac{3}{2}\alpha_{11})^2 \end{aligned} \quad (5.184)$$

From Eq. (5.184) and using Eq. (5.106) for $d\alpha_{11}$, we have

$$d\tilde{\sigma}_e = d\sigma_{11} - \frac{3}{2}c(1-M) d\epsilon_{11}^p \quad \text{for Prager's rule} \quad (5.185)$$

Using Eq. (5.105) for $d\tilde{\sigma}_e$ and noting that $d\sigma_{11}$ and $d\epsilon_{11}^p$ are equal to $d\sigma_e$ and $d\epsilon_p$, respectively, in the uniaxial case, we obtain

$$\frac{d\sigma_e}{d\epsilon_p} = [M(\tilde{H}_p - \frac{3}{2}c) + \frac{3}{2}c] = H_p \quad (5.186)$$

Here, the definition of the plastic modulus H_p , Eq. (5.96), has been used. Since M is an arbitrary material constant and Eq. (5.162) must be valid for any value of M , it follows that

$$c = \frac{2}{3}H_p, \quad \bar{H}_p = H_p. \quad (5.187)$$

Finally, the substitution of Eq. (5.187) into (5.182) gives the scalar function \bar{h} in the simple form

$$\bar{h} = 4(3G + H_p)\bar{\sigma}_e^2 \quad (5.188)$$

Therefore, the elastic-plastic stiffness tensor for von Mises material with the associated mixed hardening rule is obtained as

$$C_{ijkl}^{ep} = C_{ijkl} - \frac{36G^2}{\bar{h}} \bar{s}_{ij} \bar{s}_{kl} \quad (5.189)$$

It should be noted that $\bar{\sigma}_e$ and \bar{s}_{ij} are reduced stress values, i.e., they are referred to the stress space with its origin at the current center of the kinematically translated yield surface.

For Ziegler's hardening rule and using Eq. (5.163) instead of Eq. (5.162) for A_{ii} , we obtain the scalar function \bar{h} as

$$\bar{h} = [12G + 4a(1-M)\bar{\sigma}_e + 4M\bar{H}_p]\bar{\sigma}_e^2 \quad (5.190)$$

To determine the hardening parameters a and \bar{H}_p , we use Eq. (5.107) instead of Eq. (5.106) for $d\alpha_{ii}$ in Eq. (5.184) and obtain the counterpart of Eq. (5.185)

$$d\bar{\sigma}_e = d\sigma_{11} - a(1-M)d\epsilon_p \bar{\sigma}_{11} \quad (5.191)$$

In a similar manner to that of Eq. (5.186), we obtain

$$\frac{d\sigma_e}{d\epsilon_p} = [M(\bar{H}_p - a\bar{\sigma}_e) + a\bar{\sigma}_e] = H_p \quad (5.192)$$

Using the same argument as for Eq. (5.187), we can conclude from Eq. (5.192) that

$$a = \frac{H_p}{\bar{\sigma}_e}, \quad \bar{H}_p = H_p \quad (5.193)$$

Finally, Ziegler's hardening rule leads to the same expression for \bar{h} , Eq. (5.188), as Prager's hardening rule for J_2 -material.

Equations (5.188) and (5.189) define the elastic-plastic tangent stiffness tensor C_{ijkl}^{ep} for the mixed-hardening von Mises material, which includes isotropic hardening, kinematic hardening, and perfectly plasticity (without hardening) as special cases. This is illustrated in the following.

(i) *Isotropic hardening case*. For this case, we have $M = 1$, $\alpha_{ij} = 0$, and $\bar{s}_{ij} = s_{ij}$. The loading function f , the scalar function h , and the elastic-plastic stiffness tensor C_{ijkl}^{ep} are

$$f(\sigma_{ij}, k) = \frac{1}{2}s_{ij}\bar{s}_{ij} - \sigma_e^2(\epsilon_e) = 0 \quad (5.194)$$

$$\bar{h} = h = 4(3G + H_p)\sigma_e^2 \quad (5.195)$$

$$C_{ijkl}^{ep} = C_{ijkl} - \frac{36G^2}{h} s_{ij} s_{kl} \quad (5.196)$$

Alternatively, using Eq. (5.141), we have

$$\begin{aligned} h &= \kappa + H_{kl} \frac{\partial g}{\partial \sigma_{kl}} \\ &= \kappa + (6G s_{kl})(3s_{kl}) = \kappa + 12G\sigma_e^2 = \frac{1}{G} + 12G\sigma_e^2 \end{aligned} \quad (5.197)$$

Comparing Eq. (5.195) with Eq. (5.197), we have

$$\bar{G} = \frac{1}{4H_p\sigma_e^2} \quad (5.198)$$

This equation is similar to Eq. (5.112) given previously in Example 5.5, but differs by a factor of 9. This is because the loading function used in Eq. (5.194) differs from the loading function used in Eq. (5.108) by a factor of 3.

(ii) *Kinematic hardening case*. For this case, we have $M = 0$ and $\bar{\sigma}_e^2 = \text{constant} = \sigma_0^2$. The loading function becomes

$$f(\sigma_{ij} - \alpha_{ij}) = \frac{1}{2}\bar{s}_{ij}\bar{s}_{ij} - \sigma_0^2 = 0 \quad (5.199)$$

The elastic-plastic tangent stiffness tensor C_{ijkl}^{ep} and the expression for the scalar function h take the same form as Eqs. (5.189) and (5.188), respectively, with $\bar{\sigma}_e = \sigma_0$.

Now let's examine the translation of the center, $d\alpha_{ij}$. According to Ziegler's hardening rule, Eq. (5.107), we have

$$d\alpha_{ij} = a d\epsilon_p \bar{\sigma}_{ij} = \frac{H_p d\epsilon_p}{\bar{\sigma}_e} \bar{\sigma}_{ij} = \frac{H_p d\epsilon_p}{\sigma_0} \bar{\sigma}_{ij} \quad (5.200)$$

in which Eq. (5.193) has been used. Note that in Eq. (5.200), $H_p d\epsilon_p = d\sigma_e = (3/2\bar{\sigma}_e)\bar{s}_{ij} ds_{ij}$, meaning that the incremental effective stress is evaluated only with respect to increments in the stress components, i.e., with constant α_{ij} .

For the special case in Example 5.4, $\sigma_x = \sigma$, $\tau_{xy} = \tau$, other stress components = 0, $H_p d\epsilon_p = (1/\sigma_0)(\bar{\sigma} d\sigma + 3\bar{\tau} d\tau)$, Eq. (5.200) leads to Eq. (5.50), as it should.

(iii) *Perfectly plastic case.* For this case, we have $M = 1$, $\alpha_{ij} = 0$, $\bar{s}_{ij} = s_{ij}$, $\bar{\sigma}_c = \sigma_0 = \text{constant}$, and $H_p = 0$. The elastic-plastic tangent stiffness takes the same form as Eq. (5.196), but the scalar function h in Eq. (5.195) becomes

$$h = 12G\sigma_0^2 = 36GJ_2 \quad (5.201)$$

Thus,

$$C_{ijkl}^{ep} = C_{ijkl} - \frac{G}{J_2} s_{ij} s_{kl} \quad (5.202)$$

which leads to Eq. (4.92), the constitutive relation for a perfectly plastic von Mises material.

EXAMPLE 5.8. Derive the stress-strain equations for isotropic-hardening Drucker-Prager material with a nonassociated flow rule.

SOLUTION. The general form of the loading function of the isotropic-hardening Drucker-Prager material can be expressed as

$$f(\sigma_{ij}, \epsilon_p) = \alpha(\epsilon_p) I_1 + \sqrt{J_2} - k(\epsilon_p) = 0 \quad (5.203)$$

In Section 4.10, the stress-strain equation for a perfectly plastic material has been presented with $\alpha = \text{constant}$ and $k = \text{constant}$. Herein, for simplicity, we shall assume that the slope of the loading surface in the $I_1-J_2^{1/2}$ space is a constant, $\alpha(\epsilon_p) = \alpha_1$, so that the hardening behavior of the material can be uniquely determined by a single uniaxial stress-strain relation through the hardening parameter $k(\epsilon_p)$

$$f(\sigma_{ij}, \epsilon_p) = \alpha_1 I_1 + \sqrt{J_2} + k(\epsilon_p) = 0 \quad (5.204)$$

As discussed previously in Section 4.10, the plastic deformation of Drucker-Prager material is always accompanied by a dilatation of volume if the associated flow rule is adopted. In this case, the rate of dilatation is controlled by the parameter α , Eq. (4.120). Herein, we will use a plastic potential function similar to the loading function, Eq. (5.204),

$$g(\sigma_{ij}) = \alpha_2 I_1 + \sqrt{J_2} \quad (5.205)$$

where $0 \leq \alpha_2 \leq \alpha_1$ is a constant. The subsequent loading surfaces and the potential surface are plotted in Fig. 5.12. The derivatives of f and g are obtained as

$$\frac{\partial f}{\partial \sigma_{ij}} = \alpha_1 \delta_{ij} + \frac{1}{2\sqrt{J_2}} s_{ij} \quad (5.206)$$

$$\frac{\partial g}{\partial \sigma_{ij}} = \alpha_2 \delta_{ij} + \frac{1}{2\sqrt{J_2}} s_{ij} \quad (5.207)$$

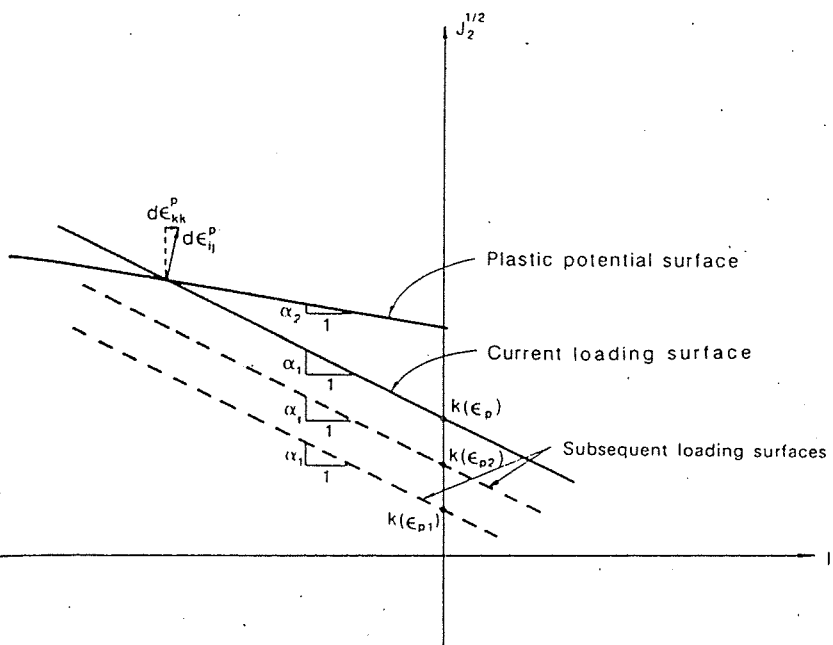


FIGURE 5.12. The loading and plastic potential surfaces for the Drucker-Prager material with a nonassociated flow rule.

Using the elastic stiffness tensor in the form

$$C_{ijkl} = (K - \frac{2}{3}G)\delta_{ij}\delta_{kl} + G(\delta_{ik}\delta_{jl} + \delta_{il}\delta_{jk}) \quad (5.208)$$

we obtain

$$H_{kl} = C_{ijkl} \frac{\partial f}{\partial \sigma_{ij}} = 3K\alpha_1 \delta_{kl} + \frac{G}{\sqrt{J_2}} s_{kl} \quad (5.209)$$

$$H_{kl}^* = C_{ijkl} \frac{\partial g}{\partial \sigma_{ij}} = 3K\alpha_2 \delta_{kl} + \frac{G}{\sqrt{J_2}} s_{kl} \quad (5.210)$$

Since the loading function is not expressed as a function of ϵ_{ij}^p explicitly, we have $\partial f / \partial \epsilon_{ij}^p = 0$. To determine the scalar function h defined in Eq. (5.132), we also need to obtain $dk/d\epsilon_p$ and the parameter C . The effective stress σ_e for Drucker-Prager material has been derived in Section 5.5, Eq. (5.79),

$$\sigma_e = \frac{\sqrt{3}(\alpha_1 I_1 + \sqrt{J_2})}{1 + \sqrt{3}\alpha_1} \quad (5.211)$$

Using eqs. (5.204) and (5.211), we can express k in terms of σ_e

$$k = \frac{1 + \sqrt{3}\alpha_1}{\sqrt{3}} \sigma_e$$

from which we obtain

$$\frac{dk}{d\epsilon_p} = \frac{1 + \sqrt{3}\alpha_1}{\sqrt{3}} \frac{d\sigma_e}{d\epsilon_p} = \frac{1 + \sqrt{3}\alpha_1}{\sqrt{3}} H_p \quad (5.212)$$

where H_p is determined from a uniaxial tension stress-strain curve, $d\sigma = H_p d\epsilon$.

The effective strain, ϵ_p , has been derived for the associated flow rule case in Section 5.5. Here, we shall follow the same procedure and derive the expression of $d\epsilon_p$ for a nonassociated flow rule case.

$$\begin{aligned} d\epsilon_p &= \frac{dW_p}{\sigma_e} = \frac{\sigma_{kl} d\epsilon_{kl}^p}{\sigma_e} \\ &= \frac{\sigma_{kl} \frac{\partial g}{\partial \sigma_{kl}}}{\sigma_e} d\lambda = \frac{\sigma_{kl} \frac{\partial g}{\partial \sigma_{kl}}}{\sigma_e} \frac{\sqrt{d\epsilon_{ij}^p d\epsilon_{ij}^p}}{\sqrt{\frac{\partial g}{\partial \sigma_{st}} \frac{\partial g}{\partial \sigma_{st}}}} = C \sqrt{d\epsilon_{ij}^p d\epsilon_{ij}^p} \end{aligned} \quad (5.213)$$

in which we have used Eq. (5.83) as the definition of $d\epsilon_p$. From the above equation, we have

$$C = \frac{\sigma_{kl} \frac{\partial g}{\partial \sigma_{kl}}}{\sqrt{\frac{\partial g}{\partial \sigma_{st}} \frac{\partial g}{\partial \sigma_{st}}}} \sigma_e \quad (5.214)$$

Substituting Eqs. (5.206) to (5.214) into (5.132), we can express the scalar function h as

$$h = G + 9K\alpha_1\alpha_2 + \frac{\alpha_2 I_1 + \sqrt{J_2}}{3k} (1 + \sqrt{3}\alpha_1)^2 H_p \quad (5.215)$$

Finally, we obtain the elastic-plastic tangent stiffness tensor as

$$\begin{aligned} C_{ijkl}^p &= C_{ijkl} - \frac{1}{h} H_{ij}^* H_{kl} \\ &= C_{ijkl} - \frac{1}{h} \left(3K\alpha_1 \delta_{kl} + \frac{G}{\sqrt{J_2}} s_{kl} \right) \left(3K\alpha_2 \delta_{ij} + \frac{G}{\sqrt{J_2}} s_{ij} \right) \end{aligned} \quad (5.216)$$

As noted previously in Section 5.7.2, for a nonassociated flow rule material, the stiffness C_{ijkl}^p , as given in Eq. (5.216), is not symmetric. However, for a value of the parameter α_2 in the range $0 \leq \alpha_2 \leq \alpha_1$, C_{ijkl}^p is still positive definite. The plastic volume change or dilatation has the value

$$d\epsilon_{kk}^p = 3\alpha_2 d\lambda \quad (5.217)$$

By adjusting the value of α_2 , the rate of dilatation of volume of the material can be controlled from 0 (incompressible) up to $3\alpha_1 d\lambda$.

Consider the following three special cases:

Case (i): *Associated flow rule case*. For this case, $\alpha_2 = \alpha_1 = \alpha$, we have

$$h = G + 9K\alpha^2 + \left(\alpha + \frac{1}{\sqrt{3}} \right)^2 H_p \quad (5.218)$$

$$C_{ijkl}^{sp} = C_{ijkl} - \frac{1}{h} \left(3K\alpha \delta_{kl} + \frac{G}{\sqrt{J_2}} s_{kl} \right) \left(3K\alpha \delta_{ij} + \frac{G}{\sqrt{J_2}} s_{ij} \right) \quad (5.219)$$

Furthermore, if a perfectly plastic behavior is assumed, Eqs. (5.218) and (5.219) lead to Eq. (4.126) for the perfectly plastic Drucker-Prager material, as they should.

Case (ii): *Drucker-Prager surface used as the plastic potential surface for the von Mises material*. For this case, $\alpha_1 = 0$, $\alpha_2 > 0$, we have

$$h = G + \frac{\alpha_2 I_1 + \sqrt{J_2}}{3k} H_p \quad (5.220)$$

$$C_{ijkl}^{sp} = C_{ijkl} - \frac{1}{h} \left(3K\alpha_2 \delta_{ij} + \frac{G}{\sqrt{J_2}} s_{ij} \right) \frac{G}{\sqrt{J_2}} s_{kl} \quad (5.221)$$

and the von Mises material is no longer plastically incompressible, and the rate of dilatation is given by Eq. (5.217).

Case (iii): *von Mises surface used as the plastic potential surface for the Drucker-Prager material*. For this case, $\alpha_1 > 0$, $\alpha_2 = 0$, we have

$$h = G + \frac{\sqrt{J_2}}{3k} (1 + \sqrt{3}\alpha_1)^2 H_p \quad (5.222)$$

$$C_{ijkl}^{sp} = C_{ijkl} - \frac{1}{h} \frac{G}{\sqrt{J_2}} s_{ij} \left(3K\alpha_1 \delta_{kl} + \frac{G}{\sqrt{J_2}} s_{kl} \right) \quad (5.223)$$

and the material becomes plastically incompressible, $d\epsilon_{kk}^p = 0$.

References

- Budiansky, B., 1959. "A Reassessment of Deformation Theories of Plasticity," *Journal of Applied Mechanics*, 26:259-264.
- Chen, W. F., 1982. *Plasticity in Reinforced Concrete*, McGraw-Hill, New York.
- Drucker, D.C., "A More Fundamental Approach to Plastic Stress-Strain Relation," Proc. 1st National Congress of Applied Mechanics, ASME, Chicago, 1951, pp. 487-491.
- Drucker, D.C., 1956. "On Uniqueness in the Theory of Plasticity," *Quarterly of Applied Mathematics* 14:35-42.
- Drucker, D.C., 1960. Plasticity. In: J.N. Goodier and N.J. Hoff (Editors), *Structural Mechanics*, Pergamon Press, London, pp. 407-445.

- Hill, R., 1950. *The Mathematical Theory of Plasticity*, Oxford University Press, London.
- Hodge, P.G., Jr., 1957. "Discussion of [Prager (1956)]," *Journal of Applied Mechanics* 23:482-484.
- Martin, J.B., 1975. *Plasticity: Fundamentals and General Results*, MIT Press, Cambridge.
- Mroz, Z., 1963. "Non-Associated Flow Laws in Plasticity," *Journal de Mécanique* II(1):21-42.
- Prager, W., 1955. "The Theory of Plasticity: A Survey of Recent Achievements (James Clayton Lecture)," *Institute of Mechanical Engineering* 169:41-57.
- Prager, W., 1956. "A New Method of Analyzing Stress and Strains in Work-Hardening Solids," *Journal of Applied Mechanics, ASME* 23:493-496.
- Ziegler, H., 1959. "A Modification of Prager's Hardening Rule," *Quarterly of Applied Mathematics* 17:55-65.

PROBLEMS

- 5.1. In a deformation theory, we assume the total stress-strain relation has the form

$$\epsilon_{ij} = aI_1\delta_{ij} + (b + cJ_2^2)s_{ij}$$

(a) Determine the material constants a , b , and c if the material response curves are approximated as follows.

(i) In a simple shear test ($\tau_{xy} = \tau_{yx} = \tau$, other $\sigma_{ij} = 0$, and $\gamma_{xy} = \gamma$):

$$\gamma = \frac{\tau}{28,000} + 27 \left(\frac{\tau}{700} \right)^5, \quad \tau \text{ in MPa}$$

(ii) In a hydrostatic stress test ($\sigma_x = \sigma_y = \sigma_z = p$, others = 0):

$$\epsilon_v = \frac{3}{2} \left(\frac{p}{7 \times 10^4} \right), \quad p \text{ in MPa}$$

(b) An element of the above material is subjected to a loading history which produces the following stress state:

$$\sigma_{ij} = \begin{bmatrix} 140 & 0 & 56 \\ 0 & 70 & -42 \\ 56 & -42 & 0 \end{bmatrix} \text{ MPa}$$

Predict the corresponding components of strain ϵ_{ij} .

- 5.2. An element of von Mises kinematic-hardening material is subjected to biaxial loadings. A stress increment $(d\sigma_1, d\sigma_2)$ is now imposed on a stress state (σ_1, σ_2) which lies on the yield surface. The stress increment satisfies the loading condition. Determine the coordinate change of the center of the loading surface, $d\alpha_{ij}$, based on Ziegler's hardening rule.

- 5.3. For biaxial states of stresses (σ_1, σ_2) with $\sigma_3 = 0$, write down the incremental plastic strain equation in component forms for the Tresca material in various regimes, assuming the associated flow rule.

- 5.4. The stress-strain curve of a metal under a simple tension test is assumed to be given by

$$\epsilon = \epsilon^e + \epsilon^p = \frac{\sigma}{E} \left[1 + \left(\frac{\sigma}{\sigma_0} \right)^{2n} \right]$$

in which $E = 2(1+\nu)G$ is the elastic modulus, σ_0 = initial tensile yield stress, and n = given material parameter. Assume that the metal is incompressible. Based on the isotropic-hardening von Mises theory, obtain the stress-strain relation

$$2G d\epsilon_{ij} = ds_{ij} + \frac{2n+1}{2} \left(\frac{J_2}{k^2} \right)^{n-1} s_{ij} \left(\frac{dJ_2}{k^2} \right)$$

where k is the initial yield stress in pure shear.

- 5.5. A thin-walled circular tube is subjected to combined axial-tension and twisting-moment loadings. A stress state with $\sigma = \sigma_0$ and $\tau = \sigma_0/\sqrt{3}$ is reached in the wall of the tube. The stress-strain relation of the material in simple tension is given by

$$\epsilon = \begin{cases} \frac{\sigma}{E} & (\sigma < \sigma_0) \\ \frac{\sigma_0}{E} + \frac{\sigma - \sigma_0}{E_p} & (\sigma \geq \sigma_0) \end{cases}$$

which is an elastic-linear-hardening plastic stress-strain relation with constant elastic modulus E and plastic modulus E_p , and σ_0 is the initial yield stress. Assume the material is of the isotropic-hardening von Mises type. Find the state of strain (ϵ, γ) corresponding to the given state of stress $(\sigma_0, \sigma_0/\sqrt{3})$ for the following loading paths (see Fig. P5.5):

- (i) Normal stress σ first increases up to σ_0 and then remains constant. Shear stress τ increases to $\sigma_0/\sqrt{3}$ (path OCB).
- (ii) Shear stress τ first increases up to $\sigma_0/\sqrt{3}$ and then remains constant. Normal stress σ increases to σ_0 (path OAB).
- (iii) Stresses σ and τ increase with a constant ratio of $\sigma/\tau = \sqrt{3}$ until $\sigma = \sigma_0$ and $\tau = \sigma_0/\sqrt{3}$ (path OB).

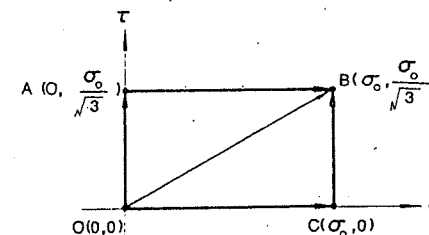


FIGURE P5.5

